

HYDRAULIC EVALUATION OF LYSIMETERS VERSUS
ACTUAL EVAPOTRANSPIRATIVE CAPS

By

Ramil Garcia Mijares

A DISSERTATION

Submitted to
Michigan State University
in partial fulfillment of the requirements
for the degree of

DOCTOR OF PHILOSOPHY

Civil Engineering

2011

ABSTRACT

HYDRAULIC EVALUATION OF LYSIMETERS VERSUS ACTUAL EVAPOTRANSPIRATIVE CAPS

By

Ramil Garcia Mijares

The ability to quantify percolation through a soil profile is one of the important considerations for geoenvironmental systems. Reliable estimates of percolation through natural soil deposits help in determining local groundwater recharge rates. For landfills, accurate measurement of percolation through the cap is necessary for permitting earthen final covers. Even though percolation is generally the smallest component among water balance parameters, quantifying its magnitude is environmentally critical and key in evaluating the overall hydraulic performance of final covers. Direct estimation of percolation through a soil cover is typically achieved using pan lysimeters which consist of a drainage layer underlain by an impermeable geomembrane liner. The presence of this hydraulic barrier in lysimeter, which is used to facilitate the collection and measurement of percolation, alters the hydraulics of the system. This dissertation aimed to evaluate the difference in hydraulic performance of a lysimeter versus actual earthen cap with underlying landfilled waste. Two uncompacted and one compacted field-scale earthen cap test sections were built and instrumented at a landfill near Detroit, Michigan to investigate the hydraulic difference between an actual cap (underlain by waste) and corresponding lysimeter which was used to directly measure percolation. Lysimeter pans were installed in the middle of each test sections and the instrumented area was expanded upslope and downslope of the lysimeter to monitor the soil water storages within and

beyond the lysimeter footprint. About 35 sensors were installed in each of the test sections to monitor water contents, water potentials, soil temperatures, water levels, and gas pressures. The field results show soil water storage values for the uncompacted test sections that were underlain by waste were typically greater than those for the corresponding lysimeters. For the compacted test section, there was no significant difference between the soil water storage for the actual cap and the lysimeter. Using the single porosity numerical models UNSAT-H and Vadose/W, the field measured percolation in the lysimeter as well as the variation in soil water storages were predicted with an acceptable accuracy for the compacted test section. The presence of macropore flow through large clods in uncompacted test sections is not accounted for in these single porosity models. A numerical analysis showed that when a lysimeter underestimates the soil water storage of an actual earthen cap, it corresponds to greater actual percolation across the interface between the soil cover and the underlying waste. A lysimeter overestimates percolation because the infiltrated water drained into the lysimeter is immediately removed and is therefore not available for removal by evapotranspiration. Field-scale simulations also showed that the magnitude of capillary barrier effect introduced by the drainage layer in the lysimeters is negligible when the saturated hydraulic conductivity of the soil cover is equal to or less than 10^{-5} cm/s.

Keywords: Landfill final covers, alternative earthen caps, lysimeter, field-scale testing and instrumentation; water balance, municipal solid waste, UNSAT-H, Vadose/W.

To
Mommy[†]
and
Daddy[†]

ACKNOWLEDGMENTS

I would like to express my deepest gratitude and appreciation to the following individuals and institutions for their valuable contributions for making this dissertation and my graduate study in the U.S. a successful endeavor.

Prof. Milind V. Khire, my supervisor and graduate advisor, for his continued support and guidance. I have been privileged to have an advisor who imposes a high standard on research. His perceptive comments and constructive criticisms helped me finish this dissertation and published papers. Thank you for the opportunity to be one of your students, Prof. Khire. Thank you for entrusting me a variety of projects, I learned a lot from them. I especially enjoyed the times we worked together in the field. Thank you for the motivation and advice you have shared with me, I really appreciate it.

Prof. Thomas Wolff, Prof. Phanikumar Mantha, and Prof. Remke van Dam, my Ph.D. Guidance Committee members, for the comments and suggestions to further improve this manuscript; Prof. Shu-Guang Li and Prof. Karim Chatti, my Examining Committee members, for the positive evaluation in my Ph.D. qualifying examination.

The Environmental Research and Education Foundation (EREF) and Waste Management, Inc. for funding the projects presented in this study; the Department of Civil and Environmental Engineering, the College of Engineering, and the Graduate School of Michigan State University for the research/teaching assistantships and fellowship awards to support my graduate study; the United States Universities Council for Graduate Education and Research (USUCGER) and the Geo-Institute of the

American Society of Civil Engineers (ASCE) for the travel grants to attend and present my papers in the conference.

Terry Johnson, Eric Wallis, and Paul Mazanec of Waste Management, Inc. for their assistance on the field project at Woodland Meadows Landfill; Jason Ritter of Campbell Scientific, Inc. for the technical support in programming the data acquisition system used in my field and lab studies.

The faculty and staff of the Department of Civil and Environmental Engineering at Michigan State University, headed by Prof. Ronald Harichandran, for providing an excellent workplace where one can have an enjoyable atmosphere for doing research and teaching; special thanks to James Brenton, and his student assistants, for the technical assistance in the fabrication and repair of all the apparatus and equipment I used in my experiments; thank you also to Lori Lerner, Laura Taylor, Mary Mroz, and Margaret Conner for their assistance in processing all the paperworks and performing other administrative functions.

My family and relatives for the unending support, love, and patience. Thank you for the sacrifices. Thank you for the prayers. Through the years, I have been blessed with a big extended family that is very supportive especially when my parents passed away.

My colleagues and friends, who constantly supported me, thank you for the camaraderie and the friendship.

And above all, to the Almighty God, for the countless blessings He has given me and for always providing His eternal guidance that allows me to face the challenges that life has to offer.

TABLE OF CONTENTS

LIST OF TABLES	x
LIST OF FIGURES	xi
KEY TO ABBREVIATIONS	xvi
KEY TO SYMBOLS.....	xix
INTRODUCTION.....	1
BACKGROUND ON LANDFILL FINAL COVERS	1
ALTERNATIVE EARTHEN COVERS	3
LYSIMETRY	5
Effect of Lower Boundary	7
Capillary Barrier Effect	8
NUMERICAL MODELS.....	9
OBJECTIVES	10
METHODOLOGY	11
DISSERTATION ORGANIZATION	12
REFERENCES	15
PAPER NO. 1: FIELD-SCALE EVALUATION OF LYSIMETERS VERSUS	
ACTUAL EARTHEN COVERS	18
ABSTRACT	18
INTRODUCTION.....	19
OBJECTIVE.....	21
DESIGN AND CONSTRUCTION OF TEST SECTIONS	21
Test Section Layout.....	22
Test Section Construction.....	23
<i>Lysimeter Installation</i>	25
<i>Soil Placement</i>	26
<i>Pump Set-up</i>	29
INSTRUMENTATION.....	30
Water Level and Pressure Transducers	31
Water Content Sensors	32
Soil Suction and Temperature Sensors.....	33
Percolation Monitoring.....	34
RESULTS AND DISCUSSION	37
Soil Temperatures.....	37
Soil Water Storage.....	38
<i>Phase 1: Uncompacted North and South Test Sections</i>	38
<i>Phase 2: Compacted North and Uncompacted South Test Sections</i>	43
SUMMARY AND PRACTICAL IMPLICATIONS	47
REFERENCES	50

PAPER NO. 2: FIELD DATA AND NUMERICAL MODELING OF WATER BALANCE OF LYSIMETER VERSUS ACTUAL EARTHEN CAP	52
ABSTRACT	52
INTRODUCTION.....	53
OBJECTIVE.....	54
FIELD-SCALE TEST SECTION	55
Soil Properties	57
Instrumentation.....	59
NUMERICAL WATER BALANCE MODELING.....	61
INPUT PARAMETERS FOR UNSAT-H	61
Soil Properties	63
MSW Properties	63
Meteorological Data	68
Initial Conditions	68
Numerical Control Parameters	69
FIELD DATA	69
Soil Water Storage.....	69
SUMMARY AND CONCLUSIONS.....	80
APPENDIX	83
Material Properties	84
Uncompacted Test Section Simulations.....	89
REFERENCES.....	98

PAPER NO. 3: EFFECT OF UNDERLYING WASTE LAYER ON SOIL WATER STORAGE AND PERCOLATION ESTIMATES FOR LANDFILL EARTHEN CAPS	101
ABSTRACT	101
INTRODUCTION.....	101
LYSIMETER VERSUS ACTUAL ET CAP	102
OBJECTIVE.....	105
WATER BALANCE MODEL.....	105
Material Properties	107
Meteorological Data	112
Initial and Boundary Conditions and Numerical Control Parameters	113
RESULTS.....	116
Semi-arid Climate.....	116
Humid Climate	121
SUMMARY AND CONCLUSIONS.....	124
REFERENCES.....	127

PAPER NO. 4: EVALUATION OF GEOSYNTHETIC CAPILLARY BREAK IN EARTHEN COVER LYSIMETERS.....	130
ABSTRACT	130
INTRODUCTION.....	130
OBJECTIVES	134
NUMERICAL MODELING.....	135

Material Properties	135
Initial and Boundary Conditions and Numerical Control Parameters	140
RESULTS.....	142
Constant Infiltration Simulations	142
Practical Implications	146
Field-scale Simulations	150
<i>Semi-arid Climate</i>	150
<i>Humid Climate</i>	155
SUMMARY AND CONCLUSIONS.....	162
REFERENCES.....	164

**PAPER NO. 5: NUMERICAL ASSESSMENT OF PAN LYSIMETERS USED
FOR ESTIMATION OF GROUNDWATER RECHARGE FOR NATURAL
SYSTEMS..... 167**

ABSTRACT	167
INTRODUCTION.....	168
OBJECTIVE.....	169
LABORATORY SOIL COLUMN	170
NUMERICAL MODELING.....	172
Material Properties	175
<i>Laboratory Soil Column</i>	175
<i>Field-scale Simulations</i>	177
Initial and Boundary Conditions	177
<i>Laboratory Soil Column</i>	177
<i>Field-scale Simulations</i>	179
Numerical Control Parameters	180
RESULTS.....	180
Laboratory Soil Column	180
Field-scale Simulations	184
<i>Semi-arid Climate</i>	184
<i>Sub-humid Climate</i>	189
<i>Practical Implications</i>	192
SUMMARY AND CONCLUSION.....	195
REFERENCES.....	197

SUMMARY AND CONCLUSIONS 199

LIST OF TABLES

Table 1-1: Properties of cover soils used in the test sections.	27
Table 2-1: Physical properties of the soils.	59
Table 2-2: Saturated and unsaturated hydraulic properties of the soils and waste.	64
Table 2-3: Saturated and unsaturated hydraulic properties of the cap components for the uncompacted test section.	84
Table 3-1: Saturated and unsaturated hydraulic properties of soils used in the instrumented field test sections of Khire et al. (1997).	108
Table 3-2: Saturated and unsaturated hydraulic properties of geotextile and waste used in the simulations.	109
Table 4-1: Saturated and unsaturated hydraulic properties.	137
Table 5-1: Saturated and unsaturated hydraulic properties of the materials used to build the laboratory soil column.	172
Table 5-2: Saturated and unsaturated hydraulic properties of the soils used to simulate groundwater recharge rates.	177

LIST OF FIGURES

Figure I-1:	Final cover system for MSW landfills (EPA 1992).	2
Figure I-2:	Evapotranspirative caps: monolithic caps (a) and capillary barriers (b).	4
Figure I-3:	Schematic of a typical lysimeter showing the water balance parameters.	6
Figure I-4:	Conceptual model of evapotranspirative caps consisting of lysimeter only (a); and actual cap (b) with underlying waste (Khire and Mijares 2008).....	8
Figure 1-1:	Typical cross-section of instrumented three field test sections.....	24
Figure 1-2:	Proctor compaction curves and field water contents and unit weights.	28
Figure 1-3:	Comparison between on-site and NOAA recorded precipitation.....	30
Figure 1-4:	Water contents measured in the field using water content reflectometers versus using Shelby tube samples.	33
Figure 1-5:	Lysimeter water level, volume, and percolation relations.....	35
Figure 1-6:	TDR and water level sensor correlation.	36
Figure 1-7:	Seasonal temperature variation across the test sections.	37
Figure 1-8:	Soil water storages (a); and cumulative precipitation and percolation (b) for uncompacted test sections.	39
Figure 1-9:	Correlation between measured soil water storages for lysimeters versus actual caps for uncompacted test sections.....	41
Figure 1-10:	Water contents in the test section and in the underlying waste.....	42
Figure 1-11:	Soil water storage and cumulative precipitation and percolation for compacted north test section (a); and uncompacted south test section (b).	44
Figure 1-12:	Correlation between measured soil water storages for lysimeter versus actual cap for the compacted north test section.....	46
Figure 2-1:	Cross-section of instrumented field test section.....	56
Figure 2-2:	Proctor compaction curves and field water contents and unit weights.	58

Figure 2-3:	Conceptual model for numerical simulation of a lysimeter (a); and an actual cap with underlying waste (b).....	62
Figure 2-4:	Measured water retention curves (a); and unsaturated hydraulic conductivity functions (b) for the waste.....	66
Figure 2-5:	Measured water contents (a); and gas pressures and suctions (b) in the waste.....	67
Figure 2-6:	Measured soil water storages and surficial temperatures for the lysimeter and actual caps.....	70
Figure 2-7:	Correlation between measured soil water storage for an actual cap and its corresponding lysimeter.	71
Figure 2-8:	Measured volumetric water contents for the lysimeter (a) and actual cap (b).....	73
Figure 2-9:	Measured water content profiles for the lysimeter and actual caps on 1 Feb. (a) and 1 Oct. 2010 (b).	74
Figure 2-10:	Measured and simulated cumulative percolation for the lysimeter and the actual cap.	75
Figure 2-11:	Measured and simulated soil water storage for the lysimeter.	77
Figure 2-12:	Simulated soil water storage for the lysimeter and the actual cap.	78
Figure 2-13:	Field water contents and unit weights for the uncompacted test section. ..	83
Figure 2-14:	Measured soil water characteristic curves (a); and predicted hydraulic conductivity function (b) for the cap components for uncompacted test section.....	86
Figure 2-15:	Typical mesh used for modeling in Vadose/W for: a lysimeter only (a); and an actual earthen cap with underlying waste (b).	88
Figure 2-16:	Field measured and numerically simulated cumulative percolation for the uncompacted test section.....	89
Figure 2-17:	Measured volumetric water contents for the lysimeter (a) and actual cap (b).....	91
Figure 2-18:	Calculated hydraulic gradient across the bottommost two sensors for the lysimeter and actual cap in the uncompacted test section.	92
Figure 2-19:	Field measured and numerically simulated soil water storage for the uncompacted test section.....	93

Figure 2-20: Correlation between measured soil water storage for actual cap versus lysimeter for the uncompacted test section.	94
Figure 2-21: Correlation between the simulated soil water storage for an actual cap versus its corresponding lysimeter with varying hydraulic properties of soil cover (Mijares et al. 2010).....	95
Figure 3-1: Conceptual model for numerical simulation of alternative capping system consisting of a lysimeter only (a); and a typical ET cap with underlying waste (b).	106
Figure 3-2: Soil water characteristic curves (a); and hydraulic conductivity functions (b) for the soils used in the Wenatchee test section, nonwoven geotextile, and MSW.	114
Figure 3-3: Soil water characteristic curves (a); and hydraulic conductivity functions (b) for the soils used in the Atlanta test section, nonwoven geotextile, and MSW.....	115
Figure 3-4: Simulated cumulative percolation and soil water storage for Wenatchee soil, with 0.6-m thick storage layer, in a semi-arid climate boundary condition.....	117
Figure 3-5: Simulated soil water storage for actual cap versus lysimeter for Wenatchee soil, with 0.6-m thick storage layer, in a semi-arid climate boundary condition.....	119
Figure 3-6: Simulated cumulative percolation and soil water storage for Wenatchee soil, with 0.9-m thick storage layer, in a semi-arid climate boundary condition.....	120
Figure 3-7: Simulated cumulative percolation and soil water storage for Atlanta soil, with 0.9-m thick storage layer, in a humid climate boundary condition.....	121
Figure 3-8: Simulated soil water storage for actual cap versus lysimeter for Atlanta soil, with 0.9-m thick storage layer, in a humid climate boundary condition.....	122
Figure 3-9: Simulated cumulative percolation and soil water storage for Atlanta soil, with 1.5-m thick storage layer, in a humid climate boundary condition.....	124
Figure 4-1: Conceptual model used to simulate a lysimeter without (a) and with (b) a nonwoven GT and an actual cap with waste layer (c).	136
Figure 4-2: Measured soil water characteristic curves (a); and predicted hydraulic conductivity function (b) for nonwoven geotextile and MSW.....	138

Figure 4-3:	Unsaturated hydraulic conductivity functions of the cap soils and the underlying nonwoven GT to illustrate the contrast in $K(\psi)$ relationships which is conducive to the occurrence of capillary barrier effect.	139
Figure 4-4:	Simulated cumulative percolation and soil water storage for OK110 fine sand under specified flux boundary condition.	143
Figure 4-5:	Simulated cumulative percolation and soil water storage for SM soil under specified flux boundary condition.	144
Figure 4-6:	Simulated cumulative percolation and soil water storage for SM-ML soil under specified flux boundary condition.	145
Figure 4-7:	Water retention curves (a); and unsaturated hydraulic conductivity functions (b) for fine-textured soil cap and coarse-textured GT or MSW.	147
Figure 4-8:	Relative magnitude of capillary barrier effect as a function of applied specified flux for SM and SM-ML soils.	149
Figure 4-9:	Simulated cumulative percolation and soil water storage for Wenatchee soil under semi-arid climate boundary condition.	151
Figure 4-10:	Simulated cumulative percolation and soil water storage for SM soil under semi-arid climate boundary condition.	152
Figure 4-11:	Simulated cumulative percolation and soil water storage for SM-ML soil under semi-arid climate boundary condition.	153
Figure 4-12:	Simulated soil water storage for lysimeter with GT versus without GT under semi-arid climate boundary condition.	155
Figure 4-13:	Simulated cumulative percolation and soil water storage for Atlanta soil under humid climate boundary condition.	156
Figure 4-14:	Simulated cumulative percolation and soil water storage for SM soil under humid climate boundary condition.	157
Figure 4-15:	Simulated cumulative percolation and soil water storage for SM-ML soil under humid climate boundary condition.	158
Figure 4-16:	Simulated soil water storage for lysimeter with GT versus without GT under humid climate boundary condition.	160
Figure 4-17:	Annual percolation difference between lysimeter without GT and lysimeter with GT for semi-arid (a); and humid climates (b).	161

Figure 5-1:	Photo and schematic of instrumented laboratory soil column.	171
Figure 5-2:	Water retention curves (a); and predicted hydraulic conductivity functions (b) for the materials used in the laboratory soil column.....	176
Figure 5-3:	Soil water characteristic curves (a); and predicted hydraulic conductivity functions (b) for the soils used to simulate groundwater recharge rates.....	178
Figure 5-4:	Measured and simulated UNSAT-H cumulative percolation and soil water storage for OK110 sand column.....	181
Figure 5-5:	Measured and simulated water content profile for OK110 fine sand column at breakthrough.....	183
Figure 5-6:	Schematic of a lysimeter (a); and a monolithic natural system (b) used to estimate natural groundwater recharge rates.....	185
Figure 5-7:	Simulated natural groundwater recharge rates and lysimeter percolations for SP soil in a semi-arid climate.....	186
Figure 5-8:	Simulated natural groundwater recharge rates and lysimeter percolations for SM soil in a semi-arid climate.	188
Figure 5-9:	Simulated natural groundwater recharge rates and lysimeter percolations for SP-SM soil in a semi-arid climate.....	189
Figure 5-10:	Simulated natural groundwater recharge rates and lysimeter percolations for SM soil in a sub-humid climate.	190
Figure 5-11:	Simulated natural groundwater recharge rates and lysimeter percolations for SM-ML soil in a sub-humid climate.	191
Figure 5-12:	Simulated natural groundwater recharge rates and lysimeter percolations for ML soil in a sub-humid climate.	192
Figure 5-13:	Ratio of natural groundwater recharge and percolation estimates for various lysimeter profile thicknesses in semi arid (a); and sub-humid (b) climates.	193
Figure 5-14:	Ratio of natural groundwater recharge and percolation estimates for various saturated hydraulic conductivity of the soil.....	194

KEY TO ABBREVIATIONS

1-D	=	one-dimensional
2-D	=	two-dimensional
ASTM	=	American Society for Testing and Materials
BGS	=	below ground surface
CB	=	bottom nest of the compacted north test section
CFR	=	Code of Federal Regulations
CL	=	lean clay
CM	=	middle nest of the compacted north test section
CT	=	top nest of the compacted north test section
ET	=	evapotranspiration/evapotranspirative
GCL	=	geosynthetic clay liner
GDL	=	geocomposite drainage layer
GP	=	uniformly graded gravel
GT	=	nonwoven geotextile; unit gradient boundary at the base of the nonwoven geotextile that lines the OK110 soil column
GW	=	constant water table at the base of a 90-cm thick coarse gravel that was hypothetically placed underneath the OK110 soil column
HDMP	=	heat dissipation matric potential
HDPE	=	high-density polyethylene
IPM	=	instantaneous profile method
LL	=	liquid limit

MDE	=	Maryland Department of the Environment
ML	=	low plasticity silt
MSW	=	municipal solid waste
NB	=	bottom nest of the uncompacted north test section
NM	=	middle nest of the uncompacted north test section
NOAA	=	National Oceanic and Atmospheric Administration
NT	=	top nest of the uncompacted north test section
OK 110	=	uniformly graded fine sand
P/PET	=	precipitation to potential evapotranspiration ratio
PE/P	=	potential evaporation to precipitation ratio
PI	=	plasticity index
PVC	=	polyvinyl chloride
RCRA	=	Resource Conservation and Recovery Act
SAIC	=	Science Applications International Corporation
SB	=	bottom nest of the uncompacted south test section
SM	=	silty sand; middle nest of the uncompacted south test section
SM-ML	=	nonplastic sandy silt
SP	=	uniformly graded medium sand
SP-SM	=	poorly graded sand with silt
ST	=	top nest of the uncompacted south test section
SWS	=	soil water storage
TDR	=	time domain reflectometry
UG	=	unit gradient boundary at the base of the monolithic OK110 soil column

US = United States

USCS = Unified Soil Classification System

USEPA = United States Environmental Protection Agency

WL = waste layer

KEY TO SYMBOLS

A	=	curve fitting parameter for Haverkamp et al. (1977) function
B	=	curve fitting parameter for Haverkamp et al. (1977) function
C_c	=	coefficient of gradation
C_u	=	uniformity coefficient
D_{10}	=	effective size or diameter in the particle-size distribution curve corresponding to 10% finer
D_{50}	=	diameter in the particle-size distribution curve corresponding to 50% finer
D_{60}	=	diameter in the particle-size distribution curve corresponding to 60% finer
E	=	surface evaporation
ET	=	evapotranspiration
G_s	=	specific gravity of soil solids
K	=	saturated hydraulic conductivity
K_{int}	=	ordinate of the intersection of unsaturated hydraulic conductivity functions for the coarse-textured and fine-textured materials where $K(\psi_c) = K(\psi_f)$
$K_L(\psi)$	=	unsaturated hydraulic conductivity for a given ψ
K_s	=	saturated hydraulic conductivity
K_{sat}	=	saturated hydraulic conductivity
K_{SL}	=	saturated hydraulic conductivity of the storage layer

$K_T(\psi)$	=	isothermal water vapor conductivity for a given ψ
K_{WL}	=	saturated hydraulic conductivity of municipal solid waste
K_ψ	=	unsaturated hydraulic conductivity
$k(\psi)$	=	hydraulic conductivity of the porous media for a given ψ
$K(\psi)$	=	unsaturated hydraulic conductivity
$K(\psi_f)$	=	unsaturated hydraulic conductivity for a fine-textured material with ψ_f
n	=	curve fitting parameter for van Genuchten (1980) function
p	=	estimated lysimeter percolation (mm)
P	=	precipitation
P_r	=	percolation; basal percolation
q	=	applied or specified flux
q_{VT}	=	thermal vapor flux density
RO	=	surface runoff
S	=	degree of saturation; sink term that represents the water uptake by vegetation as a function of both depth and time
t	=	time
T	=	plant transpiration
V	=	equivalent volume of water stored in the lysimeter (gal)
x	=	period measured by the water content reflectometer (μs)

z	=	vertical coordinate; depth of water in the lysimeter (cm)
α	=	curve fitting parameter for van Genuchten (1980) function; curve fitting parameter for Haverkamp et al. (1977) function
β	=	curve fitting parameter for Haverkamp et al. (1977) function
γ_d	=	dry unit weight
Δ	=	change
ΔS	=	change in soil water storage
θ	=	volumetric water content
θ_c	=	volumetric water content for a coarse-textured material
θ_f	=	volumetric water content for a fine-textured material
θ_r	=	residual water content
θ_s	=	saturated water content
ψ	=	matric suction head
Ψ	=	matric suction
Ψ_c	=	matric suction for a coarse-textured material
Ψ_f	=	matric suction for a fine-textured material
Ψ_{int}	=	abscissa of the intersection of unsaturated hydraulic conductivity functions for the coarse-textured and fine-textured materials where $\Psi_c = \Psi_f$
ω	=	gravimetric water content

INTRODUCTION

BACKGROUND ON LANDFILL FINAL COVERS

Landfills are the most widely used facilities for disposal of municipal solid wastes (MSW). The United States Environmental Protection Agency (USEPA) estimated that there are about 1,750 active landfills across the country as of 2006 and over 10,000 old municipal landfills. Current per capita waste generation in the U.S. is about 4.6 pounds per person per day which would translate to a total of roughly 250 million tons of MSW per year. Even though efforts to recycle wastes have significantly increased, approximately 55% of MSW is still being disposed off into landfills (EPA 2007).

Once these landfills reach their volumetric capacity and are scheduled for closure, final cover systems are installed. Final cover systems are used to control the amount of moisture infiltrating into the wastes, separate wastes from disease vectors and other nuisances, control landfill gas emissions and odors, and meet aesthetic requirements. Well-designed landfill final covers also promote good surface drainage, resist erosion, prevent slope failure, minimize long-term maintenance, and provide suitability for other eventual use of the site. Potential end-uses for closed MSW landfills are nature or recreation park, wilderness area or animal refuge, golf course, ski or toboggan hill, and parking lot (EPA 1995).

Conventional designs for landfill final cover systems are based on the requirements set forth in the Resource Conservation and Recovery Act (RCRA). Under RCRA Subtitle D (40 CFR 258.60), the minimum criteria for final cover system for MSW landfills depend on the existing bottom liner system. Accordingly, landfill final

cover system must have a permeability less than or equal to that of the bottom liner system, or less than or equal to 10^{-5} cm/s, whichever is less. A minimum 18 inches of this earthen material shall be used to minimize infiltration through the closed landfill unit. It must also have a minimum 6 inches of soil erosion layer that is capable of sustaining native plant growth.

Figure I-1 shows an example of a typical RCRA Subtitle D landfill final cover system. This design has been imposed to restrict the flow of water through the cover and into the waste. Such design would prevent the landfill from filling up with leachate that is primarily generated from infiltration of precipitation. This phenomenon is commonly referred to as “bathtub effect” and is therefore highly unwanted.

In practice, the presence of a geomembrane in the bottom liner system infers the use of a geomembrane in the final cover system (SAIC 2000). Installation of these conventional final covers that use geomembrane costs between \$80,000 and \$500,000 per acre (MDE 2003), with the bulk of the expenses allotted for the use of the geomembrane.

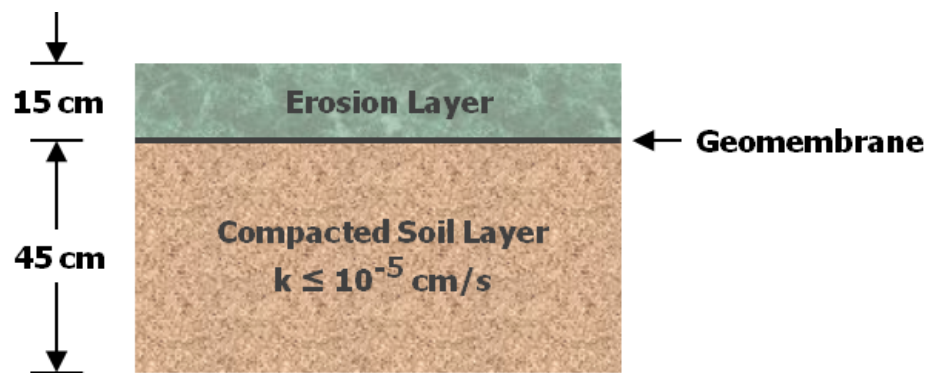


Figure I-1: Final cover system for MSW landfills (EPA 1992).

“For interpretation of the references to color in this and all other figures, the reader is referred to the electronic version of this dissertation.”

ALTERNATIVE EARTHEN COVERS

In lieu of RCRA design, RCRA guidelines also stipulate that alternative designs may be approved by regulatory agencies if it can be demonstrated that the proposed alternative provides equivalent performance with regard to reduction in percolation, erosion protection, and other applicable criteria.

Several alternative final cover designs have been proposed and investigated in the past decade (Benson and Khire 1995; Nyhan et al. 1997; Ward and Gee, 1997; Stormont and Morris 1998; Khire et al. 1999; Benson et al 2002; Albright et al. 2003; Scanlon et al. 2005). Collectively, the mechanisms in which these alternative final covers perform rely on the water-holding capability of native soils and a huge percentage of precipitation returns to the atmosphere through evapotranspiration. Hence the term “evapotranspirative caps” is often used to refer to these alternative final covers.

Evapotranspirative caps are often classified into two types: (1) monolithic caps and (2) capillary barriers. Monolithic caps have relatively simple cross-sectional profile consisting of 6 to 18 inches thick of topsoil layer underlain with a thick storage layer of earthen material with low hydraulic conductivity and high water storage capacity. The topsoil layer provides medium for vegetative growth for effective erosion protection and removal of water from the soil through transpiration. The thickness of the storage layer is designed such that most infiltration during “wet season” is stored in the soil until withdrawn back by evapotranspiration. Capillary barriers consist of finer-grained soil layer underlain with coarser-grained layer. The contrast in hydraulic properties between the two layers forms a capillary interface forcing water to be stored in the finer-grained layer and delaying or preventing infiltration into the underlying coarser-grained layer.

Capillary barriers also usually have a topsoil layer for plant growth and erosion protection. Figure I-2 shows the general profile of the two most commonly used evapotranspirative cap designs.

Distinct difference between RCRA Subtitle D final covers and evapotranspirative caps is the absence of geomembrane in the latter. This directly translates to significant cost reduction in landfill final cover installation. Hauser et al (2001) estimated the benefits and costs advantages for evapotranspirative caps and has shown a potential savings of 50% on landfill cover construction costs. Long-term performance of evapotranspirative caps is also anticipated as the root system of its vegetation develops through time improving slope stability in contrast with prescribed caps where slope failure has been a great concern. The inherent high cost of prescriptive caps and its uncertain long-term performance has led to initiate extensive research on evapotranspirative caps.

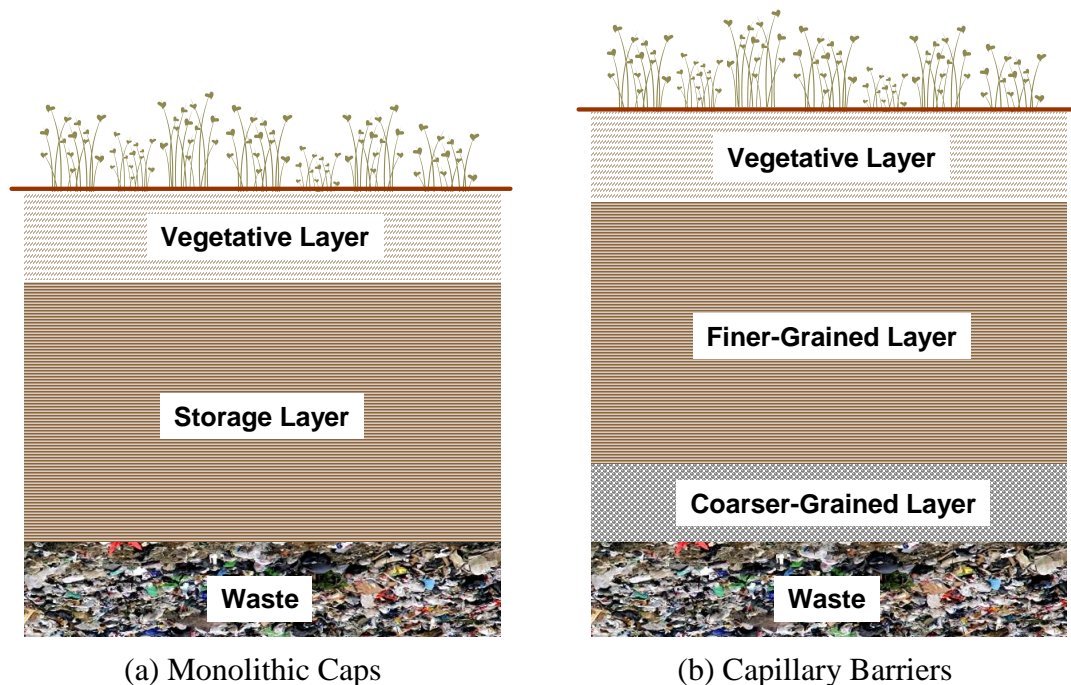


Figure I-2: Evapotranspirative caps: monolithic caps (a) and capillary barriers (b).

LYSIMETRY

As per RCRA regulations, acceptance of alternative designs including evapotranspirative caps for landfill final covers requires field demonstration to assess its performance under site-specific field conditions. Demonstration of hydraulic equivalency is usually attained when the resulting percolation rate from evapotranspirative cap is less than or equal to the percolation rate from prescribed final covers under identical field conditions (SAIC 2000).

In order to evaluate equivalent performance of evapotranspirative caps with the prescribed final covers, direct quantitative method of estimating the amount of percolated water across the landfill cap is needed (Benson et al 2001). This is typically accomplished by installing water-balance lysimeters wherein an entire cross-section of evapotranspirative cap is underlain with an impermeable geomembrane allowing collection of drainage through this bottom boundary. Key feature of a lysimeter is the ability to directly measure percolation rate and with a good precision of about 0.5 mm/yr (Benson et al. 1994; Ward and Gee 1997).

Figure I-3 shows a typical layout of a lysimeter. A high-density polyethylene geomembrane is usually used to line the lysimeter. Most lysimeters include a gravel or geosynthetic drainage layer at the soil and geomembrane interface to direct the percolation to the collection system (Benson et al. 2001). Aside from percolation measurements, lysimeters are also used to measure the changes in the soil water storage of the cap. This is accomplished either directly through weighing or monitoring the water content across the profile using water content sensors. A diversion berm is constructed along the perimeter in order to divert surface runoff from upslope of the lysimeter while

directing the surface runoff within the monitoring area to the collection system. Precipitation is usually measured at the site using a tipping bucket.

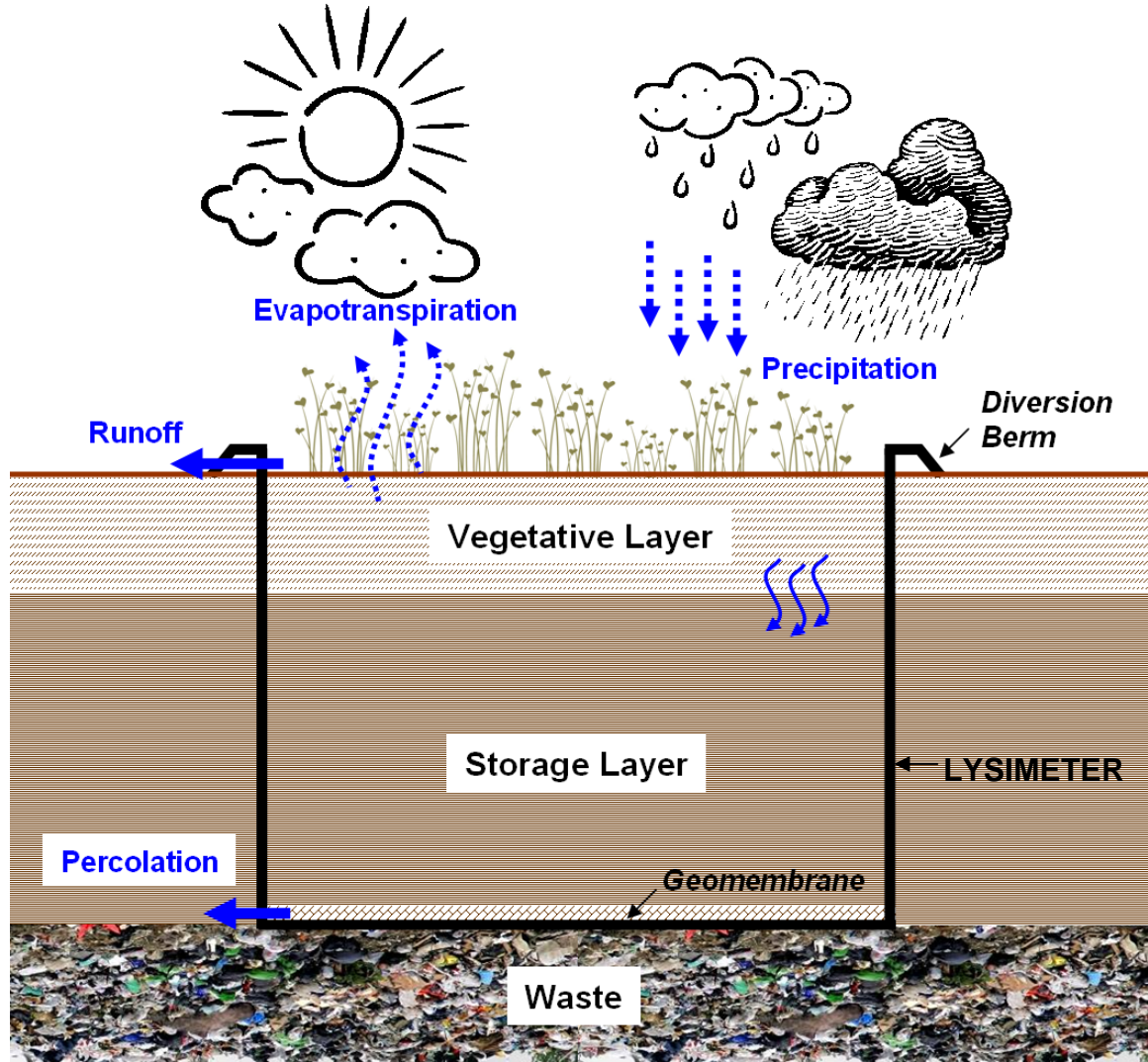


Figure I-3: Schematic of a typical lysimeter showing the water balance parameters.

Water balance of the lysimeter can be expressed as:

$$ET = P - P_r - RO - \Delta S \quad (I-1)$$

where ET is evapotranspiration, P is precipitation, P_r is percolation, RO is surface runoff, and ΔS is the change in soil water storage during a specified period of time. Hence, evapotranspiration can be estimated if precipitation, percolation, runoff and soil water storage are measured. The calculated evapotranspiration is often compared to the site-specific estimates of potential evapotranspiration to confirm the accuracy of the estimate.

Effect of Lower Boundary

The most significant disadvantage of using lysimeters to estimate percolation rate is the presence of artificial no-flow boundary induced by the hydraulic barrier at the base of the lysimeter (Abichou et al. 2006). This bottom boundary, which does not exist in an actual landfill final cover, prevents the upward and downward flux of liquid and vapor across the base of the lysimeter thereby possibly underestimating or overestimating the actual percolation rate.

Several studies have identified this concern (Benson et al. 2001; Abichou et al. 2006). However, there has been a lack of data in the literature where the effect of this artificial boundary on percolation is quantified until Khire and Mijares (2008) presented a result from numerical modeling of lysimeters versus the corresponding actual evapotranspirative caps covering a waste layer as shown in Figure I-4. Results of the numerical analyses indicated that percolation rates obtained from lysimeters are conservative by factors ranging from 2 to 10.

Lysimeter is the only available tool that directly estimates percolation through evapotranspirative caps (Benson et al. 2001; Albright et al. 2002). Hence detailed

understanding on its ability to capture actual flux on landfill covers is highly indispensable. Percolation values measured in the lysimeters need to be re-evaluated by carrying-out numerical modeling that incorporates the underlying waste for actual evapotranspirative cap scenarios (Khire and Mijares 2008).

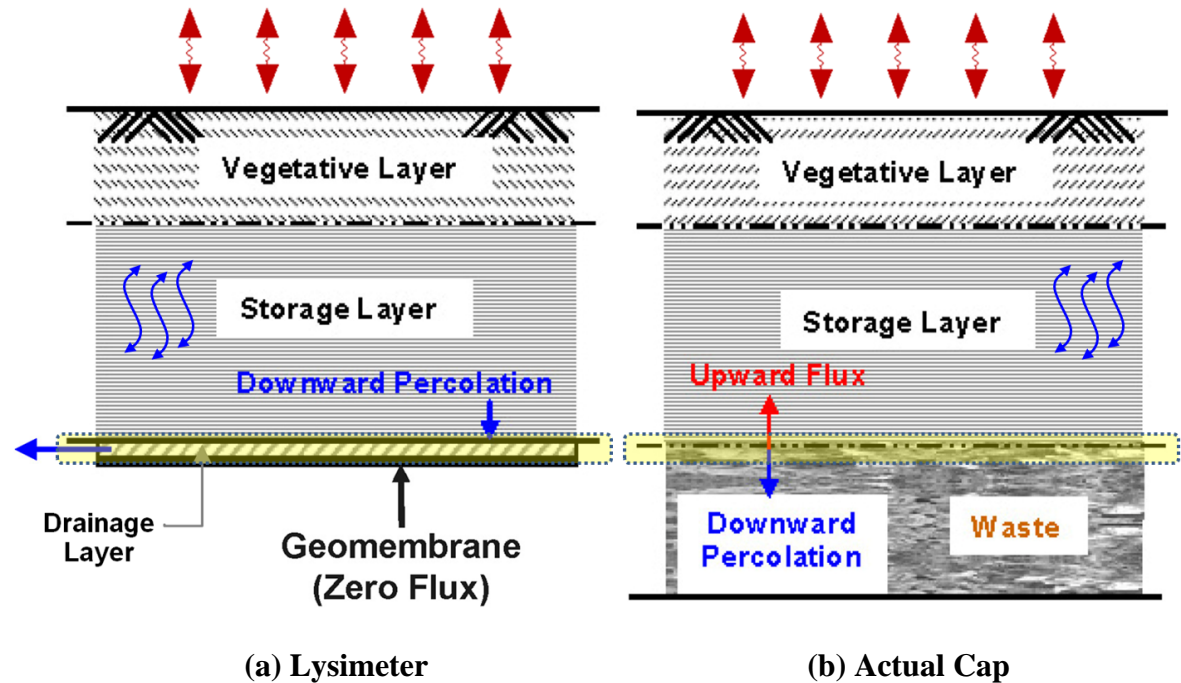


Figure I-4: Conceptual model of evapotranspirative caps consisting of lysimeter only (a); and actual cap (b) with underlying waste (Khire and Mijares 2008).

Capillary Barrier Effect

The use of a geocomposite drainage layer at the base of the lysimeter to facilitate the collection and measurement of percolated water through the earthen cap has been perceived to create a capillary barrier effect (Stormont and Morris 2000; Scanlon et al. 2005). This geocomposite drainage layer which is placed above the geomembrane that lines conventional pan lysimeter consists of a geonet sandwiched between two nonwoven

geotextiles. Published studies indicate that non-woven geotextiles have water retention function that is similar to those of coarse-textured soils such as sands and gravels creating a capillary break with the overlying fine-textured cover soil (Iryo and Rowe 2003; Park and Fleming 2006; Bathurst et al. 2007).

Benson et al. (2005) and Bohnhoff et al. (2009) investigated the effect of capillary break on percolation estimates by conducting parametric evaluation using several water balance models. They reported that regardless of the capillary break, predicted percolation was less than field measured percolation. Due to the inherent uncertainty in the field boundary condition, it is critical to identify when the presence of capillary barrier effect will be significant or minimal on the measured percolation.

NUMERICAL MODELS

Several models have been developed to simulate the water balance of earthen caps. Among these, the numerical models UNSAT-H (Fayer 2000) and VADOSE/W (Geo-Slope 2007) are among the commonly used in engineering practice for simulating water balance in saturated and unsaturated porous media (Benson 2007). In this study, these three computer models were used to simulate the hydrology of landfill earthen final covers.

Each model numerically solves a modified form of Richards' equation to estimate the flow of water through both saturated and unsaturated soil media. A one-dimensional (1-D) form of Richards' equation can be expressed as follows:

$$\frac{\partial \theta}{\partial t} = \frac{\partial}{\partial z} \left[k(\psi) \frac{\partial \psi}{\partial z} + k(\psi) \right] - S \quad (\text{I-2})$$

where θ is the volumetric water content, ψ is the matric suction head, $k(\psi)$ is the corresponding hydraulic conductivity of the porous media for a given ψ , S is the sink term, z is the vertical coordinate, and t is the time. UNSAT-H is a 1-D code that uses finite-difference scheme in solving Equation I-2. VADOSE/W is a finite-element model that can be run either under 1-D or two-dimensional (2-D) modes. These numerical models have been extensively used in simulating landfill final covers (Khire et al. 1997; Roesler et al. 2002; Benson et al. 2004; Bohnhoff et al. 2009).

The use of numerical models to predict percolation rates and compare it to measured values obtained from lysimeters has been widely considered (Khire et al. 1997; Khire et al. 2000; Albright et al. 2004; Benson et al. 2005). However it has been reported that these models failed to capture pulses of field measured percolation rates due to inability of these models to account water flow through preferential flow paths in soil (Khire et al. 1997). The formation of macrodefects or fractures on soils greatly influences the water balance parameters, especially percolation.

OBJECTIVES

The key objectives of this dissertation are to: (1) build and instrument large-scale evapotranspirative landfill final cover test sections that are capable of monitoring the difference between the hydraulic performance of a lysimeter and the corresponding actual cap (underlain by waste) under field conditions; (2) assess the capability of numerical models in predicting the water balance of an earthen cover with a vented lysimeter pan that does not use geocomposite drainage layer; (3) conduct field-scale simulations to determine the effect of the underlying landfilled waste on percolation estimates for actual

caps; and (4) determine key considerations regarding the occurrence of capillary barrier effect and its implications on percolation when using conventional pan lysimeter that use the synthetic geocomposite drainage layer.

METHODOLOGY

Field-scale evapotranspirative caps were constructed in a landfill located near Detroit, Michigan which is operated by Waste Management, Inc. Two tests sections, each having a dimension of 15 m by 30 m, were built on top of a landfill site that is scheduled for final closure. Performance monitoring for the test sections was divided into two phases: (1) uncompacted earthen cover investigation from September 2007 to September 2009; and (2) compacted earthen cover investigation from October 2009 to present.

In order to measure the net percolation across the caps, 8.5 m x 8.5 m x 0.6 m deep vented lysimeters (with provisions for pressure control) were constructed in the middle of each test section. The rest of the test section was built on an existing intermediate cover that is temporarily covering the underlying waste that was placed in the landfill cell in 1990s. The instrumented area of the test section was expanded upslope and downslope of the lysimeter to monitor the water content within and beyond the lysimeter footprint in order to assess the resulting flux between actual evapotranspirative cover and underlying waste.

Over 70 sensors consisting of time domain reflectometry-based water content and heat dissipation matric potential sensors as well as an automated meteorological station were installed at the site. Water balance parameters as well as gas pressures within the cap and the waste were monitored. The data obtained from the field investigation were

used to evaluate the hydraulic differences between a lysimeter and the corresponding actual cap. A numerical study was conducted to determine the effect of the underlying landfilled waste on percolation estimates for actual caps and the presence of capillary barrier effect introduced by the geocomposite in the drainage layer on lysimeters.

DISSERTATION ORGANIZATION

This dissertation has been organized into five sections. Each section is written as a standalone technical paper.

The first paper describes the design and construction of field-scale evapotranspirative cap test sections that were built to evaluate the difference in the hydraulic performance of a lysimeter versus actual cap (with underlying intermediate cover or waste). The unique design of these fully instrumented test sections allows comparative evaluation between the water balance of a lysimeter and actual cap under field meteorological conditions.

The second paper compares the measured water balance data obtained from the field test sections to the predictions made using the numerical models UNSAT-H and VADOSE/W. The calibrated numerical model was used to estimate the percolation across the interface between the soil cap and underlying waste.

The third paper evaluates the effect of the underlying landfilled waste on percolation estimates for actual caps. Long-term field-scale simulations using UNSAT-H were conducted to determine the correlation between the soil water storage and percolation estimates for an actual cap and its corresponding lysimeter.

The fourth paper discusses the occurrence of capillary barrier effect when using geocomposites as drainage layer at the base of the lysimeters. A numerical investigation using UNSAT-H was performed to assess capillary break over different soil types subjected to a wide range of specified fluxes. The fundamental mechanism involved when capillary barrier effect occurs was presented and several lysimeter field case studies were re-analyzed to map key factors that identify significant capillary barrier effect.

The fifth paper presents a numerical method to estimate the natural recharge in a vadose zone system using water balance models. A simple 1-D laboratory column test was conducted to verify the proposed approach.

REFERENCES

REFERENCES

- Abichou, T., Liu, X., Tawfiq, K. (2006). "Design Considerations for Lysimeters Used to Evaluate Alternative Earthen Final Covers," *Journal of Geotechnical and Geoenvironmental Engineering*, 132 (12): 1519 – 1525.
- Albright, W., Gee, G., Wilson, G., and Fayer, M. (2002). "Alternative Cover Assessment Project: Phase I Report," Publication No. 41183. Report to US EPA. Desert Research Institute, NV.
- Albright, W., Benson, C., Gee, G., Abichou, T., Roesler, A., and Rock, S. (2003), "Evaluating the Alternatives," *Civil Engineering*, 73 (1): 70-75.
- Albright, W., Benson, C., Gee, G., Roesler, A., Abichou, T., Apiwantragoon, P., Lyles, B., and Rock, S. (2004). "Field Water Balance of Landfill Final Covers," *Journal of Environmental Quality*, 33 (6): 2317-2332.
- Bathurst, R., Ho, A., and Siemens, G. (2007). "A Column Apparatus for Investigation of 1-D Unsaturated-Saturated Response of Sand-Geotextile Systems," *Geotechnical Testing Journal*, 30 (6): 1-9.
- Benson, C. (2007). "Modeling Unsaturated Flow and Atmospheric Interactions," *Theoretical and Numerical Unsaturated Soil Mechanics*, 113: 187-201.
- Benson, C. and Khire, M. (1995). "Earthen Covers for Semi-Arid and Arid Climates," *Landfill Closures*, GSP No. 53, ASCE, Reston, VA: 201-217.
- Benson, C., Bosscher, P., Lane, D., and Pliska, R. (1994). "Monitoring System for Hydrologic Evaluation of Landfill Final Covers," *Geotechnical Testing Journal*, 17 (2): 138-149.
- Benson, C., Abichou, T., Albright, W., Gee, G., and Roesler, A. (2001). "Field Evaluation of Alternative Earthen Final Covers," *International Journal of Phytoremediation*, 3 (1): 105-127.
- Benson, C., Albright, W., Roesler, A., and Abichou, T. (2002). "Evaluation of Final Cover Performance: Field Data from the Alternative Cover Assessment Program (ACAP)," *Proceedings, Waste Management 2002*, Tucson, AZ.
- Benson, C., Bohnhoff, G., Apiwantragoon, P., Ogorzalek, A., Shackelford, C., and Albright, W. (2004). "Comparison of Model Predictions and Field Data for an ET Cover," *Proceedings, Tailings and Mine Waste 2004*, Balkema, Leiden, Netherlands: 137-142.
- Benson, C., Bohnhoff, G., Ogorzalek, A., Shackelford, C., Apiwantragoon, P., and Albright, W. (2005). "Field Data and Model Predictions for an Alternative Cover," *Waste Containment and Remediation*, GSP No. 142, ASCE, Reston, VA: 1-12.

- Bohnhoff, G., Ogorzalek, A., Benson, C., Shackelford, C., and Apiwantragoon, P. (2009). "Field Data and Water-Balance Predictions for a Monolithic Cover in a Semiarid Climate," *Journal of Geotechnical and Geoenvironmental Engineering*, 135 (3): 333–348.
- EPA. (1992). "Subtitle D Clarification." 40 CFR 257 and 258. Federal Register.
- EPA. (1995). "Decision Maker's Guide to Solid Waste Management, Volume II," EPA 530-R-95-023.
- EPA. (2007). "Municipal Solid Waste Generation, Recycling, and Disposal in the United States: Facts and Figures for 2006," EPA 530-F-07-030.
- Fayer, M. (2000). "UNSAT-H Version 3.0: Unsaturated Soil Water and Heat Flow Model – Theory, User Manual, and Examples." PNNL-13249, Pacific Northwest Laboratories, Richland, Washington.
- Geo-Slope. (2007). "Vadose Zone Modeling with VADOSE/W 2007: An Engineering Methodology," Geo-Slope International Ltd, Alberta, Canada.
- Hauser, V. L., Weand B. L., and Gill, M. D. (2001). "Natural Covers for Landfills and Buried Waste," *Journal of Environmental Engineering*, 127 (9): 768-775.
- Iryo, T., and Rowe, R. (2003). "On the Hydraulic Behavior of Unsaturated Nonwoven Geotextiles," *Geotextiles and Geomembranes*, 21: 381-404.
- Khire, M., and Mijares, R., 2008, "Influence of the Waste Layer on Percolation Estimates for Earthen Caps Located in a Sub-humid Climate," *Proceedings, GeoCongress 2008*, GSP No. 177, Geotechnics of Waste Management and Remediation, ASCE, Reston, VA: 88-95.
- Khire, M., Benson, C., and Bosscher, P. (1997). "Water Balance Modeling of Earthen Final Covers," *Journal of Geotechnical and Geoenvironmental Engineering*, 123 (8): 744-754.
- Khire, M., Benson, C., and Bosscher, P. (1999). "Field Data From a Capillary Barrier and Model Predictions with UNSAT-H," *Journal of Geotechnical and Geoenvironmental Engineering*, 125: 518–528.
- Khire, M., Benson, C., and Bosscher, P. (2000). "Capillary Barriers: Design Variables and Water Balance," *Journal of Geotechnical and Geoenvironmental Engineering*, 126 (8): 695-708.
- MDE. (2003). "Estimated Costs of Landfill Closure Fact Sheet," Maryland Department of the Environment, Baltimore, MD.

- Nyhan, J., Schofield, T., and Starmer, R. (1997). "A Water Balance Study of Four Landfill Cover Designs Varying in Slope for Semi-Arid Region," *Journal of Environmental Quality*, 26: 1385-1392.
- Park, K., and Fleming, I. (2006). "Evaluation of a Geosynthetic Capillary Barrier," *Geotextiles and Geomembranes*, 24: 64-71.
- Roesler, A., Benson, C., and Albright, W. (2002). "Field Hydrology and Model Predictions for Final Covers in the Alternative Assessment Program – 2002," Geo-Engineering Report 02-08. University of Wisconsin, Madison.
- SAIC. (2000). "Quality Assurance Project Plan, Alternative Cover Assessment Project," Science Applications International Corporation, Report to USEPA Contract No. 68-C5-0036.
- Scanlon, B., Reedy, R., Keese, K., and Dwyer, S. (2005). "Evaluation of Evapotranspiration Covers for Waste Containment in Arid and Semiarid Regions in the Southwestern USA," *Vadose Zone Journal*, 4: 55-71.
- Stormont, J. and Morris, C. (1998). "Method to Estimate Water Storage Capacity of Capillary Barriers," *Journal of Geotechnical and Geoenvironmental Engineering*, 124 (4): 297 – 302.
- Stormont, J., and Morris, C. (2000). "Characterization of Unsaturated Nonwoven Geotextiles," *Proceedings, Geo-Denver 2000*, GSP No. 99, Advances in Unsaturated Geotechnics, ASCE, Reston, VA: 153–164.
- Ward, A. and Gee, G. (1997). "Performance Evaluation of a Field-Scale Surface Barrier," *Journal of Environmental Quality*, 26: 694-705.

PAPER NO. 1: FIELD-SCALE EVALUATION OF LYSIMETERS VERSUS ACTUAL EARTHEN COVERS

ABSTRACT

This paper presents the design, construction, and monitoring of two uncompacted and one compacted clay field-scale test sections that were built and instrumented at a landfill near Detroit (Michigan) to capture the differences in the hydraulic and hydrologic responses of actual caps overlying the municipal solid waste (MSW) versus the corresponding lysimeters. While the lysimeter pans were installed in the middle of each of the three test sections to measure percolation, the instrumented area of the test section was expanded upslope and downslope of the lysimeter to evaluate the effect of the lower boundary. About 35 sensors were installed in each of the three test sections to monitor water contents, water potentials, soil temperatures, water levels, and gas pressures. The soil water storages for the uncompacted test sections that were underlain by the waste were typically greater than those for the corresponding lysimeters. However, for the compacted test section, there was no significant difference between the soil water storage for the actual cap and the lysimeter. The percolation for the compacted clay test section was about few millimeters per year versus it was in tens of centimeters for the uncompacted test sections due to about two orders greater field hydraulic conductivities. The field data collected in this project validates previously published numerical results regarding hydraulic differences in lysimeters versus actual caps.

INTRODUCTION

Earthen covers, or evapotranspirative (ET) caps, or ET final covers are synonyms for alternative form of final covers that have been permitted in the U.S. for municipal solid waste (MSW) landfills during the last two decades. Field-scale hydrologic evaluation of ET covers requires direct or indirect method of quantifying percolation through the soil covers. For direct quantification, it is typically accomplished by installing water-balance lysimeters where the earthen cap is underlain by a drainage layer which is underlain by an impermeable geomembrane to facilitate the collection of all percolation through the bottom boundary. Key feature of a lysimeter is the ability to directly measure percolation rate with a precision of about 0.5 mm/yr (Benson et al. 1994; Ward and Gee 1997; Albright et al. 2002).

Lysimeter studies have been performed since the end of the 17th century (Seiler and Gat 2007). In the past, lysimeters are generally constructed using deep cylindrical pots with an open surface area of about 1 m^2 . These cylindrical lysimeters were typically used for estimating groundwater recharge and were mechanically balanced to accurately measure fluctuations in soil water storage and measure the deep percolation. For landfill final cover application, pan lysimeters are more common. These lysimeters have much larger surface area to capture the field-scale heterogeneities such as soil macropores and fractures (Benson et al. 1994; Khire et al. 1997).

Changes in the soil water storage are determined by installing water content sensors to monitor the water content across the soil cover profile. A diversion berm is usually placed around the perimeter of the lysimeter in order to divert surface runoff from

upslope of the lysimeter while directing the surface runoff within the lysimeter to the collection system. Water balance of pan lysimeter can be expressed using Equation 1-1.

$$ET = P - P_r - RO - \Delta S \quad (1-1)$$

where ET is evapotranspiration, P is precipitation, P_r is percolation, RO is surface runoff, and ΔS is the change in the soil water storage during a specified period of time. ET is estimated if all other parameters in Equation 1-1 are measured. The estimated ET is then compared from site-specific estimates of potential and actual ET.

While a lysimeter allows measurement of percolation through the test section, it is important to evaluate the magnitude of percolation from a lysimeter versus through the actual cover constructed on the waste surface. The lower boundary of a lysimeter is a zero flux boundary with lateral drainage occurring through a geocomposite or gravel drainage layer (Khire et al. 1997; Abichou et al. 2006). The bottom boundary in an actual landfill final cover allows upward and downward flux of liquid, vapor and heat across the interface of the waste (Khire and Mijares 2008). Hence, even though lysimeters represent one of the best means of measuring percolation through a soil cover, it alters the hydraulics and hydrology of the system.

Khire and Mijares (2008) carried out numerical modeling of lysimeters versus the corresponding actual earthen caps placed on a waste layer using the 2-D water balance model Vadose/W (Geo-Slope 2007). Results from this numerical study indicate that percolation rates obtained from lysimeters are greater than those for earthen caps that are

underlain by MSW. Mijares et al. (2010) illustrated numerically that the soil water storage for lysimeters is typically less than that for earthen caps that are underlain by MSW and that greater soil water storage capacity corresponds to a lower percolation rate. Because regulations often require percolation to be relatively small, it is critical to evaluate the equivalency of percolation measured by a lysimeter to an equivalent cap that is underlain by MSW. Geo-Slope (2007), Bews et al. (1997), and Parent et al. (2006) have presented numerical results of lysimeters and the effect of depth of lysimeter pan on the percolation measured by lysimeter. Geo-Slope (2007) study is based on fixed infiltration upper boundary. In addition, the lysimeter simulated in Geo-Slope (2007) is horizontal. The field study presented in this paper focuses on inclined lysimeter which had atmospheric boundary (transient flux).

OBJECTIVE

The key objective of the field study presented in this paper is to assess the hydraulic and hydrologic differences between an actual cap and the corresponding lysimeter. In order to meet the objective, three earthen cap test sections were instrumented and field data was collected for a period ranging from one to three years.

DESIGN AND CONSTRUCTION OF TEST SECTIONS

Field-scale ET caps were constructed at a landfill located near Detroit, Michigan. The landfill site is situated in a sub-humid climate where the average annual precipitation is approximately 84 cm and potential evaporation to precipitation ratio (PE/P) is about 1.2. Two tests sections, each 15 m wide by 30 m long, were built on the westward facing side

slope of the landfill. Performance monitoring for the test sections was divided into two phases: (1) uncompacted earthen cover investigation from September 2007 to September 2009; and (2) compacted earthen cover investigation from October 2009 to present. To construct the test sections that represent an ET final cover for the site, native glacial till soils (USCS Classification: CL) were used for constructing the soil water storage layer.

The Phase 1 construction and monitoring consisted of assessing the earthen caps under a scenario where the native clay was not compacted. The reason the test sections were not compacted was to simulate a conservative scenario for higher overall hydraulic conductivity of the storage layer of the cap, potentially resulting in less increase or no increase in the overall hydraulic conductivity of the clay due to root penetration and desiccation. In addition, to enhance ET from the test sections by providing more pore space for the plant roots to reach greater depths quickly in the test sections. The Phase 2 consisted of constructing and evaluating a test section that was compacted at dry of optimum water contents to reduce the overall hydraulic conductivity of the cap which is the typical practice for covers designed as hydraulic barriers.

Test Section Layout

During the Phase 1, which was completed in September 2007, two 15 m by 30 m field test sections were constructed side-by-side on a landfill side slope. These dimensions were selected based on previous field studies which indicated that these dimensions are large enough to capture the field-scale effects (Khire et al. 1997; Albright et al. 2002). Average slope in the area is about 1V to 6H consisting of an existing intermediate cover that was placed in the landfill cell in 1990s. One test section was located on the north side

and the other on the south side. In the Phase 2, during October 2009, the north test section was excavated and removed and a new compacted test section was constructed and instrumented. However, the south test section constructed in the Phase 1 is still being monitored. The north and south test sections constructed in the Phase 1 consisted of 1.0 m and 1.5 m thick uncompacted native clay cover overlain with a 0.3-m thick topsoil layer, respectively. In Phase 2, the new north test section was constructed using 1.5-m thick compacted native clay overlain with a 0.3-m thick topsoil layer.

Figure 1-1 shows the typical cross-section of the instrumented test sections illustrating the relative locations of the sensor nests including the lysimeter pan. The lysimeter consisted of a trapezoidal excavation in the middle of each of the test sections having plan view dimensions of about 8.5 m x 8.5 m x 0.6 m deep. As shown in Figure 1-1, the instrumented area of the test section was expanded upslope and downslope of the lysimeter to monitor the water contents, water potentials, and soil temperatures within and beyond the lysimeter footprint to assess and compare the hydrologic response of the lysimeter versus the actual earthen cap placed on the underlying waste.

Test Section Construction

Construction of the uncompacted field test sections was undertaken from August to September 2007. The construction began with excavating and scraping off the intermediate cover followed by the installation of pan lysimeter in the middle of each of the test sections. The clay cover was placed using a track dozer to build the earthen cap. The clay lift thickness was 30 cm. A specialized company was subcontracted to install

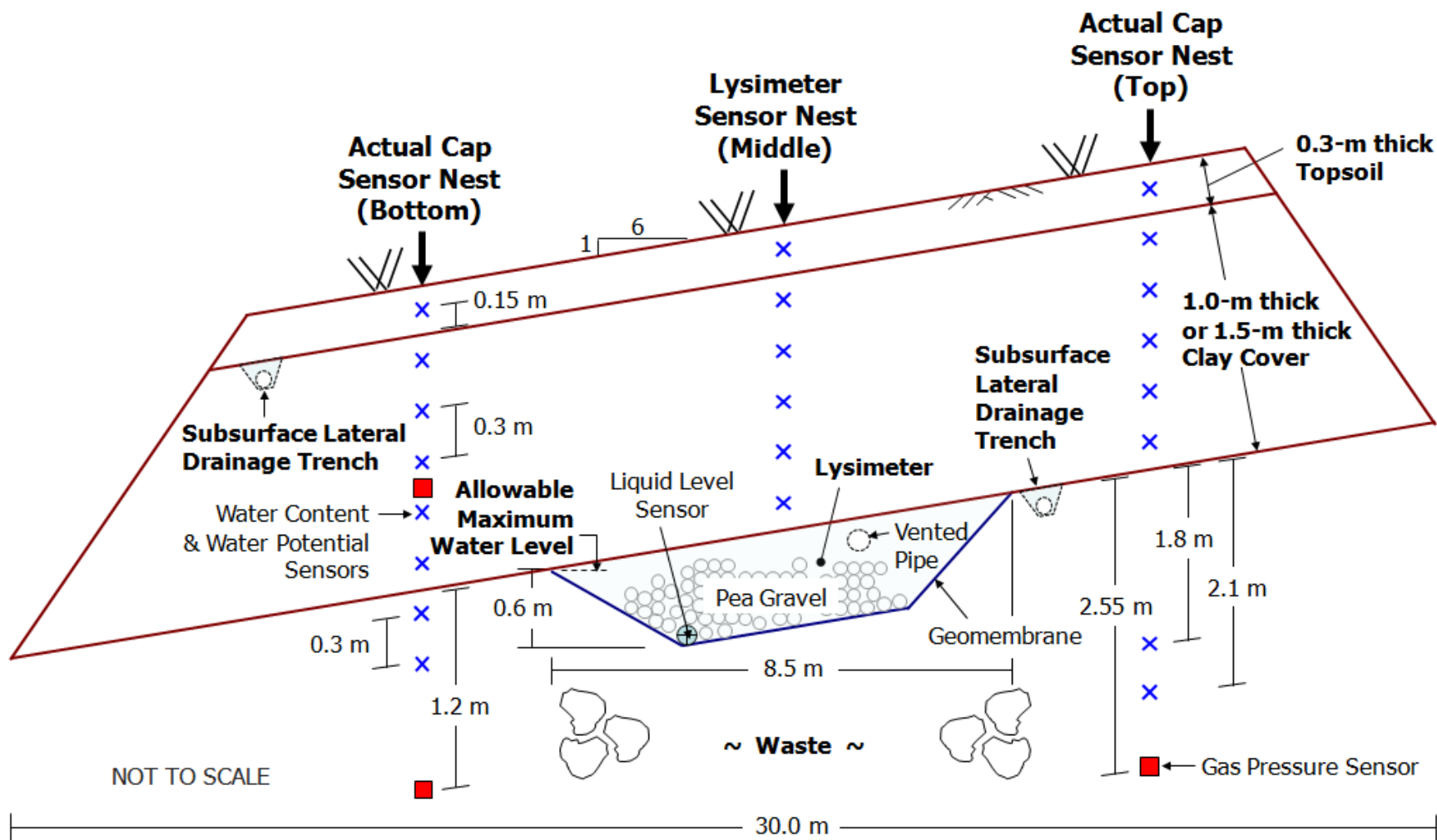


Figure 1-1: Typical cross-section of instrumented three field test sections.

sensors in the MSW underlying the top and bottom sensor nests as shown in Figure 1-1. The entire test section was seeded with native grass seeds to promote vegetation growth for erosion protection and to enhance ET. A 1.5 m deep diversion trench was constructed upslope of the test sections to divert surface runoff from uphill.

In the Phase 2, during October 2009, the north test section was excavated and removed and a new compacted test section was constructed and instrumented.

Lysimeter Installation

In order to directly measure percolation, an 8.5 m by 8.5 m lysimeter pan with an average depth of 0.6 m was installed in the middle of each of the three test sections (Figure 1-1). The lysimeter was lined using a geosynthetic clay liner (GCL) overlain by a 1.5 mm thick high-density polyethylene (HDPE) geomembrane. The lysimeter pan was filled with clean pea gravel having an average hydraulic conductivity equal to 1 cm/s. An insect mesh made up of polymer having an average opening size of 1 mm was placed on the top of the gravel surface before the clay was placed to minimize the intrusion of fines into the lysimeter. A perforated 7.5 cm diameter HDPE pipe was installed in the upper 10 cm of the pea gravel and vented to the atmosphere to create a vented drainage boundary (Figure 1-1). This boundary can be subjected to a fixed or variable pressure (or suction) to create other boundary condition effects for future research studies. During the phases of the study presented in this paper, the upper boundary of the gravel layer was at atmospheric pressure. The lower boundary was impermeable to allow collection and monitoring of percolation. Mijares et al. (2010) carried out numerical modeling of the lysimeters using UNSAT-H and Vadose/W and showed that while the pea gravel

drainage layer theoretically could act as a capillary break, practically, it did not perform as a capillary break.

Quantity of water percolated through the cap directly above the lysimeter has been measured by a water level transducer placed at the bottom of each lysimeters as shown in Figure 1-1. A 30 cm long time domain reflectometry (TDR) water content sensor was vertically placed in the gravel next to the water level transducer to have a back-up measurement of the water level for data verification. Another water level transducer and a TDR water content sensor were installed about halfway upslope within the lysimeter. The lower water level sensor was placed inside a 10 cm diameter HDPE perforated HDPE pipe placed at the bottom of the lysimeter pan which ran across the entire width (8.5 m) of the lysimeter. A set of two 1 cm diameter flexible HDPE tubing was placed in the conduit to pump the drainage collected in the lysimeter.

Soil Placement

Native clay (CL) was used to construct the earthen cover test sections and was obtained from on-site borrow pits. During Phase 1, the soil was placed with minimal compaction effort using a track dozer at its natural water content of about 10%. The clay was placed in 30 cm thick lifts. Soil samples were collected for further laboratory testing and characterization. Table 1 shows the physical properties of the soils used for the test sections. Low plasticity clay was used for the soil water storage/hydraulic barrier layer in the soil cover whereas low plasticity silt was used for the topsoil layer. The hydraulic conductivity of the uncompacted clay was measured in the field using a 1 m by 1 m single-ring infiltrometer (ASTM D5126; Guyonnet et al. 2000) and the average value of

the conductivity is 10^{-4} cm/s. The water contents and dry unit weights of the uncompacted clay were measured in the field using Shelby tube samples collected from the various lifts (Figure 1-2). The dry unit weight of the uncompacted clay was about 85% of the maximum dry unit weight for the Standard Proctor effort.

Table 1-1: Properties of cover soils used in the test sections.

Property	Topsoil	Storage Layer (Native Glacial Till)
USCS Classification	ML	CL
D ₁₀ (mm)	0.00092	0.00020
D ₅₀ (mm)	0.070	0.0065
D ₆₀ (mm)	0.091	0.014
Cu	99	70
Cu	11	0.70
Liquid Limit (LL)	25	29
Plasticity Index (PI)	3	13
Optimum Water Content (%) for Standard Proctor Effort	15.7	13.4
Maximum Dry Unit Weight (kN/m ³) for Standard Proctor Effort	17.4	18.5
Hydraulic Conductivity (cm/s) – Uncompacted Test Sections	1×10^{-4} (Lab)	1×10^{-4} (Field)
Hydraulic Conductivity (cm/s) – Compacted Test Sections	1×10^{-4} (Lab)	2×10^{-7} (Lab) 1×10^{-6} (Field)

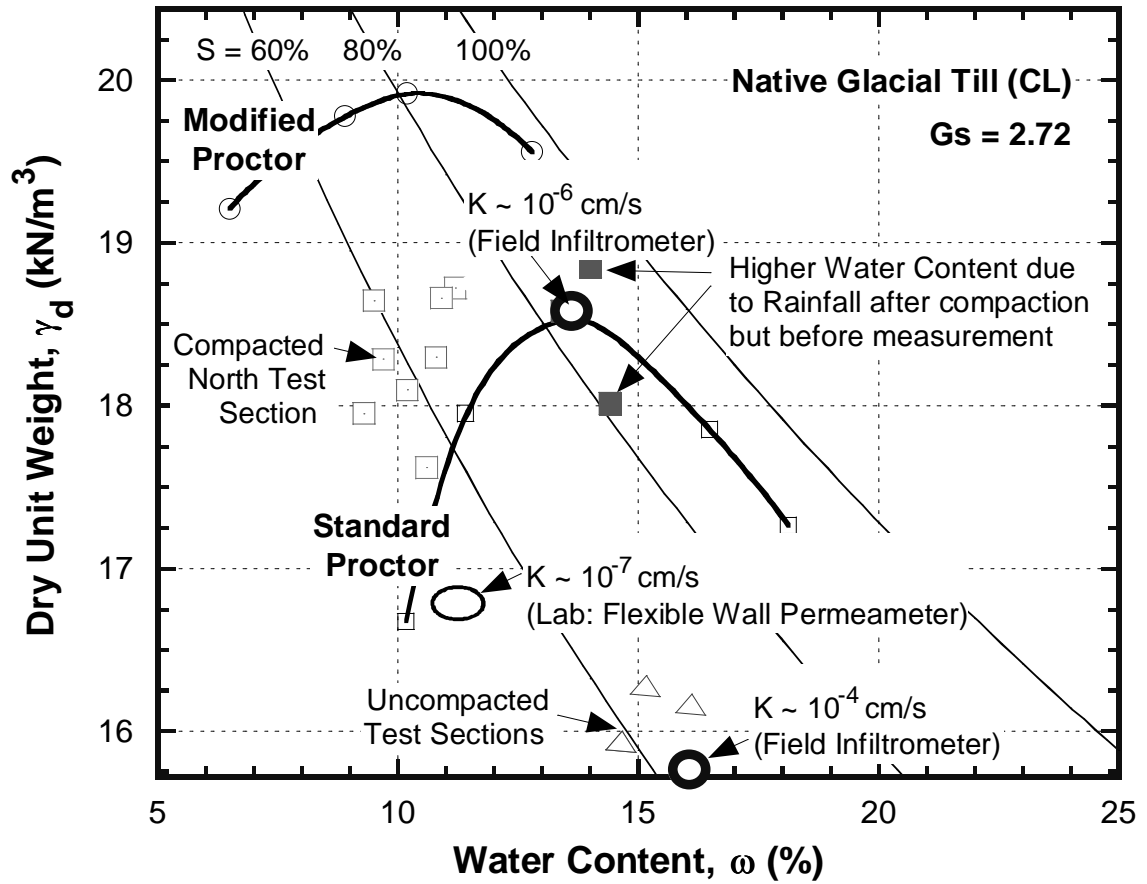


Figure 1-2: Proctor compaction curves and field water contents and unit weights.

For Phase 2, where a compacted clay cover was constructed, the clay from the same borrow area was used to build the test section. The clay lifts were compacted using a sheepfoot compactor at the dry of optimum water content. The clay was compacted in 30-cm thick lifts. The water content and dry unit weight of the compacted clay was measured using a nuclear gauge (Figure 1-2). The field water contents, on average, are about 4% dry of the optimum water content. The field dry unit weights, on average, are about 98% of the maximum dry unit weight for the Standard Proctor effort. The average hydraulic conductivity measured using 10 cm diameter sample in a flexible wall

permeameter was 2.2×10^{-7} cm/s (ASTM D5084). The hydraulic conductivity of the compacted clay was also measured in the field using a 1 m by 1 m single-ring infiltrometer and the average value of the conductivity is 10^{-6} cm/s. The field conductivity is representative of the test sections because the size of the clay sampled is larger than the size of the clay clods observed in the field. A 30 cm thick topsoil layer consisting of uncompacted silt was placed on top of the compacted clay using a track dozer and seeded to grow native grass and shrubs.

Pump Set-up

A pumping system was installed at the site for the removal of percolated water that was collected by the lysimeter pan. A 0.5-hp self-priming utility pump was attached to the drainage tubes that extended from the lowest point in the lysimeter pan (Figure 1-1). The lower boundary of the lysimeter was impermeable to collect and store the percolation until it was pumped. The upper boundary of the gravel layer was vented to the atmosphere to maintain atmospheric pressure on the lysimeter pan which is consistent with previous lysimeter studies. A check valve was used at the inlet port of the pump to maintain sufficient amount of water inside the pump for self priming. The pumps discharged outside and below the catchment of the monitoring area.

The pump was controlled remotely using an electrical relay switch which was turned on or off based on the level of water in the lysimeter pan. The lysimeter was not allowed to overflow by monitoring the water level in the lysimeter on a weekly basis based on the readings continuously recorded by the datalogger for all the sensors at 30-min interval over a period that ranged from 1 to 3 years for the three test sections.

INSTRUMENTATION

Instrumentation at the site consisted of two weather stations and sensors to monitor in-situ volumetric water contents, soil water potentials, temperatures, gas pressures, and water levels of percolated water in the lysimeter pans. Figure 1-3 illustrates the comparison of the measured precipitations from the two on-site weather stations and a weather station located about 15 km from the site that is monitored by National Oceanic and Atmospheric Administration (NOAA) which also included the snow measurements.

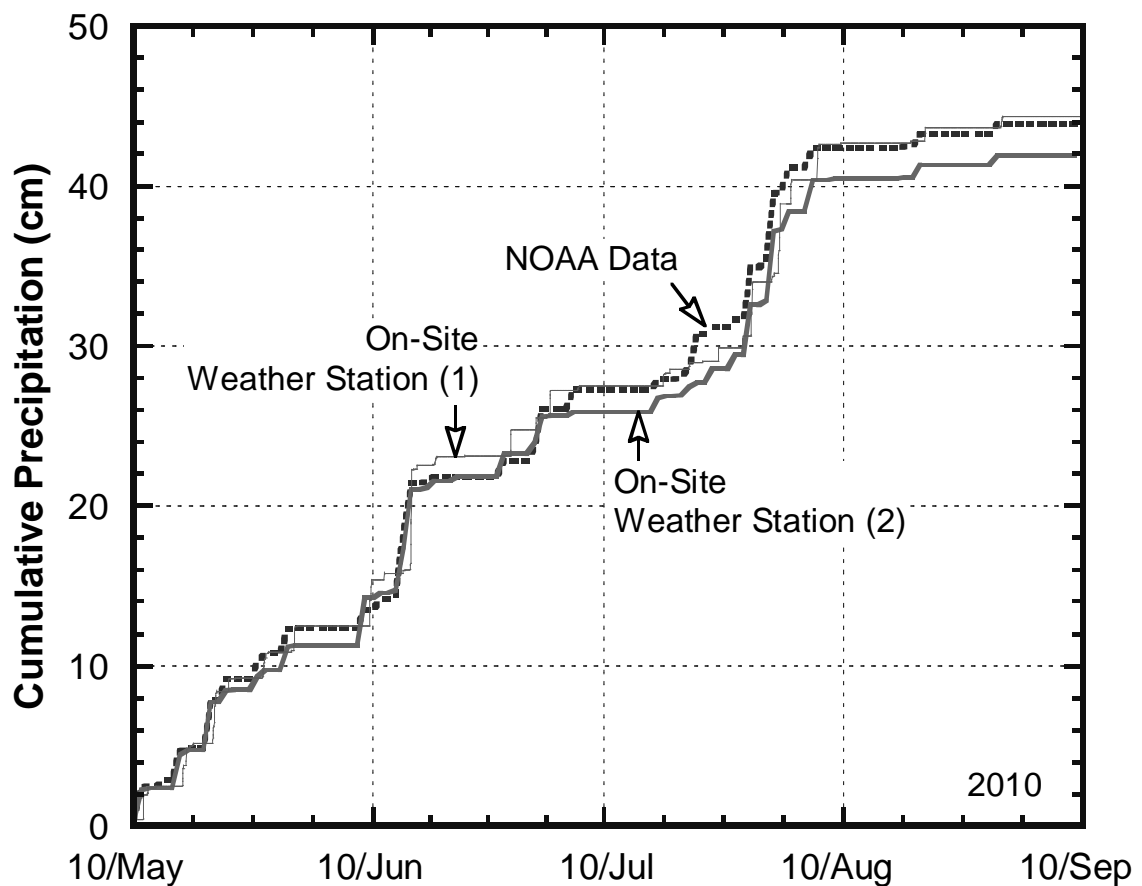


Figure 1-3: Comparison between on-site and NOAA recorded precipitation.

Nests of sensors were installed upslope and downslope of the lysimeter pans in all test sections as shown in Figure 1-1. The instrumentation also extended into the underlying MSW to about 4.4 m depths below the earthen caps. The weather stations recorded: hourly precipitation and air temperatures, barometric pressures, relative humidity, wind speed, and solar radiation. The data was recorded using a datalogger installed at the site which was accessed remotely using a wireless modem.

Water Level and Pressure Transducers

Pressure transducers were used to measure the water level in the lysimeter pans. The pressure transducers are made by Keller (Model No. CS431). These sensors have a measurement range of 0 to 90 cm with 0.1% accuracy. Similar transducers rated for a higher pressure of up to 105 kPa were used to monitor the gas pressures in the cap and the underlying MSW. These sensors are 8.5 cm long and have a diameter of 1.2 cm. The sensor provides a temperature-compensated analog output proportional to the ambient pressure or the water level above the transducer. It also consists of a 2-mm diameter vent tube that connects the hollow chamber behind the diaphragm to the atmosphere, therefore requiring no barometric pressure compensation. A thermistor is embedded within the transducer to measure ambient temperature to correct errors in the vibrating wire measurement caused by the changes in the temperature. Prior to installation in the field, the pressure transducers were calibrated and tested for accuracy.

Water Content Sensors

Volumetric water contents were measured using time domain reflectometers manufactured by Campbell Scientific (Model CS 616). The sensor consisted of two stainless steel rods, each 30 cm long with a diameter of 3.2 mm spaced 3.2 cm apart. A calibration curve was developed for the soils used to build the test sections as well as for the MSW that existed below the test sections. Equation 1-2 presents the calibration equation that converts the time period, x (μ s) measured by the water content reflectometer to the volumetric water content (θ) of the clay (CL) used as the storage layer.

$$\theta = 3.86\text{E-}05x^3 - 2.55\text{E-}03x^2 + 6.89\text{E-}02x - 6.15\text{E-}01 \quad (1-2)$$

Accuracy of the field measured water contents using the water content reflectometers were checked from time to time by collecting soil samples from various depths within the test sections which included the topsoil as well as the underlying clay. The destructive samples were collected from outside the footprint of the lysimeter or at least 8 m away from any instrumentation to minimize any influence on the long-term measurements. Figure 1-4 shows the water content profile obtained from the samples collected in the field (October 2009) compared to the water content profile obtained using the in-situ water content reflectometers at the time of the physical sampling. The calibrated water contents measured by the sensors closely match the field measurements using Shelby tube samples. Equation 1-3 presents the calibration equation that converts

the time period, x (μ s) measured by the water content reflectometer to the volumetric water content (θ) of MSW that was sampled from below the test sections.

$$\theta = (47.58 - 1.04x)^{-0.83} \quad (1-3)$$

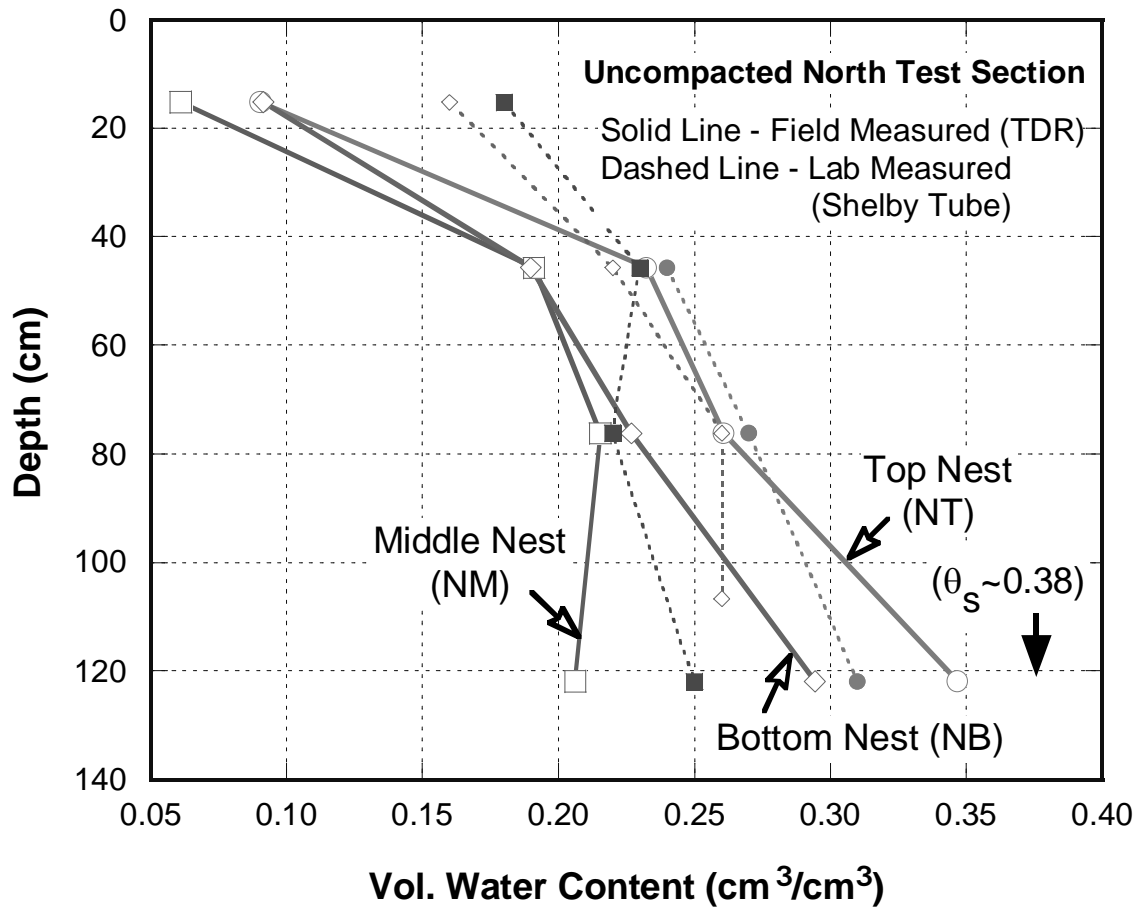


Figure 1-4: Water contents measured in the field using water content reflectometers versus using Shelby tube samples.

Soil Suction and Temperature Sensors

Heat dissipation matric potential (HDMP) sensors were used to measure the soil water potential in the field. The sensor is manufactured by Campbell Scientific and has a model

number 229-L. The sensor consists of a cylindrical-shaped porous ceramic matrix with heating element and a thermocouple embedded in its center. Hence, it also measures soil temperature. The total length of the sensor is 6 cm and it has a diameter of 1.5 cm. Soil water potential is indirectly determined using heat dissipation. The sensor is gradually heated for a fixed time period by applying a current to the heating element and the increase in temperature is measured by the thermocouple. The magnitude of the temperature rise represents the heat that is not dissipated and is controlled by the water content of the porous ceramic matrix, which changes as the surrounding soil wets and dries, because water conducts heat more readily than air or vacuum.

Soil water potentials ranging from -2500 to -10 kPa can be captured using these sensors. The air entry pressure of the sensor is about -10 kPa and therefore it cannot measure potentials above this value because the matrix remains saturated until it reaches the air entry value. Because of variability of heat transfer properties among sensors, all heat dissipation sensors used in the field were calibrated individually before they were deployed in the field. The procedure is presented by Flint et al. (2002). A thermistor sensor that looks similar to a pencil was inserted in the ground surface of each of the test sections to monitor the ground freeze and thaw.

Percolation Monitoring

Percolation collected by the lysimeter pan installed in the middle of each of the three test sections was monitored by measuring the depth of water. Water levels were measured directly using two pressure transducers and indirectly using 30 cm long time domain reflectometers placed vertically next to the pressure transducers. Thus, the upper TDR

water content sensor was placed in the upper 30 cm of the gravel drainage layer which was in direct contact with the clay soil of the ET covers.

Figure 1-5 shows the calibration curve for estimating the lysimeter percolation from the depth of water ponded in the lysimeter pan. Figure 1-5 also shows the equivalent volume of water in the lysimeter as a function of the measured water level. The calibration curve was determined from volumes estimated for specific water levels using the as-built dimensions and layout of the lysimeter pan. This has been verified during pumping events wherein the water outflow rates that were independently measured are compared with the estimated rate of decrease in the volume of water stored in the

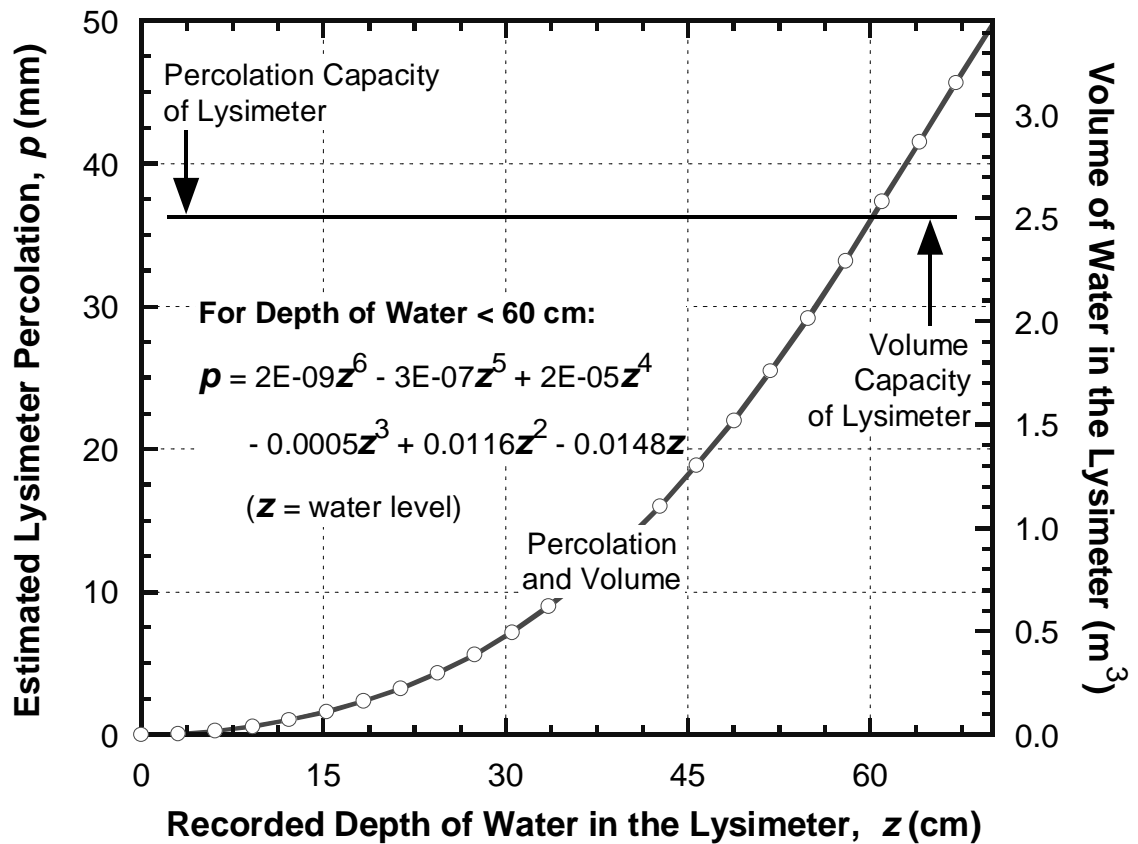


Figure 1-5: Lysimeter water level, volume, and percolation relations.

lysimeter pan. The maximum water level in the lysimeter before the lysimeter would overflow is 60 cm. At the maximum water level, the corresponding maximum percolation that can be recorded is about 35 mm or 2.5 m^3 . Thus, about 1 cm rise in the water level correspond to about 0.5 mm percolation.

Figure 1-6 shows the use of TDR sensors to indirectly monitor and confirm the water level in the lysimeters. Figure 1-6 shows that the water content versus the water level relationship is close to linear. While the water content readings recorded by the TDR sensors installed in the gravel drainage layer of the lysimeters were never used to

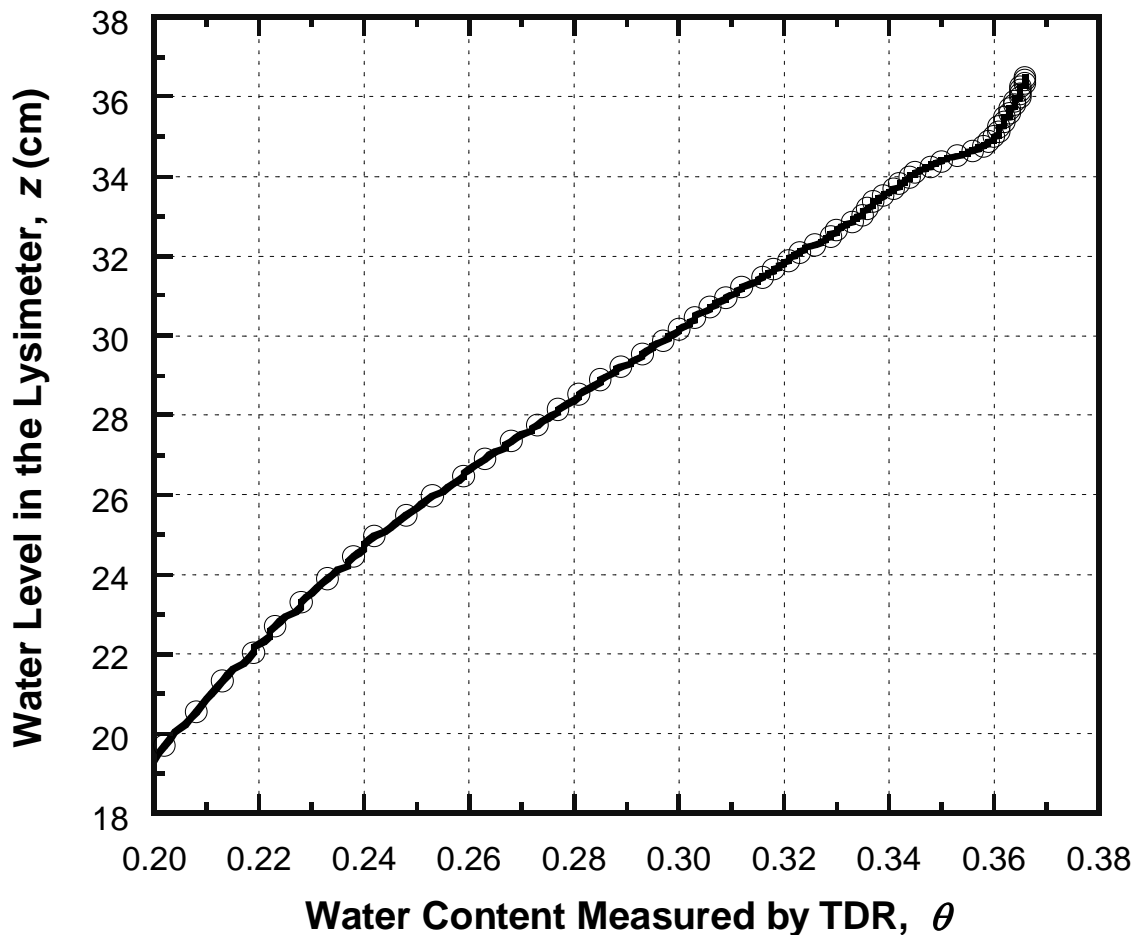


Figure 1-6: TDR and water level sensor correlation.

estimate the quantity of percolation, the data served as an independent check on water levels monitored by the pressure transducers. The pressure transducer readings coupled with outflow measurements were used to monitor percolation.

RESULTS AND DISCUSSION

Soil Temperatures

Figure 1-7 presents an example of seasonal variation of soil temperatures observed across the uncompacted south test section. The plot shows the values measured by the temperature probe placed on the ground surface as well as the built-in thermistor in heat

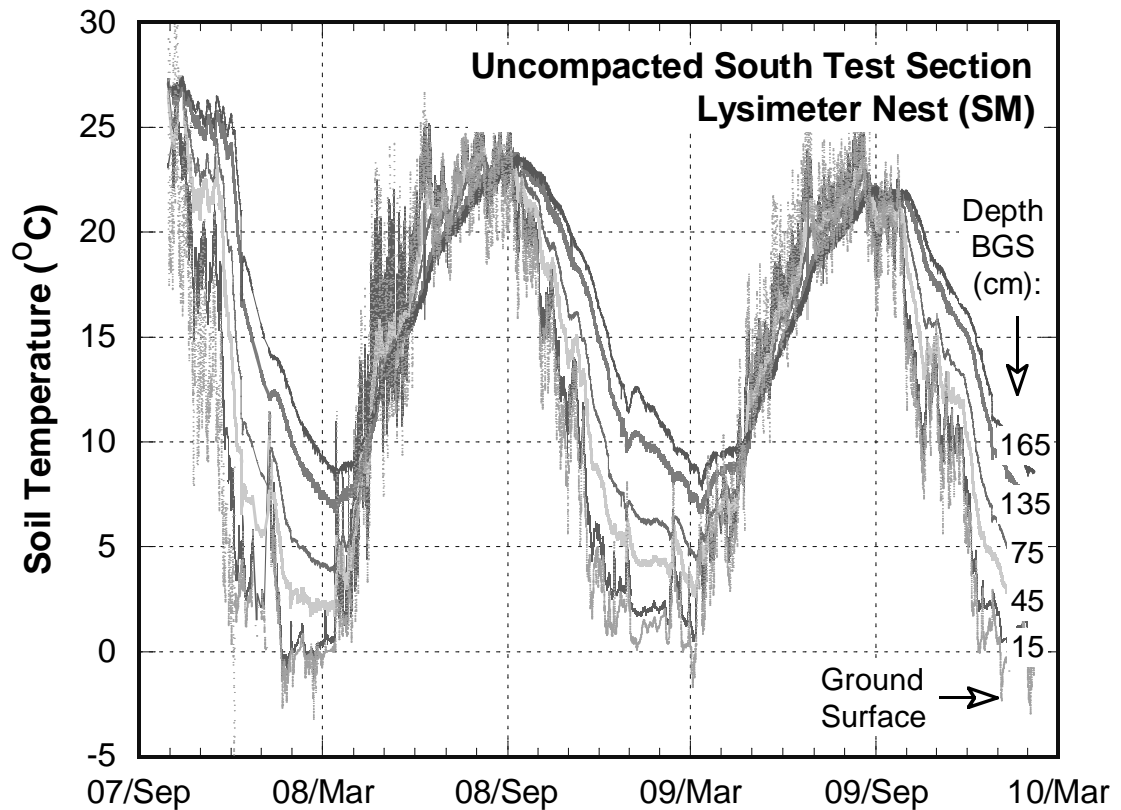


Figure 1-7: Seasonal temperature variation across the test sections.

dissipation matric water potential sensors installed at various depths at the middle nest of the uncompacted south test section. The expected trend is evident in the data wherein the soil temperature drops during winter and peaks during summer. It can also be seen that the soil temperature on the ground surface fluctuates significantly since it is directly exposed to atmospheric condition. On the other hand, the soil temperatures at succeeding depths show successive damping of fluctuations. This pattern is also observed for the other nests of sensors from both test sections.

Soil Water Storage

Phase 1: Uncompacted North and South Test Sections

Soil water storage of all three test sections (Phases 1 and 2) was calculated by integrating the recorded volumetric water contents across the profile using the 30-min readings. Figure 1-8 presents the measured soil water storages obtained from the sensor nests placed within the lysimeters versus upslope and downslope of the lysimeters constructed during the Phase 1. Percolation was measured for the middle nest of sensors which was installed above the lysimeter pan.

Figure 1-8(a) shows that, generally, the soil water storages for the portions of the test sections that are placed on the MSW (NT, ST, NB) are greater than those for the portions placed above the lysimeters (NM and SM). For the uncompacted north test section, the average soil water storage for the lysimeter nest (NM) was 31.2 cm whereas the storages were 40.3 cm and 33.1 cm for the top (NT) and bottom (NB) nests, respectively, that were placed in the portions of the test sections which were underlain by

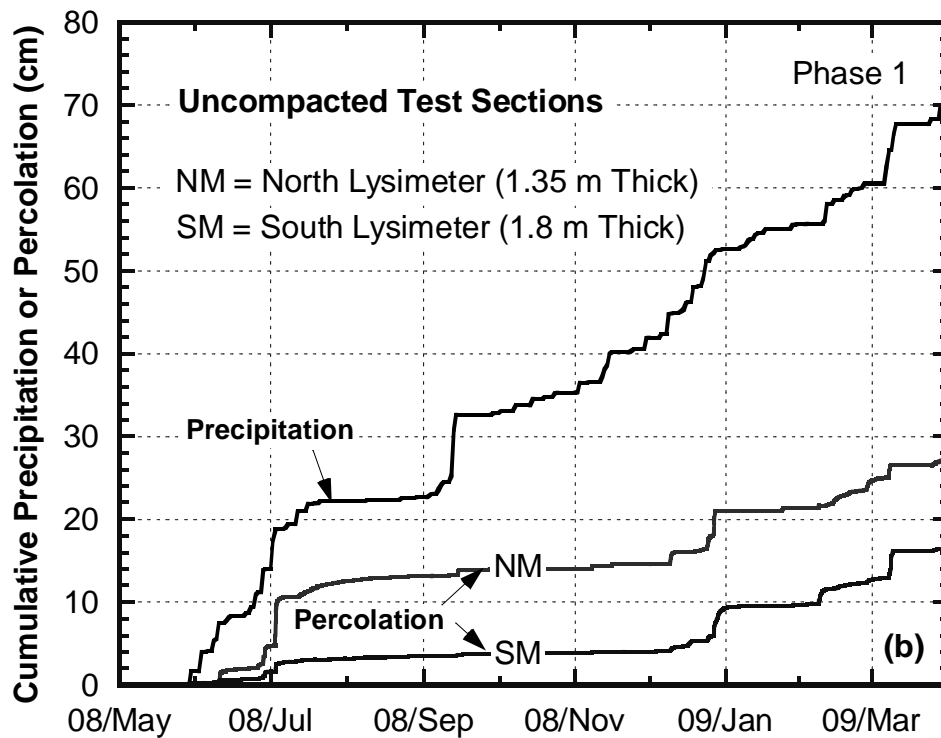
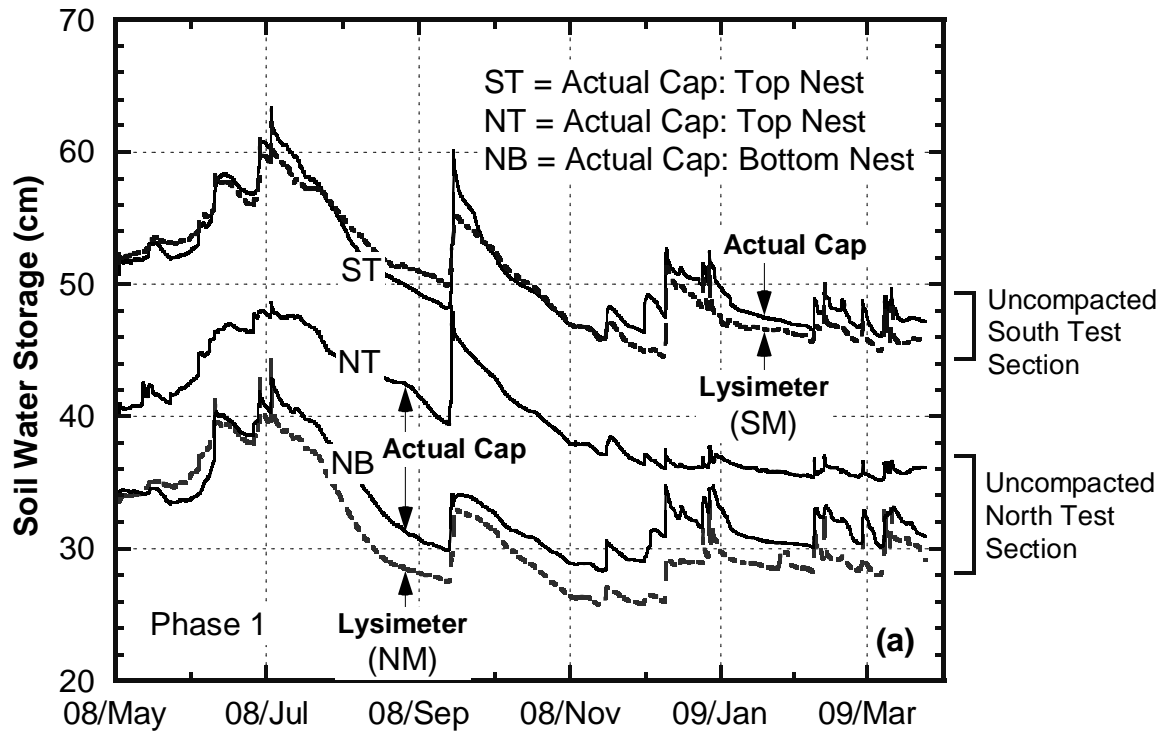


Figure 1-8: Soil water storages (a); and cumulative precipitation and percolation (b) for uncompacted test sections.

MSW. The peak soil water storage for NM was 44.2 cm whereas it was 48.6 cm and 42.9 cm for NT and NB, respectively. The average soil water storage for the lysimeter is less than that for the actual caps.

For the uncompacted south test section, which had about additional 45 cm of clay compared to the north test section, the average soil water storage for the lysimeter nest (SM) was 50.5 cm whereas the storage was 51.0 cm for the top (ST) nest that was placed above the MSW (Figure 1-1). The peak soil water storage for SM was 62.2 cm whereas it was 63.3 cm for ST. The bottom nest in the south test section was placed in the existing intermediate cap placed on the landfill cell in 1996. Data for that nest is not presented in this paper. That data is being used to assess long-term changes in the water holding capacity of the test sections. During July to September 2008, the soil water storage in the upper portion of the south test section (ST) drops below the lysimeter portion of the test section (SM). During this period, according to Figure 1-8(b), relatively small precipitation and percolation were recorded. This shows that the soil water storage was depleted primarily due to ET.

Figure 1-9 shows the comparison of measured soil water storages for the actual caps in the north and south test sections versus the soil water storages for the corresponding lysimeters. The 1:1 line indicates equal soil water storages for the lysimeter and the actual cap for the measurements done at the same moment. The points above the line indicate that the soil water storage for the actual cap is greater than that for the corresponding lysimeter and vice versa. About 97% of the data points cluster together above the 1:1 line for the north test section while about 69% of the data for the south test section. The average of the ratios of soil water storages for the actual caps to those for the

corresponding lysimeters for the uncompacted north and south test sections are 1.17 and 1.00, respectively.

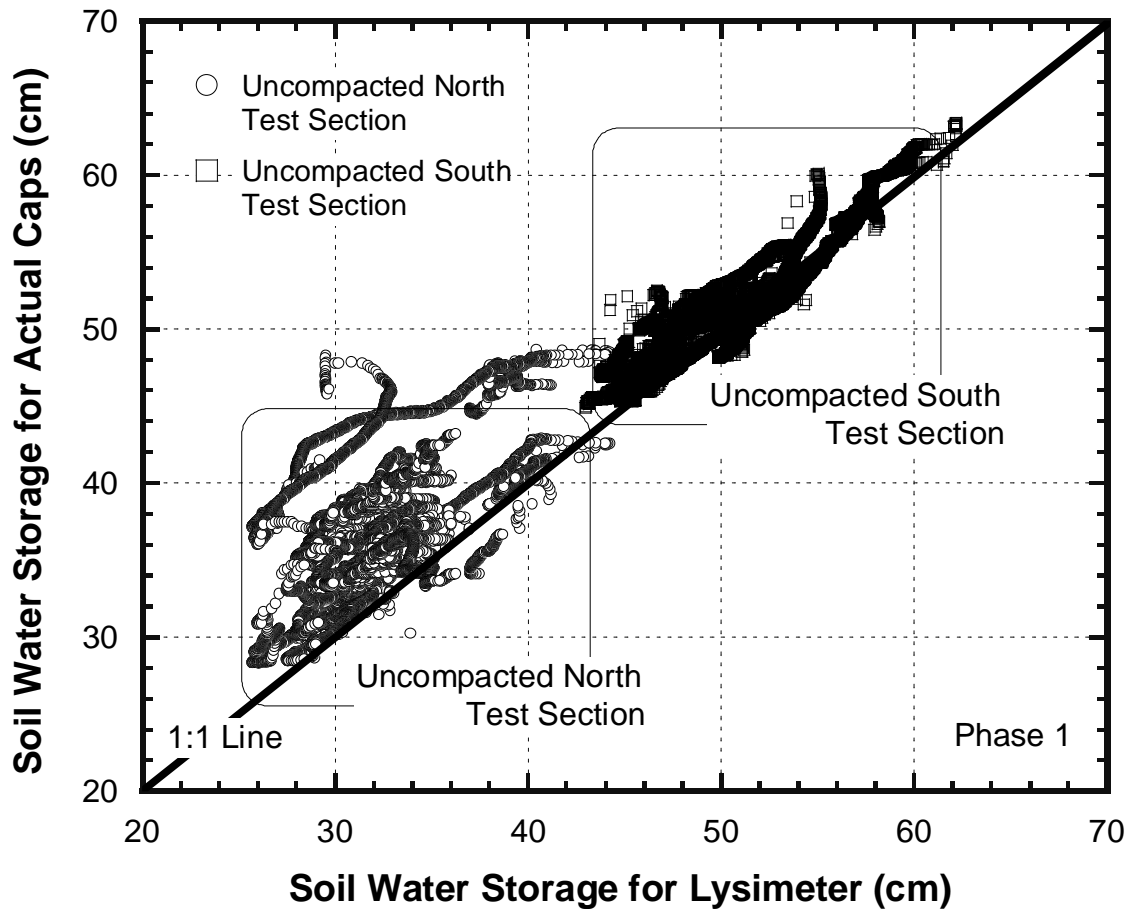


Figure 1-9: Correlation between measured soil water storages for lysimeters versus actual caps for uncompacted test sections.

Using the numerical model Vadose/W, Mijares et al. (2010) demonstrated that the soil water storages for lysimeters are expected to be less than those for the corresponding actual caps because depending upon the soil water retention functions, the soil cover in the actual cap is able to pull water upwards from the waste layer to maintain its higher soil water storage. In addition, they also concluded that as the thickness of the cap

increases, the difference in soil water storages between the actual cap and the corresponding lysimeter shrinks. Thus, the soil water storage of the south lysimeter, which is thicker than the north test section, is closer to the corresponding cap. Furthermore, Mijares et al. (2010) also numerically demonstrated that greater soil water storage represents lower percolation. Hence, while percolation values for the actual caps cannot be measured in the absence of a lysimeter, it can be inferred that the percolation measured in the uncompacted north lysimeter is on the conservative side compared to the percolation that must have entered into the waste in the north test section while the percolation measured in the uncompacted south lysimeter is closer to the percolation that must have entered into the waste in the south test section.

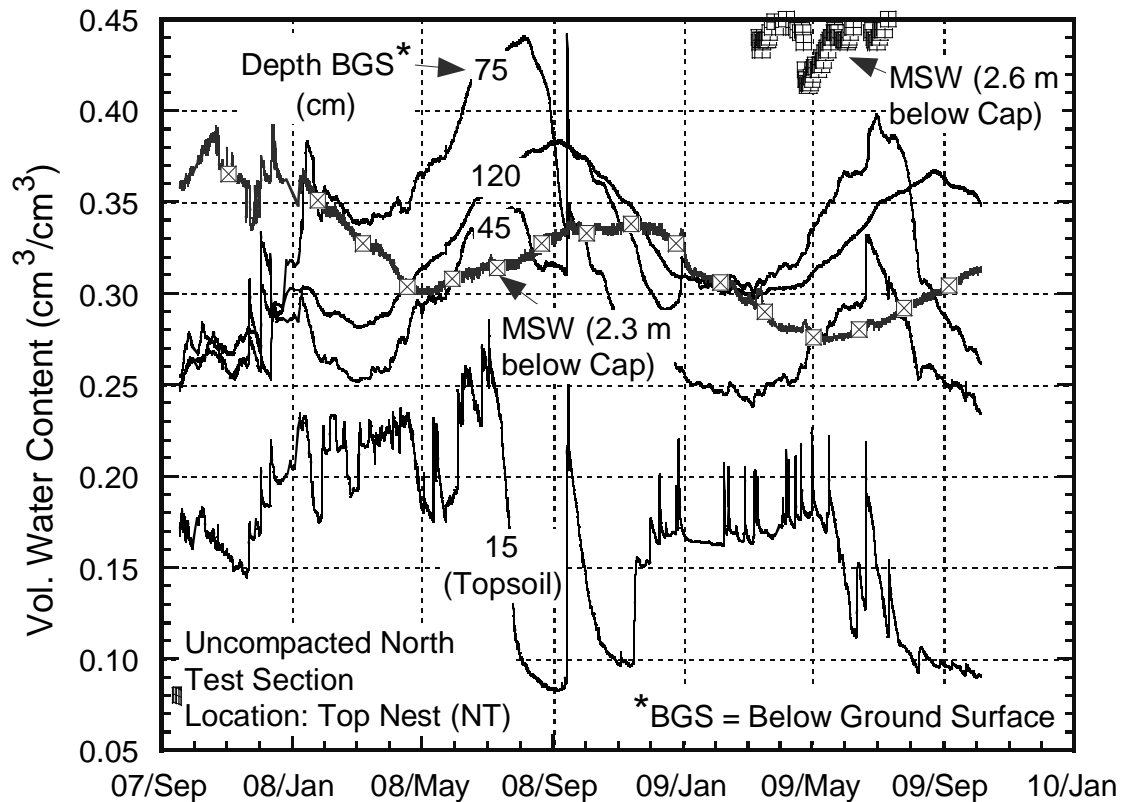


Figure 1-10: Water contents in the test section and in the underlying waste.

Figure 1-10 shows the water contents measured in the NT nest of the north test section. Figure 1-10 shows that the changes in the water contents during a given period of time are greater at shallower depths compared to at deeper depths. In addition, the increase or decrease in the water contents from top down (or opposite direction) follows a relatively sequential pattern similar to sinusoidal waves with phase shift. The water content of the underlying waste also increases and decreases as the water contents of the clay cap increase or decrease. Thus, in an actual cap, there is continuity in the water flux across the cap and the waste interface which impacts the magnitude of the flux depending upon the hydraulic properties of the cap and the waste (Mijares and Khire 2008).

Phase 2: Compacted North and Uncompacted South Test Sections

The soil water storages and cumulative percolation for the compacted north test section constructed during the Phase 2 of the project are presented in Figure 1-11. The Phase 2 data spans from the end of October 2009 to October 2010. For comparison, the soil water storages and cumulative percolation for the uncompacted south test section are presented in Figure 1-11(b). The compacted north and uncompacted south test sections are both 1.8 m thick and contain 1.5 m thick native clay storage layer. Comparison of Figures 1-11(a) and (b) demonstrates that the changes in the soil water storage for the uncompacted test section are larger and steeper following precipitation events or when the soils dry out between the successive precipitation events. The compacted test section, which has about two orders lower hydraulic conductivity compared to the uncompacted test section, is shedding more water as runoff (or lateral flow within the vegetative layer)

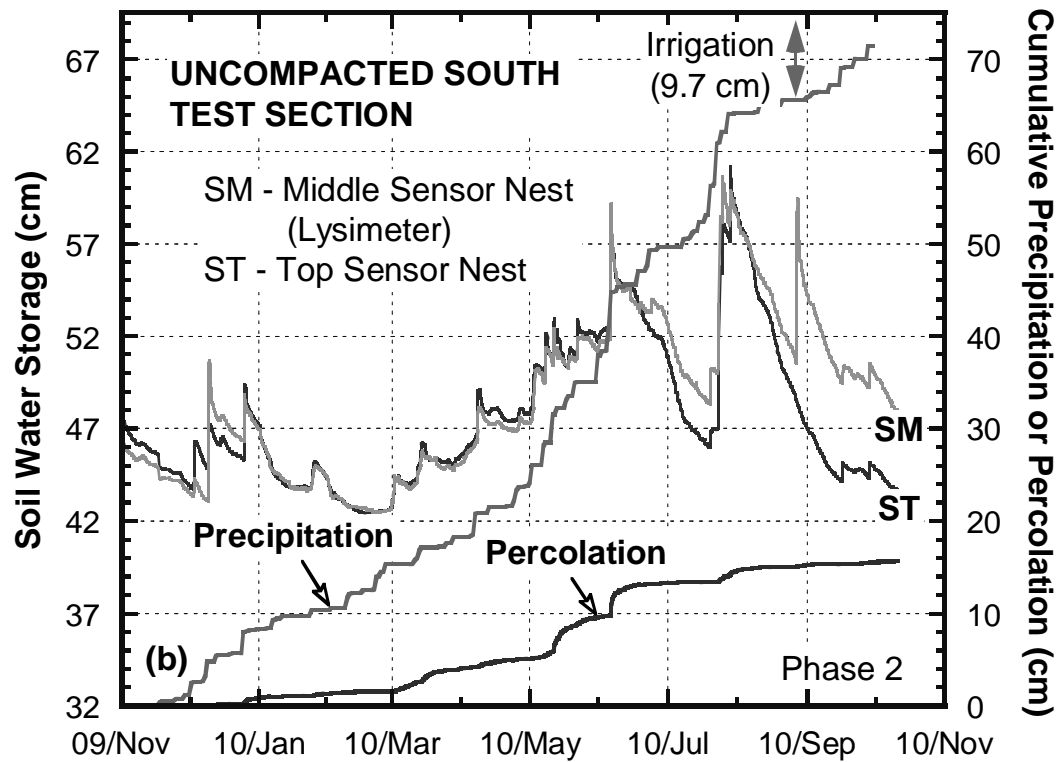
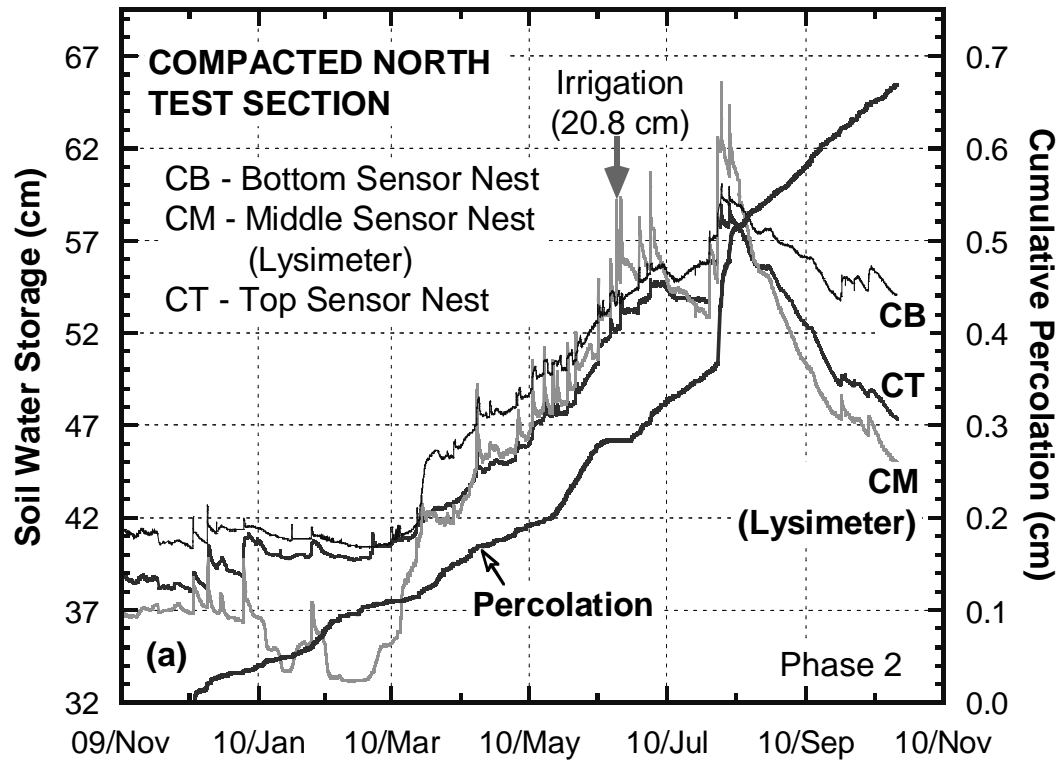


Figure 1-11: Soil water storage and cumulative precipitation and percolation for compacted north test section (a); and uncompact south test section (b).

and hence not showing increase in the storage as rapid as seen for the uncompacted test sections.

The compacted test section reached peak soil water storage of about 65.6 cm versus the uncompacted test section that reached peak storage of about 60.7 cm which occurred at about the same time as that for the compacted test section. Due to lower hydraulic conductivity, the compacted test section was able to store more water. More soil water storage translates into lower percolation (Mijares et al. 2010). The compacted test section had about 6.7 mm of percolation during the one year monitoring period and a majority of the percolation was observed when the soil water storage peaked in July 2010 (Figure 1-11a). During the same time period, the uncompacted south test section had 157 mm of cumulative percolation.

Figure 1-12 shows the comparison of measured soil water storages for the actual cap in the compacted north test section versus the soil water storages for the corresponding lysimeter. About 80% of the data points are above and about 20% of the data points are below the 1:1 line for the compacted test section. The average of the ratios of soil water storages for the actual caps to those for the corresponding lysimeter for the compacted north test section is 1.07. This average value of the ratio is about the same as that for the uncompacted south test section. Mijares et al. (2010) concluded that as the thickness of the cap increases or the hydraulic conductivity of the cap decreases, the difference in soil water storages between the actual cap and the corresponding lysimeter shrinks. Hence, due to lower hydraulic conductivity, the soil water storage of the compacted north lysimeter is about the same as the corresponding actual cap.

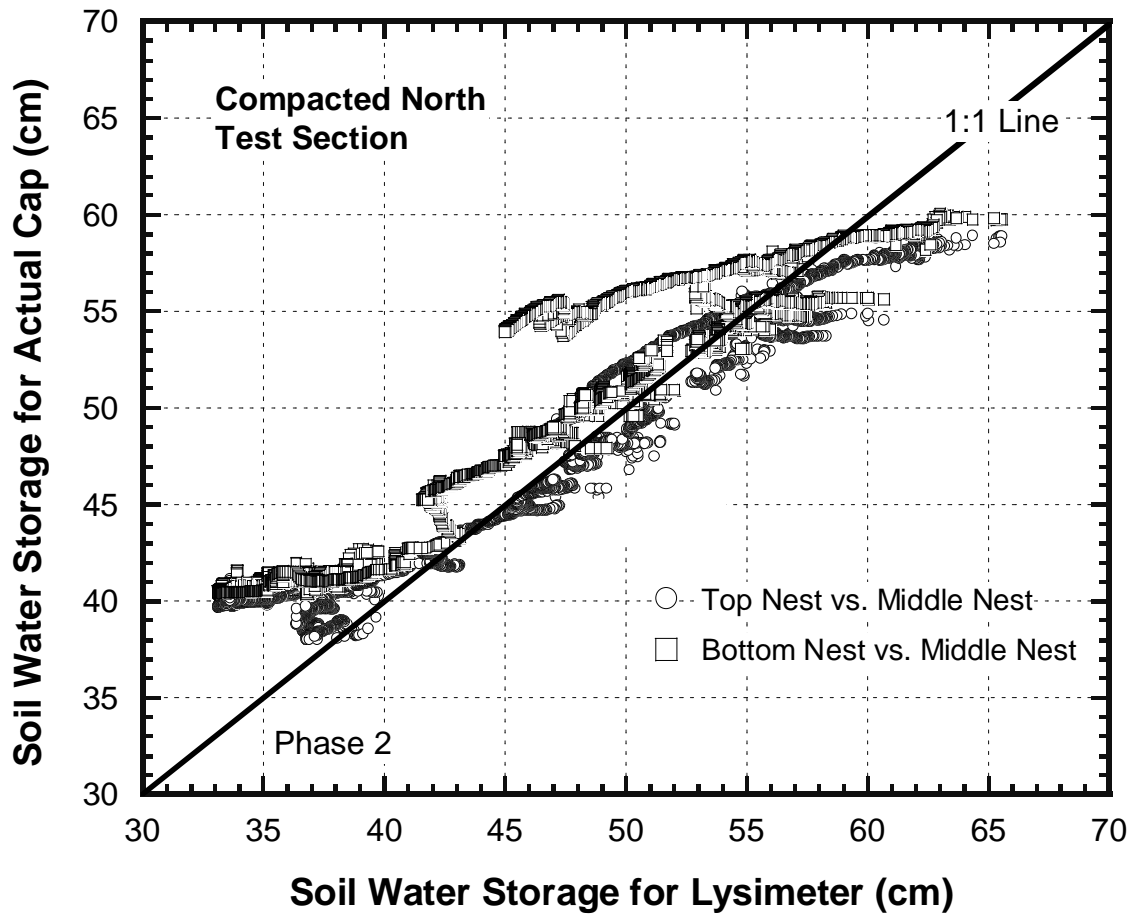


Figure 1-12: Correlation between measured soil water storages for lysimeter versus actual cap for the compacted north test section.

Using numerical simulations carried out using Vadose/W, Mijares et al. (2010) demonstrated that when the soil water storage of the lysimeter is about the same as that for the actual cap, the percolation measured from the lysimeter can be assumed representative of the percolation entering the waste in an actual cap. Hence, while percolation values for the actual caps cannot be measured in the absence of a lysimeter, it can be inferred that the percolation measured from the compacted north lysimeter (~ 6.7 mm/yr) is closer to the percolation that must have entered into the waste in the compacted north test section.

SUMMARY AND PRACTICAL IMPLICATIONS

This paper presents the design and construction of two uncompacted and one compacted field-scale earthen cap test sections that were built and instrumented at a landfill to evaluate the differences in the hydraulic and hydrologic response of actual caps (underlain by the waste) versus the corresponding lysimeters which are used to measure percolation. Lysimeter pans were installed in the middle of each of the three test sections. The instrumented area of the test section was expanded upslope and downslope of the lysimeter to monitor the soil water storages within and beyond the lysimeter footprint to evaluate the effect of lysimeter lower boundary.

About 35 sensors were installed in each of the three test sections to monitor water contents, water potentials, soil temperatures, water levels, and gas pressures. The data collected during the Phase 1 shows the hydrologic performance of two uncompacted test sections having 1.35 m and 1.8 m total thicknesses. The Phase 2 data shows the hydrologic performance of two test sections having the same thickness (1.8 m) but different hydraulic conductivities ($\sim 10^{-4}$ cm/s and 10^{-6} cm/s) due to one being compacted and the other not.

The soil water storages for the uncompacted test sections underlain by the waste were typically greater than those for the corresponding lysimeters. However, for the compacted north test section constructed in the Phase 2, there was no significant difference observed between the soil water storages for the actual cap and the lysimeter. The field data collected in this project validates the numerical findings of Khire and Mijares (2008) and Mijares et al. (2010) which demonstrated that lysimeters would underestimate the soil water storage and overestimate the percolation. However, the

difference in these parameters for lysimeters and actual caps shrink as the thickness of the cap is increased and/or the hydraulic conductivity is lowered.

REFERENCES

REFERENCES

- Abichou, T., Liu, X., and Tawfiq, K. (2006). "Design Considerations for Lysimeters Used to Evaluate Alternative Earthen Final Covers," *Journal of Geotechnical and Geoenvironmental Engineering*, 132 (12): 1519-1525.
- Albright, W., Gee, G., Wilson, G., and Fayer, M. (2002). "Alternative Cover Assessment Project: Phase I Report," Publication No. 41183, Report to US EPA, Desert Research Institute, NV.
- Benson, C., Bosscher, P., Lane, D., and Pliska, R. (1994). "Monitoring System for Hydrologic Evaluation of Landfill Final Covers," *Geotechnical Testing Journal*, 17 (2): 138-149.
- Bews, B., O'Kane, M., Wilson, G., and Williams, D. (1997). "The Design of a Low Flux Cover System Including Lysimeters for Acid Generating Waste Rock in Semi-arid Environments," Fourth International Conference on Acid Rock Drainage, Vancouver, BC: 747-762.
- Flint, A., Campbell, G., Ellett, K., and Calissendorff, C. (2002). "Calibration and Temperature Correction of Heat Dissipation Matric Potential Sensors," *Soil Science Society of America Journal*, 66: 1439-1445.
- Geo-Slope. (2007). "Vadose Zone Modeling with VADOSE/W 2007: An Engineering Methodology," Geo-Slope International Ltd., Alberta, Canada.
- Guyonnet, D., Amraoui, N., and Kara, R. (2000). "Analysis of Transient Data from Infiltrometer Tests in Fine-Grained Soils," *Ground Water*, 38 (3): 396-402.
- Khire, M., and Mijares, R. (2008). "Influence of the Waste Layer on Percolation Estimates for Earthen Caps Located in a Sub-humid Climate," *Proceedings, GeoCongress 2008, GSP No. 177, Geotechnics of Waste Management and Remediation, ASCE, Reston, VA: 88-95.*
- Khire, M., Benson, C., and Bosscher, P. (1997). "Water Balance Modeling of Earthen Final Covers," *Journal of Geotechnical and Geoenvironmental Engineering*, 123 (8): 744-754.
- Mijares, R., Khire, M., and Johnson T. (2010). "Lysimeters Versus Actual Earthen Caps: Numerical Assessment of Soil Water Storage," *Proceedings, GeoFlorida 2010, GSP No. 199, Advances in Analysis, Modeling and Design, ASCE, Reston, VA: 2849-2858.*
- Parent, S., Cabral, A., Gras, G. and Marinho, F. (2006). "Design and Installation of Zero-Tension Lysimeter in an Inclined Cover," *Proceedings, 6th International Conference on Unsaturated Soils*, April 2-6, Carefree, AZ: 625-633.

- Seiler, K., and Gat, J. (2007). *Groundwater Recharge from Run-off, Infiltration and Percolation*, Water Science and Technology Library, Vol. 55, Springer, The Netherlands, 244 p.
- Ward, A., and Gee, G. (1997). "Performance Evaluation of a Field-scale Surface Barrier," *Journal of Environmental Quality*, 26: 694–705.

PAPER NO. 2: FIELD DATA AND NUMERICAL MODELING OF WATER BALANCE OF LYSIMETER VERSUS ACTUAL EARTHEN CAP

ABSTRACT

In order to evaluate the differences in the hydrological performance of actual earthen cap overlying municipal solid waste (MSW) versus lysimeter which is commonly used to measure the hydrologic water balance, a field-scale test section (30 m X 20 m X 2 m) of an earthen cap made up of compacted native glacial clay was constructed and instrumented at a landfill near Detroit, Michigan. Lysimeter pan was installed within the middle of the test section and the instrumented area of the test section was expanded upslope and downslope of the lysimeter to monitor water balance parameters within and beyond the lysimeter footprint to evaluate the effect of artificial drainage boundary introduced by the lysimeter. About 50 sensors were installed to monitor meteorological parameters, water contents, water potentials, soil temperatures, water levels, gas pressures, percolation, and subsurface lateral flow.

Water balance model UNSAT-H was used to simulate the water balance of the test section. UNSAT-H was able to predict the percolation relatively accurately. Relative changes or trends in the soil water storage were generally accurately captured by the numerical model. The numerical model that was validated for the lysimeter was used to simulate the water balance of the actual cap where the cap was placed on MSW. The net percolation over the monitoring period estimated by UNSAT-H across the interface between the cap and the underlying landfilled waste was negative (upward) as well as positive (downward into the waste). However, net percolation from the actual cap

estimated by UNSAT-H was relatively close to that measured by the lysimeter. Thus, the field data and modeling results indicate that the soil cap is able to pull moisture from the underlying waste under evapotranspirative gradients. In addition, the numerical simulation results indicate that soil water storage can be used as an indicator of relative percolation for the actual cap with respect to the percolation measured by the lysimeter.

INTRODUCTION

Earthen caps, also known as evapotranspirative (ET) covers, have been commonly permitted for landfills located in arid, semi-arid, and sub-humid climates (Khire et al. 1999; Albright et al. 2004; Scanlon et al. 2005) in lieu of prescriptive caps which require the use of flexible membrane liner (FML) or geomembrane (GM). Typically, evaluating the hydrologic performance of ET caps requires the installation of lysimeters at the proposed site to measure the percolation through the cap.

Because field demonstration projects usually span only for few years, numerical models are often used to predict the long-term performance of the earthen cap. Numerical studies on lysimeters typically neglect the effect of the underlying waste (Khire et al. 2000; Benson et al. 2005) because percolation is immediately collected through a drainage layer placed above the geomembrane that lines its bottom boundary. While the geomembrane allows the infiltrated water through the cap to be physically collected and measured, it prevents the upward flux of liquid and vapor from the waste mass or subgrade layer located below the cap under evapotranspirative gradients (Khire and Mijares 2008; Mijares et al. 2010). It may also alter the heat flux from the waste mass that is present below the cap which may influence the estimated percolation for the actual

cap. When proposed alternative earthen cap is approved and constructed, the geomembrane and the drainage layers used for the lysimeter during field demonstration are not placed. Several studies have identified this conceptual difference (Scanlon and Milly 1994; Abichou and Musagasa 2008; Khire and Mijares 2008). The concern stems due to the inherent hydraulic differences in the lysimeter and the actual cap influencing the percolation. The percolation needs to be relatively small (few mm per year) in order for the regulatory agencies to approve the alternative cap. Hence, the accuracy in measuring and projecting long-term percolation for the actual cap needs to be relatively high.

A field-scale demonstration project was undertaken to evaluate the use of earthen cap in Detroit, MI which is considered to have sub-humid climate. The test section was built and instrumented at a landfill site. Lysimeter pan was installed in the middle of the test section to measure percolation. Moreover, the instrumented area of the test section was expanded upslope and downslope of the lysimeter to monitor the soil water storage within and beyond the lysimeter footprint. The unique design of the test section allowed comparative hydrologic evaluation between an actual earthen cap (underlain by MSW) versus the corresponding lysimeter.

OBJECTIVE

The key objective of the study was to evaluate the hydrological differences between an actual earthen cover versus the corresponding lysimeter. Percolation and soil water storage measured from the lysimeter portion of an instrumented field-scale test section were used to verify the numerical model UNSAT-H. Because percolation cannot be

directly measured without the lysimeter pan, the validated numerical model was used to predict the percolation for the actual cap placed on the existing MSW.

FIELD-SCALE TEST SECTION

A field-scale earthen cover test section, 30 m long by 20 m long, was constructed at a landfill located in Detroit, Michigan. The site is situated in sub-humid climate where the average annual precipitation is 84 cm and has a potential evaporation to precipitation ratio (PE/P) of about 1.2. Average slope of the landfill is about 1V to 6H consisting of an existing intermediate cover that was placed on the waste in late 1990s. The test section was constructed using a 1.5-m thick native glacial till (clay) which was overlain by a 0.3-m thick topsoil layer. The clay was compacted at dry of optimum water contents to minimize potential for desiccation cracking.

Figure 2-1 shows the cross-section of the instrumented test section illustrating the relative locations of the sensor nests including the lysimeter pan. The lysimeter consisted of a trapezoidal excavation in the middle of the test section having plan view dimensions of about 8.5 m by 8.5 m with an average depth of 0.6 m. The lysimeter was lined using a geosynthetic clay liner (GCL) overlain by a 1.5 mm thick high-density polyethylene (HDPE) geomembrane. The lysimeter pan was filled with clean pea gravel having an average hydraulic conductivity equal to 1 cm/s. A polymer insect mesh having an average opening size of 1 mm was placed on top of the gravel surface before the clay was placed to physically separate the clay from the drainage gravel during field placement. An HDPE pipe having 7.5 cm diameter was installed within the pea gravel and vented to the atmosphere to create a vented drainage boundary. This boundary can be subjected to a

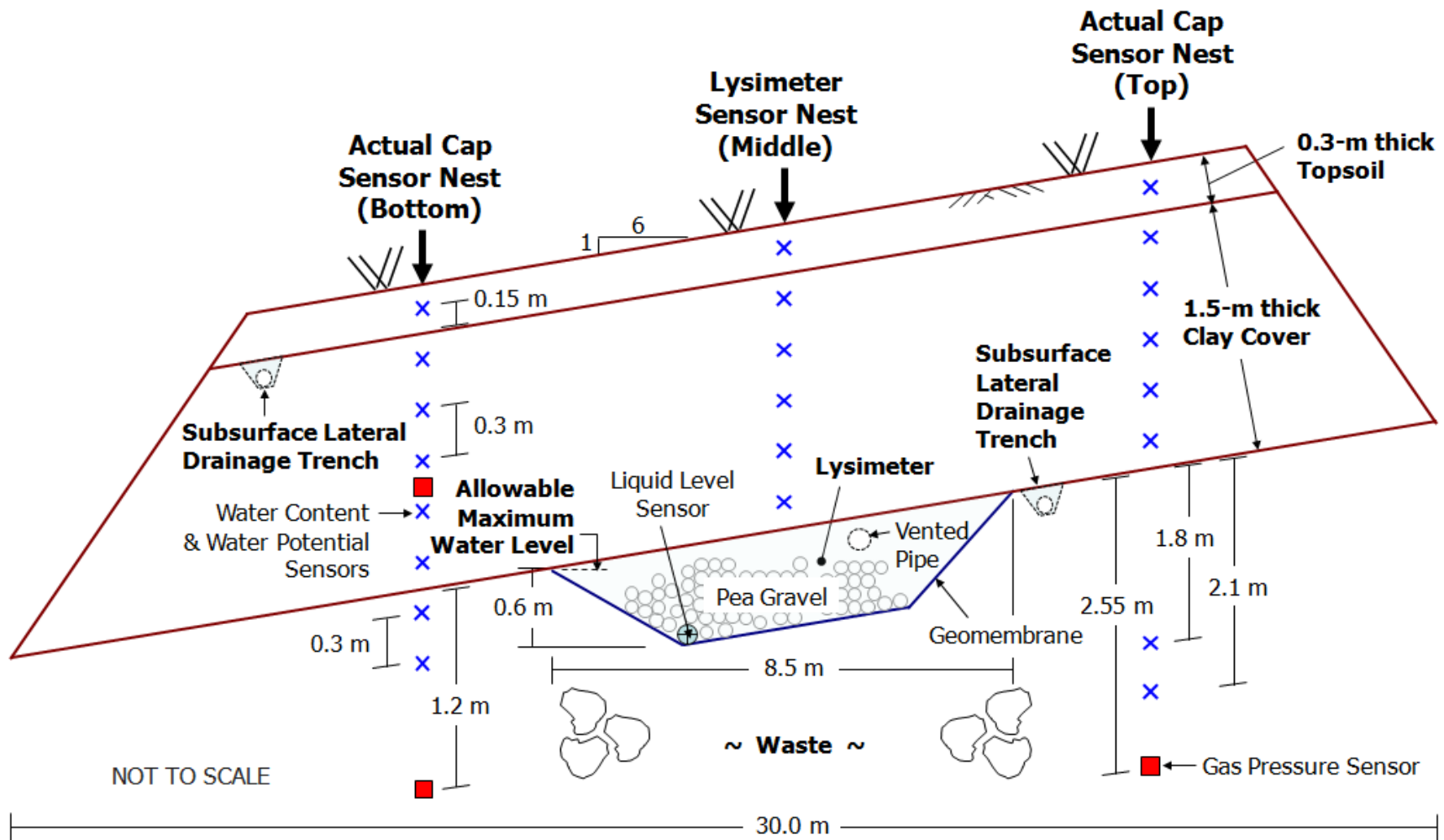


Figure 2-1: Cross-section of instrumented field test section.

fixed or variable pressure (or suction) to simulate other field conditions for future research.

The instrumented area of the test section was expanded upslope and downslope of the lysimeter (Figure 2-1) to monitor the water content, water potential, gas pressure, and soil temperature within and beyond the lysimeter footprint in order to assess and compare the hydrologic performance of the lysimeter versus the actual cover placed on the underlying waste. The upper and lower sensor nests were placed diagonally or cross slope (in plan view) with respect to the central lysimeter nest so that the sensor nests located upgradient on the slope could not influence the water balance measured by the sensor nests located downgradient.

Soil Properties

Native soil which is a glacial till was used to build the earthen cover test section. The clay was compacted in 30-cm thick lifts using a sheepsfoot compactor at dry of optimum water contents as shown on the compaction curve in Figure 2-2. Soil samples were collected for further laboratory testing and hydraulic characterization. Table 2-1 shows the physical properties of the soils used for the test sections. Low plasticity clay (CL) was used as the storage layer whereas low plasticity silt (ML) was used for the topsoil layer.

The water content and dry unit weight of the compacted clay were measured using a nuclear densometer (Figure 2-2). The field water contents, on average, are about 4% dry of the optimum water content. The field dry unit weights, on average, are about 98% of the maximum dry unit weight of the Standard Proctor effort. The hydraulic conductivity of the compacted clay was measured in the lab using 10 cm diameter

samples in a flexible wall permeameter (ASTM D5084). The average lab value of the hydraulic conductivity was 2.2×10^{-7} cm/s. The hydraulic conductivity of the compacted clay was also measured in the field using a 1 m by 1 m single-ring infiltrometer (ASTM D5126; Guyonnet et al. 2000) and the average value of the conductivity is 4.4×10^{-6} cm/s. Field conductivity was used for the modeling because it is considered more representative due to the larger size of the soil sampled. A 30 cm thick topsoil layer consisting of uncompacted silt was placed on top of the compacted clay using a track dozer and seeded to grow native grass and shrubs. Single-ring infiltrometer tests were

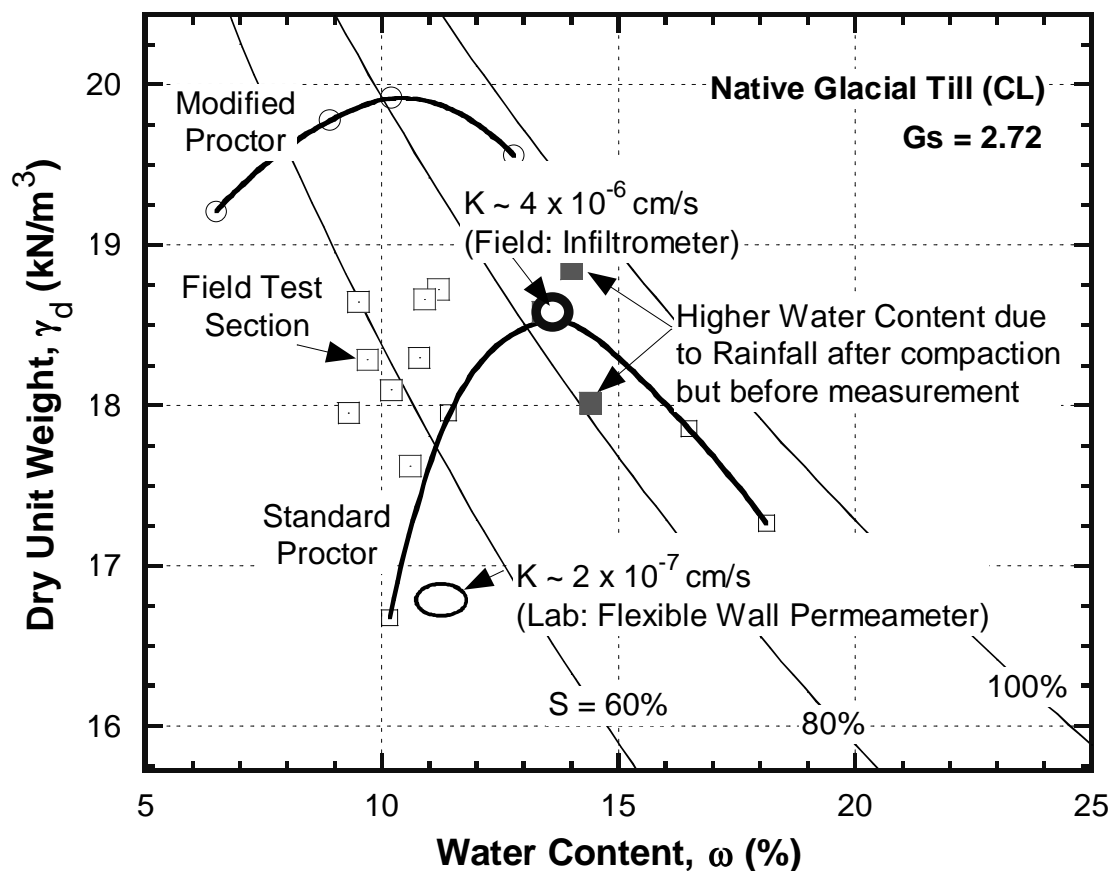


Figure 2-2: Proctor compaction curves and field water contents and unit weights.

Table 2-1: Physical properties of the soils.

Property	Topsoil	Storage Layer (Native Glacial Till)
USCS Classification	ML	CL
D ₁₀ (mm)	0.00092	0.00020
D ₅₀ (mm)	0.070	0.0065
D ₆₀ (mm)	0.091	0.014
Cu	99	70
Cc	11	0.70
Liquid Limit (LL)	25	29
Plasticity Index (PI)	3	13
Optimum Water Content (%) for Standard Proctor Effort	15.7	13.4
Maximum Dry Unit Weight (kN/m ³) for Standard Proctor Effort	17.4	18.5
Hydraulic Conductivity (cm/s)	1 x 10 ⁻² (Field)	2 x 10 ⁻⁷ (Lab) 4.4 x 10 ⁻⁶ (Field)

also carried out on the vegetative layer and the average value of the conductivity is about 1×10^{-2} cm/s.

Instrumentation

Instrumentation at the site consisted of two weather stations and sensors to monitor in-situ volumetric water contents, soil water potentials, temperatures, gas pressures, and water level of percolated water in the lysimeter pan. Subsurface lateral flow through the

topsoil layer was measured using a lateral trench connected to a tipping bucket (Figure 2-1).

Total three nests of sensors were installed within the lysimeter catchment and up-gradient and down-gradient of the lysimeter as shown in Figure 2-1. The instrumentation also extended into the underlying MSW to about 2.5 m depth below the earthen cap to monitor the water contents, temperatures, suctions, and gas pressures. The weather stations recorded precipitation, air temperature, barometric pressure, relative humidity, wind speed, and solar radiation. The data was recorded at 30-min interval using a datalogger installed at the site which could be accessed remotely using a wireless modem.

Quantity of water percolated through the cap directly above the lysimeter was measured by a water level transducer placed at the bottom of the lysimeter (Figure 2-1). A 30 cm long time domain reflectometry (TDR) water content sensor was vertically placed in the gravel next to the water level transducer to have a back-up measurement of the water level. Another water level transducer and TDR water content sensor were installed about halfway upslope within the lysimeter. The lower water level sensor was placed inside a 10 cm diameter perforated HDPE pipe placed at the bottom of the lysimeter pan which ran across the entire width (8.5 m) of the lysimeter (Figure 2-1). A set of two 1 cm diameter flexible HDPE tubing was placed in the conduit to pump the drainage collected in the lysimeter.

A 0.5-hp self-priming pump was installed at the site for the removal of percolated water that was collected in the lysimeter pan. The pump discharged water outside and below the catchment of the test section. The lysimeter recharge (percolation) was

measured and confirmed by continuously monitoring: (1) water level in the lysimeter; (2) water content of the drainage layer of the lysimeter; and (3) rate of pumped outflow.

NUMERICAL WATER BALANCE MODELING

The public domain finite-difference water balance model UNSAT-H Ver. 3.0 (Fayer 2000) was used to numerically simulate the hydrologic performance of the instrumented test section. UNSAT-H numerically solves a modified form of Richards' equation to calculate the flow of water through both saturated and unsaturated soil(s). UNSAT-H can simulate water and heat flow processes in one dimension (1-D) and is capable of simulating steady-state and transient conditions. This model has been routinely used for water balance modeling of earthen caps (Khire et al. 1997; Khire et al. 2000; Benson et al. 2005; Scanlon et al. 2005; Ogorzalek et al. 2008; Bohnhoff et al. 2009). For this study, 1-D simulations were carried out using UNSAT-H Version 3. UNSAT-H is not capable of simulating flow through macropores that may not follow capillarity and hence cannot be represented by Richards' equation. UNSAT-H also does not consider air/gas pressures. Therefore, if air/gas pressures develop during rapid infiltration events, the model is unable to simulate the flow accurately.

INPUT PARAMETERS FOR UNSAT-H

A schematic of the conceptual models used to simulate the field test section is shown in Figure 2-3. To simulate the lysimeter as represented by the middle nest (Figure 2-1), the lower boundary was assigned unit gradient to simulate the vented lower boundary. Low magnitude percolation was collected in the lysimeter throughout the year which indicates

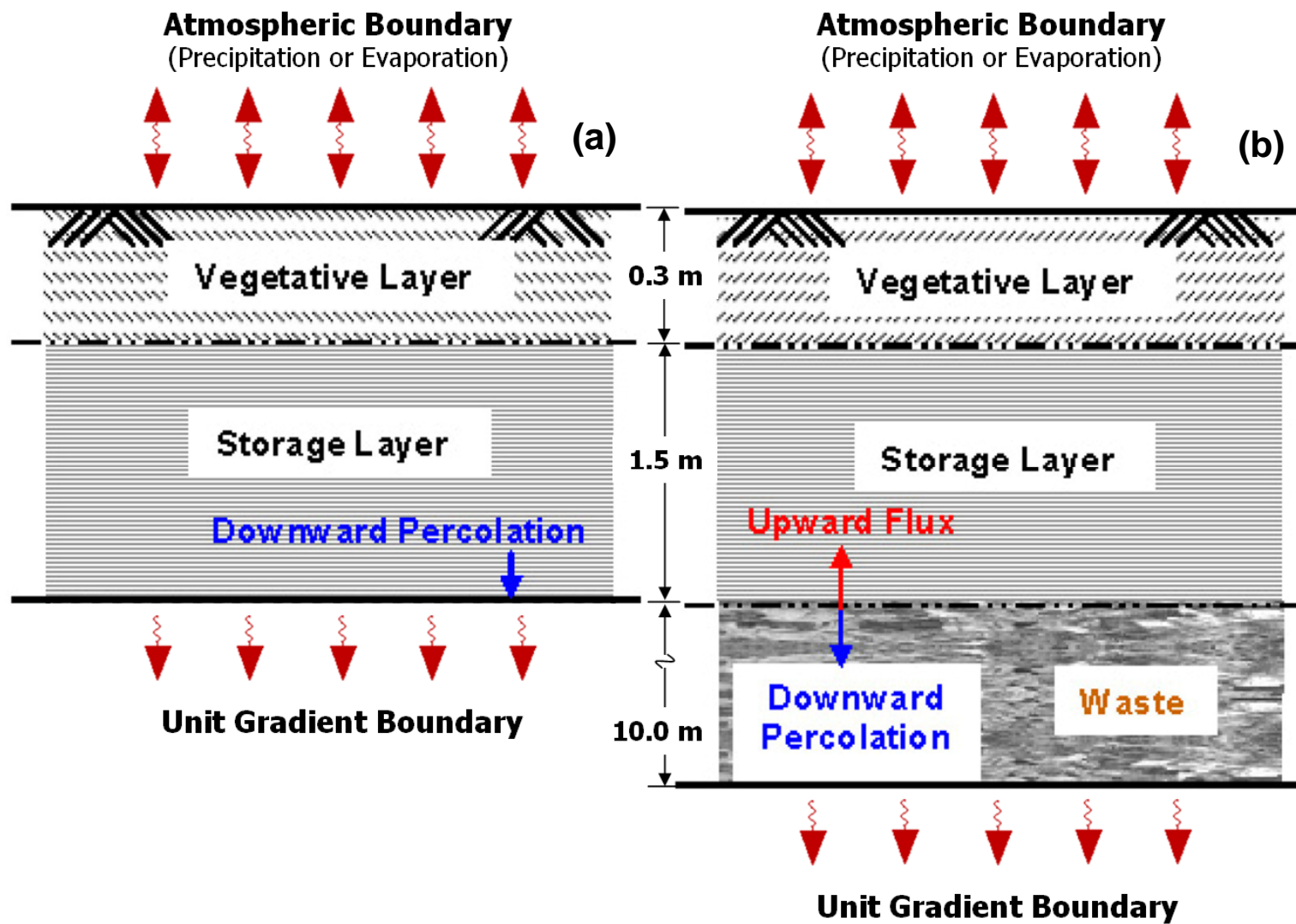


Figure 2-3: Conceptual model for numerical simulation of a lysimeter (a); and an actual cap with underlying waste (b).

that unit gradient boundary is appropriate to simulate the lysimeter. In order to simulate the actual earthen caps which are represented by the top or bottom nests (Figure 2-1) of the test section, the cap was assumed to have underlain by a 10 m thick MSW layer which is representative of the cross section at the site. The lower MSW boundary was simulated as unit gradient boundary.

Soil Properties

Table 2-1 summarizes the index, compaction, and the saturated hydraulic properties of the soils used for the test section. Table 2-2 presents the unsaturated hydraulic parameters. The soil water characteristic curves are described by Haverkamp et al. (1977) function and were obtained from the water contents and soil suctions measured in the field. The unsaturated hydraulic conductivities were estimated by applying the instantaneous profile method (Meerdink et al. 1996) to the water contents and suctions measured in the field using co-located sensors (Figure 2-1).

MSW Properties

In order to simulate the actual earthen caps located upslope and downslope of the lysimeter, numerical simulations included the underlying MSW layer. The MSW was simulated by assigning saturated and unsaturated hydraulic properties of MSW that were measured in the laboratory for MSW collected from the landfill from 6 to 12 m depths. The MSW sample was obtained using a 45 cm diameter auger. The waste, without sorting or screening, was placed in a relatively large PVC cell (30 cm diameter, 25 cm tall) to measure the saturated hydraulic conductivity using the falling head test (ASTM D5084)

Table 2-2: Saturated and unsaturated hydraulic properties of the soils and waste.

Material	θ_s (cm³/cm³)	θ_r (cm³/cm³)	α	β (1/cm)	Ks (cm/s)	A	B (1/cm)
Vegetative Layer or Topsoil (Sandy Silt; ML)	0.41	0.025	147.26	0.668	1.0×10^{-2}	6,261	2.64
Storage Layer (Lean Clay with Sand; CL)	0.35	0.033	403.87	0.658	4.4×10^{-6}	2,530,849	2.73
Landfilled Waste (Measured; MSW)	0.67	0.20	1.62	0.293	1.0×10^{-2}	1.80	1.46

and the same sample was spun in a geotechnical centrifuge at up to 40 g gravitational force added to the sample in 1 to 3 g increments to measure the water retention function (ASTM D6836). The centrifuge not only allowed the measurement of the water retention function relatively rapidly, it also simulated the normal stress experienced by the waste at the depth it was collected. The dry density of the waste at the vertical stress simulated in the centrifuge was 0.69 g/cm^3 . The method developed by Passioura (1977) was applied to the water retention data collected from the centrifuge test to estimate the unsaturated hydraulic conductivities for the waste.

The hydraulic properties measured for the waste are summarized in Table 2-2 and are plotted in Figure 2-4. The water retention function measured for the waste was also

confirmed by plotting the water contents and suctions measured in the waste at various depths during the two year monitoring period. Figure 2-5 shows the water contents, suctions, and gas pressures measured in the field at various depths in the waste. Figure 2-5(b) shows that the suctions and gas pressures are about the same (60 to 90 kPa) and are relatively constant at shallow depths (immediately below the cap). Thus, it can be assumed that the water content and gas pressures (or suctions) are in equilibrium. Hence, the water contents and suctions were plotted on the water retention function of the waste measured in the lab (Figure 2-4a). The boxed regions in Figure 2-4(a) indicate the equilibrium water contents and suctions measured in the field. Because it is expected that the waste in the landfill would vary in its composition, for comparison, the water retention function and unsaturated hydraulic conductivities measured by Kazimoglu et al. (2005, 2006) for loosely compacted MSW are also included in Figure 2-4. Kazimoglu et al. (2005, 2006) determined the waste retention properties for a waste specimen prepared in the laboratory which had composition similar to the waste found in Lyndhurst landfill in Australia that was located at shallow depth with a dry density of 0.57 g/cm^3 . Stoltz and Gourc (2007) published similar waste retention curves for loosely compacted MSW having a dry unit weight equal to 0.54 g/cm^3 . For loosely compacted MSW such as those found within landfills at shallow depth (i.e., immediately beneath the final cover), a saturated hydraulic conductivity of 10^{-3} cm/s has been reported (Mukherjee 2008; Breitmeyer et al. 2010). Hence, for modeling the actual cap and simulate possible scenarios, the hydraulic properties of the waste input to the model were for measured values as well as those published by Kazimoglu et al. (2005, 2006).

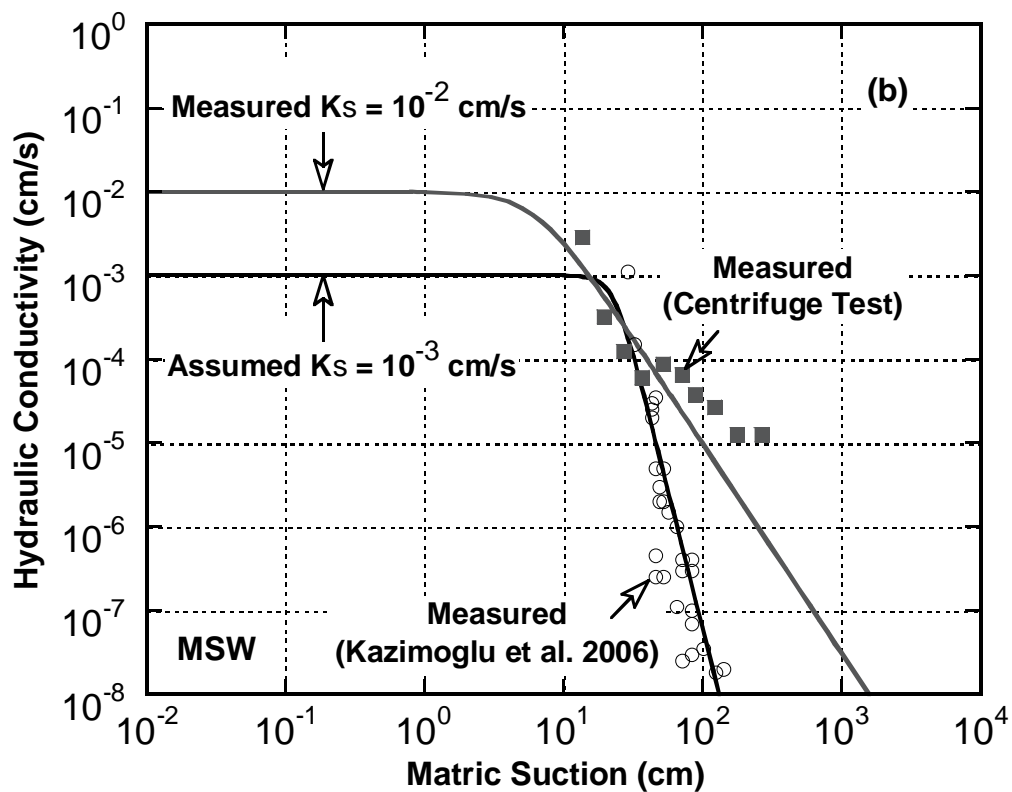
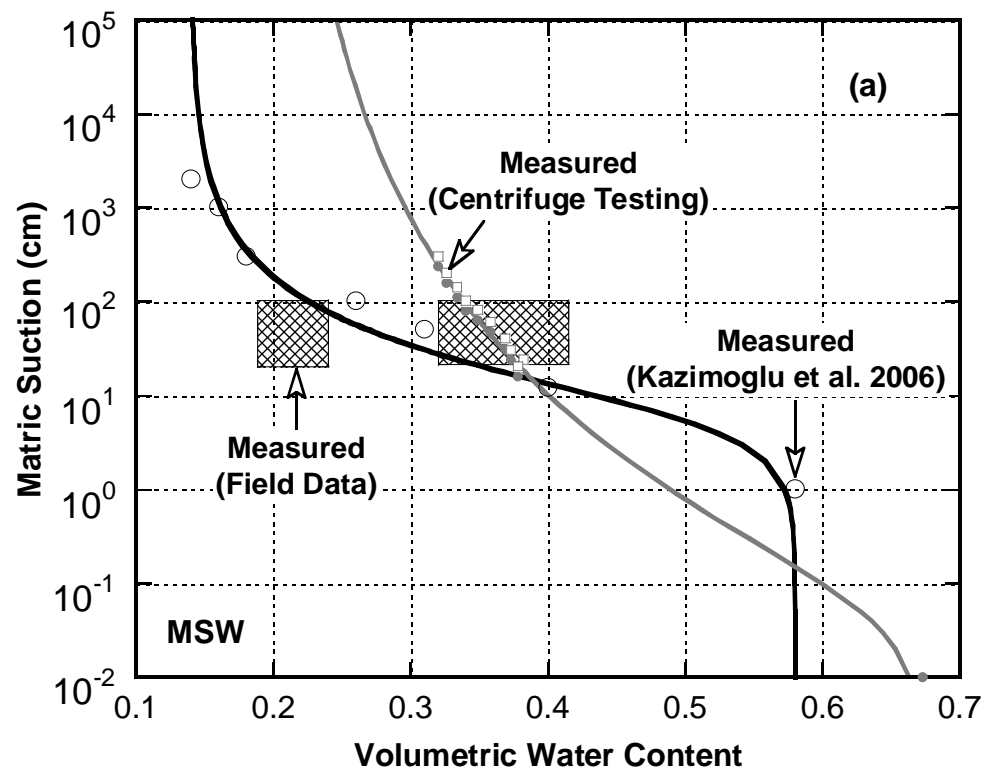


Figure 2-4: Measured water retention curves (a); and unsaturated hydraulic conductivity functions (b) for the waste.

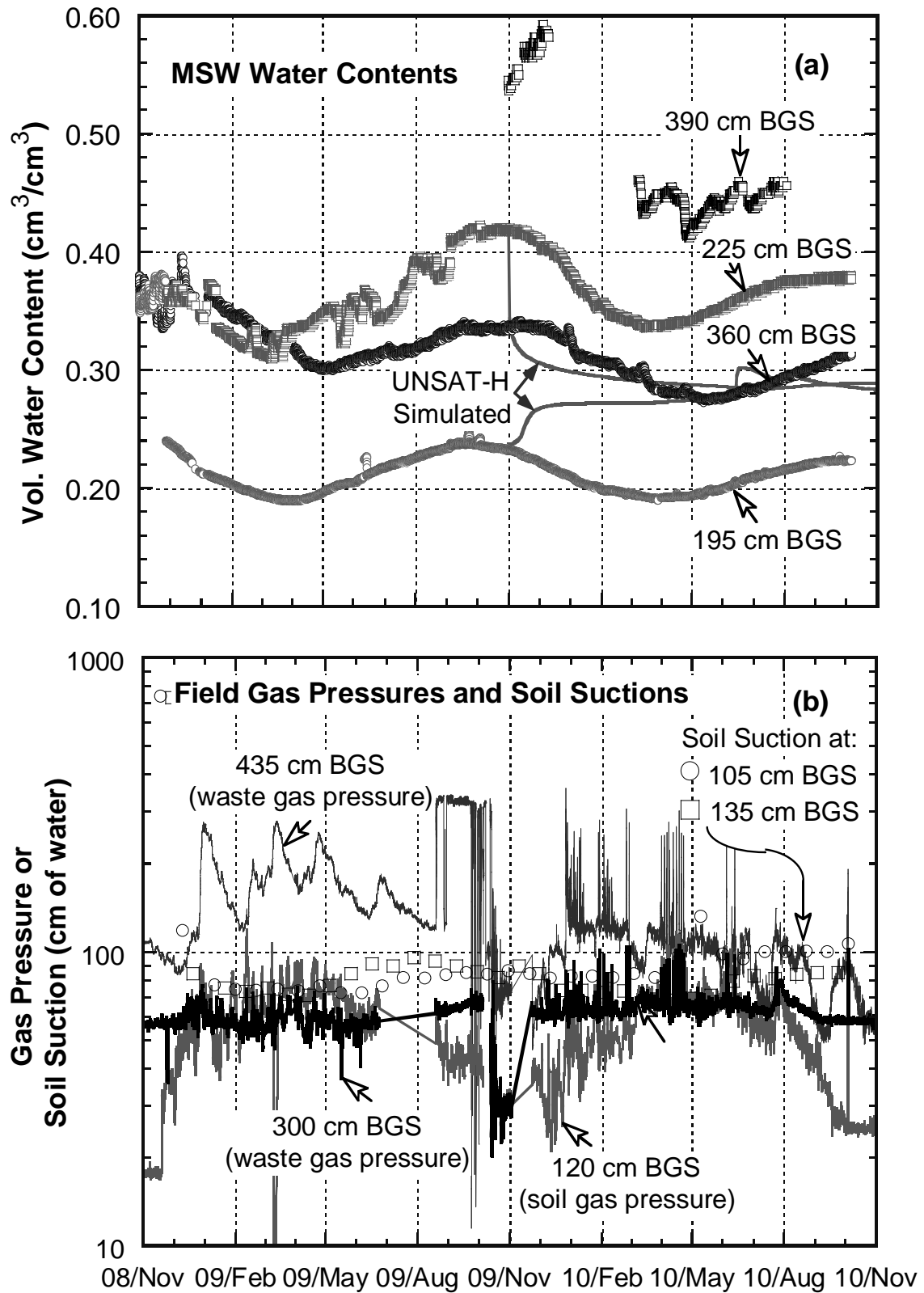


Figure 2-5: Measured water contents (a); and gas pressures and suctions (b) in the waste.

Meteorological Data

The two weather stations installed in the field provided hourly precipitation, air temperature, barometric pressure, relative humidity, wind speed and direction, and solar radiation.

UNSAT-H requires daily values for maximum and minimum air temperature, dew point temperature, total solar radiation, average wind speed, average cloud cover, and total precipitation. Daily dew point temperatures were estimated from the daily average temperature and relative humidity. Average cloud cover was assumed to be zero because net solar radiation was measured at the site. UNSAT-H assumes a sinusoidal variation in air temperature throughout the day and assumes that the daily minimum temperature occurs at 3:00 a.m. and the daily maximum temperature occurs at 3:00 p.m. The dewpoint temperature, wind speed, and cloud cover were assumed to remain constant throughout the day. The daily variation of solar radiation was approximated by a sine function with the peak value occurring at 12:00 noon. Precipitation was applied at an hourly frequency specifically during the time intervals it occurred during a particular day.

Initial Conditions

The initial conditions applied in the model were consistent with those measured in the field test section at the time corresponding to the start date of the simulation. The sensors in the underlying waste were installed a year prior to the construction of the lysimeter. Hence, the water balance simulation period was about a year, starting in Nov. 2009. Initial conditions for UNSAT-H were specified across the depth of the soil profile using the matric suctions corresponding to the measured in-situ water contents across the nest

of sensors in the test section. A variable flux boundary was applied at the ground surface (Figure 2-3) for lysimeter as well as for the actual cap(s). The variable flux boundary corresponds to infiltration rate if it is raining on a given time period or evaporation rate if otherwise.

Numerical Control Parameters

Spatial discretization of the model domain was optimized by conducting sensitivity analysis. This was done by repeatedly refining the nodal spacing until insignificant changes in simulated water balance parameters were achieved. The nodal spacing between the nodes located near the upper and lower boundaries, as well as near the interface between layers, was relatively small (~1 mm).

A maximum time step of 0.1 hr and a minimum time step of 10^{-7} hr were used for the simulations. This was necessary to accurately evaluate the extreme drying and wetting conditions typically encountered at the ground surface. At any given time step, the maximum allowable mass balance error for the whole profile was set at 10^{-5} cm. For all numerical analyses, mass balance errors of less than 1 mm/yr were achieved.

FIELD DATA

Soil Water Storage

Figure 2-6 shows the soil water storage of the test section estimated by integrating the water contents measured by the three nests of water content sensors located within the lysimeter and the actual caps located upslope and downslope of the lysimeter (see

0 1 2 3 4 5 6 7 8 9 10 11 12 13 14 15 16 17 18 19 20 21 22 23 24 25 26 27 28 29 30 31 32 33 34 35 36 37 38 39 40 41 42 43 44 45 46 47 48 49 50 51 52 53 54 55 56 57 58 59 60 61 62 63 64 65 66 67 68 69 70 71 72 73 74 75 76 77 78 79 80 81 82 83 84 85 86 87 88 89 90 91 92 93 94 95 96 97 98 99

points shown are for the period from Nov. 2009 to June 2010, which corresponds to the period before the lysimeter section was subjected to 20.8 cm irrigation which the actual caps did not receive. The 1:1 line shows the region where the soil water storage values are the same for the actual caps and the lysimeter. Points above the 1:1 line correspond to greater soil water storage for the cap compared to the lysimeter and vice versa. Figure 2-7 shows that, the soil water storage of the actual caps is about the same as the soil water storage of the lysimeter.

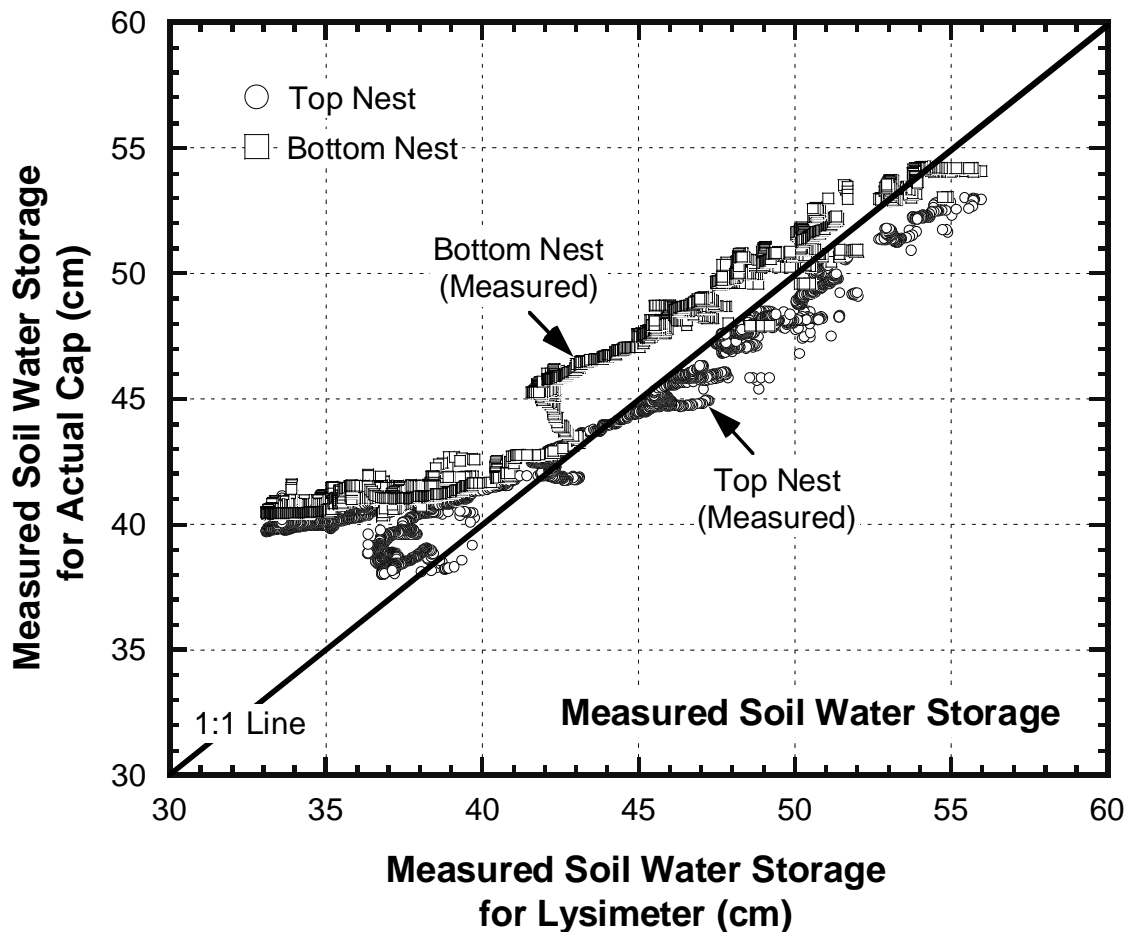


Figure 2-7: Correlation between measured soil water storage for an actual cap and its corresponding lysimeter.

Water Contents

The water contents measured at various depths within the lysimeter and the actual cap (upper nest) are presented in Figure 2-8. The water content profiles on 1 Feb. 2010 and 1 Oct. 2010, being typical for the seasons, are presented in Figure 2-9. The water content profiles of the lysimeter (Figure 2-9) show that the hydraulic gradient in the lowermost portion is downward throughout the monitoring period. This observation is consistent with the field observation that the lysimeter collected low magnitude percolation throughout the year (Figure 2-10). In addition, the water content profile of the lysimeter does not show capillary barrier effect due to the presence of gravel layer used for collecting percolation. When and if capillary barrier effect occurs, the water content of the lowest point in the upper finer-grained soil layer needs to be the highest when the percolation breakthrough occurs. Hence, while the cap in the lysimeter section is underlain by pea gravel, a coarser-grained soil, capillary barrier effect is non-existent. This observation is consistent with the finding by Mijares and Khire (2010) that when the cover soils have hydraulic conductivities less than 10^{-5} cm/s, the capillary barrier effect, even if may occur, would have insignificant effect on percolation. The cover soils of the lysimeter have hydraulic conductivity of about 4×10^{-6} cm/s.

Figure 2-9 also shows that the relative magnitudes of water contents in the actual cap are slightly but subtly different when compared to the water contents within the lysimeter section. In the actual cap, the water contents of the lowermost portion of the cap (cap and waste interface) are slightly greater than the water contents at locations above the interface. Thus, the hydraulic gradient in the actual cap at the cap and waste

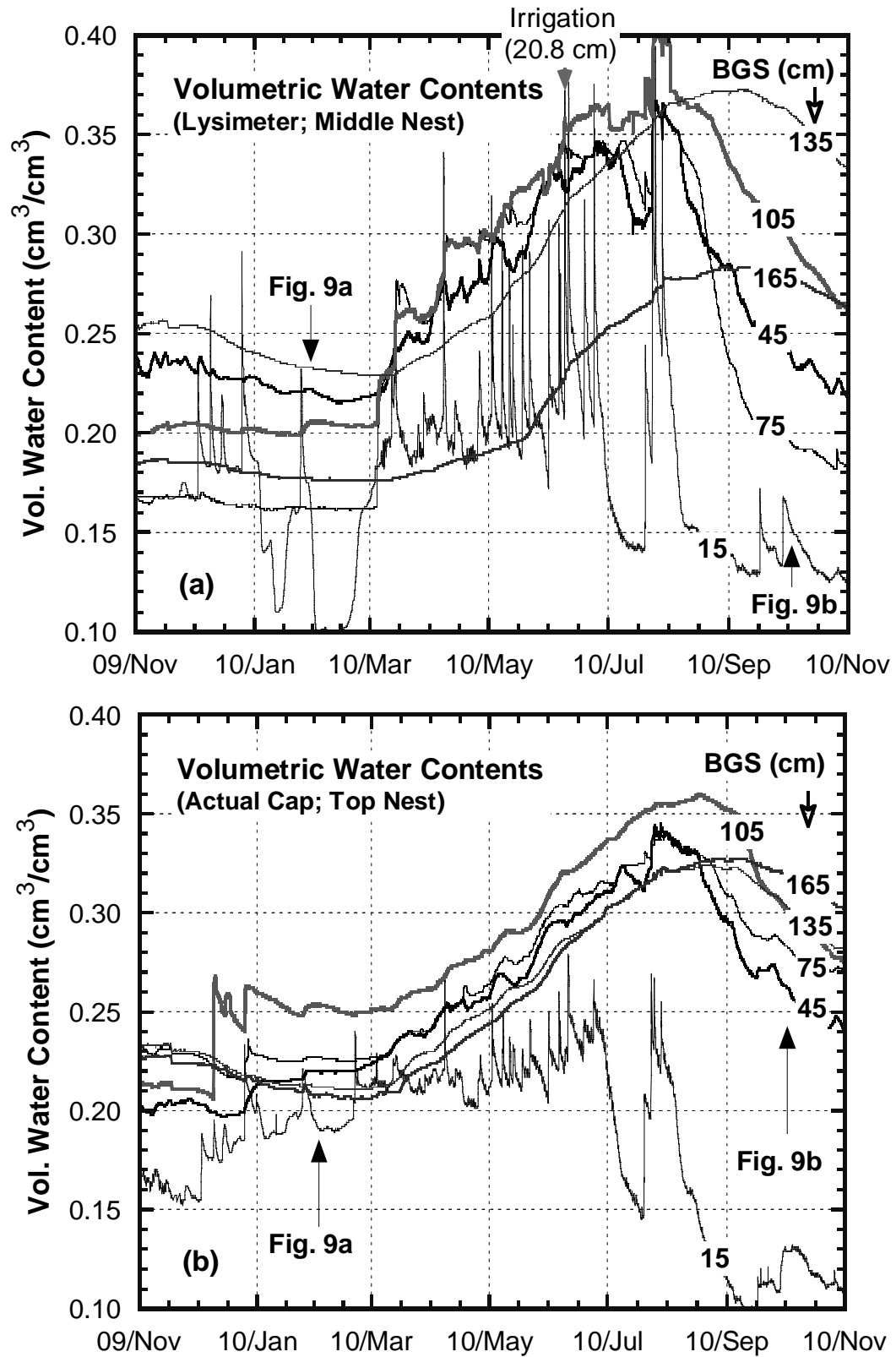


Figure 2-8: Measured volumetric water contents for the lysimeter (a) and actual cap (b).

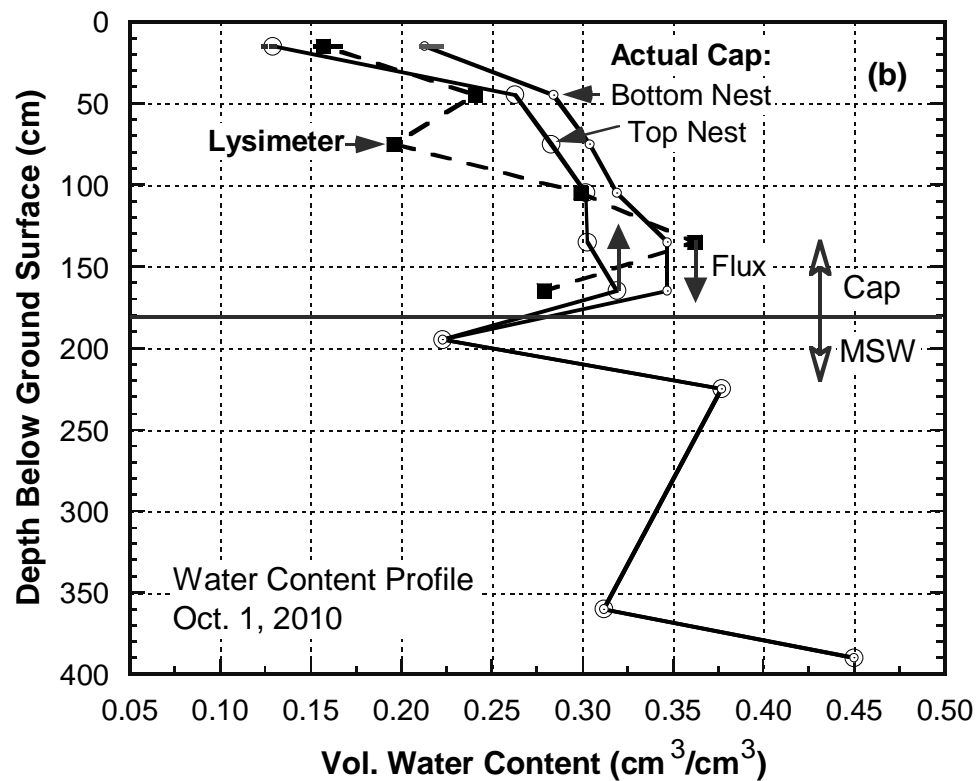
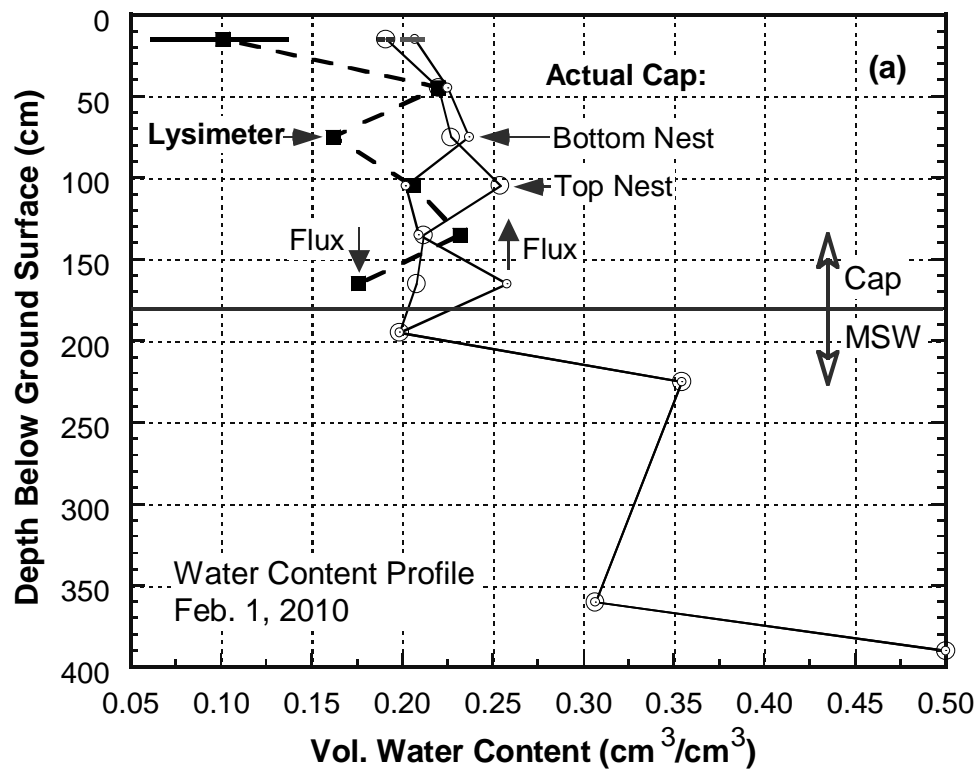


Figure 2-9: Measured water content profiles for the lysimeter and actual caps on 1 Feb. (a) and 1 Oct. 2010 (b).

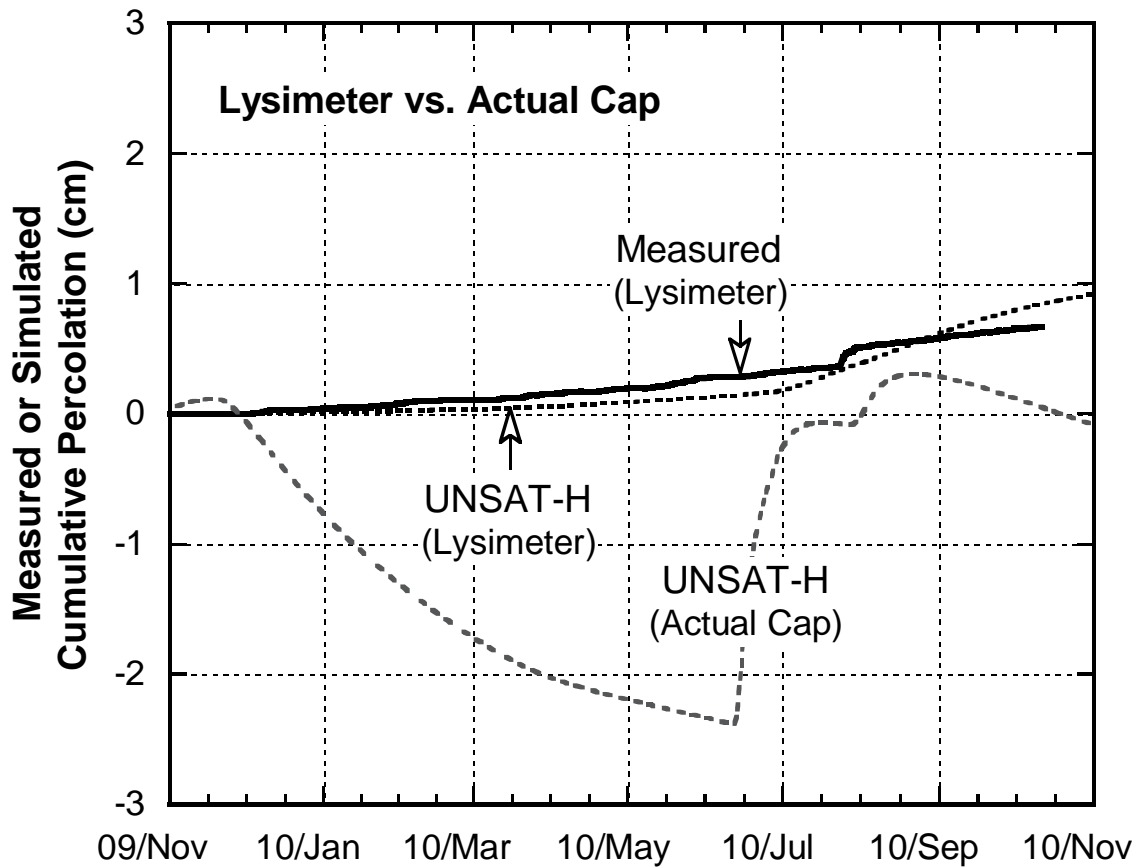


Figure 2-10: Measured and simulated cumulative percolation for the lysimeter and the actual cap.

interface is vertically upwards which would result in negative percolation into the waste. In addition, the water contents in the waste are lowest closer to the cap and waste interface and they increase deeper towards the leachate collection system. This trend in the water content profile indicates that the degree of saturation of the waste is expected to be higher near the leachate collection system, which is consistent with the field observations. However, below the cap, the waste has relatively low degree of saturation during various times of the monitoring period indicating that the magnitude of flux across the cap/waste interface would be relatively small.

NUMERICAL MODELING RESULTS

UNSAT-H simulations were conducted to predict the percolation and soil water storage for the test section for the period starting from November 2009 to October 2010. During this period, the site received 71.4 cm of precipitation. In addition, the lysimeter section was subjected to 20.8 cm of precipitation over a 48-hr period. During the monitoring period, the lateral flow collected from the topsoil layer (Figure 2-1) was negligible (~0.5 cm) and occurred only after relatively few precipitation events.

Soil Water Storage

Figure 2-11 shows the measured and simulated soil water storage for the lysimeter. The numerical model was able to capture the seasonal trends in the measured soil water storage. However, it did not predict the measured soil water storage accurately. Generally, the simulated soil storage is lower than the measured soil water storage which is also reported by Ogorzalek et al. 2008. During Winter 2010, UNSAT-H overestimated soil water storage because the model does not account the effect of frozen ground surface (Khire et al. 1999). In the field when the ground surface is frozen (Figure 2-6), subsequent infiltration is impeded whereas UNSAT-H allowed precipitation to infiltrate during this period causing the increase in soil moisture. Figure 2-6 shows that the ground surface of the lysimeter was frozen during Winter 2010 while it did not freeze for the actual cap. The heat flux from the waste in the landfill may have maintained slightly higher temperature for the actual cap compared to the lysimeter. The simulated soil water storage also showed smaller seasonal variation relative to the measured soil water storage which is similar to the findings of Fayer et al. (1992) and Khire et al. (1994). Fayer et al.

(1992) pointed out that the discrepancy is due to the overestimation of evaporation during winter and the underestimation of evaporation during the remainder of the year by UNSAT-H.

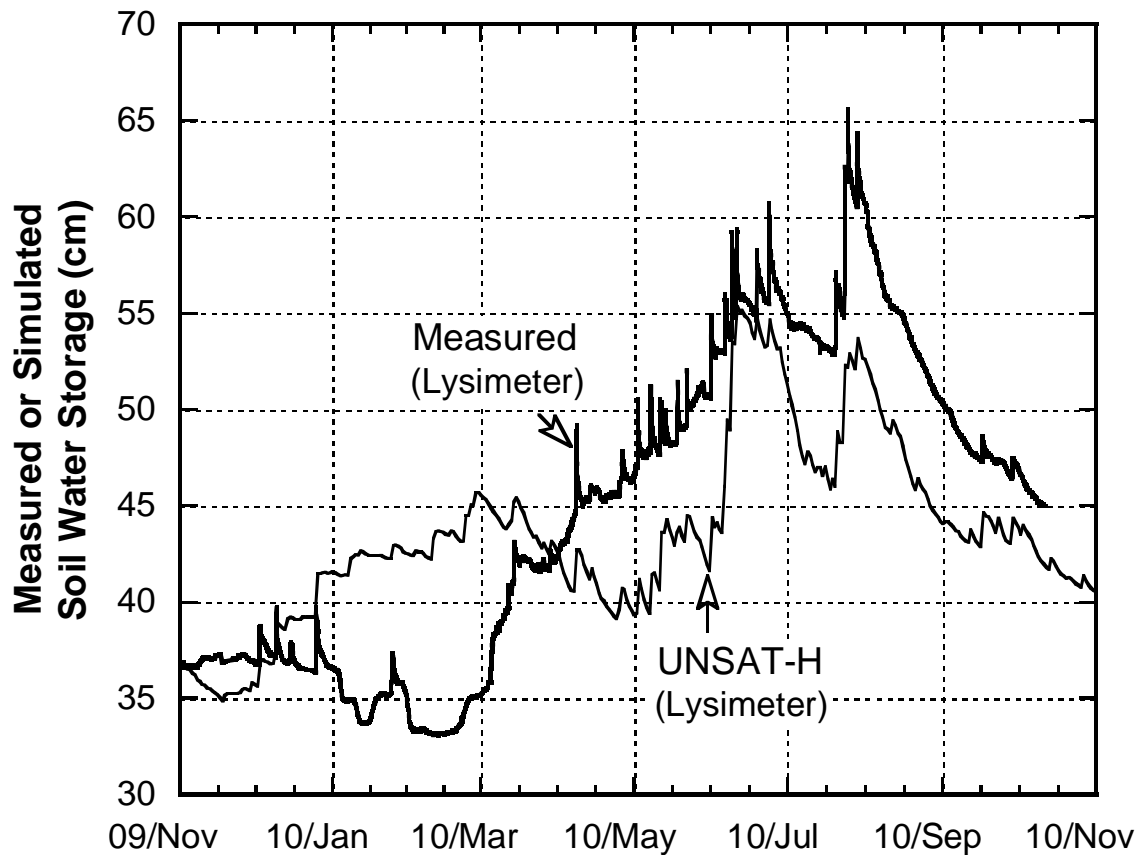


Figure 2-11: Measured and simulated soil water storage for the lysimeter.

Figure 2-12 shows the time series plot of comparison of simulated soil water storages for the lysimeter and the actual cap (underlain by MSW). Figure 2-12 shows that the soil water storage for the actual cap is always slightly greater than the soil water storage for the corresponding lysimeter except during sharp wetting events when both storages equate for a brief period of time. Measured soil water storage of the actual caps

is about the same as that for the lysimeter except when the lysimeter was subjected to irrigation wherein the lysimeter storage exceeded the actual caps and after Aug. 2010 when the soil water storage of the lysimeter steadily dropped and stayed below the storage of the actual caps (Figure 2-6).

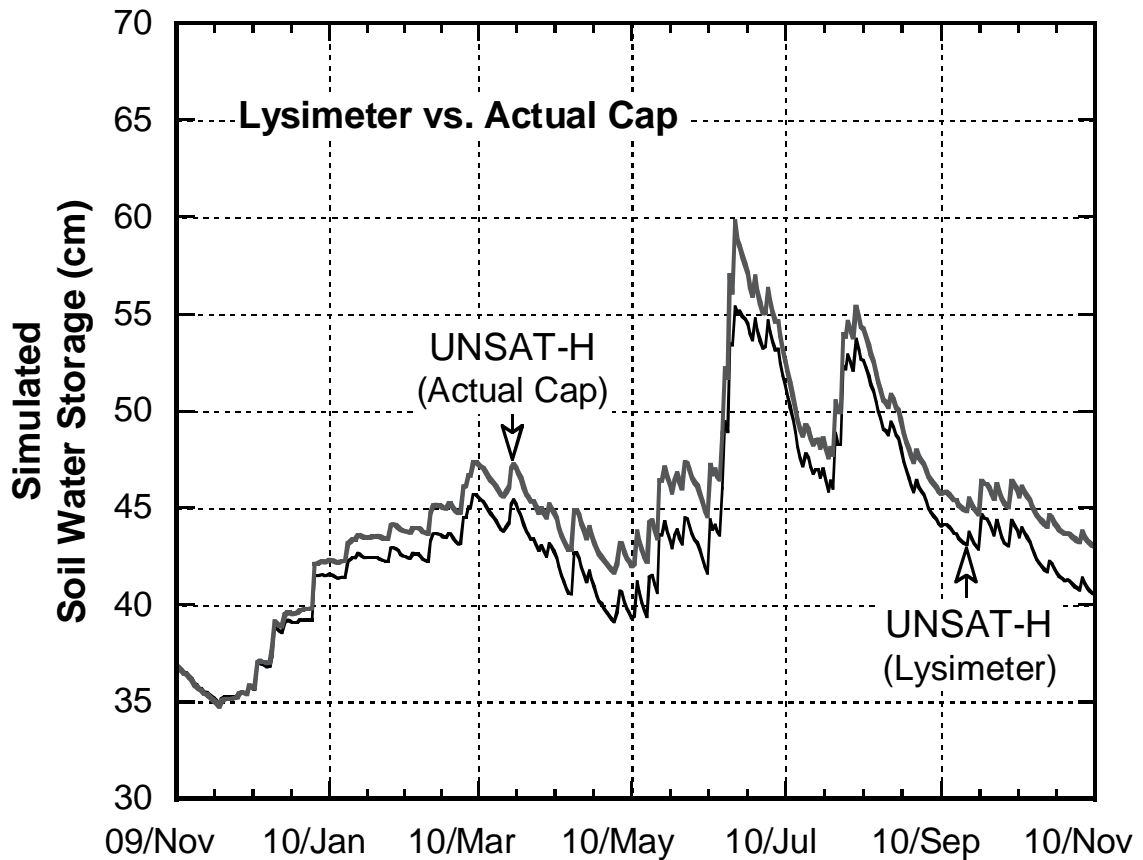


Figure 2-12: Simulated soil water storage for the lysimeter and the actual cap.

Percolation

Figure 2-10 shows the measured and simulated cumulative percolation for the lysimeter. During the one year monitoring period, the lysimeter received about 0.7 cm of percolation from about 71.4 cm of precipitation and 20.8 cm of irrigation carried out in

July 2010. The cumulative percolation predicted by UNSAT-H is relatively close to the measured percolation. There is a slight difference in the rate of change of percolation which occurred around Aug. 2010 in the field while the model simulated it in July 2010. UNSAT-H simulated volumetric water contents in test section are relatively close to the field water contents (Figure 2-8). While plants were simulated in the model, the amount of transpiration simulated by the model was negligible. It is due to the relatively short growing season in Detroit (~90 days) and less than 30 cm deep rooting depth observed in the field.

Percolation predicted by UNSAT-H for the actual caps which included the underlying waste layer with measured hydraulic properties of the waste input to the model is presented in Figure 2-10. The cumulative percolation predicted by the model was determined from the interlayer flux between the clay cover and the MSW interface. A positive value corresponds to a downward flux across the interface while a negative value corresponds to an upward flux. Figure 2-10 shows that the percolation for the actual cap is negative till about late June 2010. Negative flux indicates removal of water from the waste due to capillary pull from the overlying cap. In June 2010, the actual cap which was simulated using UNSAT-H was subjected to the 20.8 cm irrigation which the lysimeter was subjected to in the field to compare the lysimeter and actual cap under the same conditions. Figure 2-10 shows that the irrigation resulted in simulated percolation for the actual cap that was positive (downward). However, the net percolation for the actual cap simulated by UNSAT-H is about zero. It is consistent with the direction of the hydraulic gradient observed at the cap/waste interface which was mostly upward (Figure 2-9). This observation is also consistent with the simulated soil water storage

values that are presented in Figure 2-12. Figures 2-8 and 2-12 show that the simulated soil water storage for the lysimeter was lower than the actual cap and hence the simulated percolation for the lysimeter was greater than simulated percolation for the actual cap.

When Kazimoglu et al. (2005, 2006) hydraulic properties (Figure 2-4) were used to simulate the waste layer of the actual cap, the net cumulative percolation was negative (~ -2 cm) throughout the modeling period. Thus, the modeling results confirm that the percolation for the actual cap was less than the lysimeter. The results also demonstrate that even though the interlayer flux between the clay cover and the underlying MSW cannot be physically measured in the field, relative soil water storages can be used to estimate the relative magnitude of percolation for an actual cap.

SUMMARY AND CONCLUSIONS

Instrumented field-scale test section of a compacted native glacial till was constructed at a landfill located in Detroit, Michigan to compare the water balance of actual cap versus the lysimeter. Soil water contents, matric suctions, gas pressures, soil temperatures, and percolation were monitored using sensors for more than a year. The water balance model UNSAT-H was used to simulate and evaluate the differences in the hydrologic performance of an actual cap versus the corresponding lysimeter.

While the soil water storage of the lysimeter and the actual caps only had slight but subtle differences, the soil water content profiles indicated vertically downward hydraulic gradient for the lysimeter and primarily vertically upward hydraulic gradient for the actual cap throughout the monitoring period. The model predicted percolation and soil water storages were relatively similar to the field data. The model, which was

validated using the field data, predicted that the soil water storage for the actual cap would be slightly greater than that for the lysimeter and the model indicated negative as well as positive percolation with a net percolation close to zero for the actual cap.

Thus, the field data coupled with numerical modeling indicates that while percolation measured by a lysimeter for compacted clay soils which have relatively low hydraulic conductivity is greater than the percolation estimated for an actual cap which is placed on the waste, water balance of a lysimeter is relatively close to that of an actual cap. Hence, field-scale lysimeters, when designed and instrumented properly could be and should be used to assess the performance of an actual cap.

APPENDIX

APPENDIX

The numerical study presented in this paper was extended to model the field data obtained from the uncompacted test section. The uncompacted test section is identical to the compacted test section (Figure 2-1) except that the native clay that was used to build the storage layer was placed by a track dozer without any compaction effort (Figure 2-13). The reasons one of the test sections was not compacted are: (1) to simulate a conservative scenario for higher overall hydraulic conductivity of the storage layer of the cap, potentially less increase or no increase in the overall hydraulic conductivity of the clay due to root penetration and desiccation; and (2) to enhance ET from the test sections

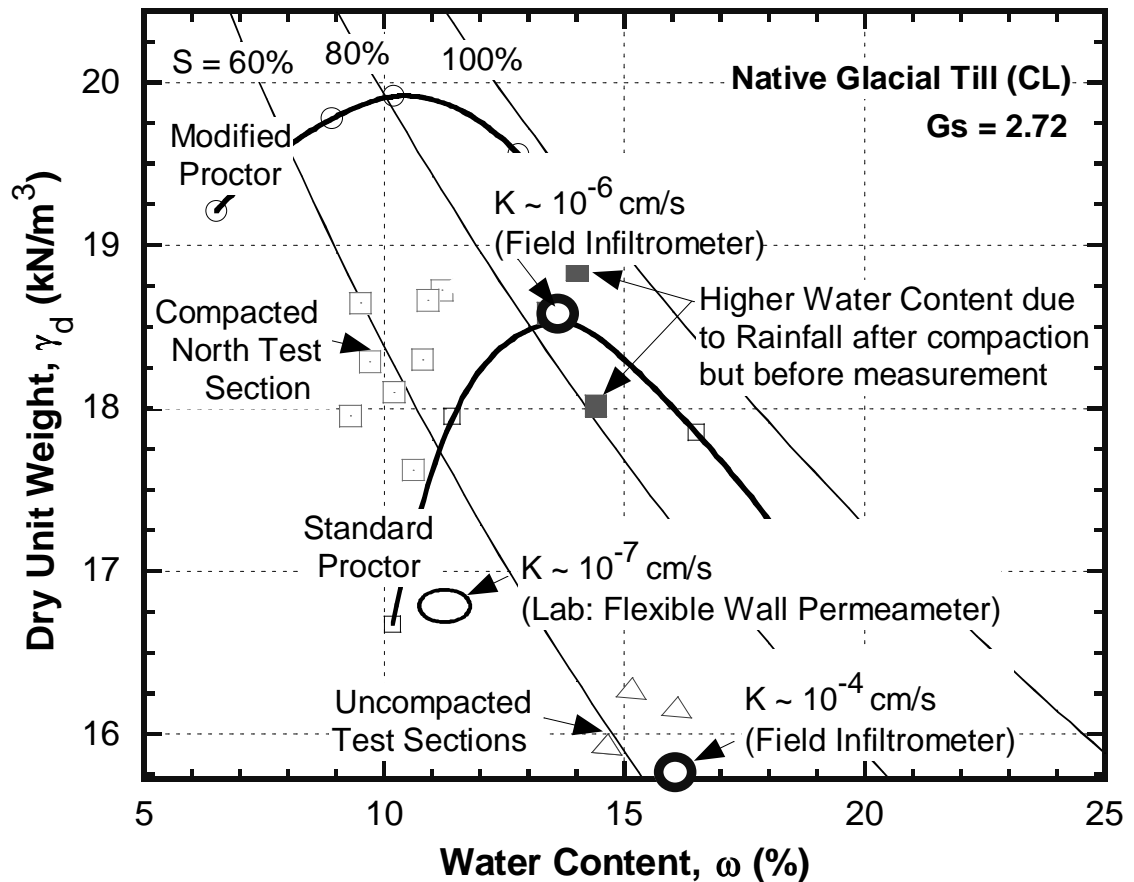


Figure 2-13: Field water contents and unit weights for the uncompacted test section.

by providing more void space for the plant roots to reach greater depths quickly in the test sections.

Material Properties

For the uncompacted test section, UNSAT-H (Fayer 2000) and Vadose/W (Geo-Slope 2007) simulations have been conducted. Table 2-3 presents the saturated and unsaturated hydraulic properties of the soils, as described in terms of the Haverkamp et al. (1977) fitting parameters, for the uncompacted test section. Field tracer tests and physical observations indicated that the uncompacted test section contained relatively large clods (15 to 60 cm in diameter) and relatively large inter-clod voids. Such field structure cannot be simulated in the lab with the conventional techniques. Hence, in order to predict the water balance of the uncompacted test section, the soil water characteristic curves and unsaturated hydraulic conductivity functions were estimated from the field

Table 2-3: Saturated and unsaturated hydraulic properties of the cap components for the uncompacted test section.

Soil	θ_s (cm ³ /cm ³)	θ_r (cm ³ /cm ³)	α	β (1/cm)	Ks (cm/s)	A	B (1/cm)
Topsoil	0.35	0.10	30	0.87	1.6×10^{-3}	120	1.14
Storage Layer	0.35	0.00	3000	0.6	1.3×10^{-4}	620	1.21
Landfilled Waste	0.58	0.14	18.74	0.972	1.0×10^{-3}	1.88×10^6	5.246

recorded water contents and water potentials. Figure 2-14(a) shows the data points from the field measurements and the fitted soil water characteristic curves. Figure 2-14(b) shows the data points obtained using instantaneous profile method (Meerdink et al. 1996) and the fitted unsaturated hydraulic conductivity function. Haverkamp et al. (1977) fitting equations were used because the soil water characteristic curves and unsaturated hydraulic conductivity functions are independently determined and described. Furthermore, Kazimoglu et al. (2005, 2006) hydraulic properties (Figure 2-4 and 2-14) were used to simulate the waste layer of the actual cap.

For UNSAT-H, the saturated and unsaturated hydraulic properties tabulated in Table 2-3 were used as input for the material properties in the simulations. For Vadose/W, apart from the hydraulic properties listed in Table 2-3, material thermal properties are also required by the program. In contrast with UNSAT-H where isothermal water flow can be specifically chosen, Vadose/W couples water and heat flow. Hence, Vadose/W requires these thermal properties as input: (1) volumetric specific heat function; and (2) thermal conductivity function. The volumetric specific heat functions were estimated using De Vries (1963) estimation method. A built-in Vadose/W tool estimates the function from the specified water retention curves. Soil mineral specific heat values of 0.8 and 1.674 kJ/g/°C were assumed for the topsoil and storage clay layer, respectively. A mass specific heat value of 0.71 kJ/g/°C was assumed for the landfilled waste. The thermal conductivity functions for each material were estimated using the built-in Vadose/W estimation tool. The thermal conductivity – volumetric water content relations were predicted using the Johansen (1975) estimation method with assumed soil

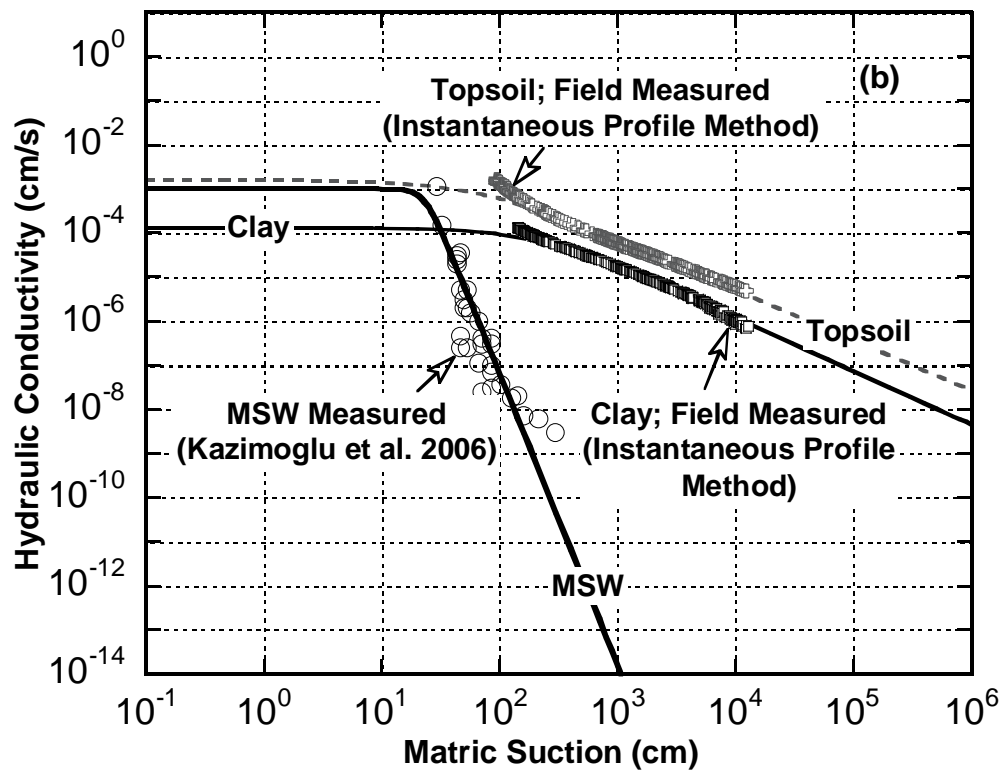
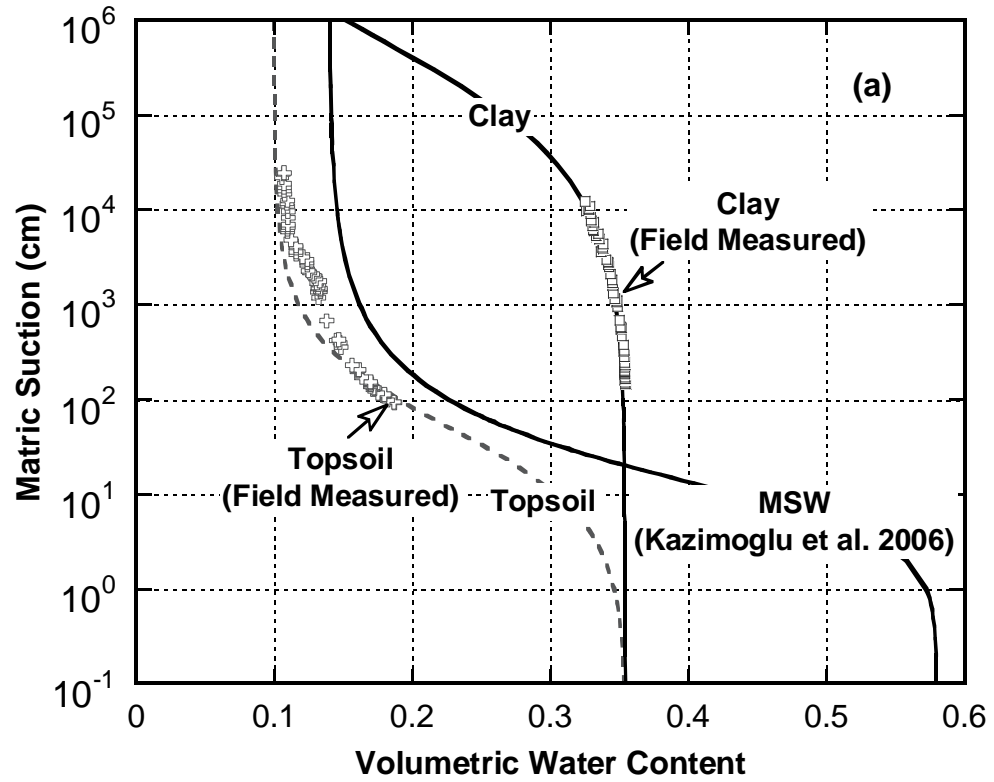


Figure 2-14: Measured soil water characteristic curves (a); and predicted hydraulic conductivity function (b) for the cap components for uncompacted test section.

mineral thermal conductivity of 280, 130, and 216 kJ/day/m/°C for the topsoil, clay cover, and landfilled waste, respectively. These typical values of thermal properties were obtained from the Vadose/W database (Geo-Slope 2007).

For Vadose/W simulations, the model requires daily values for maximum and minimum air temperature, maximum and minimum relative humidity, average wind speed, total precipitation, start and end times of precipitation, and total solar radiation or potential evapotranspiration. A sinusoidal climate distribution pattern was selected to distribute daily values of air temperature, relative humidity, solar radiation, and precipitation. The air temperature and relative humidity was assumed to be at their minimum values at sunrise and at their maximum values at 12:00 noon. The solar radiation was assumed to be zero before sunrise and after sunset and reached its peak value at 12:00 noon. The latitude of the location of the field test section (42.38° North) was used to approximate the sunrise and sunset times. Wind speed was applied as a constant value throughout the day. The daily precipitation was assumed to follow a sinusoidal distribution over the specified start and end times with its peak value occurring at the midpoint of the specified time interval.

Spatial discretization of the model domain was optimized by conducting sensitivity analysis. This was done by repeatedly refining the nodal spacing until insignificant changes in simulated water balance parameters were achieved. The nodal spacing between the nodes located near the upper and lower boundaries, as well as near the interface between layers, was relatively small (1 mm). Figure 2-15 shows the

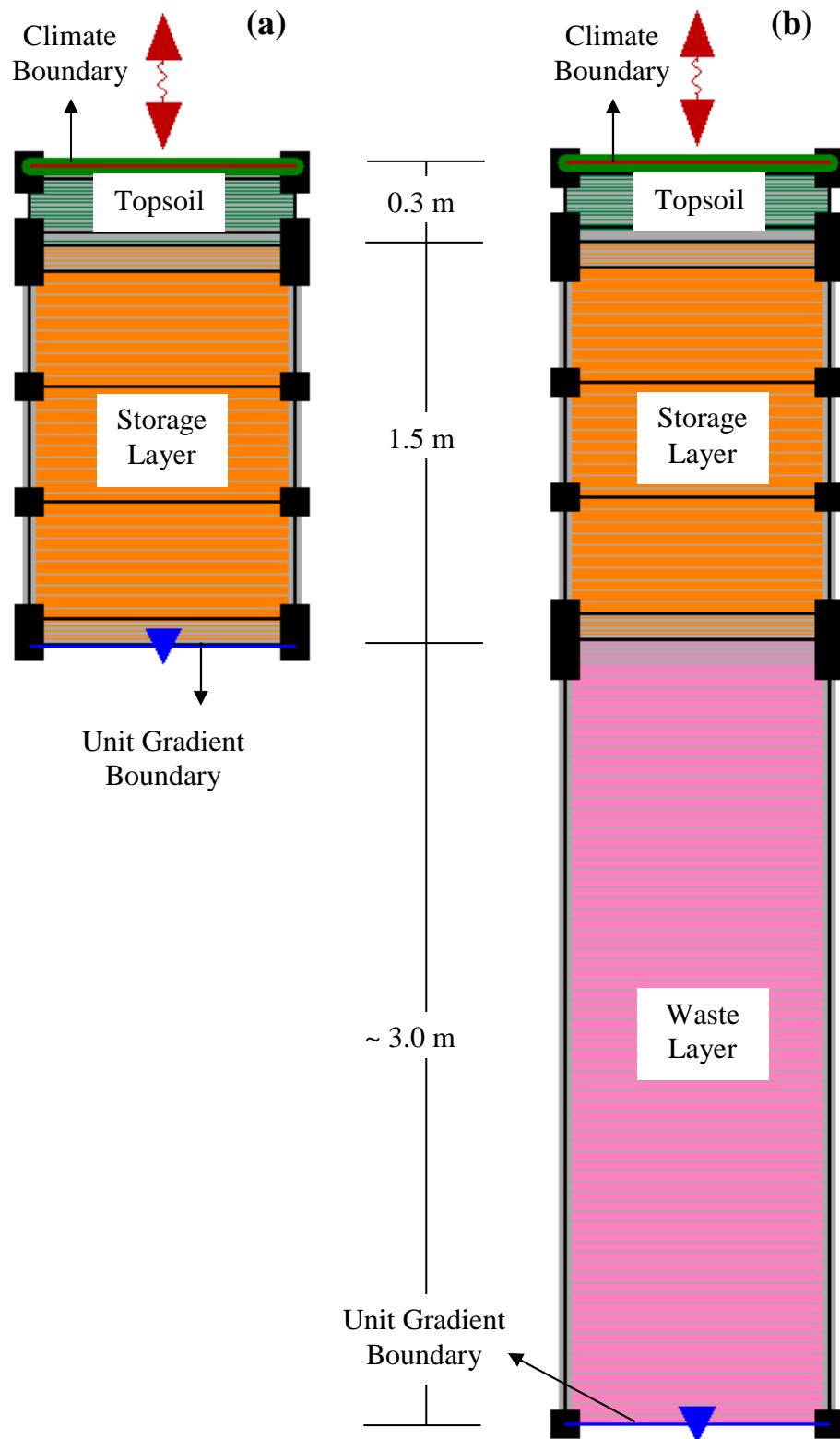


Figure 2-15: Typical mesh used for modeling in Vadose/W for: a lysimeter only (a); and an actual earthen cap with underlying waste (b).

snapshots of the model generated in Vadose/W for actual cap and its corresponding lysimeter simulations.

Uncompacted Test Section Simulations

UNSAT-H and Vadose/W simulations were conducted to predict the percolation and soil water storage for the uncompacted test section for the period from June 2008 to March 2009. During this period, the site received 68.5 cm of precipitation. Figure 2-16 shows that the cumulative percolation measured in the field from the lysimeter installed in the

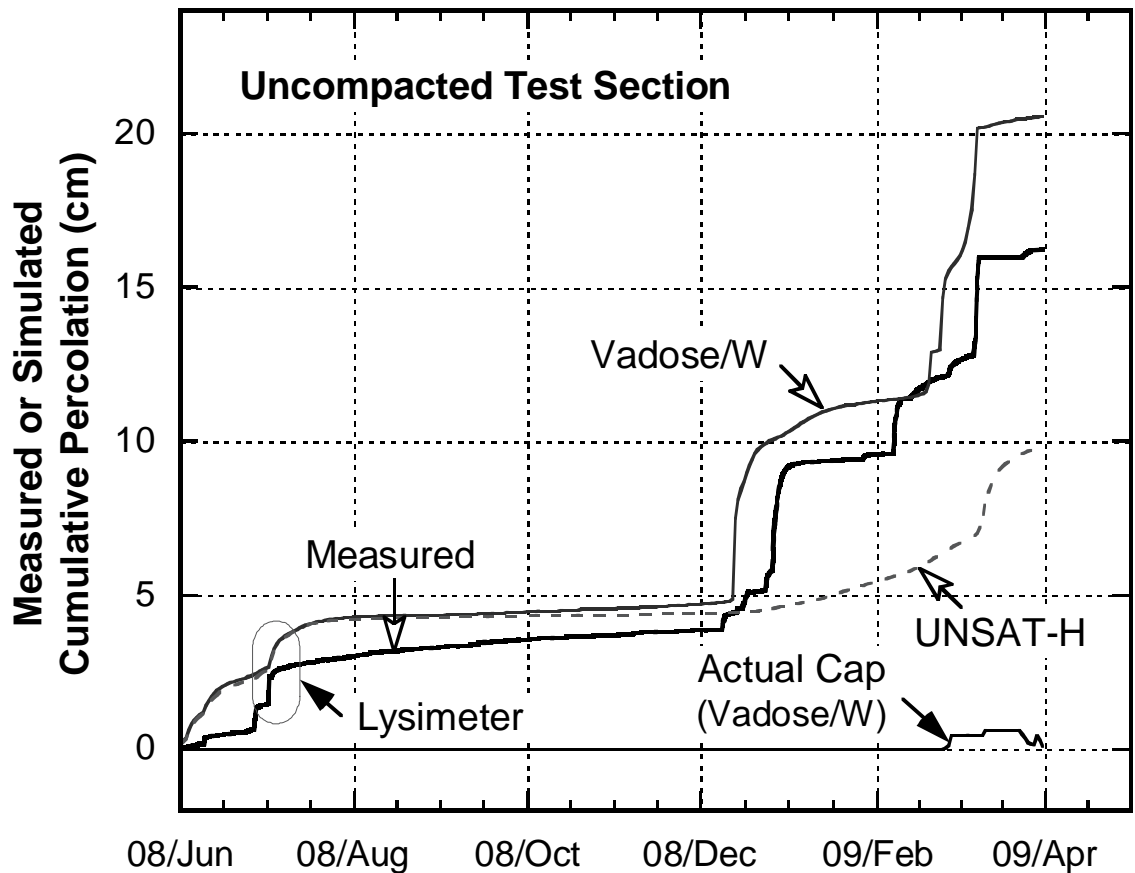


Figure 2-16: Field measured and numerically simulated cumulative percolation for the uncompacted test section.

middle of the uncompacted test section is about 16.2 cm. Since the clay cover was constructed without compaction, tracer tests and physical observations showed relatively large inter-clod voids in the clay which resulted to preferential flow for water. Hence, percolation from the uncompacted test section was significantly higher than that from the compacted test section. The percolation was about 24% of the applied precipitation. The preferential flow of water, also known as a macropore flow, is evident in Figure 2-16 as indicated by the sharp increases in the cumulative percolation plot. Figure 2-16 also shows the simulated cumulative percolation for the lysimeter using UNSAT-H and Vadose/W. UNSAT-H under predicted while Vadose/W over predicted the percolation. UNSAT-H failed to capture the sharp percolation pulses that occurred in the field. Vadose/W performed better since it was able to predict the onsets of percolation. However, the simulated percolation overestimated the field measured percolation. The simulated sharp increases in percolation also occurred earlier than those observed in the field.

Vadose/W was also used to estimate the percolation for the actual cap with underlying MSW located within the uncompacted test section. The resulting percolation across the interface between the soil cover and the underlying waste was relatively small. Upward flux of water (negative percolation) can be observed from the cumulative percolation plot. This is consistent with the data presented in Figures 2-17 and 2-18. The volumetric water contents measured at various depths within the lysimeter and the actual cap (upper nest) for the uncompacted test section are shown in Figure 2-17. The corresponding time series plot of the hydraulic gradient across the bottommost two sensors is shown in Figure 2-18. For actual cap, it can be seen that the bottommost two

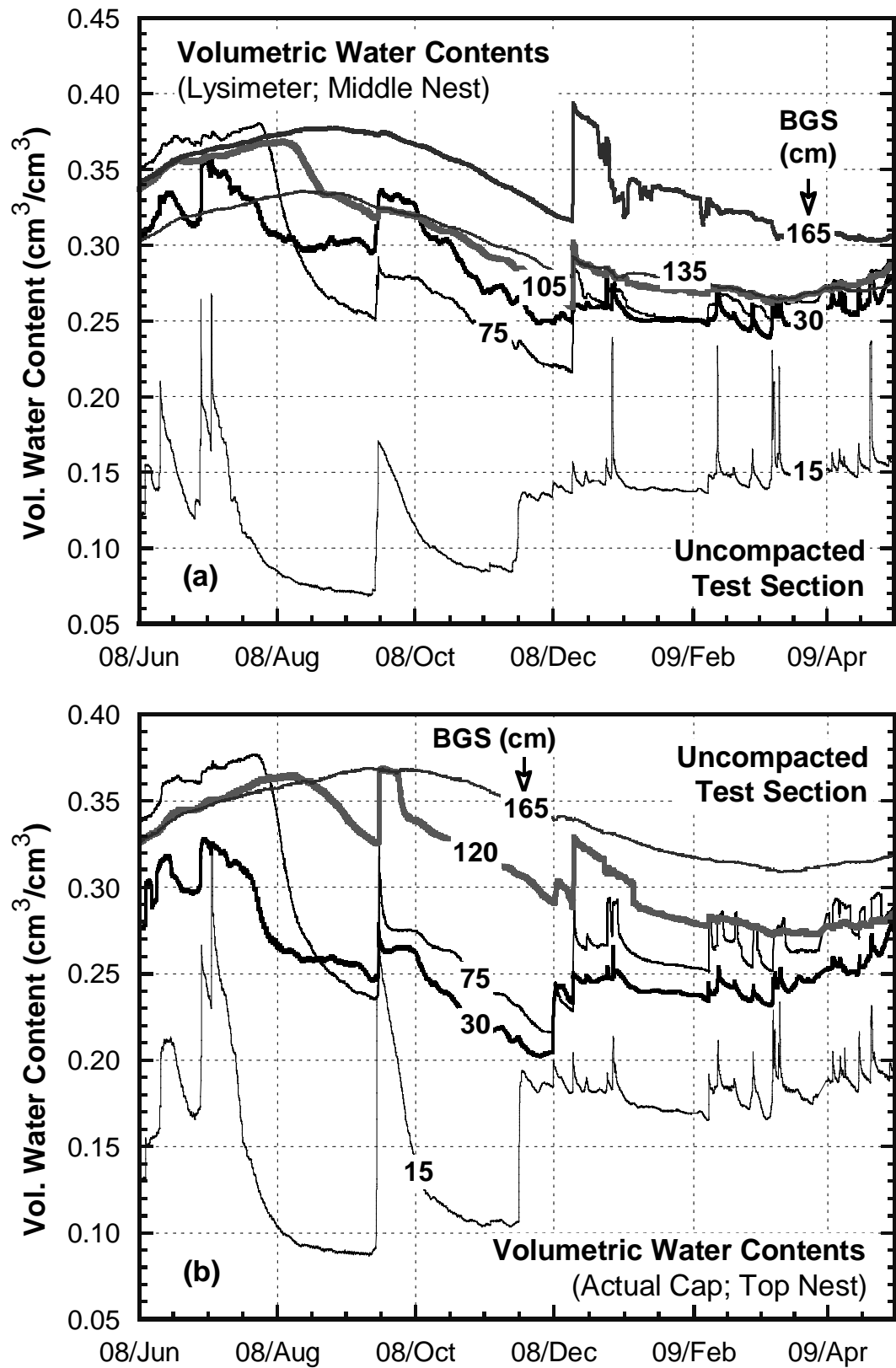


Figure 2-17: Measured volumetric water contents for the lysimeter (a) and actual cap (b).

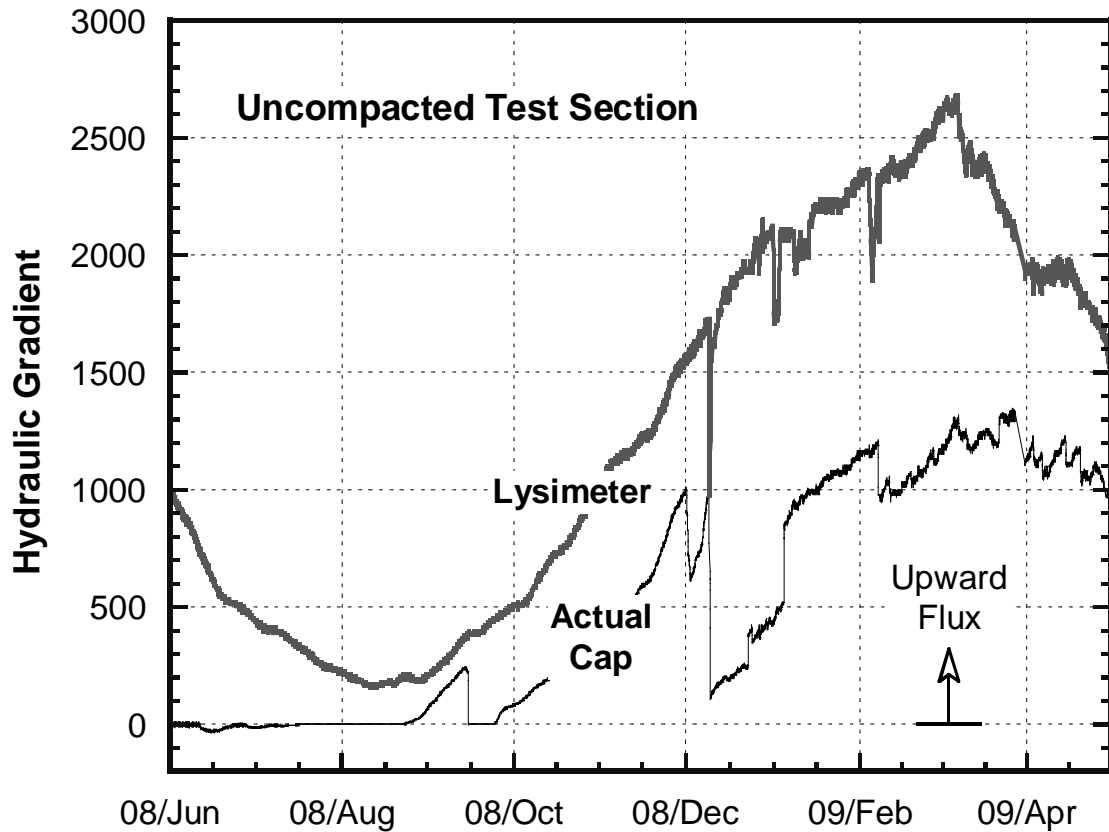


Figure 2-18: Calculated hydraulic gradient across the bottommost two sensors for the lysimeter and actual cap in the uncompacted test section.

water content readings at a given time indicate upward flux of moisture. For the lysimeter, similar observation can be seen and the resulting downward percolation observed is therefore indicative of macropore flow across inter-clod voids in the uncompacted clay test section.

Figure 2-19 shows the field measured soil water storage for the lysimeter installed in the middle of the uncompacted test section. Figure 2-19 also shows the simulated soil water storage using UNSAT-H and Vadose/W. Both numerical models were able to capture the fluctuations observed in the field. Neither models predicted the measured soil

water storage accurately. The simulated soil water storage for an actual cap with underlying MSW is generally higher compared to the simulated soil water storage for the corresponding lysimeter. This corresponds to lower percolation for the actual cap as illustrated in Figure 2-16.

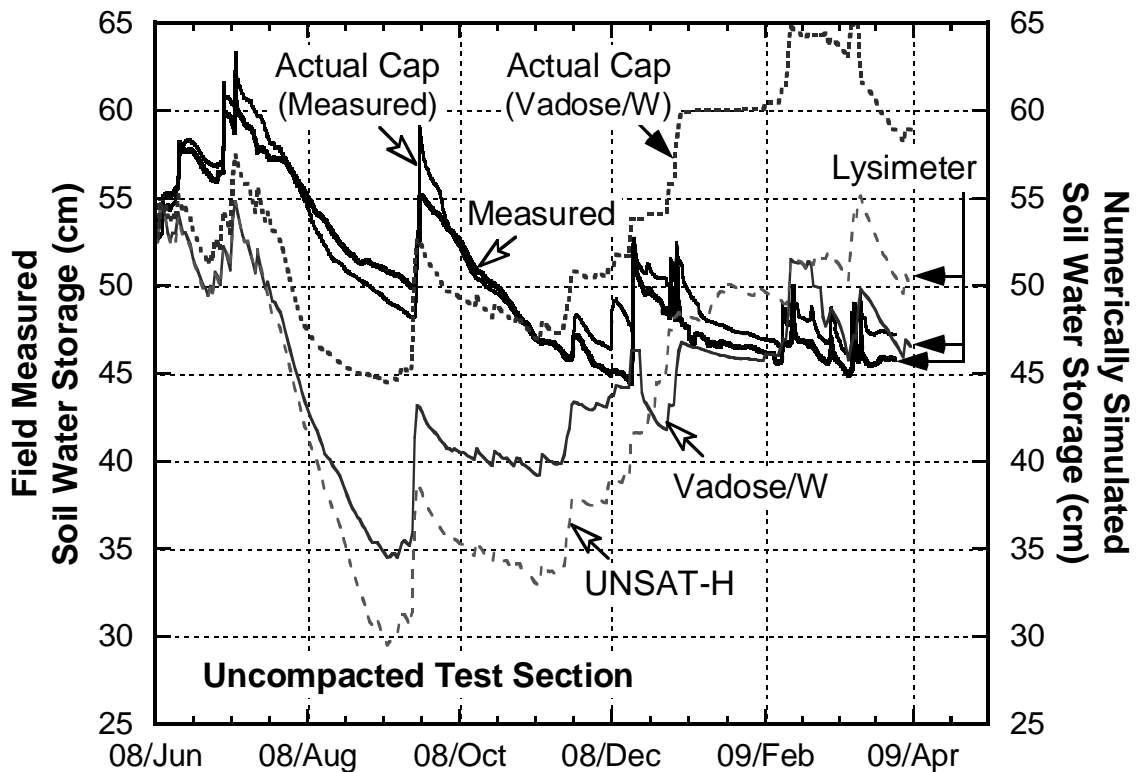


Figure 2-19: Field measured and numerically simulated soil water storage for the uncompacted test section.

Similar observation can be seen from the field measured soil water storage for an actual cap versus a lysimeter for the uncompacted test section. In contrast with the compacted test section wherein the soil water storage values for the lysimeter and the actual cap are close, Figure 2-20 shows that, for the uncompacted test section, the lysimeter has lower soil water storage than the actual cap. This is consistent with the

findings of Mijares et al. (2010). In their study, numerical simulations using Vadose/W were carried out for a range of hydraulic properties of the overlying soil cover to determine its effect on the soil water storage response of a lysimeter versus an actual cap.

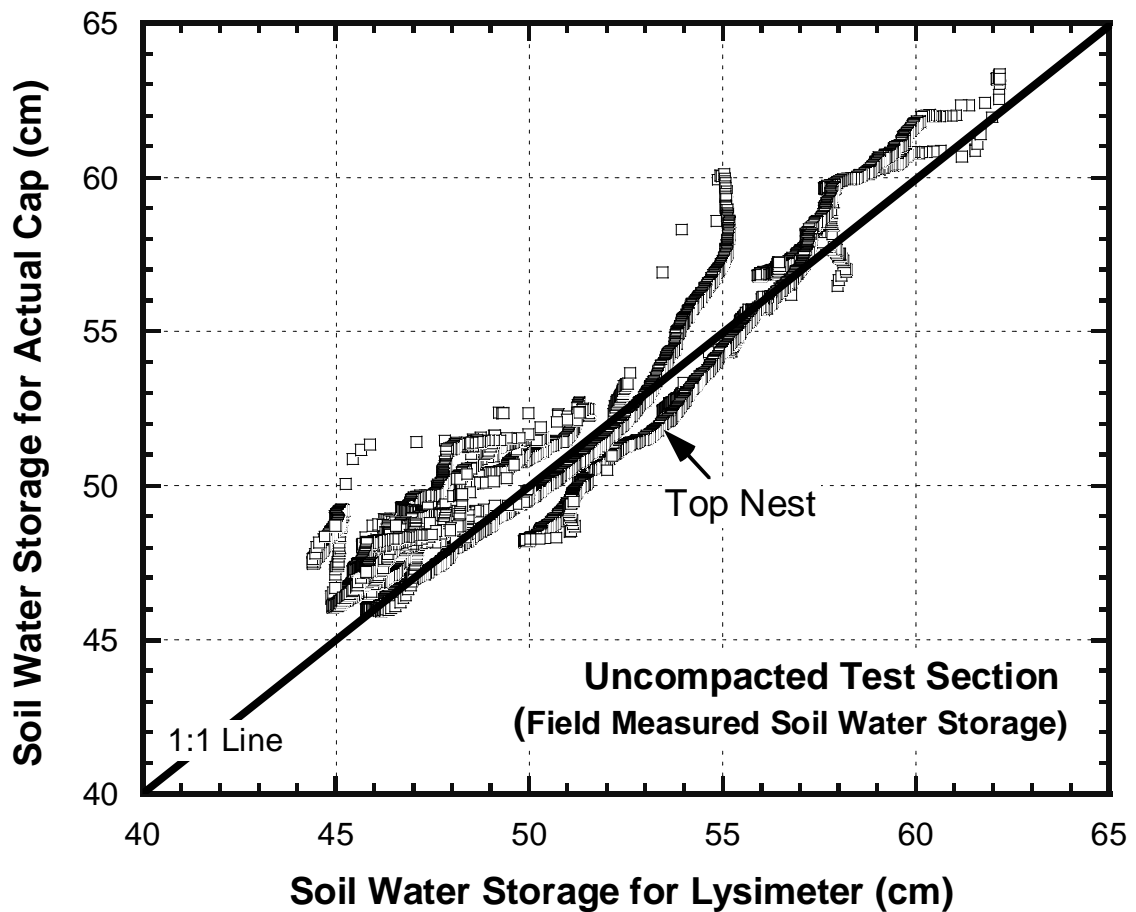


Figure 2-20: Correlation between measured soil water storage for actual cap versus lysimeter for the uncompact test section.

Figure 2-21 shows that as the saturated hydraulic conductivity of the soil cover increases, the soil water storage for a lysimeter greatly underestimates the soil water storage for an actual cap. This is because the underlying MSW acts as a capillary break due to its water retention curve that emulates a coarser soil. Mijares et al. (2010) further found out that

capillary barrier effect is significant only for a soil cover with saturated hydraulic conductivity greater than 10^{-5} cm/s. A high saturated hydraulic conductivity is evident for the uncompacted test section and therefore the measured soil water storage for the lysimeter is generally lower than the measured soil water storage for the actual cap of the uncompacted test section.

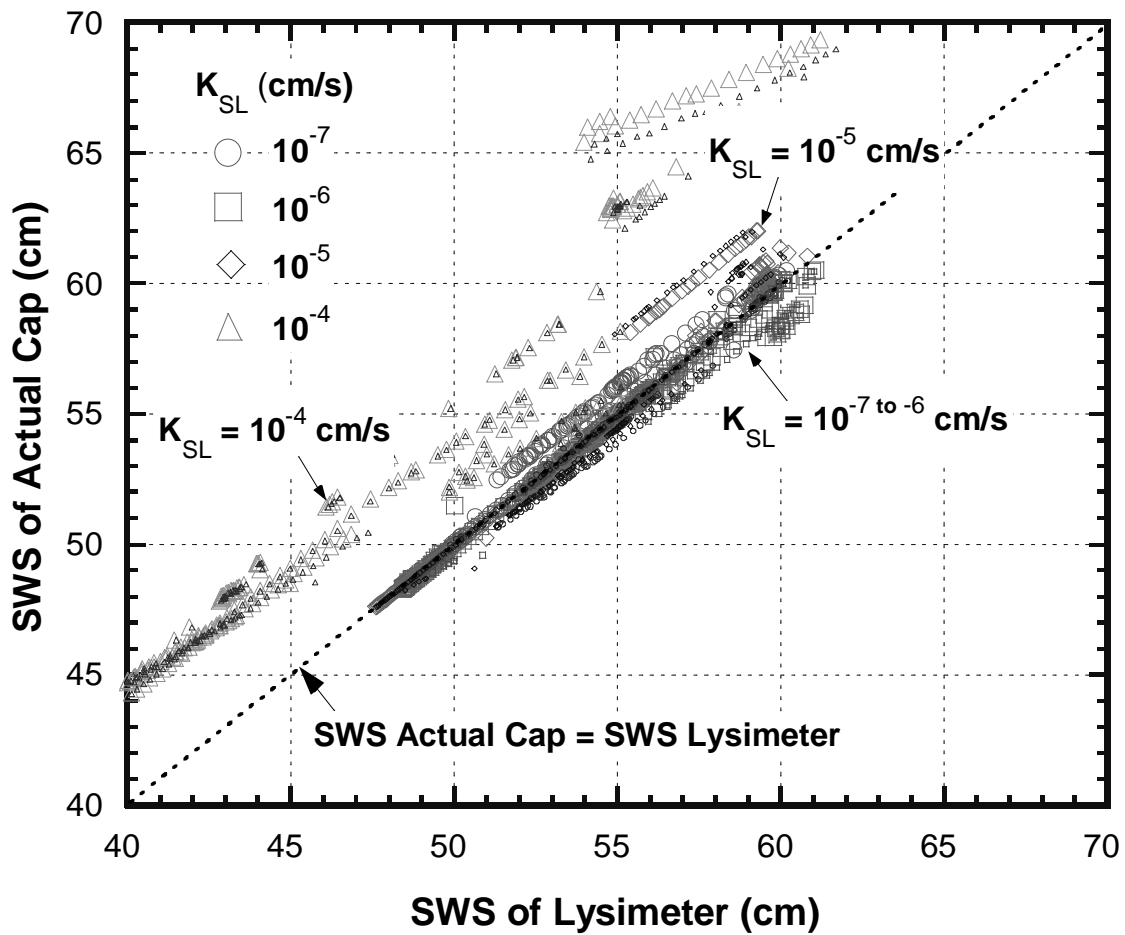


Figure 2-21: Correlation between the simulated soil water storage for an actual cap versus its corresponding lysimeter with varying hydraulic properties of soil cover (Mijares et al. 2010).

The simulation of the field response of the uncompacted test section showed that percolation obtained from the lysimeter was significantly greater than the estimated percolation of the actual cap (i.e., flux across the interface between the soil cover and underlying waste). Consequently, the simulated soil water storage of the actual cap for the uncompacted test section was generally higher compared to the simulated soil water storage of its equivalent lysimeter. This was consistent with the field measured soil water storages of both lysimeter and actual cap underlain by landfilled waste.

REFERENCES

REFERENCES

- Abichou, T., and Musagasa, J. (2008). "ET Covers: Construction and Tree Development Inside and Outside of Lysimeters," *Proceedings*, GeoCongress 2008, GSP No. 177, Geotechnics of Waste Management and Remediation, ASCE, Reston, VA: 72-79.
- Albright, W., Benson, C., Gee, G., Roesler, A., Abichou, T., Apiwantragoon, P., Lyles, B., and Rock, S. (2004). "Field Water Balance of Landfill Final Covers," *Journal of Environmental Quality*, 33 (6): 2317-2332.
- Benson, C., Bohnhoff, G., Ogorzalek, A., Shackelford, C., Apiwantragoon, P., and Albright, W. (2005). "Field Data and Model Predictions for an Alternative Cover," *Waste Containment and Remediation*, GSP No. 142, ASCE, Reston, VA: 1-12.
- Bohnhoff, G., Ogorzalek, A., Benson, C., Shackelford, C., and Apiwantragoon, P. (2009). "Field Data and Water-Balance Predictions for a Monolithic Cover in a Semiarid Climate," *Journal of Geotechnical and Geoenvironmental Engineering*, 135 (3): 333-348.
- Breitmeyer, R., Benson, C., Edil, T., and Barlaz, M. (2010). "Hydrologic Properties of Municipal Solid Waste," *Research Project Poster*, GeoEngineering Program, University of Wisconsin – Madison, Madison, WI.
- De Vries, D. (1963). "Thermal Properties of Soils," *Physics of Plant Environment*, North-Holland Publishing Company, Amsterdam, The Netherlands: 210-235.
- Fayer, M., Rockhold, M., and Campbell, M. (1992). "Hydraulic Modeling of Protective Barriers: Comparison of Field Data and Simulation Results," *Soil Science Society of America Journal*, 56: 690-700.
- Fayer, M. (2000). "UNSAT-H Version 3.0: Unsaturated Soil Water and Heat Flow Model – Theory, User Manual, and Examples," PNNL-13249, Pacific Northwest Laboratories, Richland, Washington.
- Geo-Slope. (2007). "Vadose Zone Modeling with Vadose/W 2007: An Engineering Methodology," GEO-SLOPE International Ltd., Alberta, Canada.
- Guyonnet, D., Amraoui, N., and Kara, R. (2000). "Analysis of Transient Data from Infiltrometer Tests in Fine-grained Soils," *Ground Water*, 38 (3): 396-402.
- Haverkamp, R., Valcin, M., Touma, J., Wierenga, P., and Vauchaud, G. (1977). "A Comparison of Numerical Simulation Models for One-dimensional Infiltration," *Soil Science Society of America Journal*, 41: 285-294.
- Johansen, O. (1975). "Thermal Conductivity of Soils," *Ph.D. Thesis*, University of Trondheim, Norway, CRREL Draft English Translation 637, US Army Corps of Engineers, Cold Regions Research and Engineering Laboratory, Hanover, NH.

- Kazimoglu, Y., McDougall, J., and Pyrah, I. (2005). "Moisture Retention and Movement in Landfilled Waste," *Proceedings*, GeoProb 2005: International Conference on Problematic Soils, Famagusta, Northern Cyprus, May 2005.
- Kazimoglu, Y., McDougall, J., and Pyrah, I. (2006). "Unsaturated Hydraulic Conductivity of Landfilled Waste," *Proceedings*, Unsaturated Soils 2006, GSP No. 147, ASCE, Reston, VA: 1525-1534.
- Khire, M., and Mijares, R. (2008). "Influence of the Waste Layer on Percolation Estimates for Earthen Caps Located in a Sub-humid Climate," *Proceedings*, GeoCongress 2008, GSP No. 177, Geotechnics of Waste Management and Remediation, ASCE, Reston, VA: 88-95.
- Khire, M., Benson, C., and Bosscher, P. (1994). "Final Cover Hydrologic Evaluation: Phase III," Environmental Geotechnics Report 94-4, University of Wisconsin – Madison, Madison, WI.
- Khire, M., Benson, C., and Bosscher, P. (1997). "Water Balance Modeling of Earthen Final Covers," *Journal of Geotechnical and Geoenvironmental Engineering*, 123 (8): 744-754.
- Khire, M., Benson, C., and Bosscher, P. (1999). "Field Data from a Capillary Barrier and Model Predictions with UNSAT-H," *Journal of Geotechnical and Geoenvironmental Engineering*, 125: 518–528.
- Khire, M., Benson, C., and Bosscher, P. (2000). "Capillary Barriers: Design Variables and Water Balance," *Journal of Geotechnical and Geoenvironmental Engineering*, 126 (8): 695-708.
- Meerdink, J., Benson, C., and Khire, M. (1996). "Unsaturated Hydraulic Conductivity of Two Compacted Barrier Soils," *Journal of Geotechnical and Geoenvironmental Engineering*, 122 (7): 565-576.
- Mijares, R., and Khire, M. (2010). "Evaluation of Geosynthetic Capillary Break in Earthen Cover Lysimeters," *Journal of Geotechnical and Geoenvironmental Engineering*, in review.
- Mijares, R., Khire, M., and Johnson, T. (2010). "Lysimeters versus Actual Earthen Caps: Numerical Assessment of Soil Water Storage," *Proceedings*, GeoFlorida 2010, GSP No. 199, Advances in Analysis, Modeling and Design, ASCE, Reston, VA: 2849-2858.
- Mukherjee, M. (2008). "Instrumented Permeable Blankets for Estimating Subsurface Hydraulic Conductivity and Confirming Numerical Models Used for Subsurface Liquid Injection," *Ph.D. Dissertation*, Michigan State University, East Lansing, Michigan, 278 p.

- Ogorzalek, A., Bohnhoff, G., Shackelford, C., Benson, C., and Apiwantragoon, P. (2008). "Comparison of Field Data and Water-balance Predictions for a Capillary Barrier Cover," *Journal of Geotechnical and Geoenvironmental Engineering*, 134 (4): 470-486.
- Passioura, J. (1977). "Determining Soil Water Diffusivities from One-step Outflow Experiments," *Australian Journal of Soil Research*, 15 (1): 1-8.
- Scanlon, B., and Milly, P. (1994). "Water and Heat Fluxes in Desert Soils 2: Numerical Simulations," *Water Resources Research*, 30: 721-733.
- Scanlon, B., Reedy, R., Keese, K., and Dwyer, S. (2005). "Evaluation of Evapotranspirative Covers for Waste Containment in Arid and Semiarid Regions in the Southwestern USA," *Vadose Zone Journal*, 4: 55-71.
- Stoltz, G., and Gourc, J. (2007). "Influence of Compressibility of Domestic Waste on Fluid Conductivity," *Proceedings*, 18th Congres Francais de Mecanique, Grenoble, France.
- van Genuchten, M. (1980). "A Closed-form Equation for Predicting the Hydraulic Conductivity of Unsaturated Soils," *Soil Science Society of America Journal*, 44: 892-898.

PAPER NO. 3: EFFECT OF UNDERLYING WASTE LAYER ON SOIL WATER STORAGE AND PERCOLATION ESTIMATES FOR LANDFILL EARTHEN CAPS

ABSTRACT

Lysimeters are commonly used for field-scale assessment of water balance of earthen caps, commonly referred to as alternative or evapotranspirative (ET) caps. While lysimeters can measure percolation through a cap, the lower hydraulic boundary of a lysimeter is not the same as an actual ET cap. In this study, numerical simulations of water balance of lysimeters and ET caps were carried out using UNSAT-H for a range of hydraulic properties of the cover soils and waste for semi-arid and humid climates. The numerical results show that due to the presence of waste underlying the cap, the soil water storage of an ET cap is generally greater than its corresponding lysimeter. This greater water storage capacity in an actual ET cap results in lower percolation as compared to its corresponding lysimeter. The numerical results also suggest that thicker cover soils would consistently have much lower lysimeter percolation as well as actual cap percolation. Furthermore, wetter climate, with high precipitation to potential evapotranspiration ratio, would generally have smaller difference in the soil water storage and percolation for an actual ET cap versus its corresponding lysimeter.

INTRODUCTION

When landfill reaches its capacity, a final capping system is installed. In the U.S., the minimum required design is a conventional cap which may consists of, among other components, a geomembrane liner and/or a compacted clay barrier layer [Resource

Conservation and Recovery Act (RCRA), Subtitle D, USEPA]. Capital construction cost of the conventional cap is usually greater than alternative earthen caps. RCRA includes a provision that allows alternative final cap design as long as it is capable of achieving an equivalent reduction in infiltration and protection from erosion that prescriptive caps may provide.

Several types of alternative caps, also known as earthen or evapotranspirative (ET) caps, have been considered for landfills primarily located in areas with arid and semi-arid climates (Khire et al. 1999; Albright et al. 2004; Scanlon et al. 2005). The best known method for assessing the performance of these alternative caps involves the installation of lysimeters at the proposed site to directly measure the percolation through the proposed cap. Numerical studies on lysimeters generally employ simulations that neglect the effect of the underlying waste (Khire et al. 2000; Benson et al. 2005) because percolation is collected through a drainage layer constructed above a geomembrane. While the geomembrane allows collection of infiltration through the cap, it prevents upward migration of moisture from the waste under evapotranspirative gradients. When an actual earthen cap is constructed, the geomembrane layer used for a lysimeter is not placed.

LYSIMETER VERSUS ACTUAL ET CAP

ET covers have been commonly used for landfills located in arid and semi-arid climates in lieu of prescriptive caps which require the use of geomembranes. Key advantages of ET caps include: (1) lower construction cost compared to prescriptive caps which contain a relatively expensive geomembrane layer (Hauser et al. 2001); and (2) greater soil depth

available for establishment of deeper roots for the vegetation which may reduce long-term erosion compared to the prescriptive caps. These benefits may allow additional options for end use of the landfill.

Approval of the use of an ET cover in lieu of a prescriptive cover typically requires site-specific demonstration of equivalency. Field demonstration of proposed ET cover usually entails the installation of lysimeter to directly measure the percolation through the landfill cap. These lysimeters have a relatively impermeable geomembrane at the bottom boundary to facilitate the collection of drainage in a drainage layer located immediately above the geomembrane layer (Khire et al. 1997; Benson et al. 2001).

The water balance of a lysimeter which includes percolation through the cap is a function of many site-specific and design-specific parameters including the boundary conditions. While the upper surface boundaries of a lysimeter cap and an actual ET cap are identical, the lower boundaries are significantly different. Lysimeters contain an impermeable (zero flux) lower boundary (Abichou et al 2006; Khire and Mijares 2008). This bottom boundary is hydraulically permeable in an actual ET cap. The lower zero-flux boundary in a lysimeter prevents the upward flux of liquid and vapor from the waste mass or subgrade layer located below the cap. This bottom boundary in a lysimeter may also restrict the heat flux from the waste mass present below the cap which may influence the actual percolation rate. Several studies have identified this concern (Benson et al 2001; Abichou and Musagasa 2008; Khire and Mijares 2008).

Khire and Mijares (2008) carried out numerical water balance simulations of ET caps and corresponding lysimeters. Khire and Mijares (2008) have presented the ratio of average annual percolation for an actual ET cap and average annual percolation for the

corresponding lysimeter for a range of hydraulic properties of the cap components. It has been observed that cumulative percolation for lysimeters would be typically greater than the percolation at the bottom of corresponding ET cap. Thus, percolation measured by lysimeter is conservative. Khire and Mijares (2008) showed that the percolation measured by lysimeters can be up to an order of magnitude greater than the actual cap depending upon the saturated and unsaturated hydraulic properties of the soils and underlying waste layer.

Hardt (2008) carried out numerical evaluation of percolation through ET caps and the corresponding lysimeters using the dual permeability option in HYDRUS (beta version) (Simunek et al 2008; Simunek and van Genuchten 2008). Hardt (2008) found that the magnitude of percolation measured by a lysimeter is 1 to 3 orders of magnitude greater than the percolation in an actual ET cap when soil layers of the cap contain preferential flow channels (e.g., desiccation cracks). Thus, when numerical results of Khire and Mijares (2008) are combined with findings by Hardt (2008), it can be inferred that a lysimeter will likely further overestimate the percolation as the bulk hydraulic conductivity of the cap potentially increases with the age of the cap due to various factors (Benson et al 2007). A lysimeter overpredicts percolation because the infiltrated water drained into the lysimeter is immediately removed. Hence, it is not available for removal by evapotranspiration. In ET caps, where a geomembrane does not exist below the cap, percolation into the waste may be temporarily stored in the waste and can be removed by evapotranspiration.

OBJECTIVE

While it is not possible to directly measure percolation without a lysimeter, it is possible to measure soil water storage in an ET cap using established techniques (Khire et al. 1999) and numerically estimate percolation using a calibrated model. Hence the key objective of the numerical study presented in this paper is to estimate percolation for actual ET caps using the measured soil water storage and percolation of corresponding lysimeter. In the field, the soil water storage is typically determined by integrating the water content values over the thickness of the cap. Comparative predicted soil water storage variations and percolation rates through lysimeters and actual caps (without lysimeters) were evaluated for semi-arid and humid climates for caps with varying hydraulic properties of landfilled waste.

WATER BALANCE MODEL

The finite-difference water balance model UNSAT-H (Fayer 2000) was used in this study. UNSAT-H numerically solves a modified form of Richards' equation to compute the flow of water through both saturated and unsaturated soil. This model has been routinely used for water balance modeling of earthen caps (Khire et al. 1997; Khire et al. 2000; Benson et al. 2005; Scanlon et al. 2005; Ogorzalek et al. 2008; Bohnhoff et al. 2009). For this study, one-dimensional simulations were carried out using UNSAT-H Version 3.0.

A schematic of the conceptual model used in the numerical simulations is shown in Figure 3-1. For the lysimeter, the soil cap was underlain with a geocomposite drainage layer, similar to its typical installation in the field. In order to simulate an actual cap, the

soil cap was assumed to have underlain by a 3-m thick waste layer. Additional simulations with thicker waste layer were carried out. However, thicker waste layer did not significantly influence the percolation and soil water storage of the simulated caps.

Landfill soil covers consisting of a topsoil layer and a compacted clay layer was considered in this study. This cross section is a relatively basic form for an alternative earthen cap. The compacted clay layer provides the required storage for the ET cap to temporarily store infiltrated water during wet periods and releases it back to the atmosphere during dry periods via evapotranspiration. The topsoil layer provides a medium for vegetation to develop in order to enhance transpiration. It also protects the underlying compacted clay against desiccation.

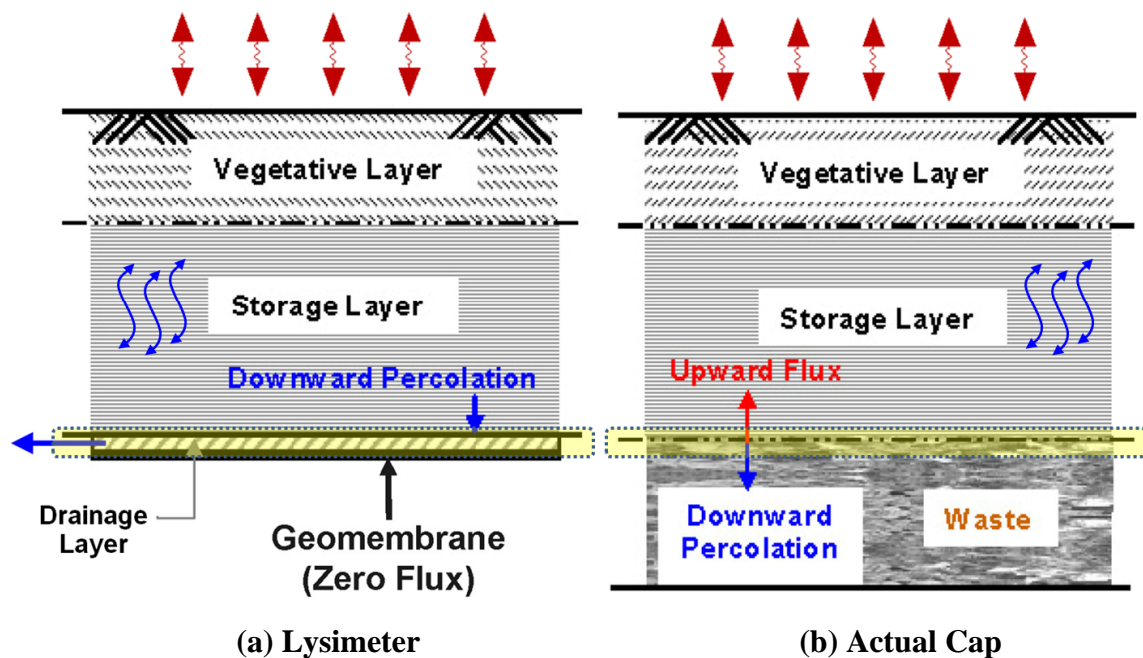


Figure 3-1: Conceptual model for numerical simulation of alternative capping system consisting of a lysimeter only (a); and a typical ET cap with underlying waste (b).

The ET caps considered in this study are based from the instrumented earthen final cover test sections built by Khire et al. (1997). A test section was constructed in East Wenatchee, Washington to assess the water balance of earthen cap in a semi-arid climate. The instrumented soil cap consisted of a 15-cm thick silty topsoil layer underlain with a 60-cm compacted Wenatchee silty clay as storage layer. A test section was also constructed in Atlanta, Georgia to assess the water balance of earthen cap in a humid climate. The instrumented soil cap also consisted of a 15-cm thick silty topsoil layer. However, a thicker storage layer was placed to accommodate the inherent wetter condition in this area. A 90-cm thick compacted Georgia red clay was used to build the test section. Underneath both test sections, a geocomposite drainage layer was placed above the textured geomembrane lining to facilitate the collection and drainage of percolated water to a measuring or monitoring device(s).

Material Properties

Table 3-1 summarizes the saturated and unsaturated hydraulic properties of the original soils used to build the instrumented test sections in Wenatchee and Atlanta (Khire et al. 1997). The soil water characteristic curve was expressed by the Haverkamp function:

$$\frac{\theta - \theta_r}{\theta_s - \theta_r} = \frac{\alpha}{\alpha + \Psi^\beta} \quad (3-1)$$

where θ is the volumetric water content for a given matric suction, Ψ ; θ_s is the saturated water content; θ_r is the residual water content; and α and β are the curve

fitting parameters. Similarly, the unsaturated hydraulic conductivity function was expressed by the Haverkamp equation:

$$\frac{K_{\Psi}}{K_S} = \frac{A}{A + \Psi^B} \quad (3-2)$$

where K_{Ψ} and K_S are the unsaturated and saturated hydraulic conductivities, respectively; and A and B are the curve fitting parameters (Haverkamp et al. 1977). Both the soil water characteristic curve and the unsaturated hydraulic conductivity data were independently measured by Khire et al. (1997).

Table 3-1: Saturated and unsaturated hydraulic properties of soils used in the instrumented field test sections of Khire et al. (1997).

Soil	θ_s (cm ³ /cm ³)	θ_r (cm ³ /cm ³)	α	β (1/cm)	K_s (cm/s)	A	B (1/cm)
Wenatchee Topsoil	0.40	0.05	80	0.60	4.5×10^{-5}	300	2.2
Wenatchee Compacted Silt Clay	0.36	0.05	72	0.60	2.2×10^{-7}	400	1.3
Atlanta Topsoil	0.40	0.08	200	0.65	1.0×10^{-4}	1	1.45
Atlanta Compacted Red Clay	0.52	0.08	17	0.40	3.2×10^{-6}	8	1.15

Table 3-2 presents the saturated and unsaturated hydraulic properties of the additional materials used in the simulations (i.e., geotextile and waste properties). Water characteristic curves were obtained from published literatures as indicated in the table. Unsaturated hydraulic conductivity functions were estimated using the closed-form van Genuchten-Mualem expression where the pore interaction term was set to 0.5 (van Genuchten 1980). Afterwards, the Haverkamp fitting parameters were determined for the water characteristic curves and unsaturated hydraulic conductivity functions.

Table 3-2: Saturated and unsaturated hydraulic properties of geotextile and waste used in the simulations.

Material	θ_s (cm³/cm³)	θ_r (cm³/cm³)	α	β (1/cm)	Ks (cm/s)	A	B (1/cm)
Geotextile (Park and Fleming 2006)	0.82	0	22307.2	3.533	1.5×10^{-1}	5.24×10^{10}	9.4
Loose Waste (Measured; Landfilled MSW)	0.67	0.20	1.62	0.293	1.0×10^{-2}	1.00×10^2	2.5
Loose Waste (Kazimoglu et al. 2006)	0.58	0.14	18.74	0.972	1.0×10^{-3}	1.88×10^6	5.246
Dense Waste (Breitmeyer et al. 2010)	0.61	0.011	10.38	0.58	4.0×10^{-5}	1.00×10^1	2.96

Hydraulic properties of nonwoven geotextile were obtained from Park and Fleming (2006). The nonwoven, polypropylene, needle-punched, continuous fiber

geotextile has a mass per unit area of 550 g/m^2 with a thickness of 4.0 mm and an opening size of 0.05 to 0.15 mm. It has similar properties to that of the geotextile used in the study of Stormont and Morris (2000). Haverkamp fitting parameters were obtained based from the data points measured by Park and Fleming (2006) for the geotextile's water retention curve.

For actual ET cap simulations, due to inherent heterogeneity of municipal solid waste (MSW), two MSW properties were considered: (1) a loosely compacted MSW typically found on landfills at shallow depth, and (2) a densely compacted MSW which is commonly found buried deep in landfills. For loose MSW, two properties were further used in the simulations.

The first was measured in the laboratory for MSW collected from the landfill from 6 to 12 m depths. The MSW sample was obtained using a 45 cm diameter auger. The waste, without sorting or screening, was placed in a relatively large PVC cell (30 cm diameter, 25 cm tall) to measure the saturated hydraulic conductivity using the falling head test (ASTM D5084) and the same sample was spun in a geotechnical centrifuge at up to 40 g gravitational force added to the sample in 1 to 3 g increments to measure the water retention function (ASTM D6836). The centrifuge not only allowed the measurement of the water retention function relatively rapidly, it also simulated the normal stress experienced by the waste at the depth it was collected. The dry density of the waste at the vertical stress simulated in the centrifuge was 0.69 g/cm^3 . The saturated hydraulic conductivity of the specimen is 10^{-2} cm/s . The method developed by Passioura

(1977) was applied to the water retention data collected from the centrifuge test to estimate the unsaturated hydraulic conductivities for the waste.

Hydraulic properties of MSW reported by Kazimoglu et al. (2005, 2006) were also assumed to represent the loose MSW layer in the actual cap. Kazimoglu et al. (2005, 2006) determined the waste retention properties for a laboratory prepared waste specimen which has composition similar to the waste found in Lyndhurst landfill in Australia that is located at shallow depth with a dry density of 0.57 g/cm^3 . Stoltz and Gourc (2007) published similar waste retention curves for loosely compacted MSW having a dry unit weight equal to 0.54 g/cm^3 . For loosely compacted MSW such as those found within landfills at shallow depth (i.e. beneath the final cover), a saturated hydraulic conductivity of 10^{-3} cm/s has been reported (Mukherjee 2008). Hence, this estimated value for MSW was adopted for this study. The corresponding predicted unsaturated hydraulic conductivity function shows good agreement, at high suction, with the measured unsaturated hydraulic conductivity function using one-step outflow method (Kazimoglu, 2006).

Since MSW is generally heterogeneous with highly varying properties, a dense MSW with lower hydraulic conductivity was also considered to determine its relative impact on the resulting soil water storage and percolation for the ET cap. Breitmeyer et al. (2010) presented the measured water characteristic curve and unsaturated hydraulic conductivity function for a dense MSW with dry density of 0.81 g/cm^3 using hanging column and multi-step outflow method, respectively. The saturated hydraulic conductivity of the specimen is $4.0 \times 10^{-5} \text{ cm/s}$. The measured and predicted unsaturated

hydraulic conductivity function show good agreement across the entire range of suction (Breitmeyer et al. 2010).

Figure 3-2 shows the water characteristic curves and the hydraulic conductivity functions for the soils used to build the instrumented test section in Wenatchee as well as the geotextile and the waste presented in Table 3-2. Figure 3-3 shows the water characteristic curves and the hydraulic conductivity functions for the soils used to build the instrumented test section in Atlanta as well as the geotextile and the waste presented in Table 3-2.

Meteorological Data

Daily meteorological data were compiled by Khire et al. (1997) for Wenatchee and Atlanta test sections. Field measurements were obtained for daily maximum and minimum air temperatures, average dew point temperature, total solar radiation, average wind speed, average cloud cover, and total precipitation. These meteorological data were used as input to UNSAT-H.

For all numerical analyses, precipitation was applied at an hourly frequency specifically during the time intervals it occurred during a particular day. The first year of field measured data for both test sections was used in the simulations. Annual precipitation for the landfill site in Wenatchee is 26.5 cm with an annual potential evapotranspiration of 109.1 cm ($P/PET \sim 0.24$). Annual precipitation for the landfill site in Atlanta is 153.6 cm with an annual potential evapotranspiration of 109.8 cm ($P/PET \sim 1.40$).

Initial and Boundary Conditions and Numerical Control Parameters

A variable flux boundary was applied at the ground surface (Figure 3-1) for the lysimeter as well as the actual cap. A unit gradient boundary condition was imposed on the lower boundary of the model domains. The unit gradient boundary used for the lysimeter was applied under two scenarios: (1) at the bottom of the compacted clay layer for lysimeter without considering the geotextile layer, and (2) at the bottom of the geotextile layer for lysimeter considering the geocomposite drainage layer. The unit gradient boundary used for the actual cap was applied at the bottom of the waste layer. Khire and Mijares (2008) and Mijares et al. (2010) have used the same lower boundary condition for simulations with waste layer. Initial conditions for UNSAT-H were specified using matric suctions corresponding to in-situ water contents measured by Khire et al. (1997) for both test sections. For actual cap simulations, the initial conditions for the waste layer were based from the matric suctions corresponding to the in-situ MSW water contents measured from the field test sections discussed in Paper No. 1.

Spatial discretization of the model domain was optimized by conducting sensitivity analysis. This was done by repeatedly refining the nodal spacing until insignificant changes in simulated water balance parameters were achieved. The nodal spacing between the nodes located near the upper and lower boundaries, as well as near the interface between layers, was relatively small (1 mm). A maximum time step of 0.1 hr and a minimum time step of 10^{-7} hr were used for all the simulations. This was necessary to accurately evaluate the extreme drying and wetting conditions typically encountered at the ground surface. At any given time step, the maximum allowable mass balance error

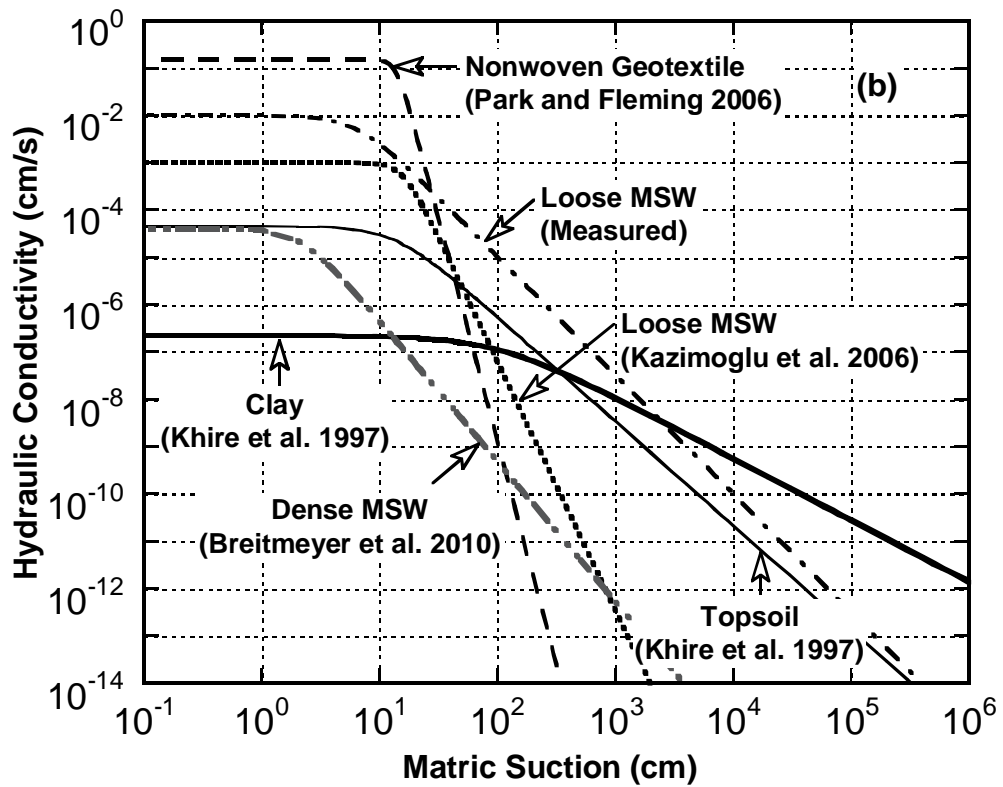
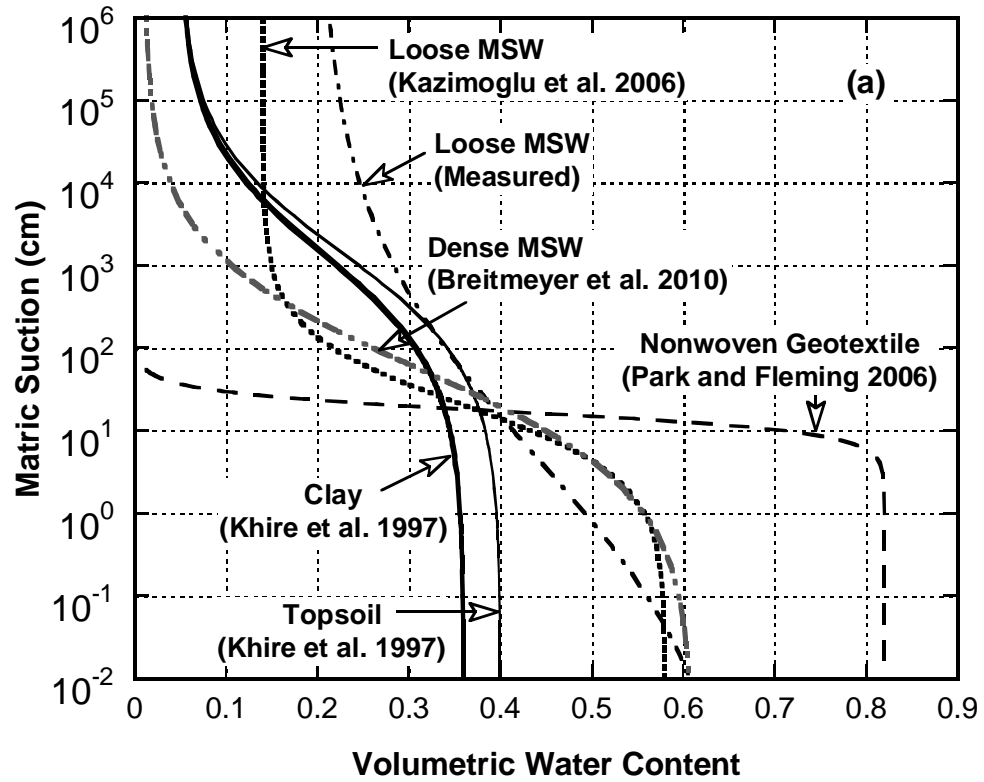


Figure 3-2: Soil water characteristic curves (a); and hydraulic conductivity functions (b) for the soils used in the Wenatchee test section, nonwoven geotextile, and MSW.

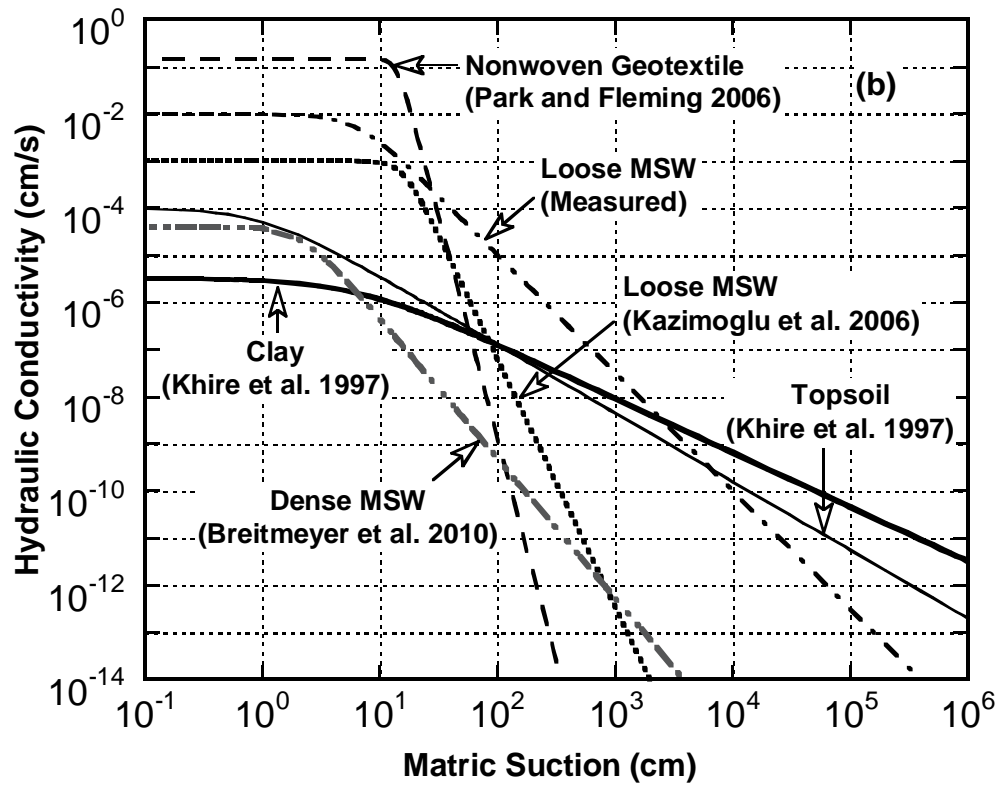
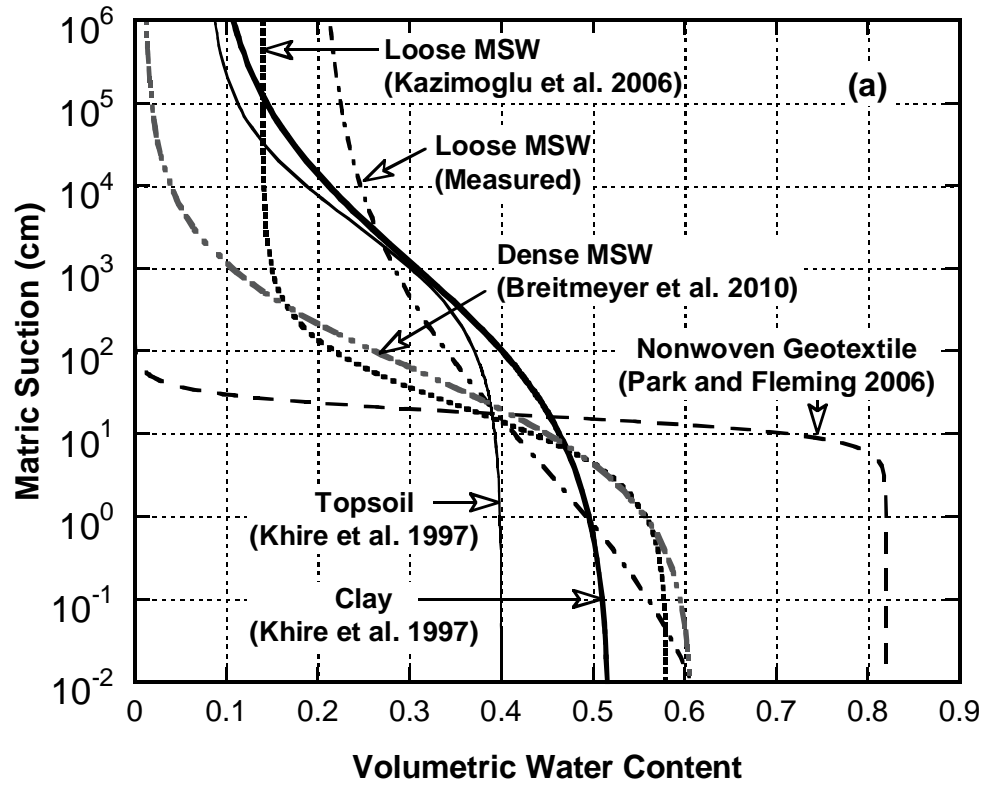


Figure 3-3: Soil water characteristic curves (a); and hydraulic conductivity functions (b) for the soils used in the Atlanta test section, nonwoven geotextile, and MSW.

for the whole profile was set at 10^{-5} cm. For all numerical analyses, total mass balance errors were less than 1%.

RESULTS

Semi-arid Climate

Figure 3-4 shows the simulated percolation and soil water storage (SWS) for the Wenatchee test section. The graph presents simulation results using the original soils used to build the instrumented earthen cover in semi-arid climate. The saturated hydraulic conductivity of the compacted silty clay cover is 2.2×10^{-7} cm/s. Field measured lysimeter percolation obtained by Khire et al. (1997) shows that the test section yielded 0.79 cm of percolation during the first year of its monitoring period. As shown in Figure 3-4, numerically simulated lysimeter percolation using unit gradient boundary at the bottom of the compacted clay layer for lysimeter (without considering the geotextile layer) relatively captured the field measured percolation. Lysimeter simulation considering a geotextile layer underneath the earthen cover showed much lower percolation compared to that without the geotextile layer.

For actual ET cap simulations, loose and dense MSW were considered underneath the earthen cover. The resulting percolation for actual ET caps corresponds to the interlayer flux across the interface between the earthen cover and the underlying landfilled waste and is a function of the hydraulic properties for the MSW layer. Positive

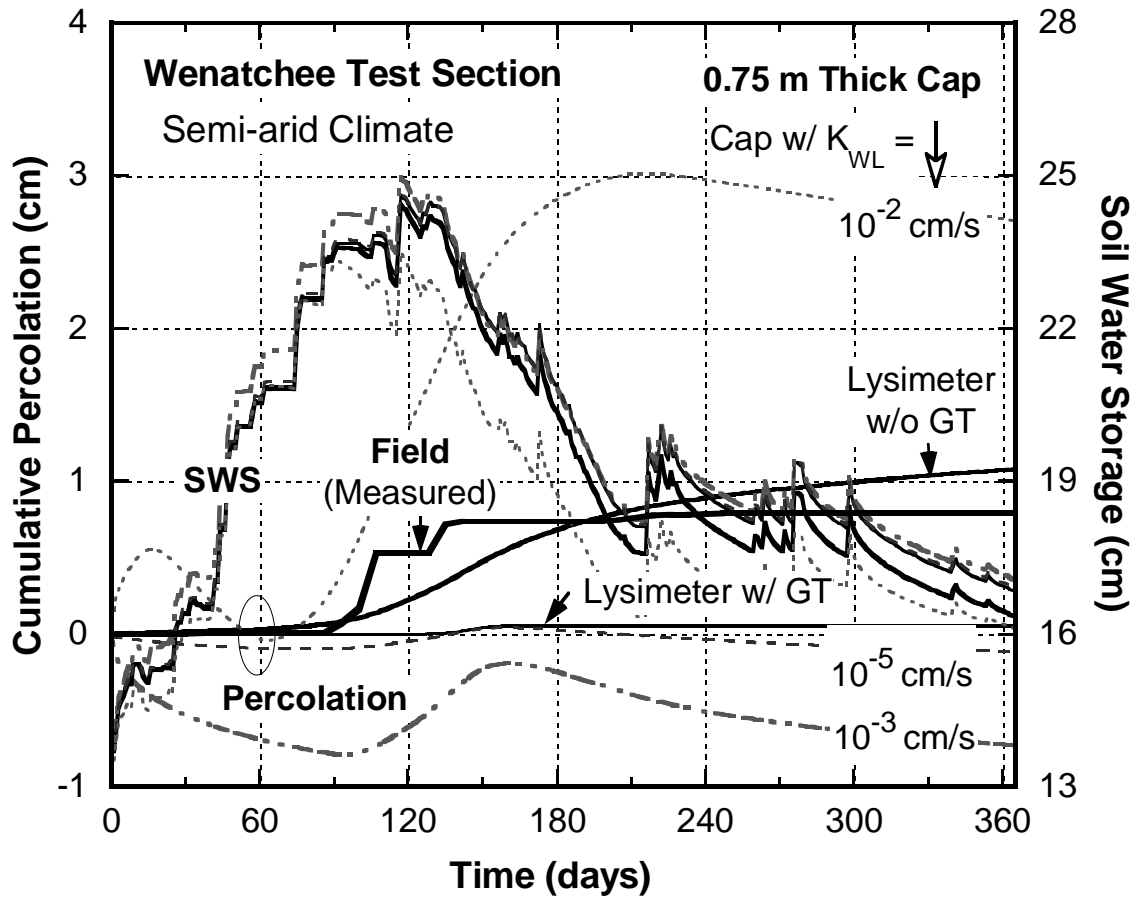


Figure 3-4: Simulated cumulative percolation and soil water storage for Wenatchee soil, with 0.6-m thick storage layer, in a semi-arid climate boundary condition.

percolation values represent downward flux of moisture from the earthen cover to the waste layer. Negative percolation values represent upward flux of moisture wherein the earthen cover pulls the moisture up from the waste layer. As shown from Figure 3-4, as the saturated hydraulic conductivity of the waste decreases, the percolation rate for the actual cap also decreases. Actual ET cap with underlying loose MSW with a saturated hydraulic conductivity of 10^{-2} cm/s and unsaturated hydraulic properties measured from centrifuge testing had percolation greater than lysimeter percolation. However, actual ET

cap percolations with typical MSW having saturated hydraulic conductivity of 10^{-3} and 10^{-5} cm/s generally have negative percolation which indicates much lower percolation than the corresponding lysimeter (i.e., lysimeter percolation is generally conservative). The reduction in percolation is attributed to: (1) the ability of the waste to impede the downward flow of water from the overlying soil cap; and (2) the temporary storage of percolated water by the underlying waste and removal of the stored water under evapotranspirative gradients as evident in Figure 3-4 showing the decrease in the cumulative percolation across the cap to waste interface. This particularly occurs during dry periods where the fine-grained soils have the capability to pull water up due to capillary action. For lysimeters, the infiltrated water drains as percolation and hence cannot be extracted later via evapotranspiration.

The reduction in percolation provided by the waste layer generally corresponds to an increase in the SWS of the overlying ET cap as compared to the corresponding lysimeter (Khire and Mijares 2010). However, due to the relatively small difference in the percolation rate between actual ET cap and lysimeter, as well as the inherently low saturated hydraulic conductivity of the cover soil, the resulting SWS of the actual ET cap and lysimeter appear similar (Figure 3-4). In order to compare the SWS, simulated SWS within actual ET caps were plotted against simulated SWS within lysimeter (without geotextile layer) for all simulations for the same time period (Figure 3-5). The 1:1 line shows the region where SWS values are the same for an actual cap and corresponding lysimeter. Points above the 1:1 line correspond to greater SWS for the cap compared to the lysimeter and vice versa. Closer look at Figure 3-5 reveals that SWS within actual ET caps are indeed generally larger than the SWS within the corresponding lysimeter for

typical MSW with K_{WL} equal to 10^{-3} and 10^{-5} cm/s, albeit small difference in magnitude. For all cases, greater soil water storage corresponded to a lower percolation or vice versa. When the difference in SWS relatively small, it is associated with relatively small difference in percolation.

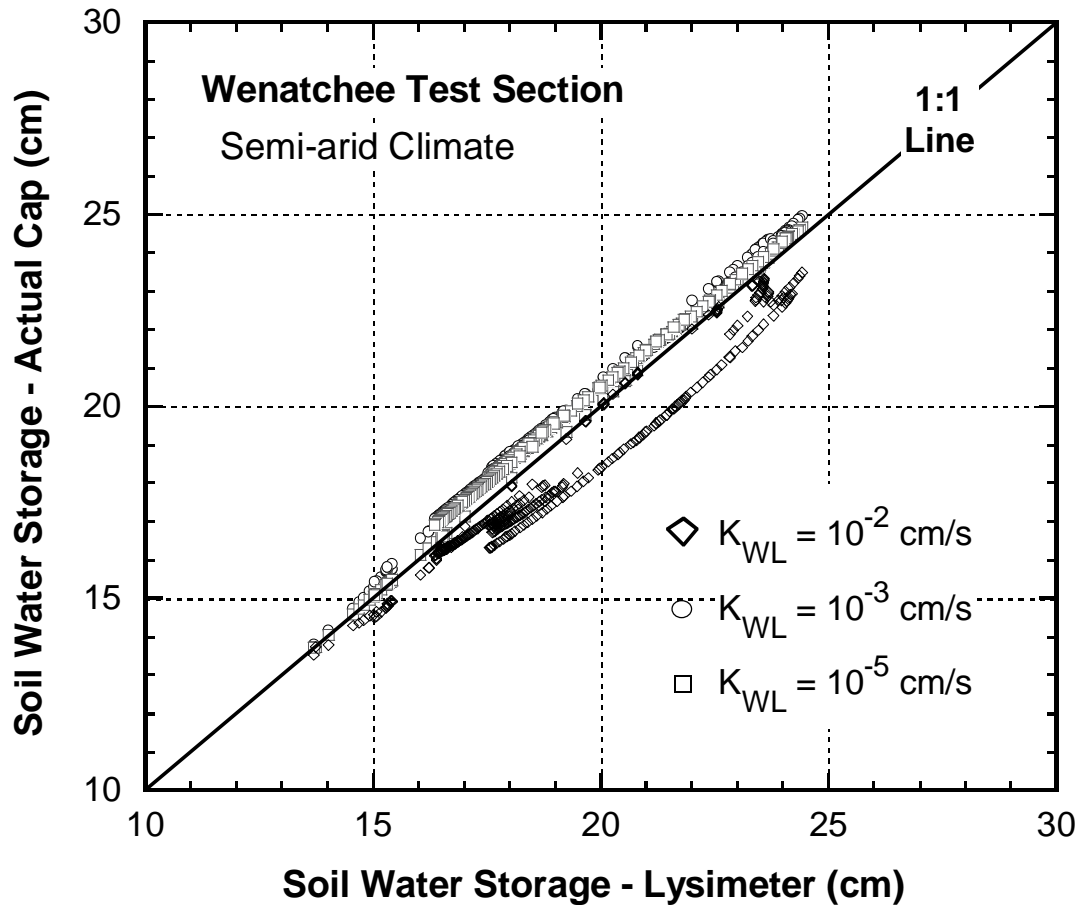


Figure 3-5: Simulated soil water storage for actual cap versus lysimeter for Wenatchee soil, with 0.6-m thick storage layer, in a semi-arid climate boundary condition.

Figure 3-6 shows the simulated percolation and SWS for actual ET caps and lysimeter consisting of Wenatchee soil with a much thicker soil cap (0.9-m thick storage layer). All other variables were kept the same. It can be seen that for lysimeter

simulations, as the thickness of the cap increases, the resulting percolation decreases. Similar trend can be observed for actual cap simulations, regardless of the hydraulic conductivity of the underlying waste. For silty clay such as the Wenatchee soil, the relatively low hydraulic conductivity produces an average percolation of about few mm per year. Simulation results show that lysimeter generally overestimates the actual ET cap by about two times.

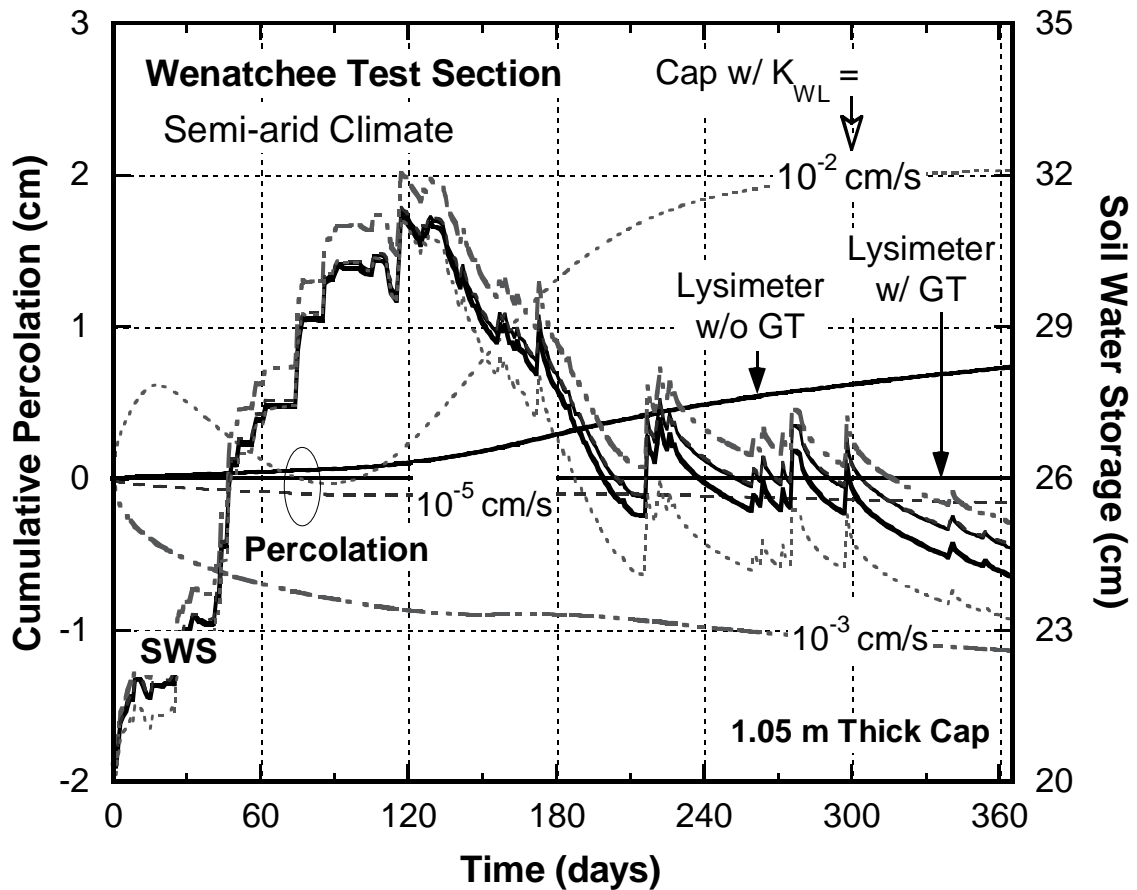


Figure 3-6: Simulated cumulative percolation and soil water storage for Wenatchee soil, with 0.9-m thick storage layer, in a semi-arid climate boundary condition.

Humid Climate

Figure 3-7 shows the simulated percolation and SWS for the Atlanta test section. The graph presents simulation results using the original soils used to build the instrumented earthen cover in a humid climate. The saturated hydraulic conductivity of the compacted clayey silt cover is 3.2×10^{-6} cm/s. Field measured lysimeter percolation obtained by Khire et al. (1997) shows that the test section yielded 12.98 cm of percolation during the first year of its monitoring period. Due to inherent high precipitation in humid climate, the test section yielded much higher percolation. Numerically simulated lysimeter

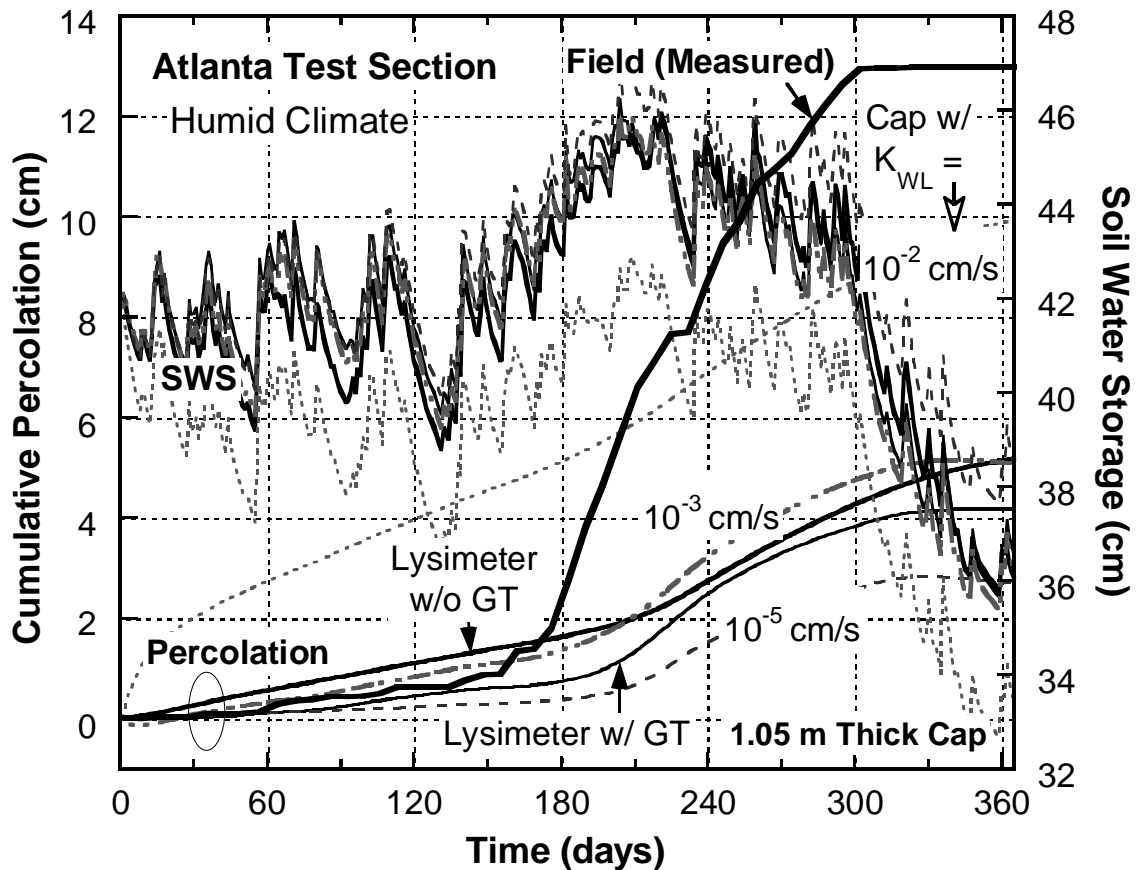


Figure 3-7: Simulated cumulative percolation and soil water storage for Atlanta soil, with 0.9-m thick storage layer, in a humid climate boundary condition.

percolation using unit gradient boundary at the bottom of the compacted clay layer for lysimeter (without considering the geotextile layer) and lysimeter simulation considering a geotextile layer underneath the earthen cover both showed much lower percolation predictions compared to the field measured percolation. Furthermore, lysimeter simulation considering a geotextile layer underneath the earthen cover still showed much lower percolation compared to that without the geotextile layer.

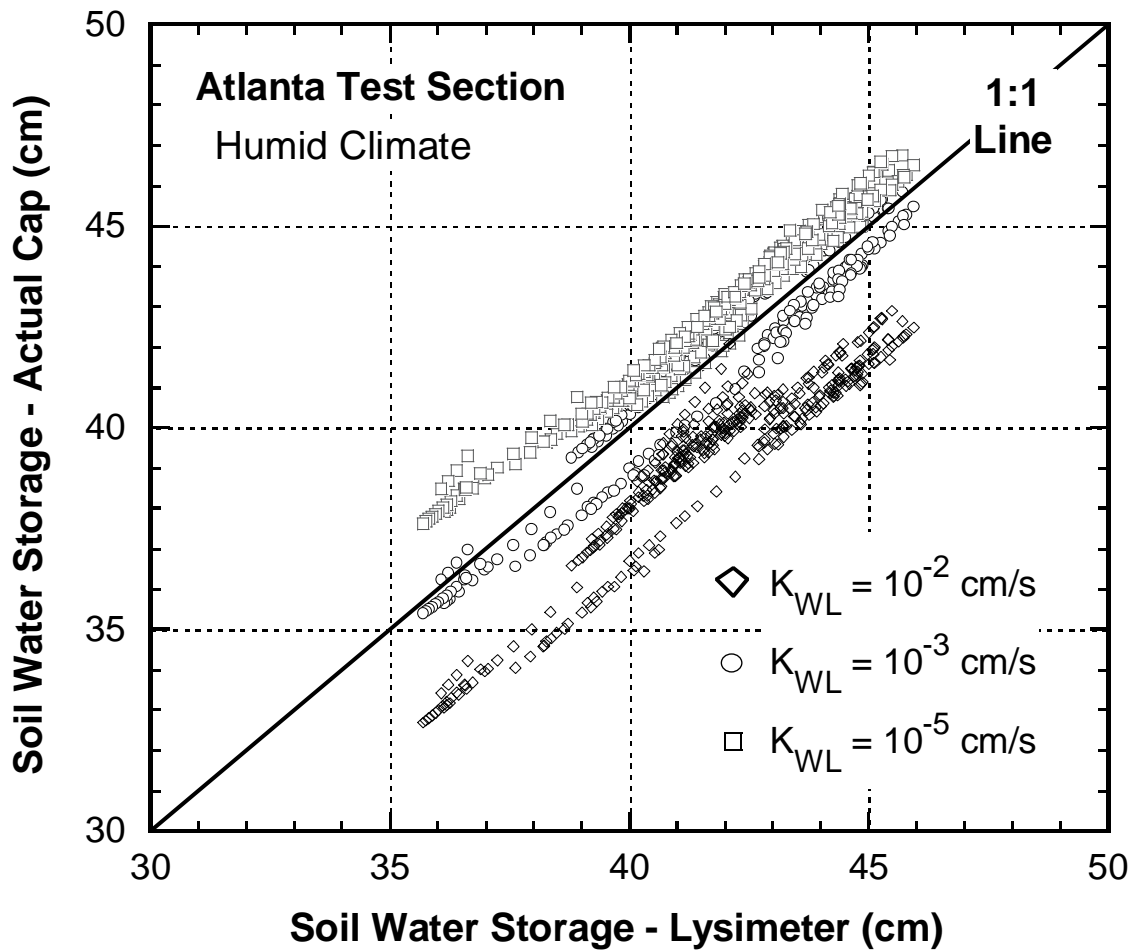


Figure 3-8: Simulated soil water storage for actual cap versus lysimeter for Atlanta soil, with 0.9-m thick storage layer, in a humid climate boundary condition.

For actual ET cap simulations, as the underlying waste is assumed to be more dense having a lower hydraulic conductivity, the percolation rate for the actual cap consistently decreases due to the reasons presented in the preceding subsection. This observation is consistent with the trends obtained for the semi-arid climate. Similarly, the SWS response of an actual ET cap and the corresponding lysimeter are close to each other (Figures 3-7 and 3-8) because the predicted percolations are about the same. It can be noted that for humid climate, net positive percolations have been observed regardless of the hydraulic properties of the underlying landfilled waste. This is because in humid climate, the magnitude of precipitation is relatively large compared to the semi-arid climate which results in the soil cover to remain relatively wet more often. Hence, the cover is less often able to develop upward hydraulic gradients to pull water from the underlying waste layer.

Figure 3-9 shows the simulated percolation and SWS for actual ET caps and lysimeter consisting of Atlanta soil with a much thicker soil cap (1.5-m thick storage layer). All other variables were kept the same. Similar to the semi-arid climate, the numerical results suggest that thicker cover soils would consistently have much lower lysimeter percolation as well as actual cap percolations. The presence of the waste layer underneath actual ET caps indeed affects the SWS response and the resulting percolation for the earthen covers. Consequently, a reduction in percolation has been observed whenever there is an increase in the SWS. The waste layer acts as a barrier that impedes, but not prevents, the downward flow of water.

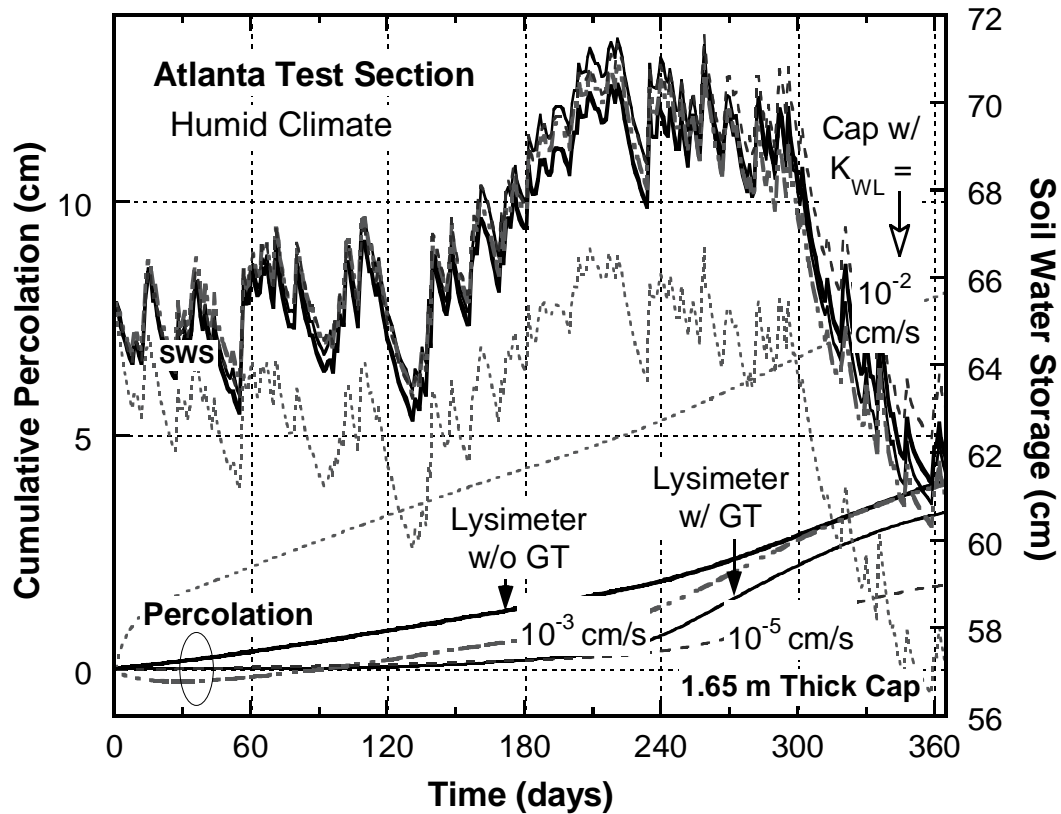


Figure 3-9: Simulated cumulative percolation and soil water storage for Atlanta soil, with 1.5-m thick storage layer, in a humid climate boundary condition.

SUMMARY AND CONCLUSIONS

Financial savings associated with ET caps and their sustainability due to more options for end use has resulted in more state regulatory agencies to consider earthen final caps. The earthen caps eliminate the use of relatively expensive geomembranes in landfill final covers. While lysimeters are commonly used to assess the water balance of alternative caps, lysimeters are not hydraulically equivalent to an actual ET cap due to the difference in the lower hydraulic boundary. Actual caps are typically underlain by permeable subgrade/waste layers. The numerical results from this study indicate that the soil water storage of an actual ET cap would generally be greater than the soil water storage of the

corresponding lysimeter. Greater soil water storage corresponds to lower percolation and vice versa. The reduction in the soil water storage capacity of lysimeters is associated with the removal of infiltrated water from the lower boundary resulting in greater percolation. In an actual ET cap, where it is underlain by waste, the percolation through the cap is generally less because of the capillary break and water storage capacity offered by the underlying waste layer. Because it is not possible to directly measure percolation without a lysimeter, the percolation values measured in the field should be re-evaluated by carrying out site-specific numerical analysis for representative field-scale hydraulic properties of the waste to simulate the long-term percolation scenario for the actual final cap. The numerical results presented in this study also suggest that thicker cover soils would consistently have much lower lysimeter percolation as well as actual cap percolation. Furthermore, wetter climate (with high precipitation to potential evapotranspiration ratio) would typically have smaller difference in the soil water storage and percolation for an actual ET cap versus its corresponding lysimeter.

REFERENCES

REFERENCES

- Abichou, T., Liu, X., and Tawfiq, K. (2006). "Design Considerations for Lysimeters Used to Evaluate Alternative Earthen Final Covers," *Journal of Geotechnical and Geoenvironmental Engineering*, 132 (12): 1519-1525.
- Abichou, T., and Musagasa, J. (2008). "ET Covers: Construction and Tree Development Inside and Outside of Lysimeters," *Proceedings, GeoCongress 2008, GSP No. 177, Geotechnics of Waste Management and Remediation*, ASCE, Reston, VA: 72-79.
- Albright, W., Benson, C., Gee, G., Roesler, A., Abichou, T., Apiwantragoon, P., Lyles, B., and Rock, S. (2004). "Field Water Balance of Landfill Final Covers," *Journal of Environmental Quality*, 33(6): 2317-2332.
- Benson, C., Abichou, T., Albright, W., Gee, G., and Roesler, A. (2001). "Field Evaluation of Alternative Earthen Final Covers," *International Journal of Phytoremediation*, 3 (1): 105-127.
- Benson, C., Bohnhoff, G., Ogorzalek, A., Shackelford, C., Apiwantragoon, P., and Albright, W. (2005). "Field Data and Model Predictions for an Alternative Cover," *Waste Containment and Remediation*, GSP No. 142, ASCE, Reston, VA: 1-12.
- Benson, C., Sawangsuriya, A., Trzebiatowski, B., and Albright, W. (2007). "Postconstruction Changes in the Hydraulic Properties of Water Balance Cover Soils," *Journal of Geotechnical and Geoenvironmental Engineering*, 133 (4): 349-359.
- Bohnhoff, G., Ogorzalek, A., Benson, C., Shackelford, C., and Apiwantragoon, P. (2009). "Field Data and Water-Balance Predictions for a Monolithic Cover in a Semiarid Climate," *Journal of Geotechnical and Geoenvironmental Engineering*, 135 (3): 333-348.
- Breitmeyer, R., Benson, C., Edil, T., and Barlaz, M. (2010). "Hydrologic Properties of Municipal Solid Waste," *Research Project Poster*, GeoEngineering Program, University of Wisconsin Madison.
- Fayer, M. (2000). "UNSAT-H Version 3.0: Unsaturated Soil Water and Heat Flow Model – Theory, User Manual, and Examples." PNNL-13249, Pacific Northwest Laboratories, Richland, Washington.
- Hardt, C. (2008). "Numerical Evaluation of Preferential Flow Through Evapotranspirative Landfill Covers," *Masters Thesis*, Michigan State University, East Lansing, Michigan, 67 p.
- Hauser, V., Weand, B., and Gill, M. (2001). "Natural Covers for Landfills and Buried Waste." *Journal of Environmental Engineering*, 127 (9): 768-775.

- Haverkamp, R., Valcin, M., Touma, J., Wierenga, P., and Vauchaud, G. (1977). "A Comparison of Numerical Simulation Models for One-Dimensional Infiltration," *Soil Science Society of America Journal*, 41: 285-294.
- Kazimoglu, Y., McDougall, J., and Pyrah, I. (2005). "Moisture Retention and Movement in Landfilled Waste," *Proceedings*, GeoProb 2005: International Conference on Problematic Soils, Famagusta, Northern Cyprus, May 2005.
- Kazimoglu, Y., McDougall, J., and Pyrah, I. (2006). "Unsaturated Hydraulic Conductivity of Landfilled Waste," *Proceedings*, Unsaturated Soils 2006, GSP No. 147, ASCE, Reston, VA: 1525-1534.
- Khire, M., and Mijares, R. (2008). "Influence of the Waste Layer on Percolation Estimates for Earthen Caps Located in a Sub-humid Climate," *Proceedings*, GeoCongress 2008, GSP No. 177, Geotechnics of Waste Management and Remediation, ASCE, Reston, VA: 88-95.
- Khire, M., Benson, C., and Bosscher, P. (1997). "Water Balance Modeling of Earthen Final Covers," *Journal of Geotechnical and Geoenvironmental Engineering*, 123 (8): 744-754.
- Khire, M., Benson, C., and Bosscher, P. (1999). "Field Data From a Capillary Barrier and Model Predictions with UNSAT-H," *Journal of Geotechnical and Geoenvironmental Engineering*, 125: 518-528.
- Khire, M., Benson, C., and Bosscher, P. (2000). "Capillary Barriers: Design Variables and Water Balance," *Journal of Geotechnical and Geoenvironmental Engineering*, 126 (8): 695-708.
- Mijares, R., Khire, M., and Johnson T. (2010). "Lysimeters Versus Actual Earthen Caps: Numerical Assessment of Soil Water Storage," *Proceedings*, GeoFlorida 2010, GSP No. 199, Advances in Analysis, Modeling and Design, ASCE, Reston, VA: 2849-2858.
- Mukherjee, M. (2008). "Instrumented Permeable Blankets for Estimating Subsurface Hydraulic Conductivity and Confirming Numerical Models Used for Subsurface Liquid Injection," *Ph.D. Dissertation*, Michigan State University, East Lansing, Michigan, 278 p.
- Ogorzalek, A., Bohnhoff, G., Shackelford, C., Benson, C., and Apiwantragoon, P. (2008). "Comparison of Field Data and Water-Balance Predictions for a Capillary Barrier Cover," *Journal of Geotechnical and Geoenvironmental Engineering*, 134 (4): 470-486.
- Park, K., and Fleming, I. (2006). "Evaluation of a Geosynthetic Capillary Barrier," *Geotextiles and Geomembranes*, 24: 64-71.

- Passioura, J. (1977). "Determining Soil Water Diffusivities from One-step Outflow Experiments," *Australian Journal of Soil Research*, 15 (1): 1-8.
- Scanlon, B., Reedy, R., Keese, K., and Dwyer, S. (2005). "Evaluation of Evapotranspirative Covers for Waste Containment in Arid and Semiarid Regions in the Southwestern USA," *Vadose Zone Journal*, 4: 55-71.
- Simunek, J., and van Genuchten, M. (2008). "Modeling Nonequilibrium Flow and Transport Processes Using HYDRUS," *Vadose Zone Journal*, 7 (2): 782-797.
- Simunek, J., van Genuchten, M., and Sejna, M. (2008). "The HYDRUS-1D Software Package for Simulating the One-Dimensional Movement of Water, Heat, and Multiple Solutes in Variably-Saturated Media: Version 4.0." Dept. of Environmental Sciences, University of California, Riverside.
- Stoltz, G., and Gourc, J. (2007). "Influence of Compressibility of Domestic Waste on Fluid Conductivity," *Proceedings*, 18th Congres Francais de Mecanique, Grenoble, France.
- Stormont, J., and Morris, C. (2000). "Characterization of Unsaturated Nonwoven Geotextiles," *Proceedings*, Geo-Denver 2000, GSP No. 99, Advances in Unsaturated Geotechnics, ASCE, Reston, VA: 153-164.
- van Genuchten, M. (1980). "A Closed-Form Equation for Predicting the Hydraulic Conductivity of Unsaturated Soils," *Soil Science Society of America Journal*, 44: 892-898.

PAPER NO. 4: EVALUATION OF GEOSYNTHETIC CAPILLARY BREAK IN EARTHEN COVER LYSIMETERS

ABSTRACT

In this study, the numerical unsaturated flow model UNSAT-H was used to evaluate the capillary break developed by nonwoven geotextile component of geocomposite drainage layer that is commonly used to collect percolation in lysimeters. Lysimeters are used to evaluate the water balance of landfill covers. The numerical modeling included constant flux simulations of coarse to fine-grained soils underlain by nonwoven geotextile followed by simulations of two instrumented lysimeters constructed in humid and semi-arid climates. Evidence of a geotextile capillary break was evident from higher soil water storage as well as a delay in the onset of percolation. The results indicate that the capillary break introduced by a nonwoven geotextile in lysimeters may be significant only when the saturated hydraulic conductivity of the soils is greater than 10^{-5} cm/s. However, irrespective of the hydraulic conductivity of the soils or the regional climate, the capillary break did not have significant impact on the long-term percolation.

INTRODUCTION

There are about 1,600 active municipal solid waste (MSW) landfills in the United States. These landfills will require a final cover once they are closed. The U.S. federal regulations imply emulating landfill liner which requires a geomembrane layer, for landfill final cover. Alternative final covers that only use earthen materials offer financial savings, greater end-use options (wood harvesting), and better long-term erosion protection due to deeper plant roots. Hence, alternative covers, which are also referred to

as evapotranspirative (ET) caps have been tested in the field since 1980s for long-term capping of municipal solid waste (MSW) landfills as well as radioactive waste sites. Since then, ET caps have been widely used in arid and semi-arid climates and are being tested and permitted in sub-humid and humid climates on a case by case basis. Often the performance of ET caps is evaluated by constructing a lysimeter to collect the percolation that infiltrates through the cap. Based on the magnitude of the annual percolation collected in the lysimeter, the ET cap is approved, disapproved, or redesigned (Khire and Mijares 2008; Mijares et al. 2010).

The lysimeter usually contains a geocomposite drainage layer (GDL) installed at the base of the ET cap to collect and drain the percolation to a measuring or monitoring device(s). This GDL, which is placed above the geomembrane that lines conventional pan lysimeter, consists of a geonet sandwiched between two geotextiles. Often the geotextile (GT) present in the GDL is nonwoven. Published studies indicate that nonwoven geotextiles have water retention function that is similar to those of coarse-textured soils such as sand and gravel (Stormont et al. 1997; Stormont and Morris 2000; Park and Fleming 2006). Hence, it has been indicated that nonwoven geotextile layer acts as a capillary break. If it acts as a capillary break, it allows greater storage of moisture in the soil layers above the geotextile before the percolation breakthrough occurs. In addition, a capillary break can reduce the total percolation by enhancing evapotranspiration because more soil water is available for an extended duration for potential removal via evaporation and transpiration (Benson and Khire 1995; Ward and Gee 1997; Khire et al. 2000).

Capillary break occurs during unsaturated conditions at the interface between the fine-textured soil cover and underlying coarse-textured material. The contrast in the unsaturated hydraulic conductivity, under relatively high matric suctions, between the two layers impedes the downward movement of water. This will result in the buildup of moisture in the overlying finer layer and consequently decrease its matric suction especially near the interface. Once the matric suction at the interface drops to the water-entry suction of the coarse-textured material, capillary barrier is breached and water will continue to infiltrate into the underlying coarse layer.

Several studies have been published to understand the physics of capillary barrier effect between fine-grained and coarse-grained soils. Laboratory tests have been conducted to observe capillary break (Baker and Hillel 1990; Stormont and Anderson 1999; Tami et al. 2004) and field-scale demonstration projects have been implemented to assess its performance (Nyhan et al. 1990; Ward and Gee 1997; Khire et al. 1999; Benson et al. 2002; Albright et al. 2004; Ogorzalek 2008). However, limited actual case studies have addressed the magnitude of capillary barrier effect when nonwoven GT is used. Although numerical studies have shown that capillary break develops when a geotextile is placed below a fine-textured soil (Iryo and Rowe 2003; Park and Fleming 2006), physical evidence showing the magnitude of capillary barrier effect due to nonwoven GT on percolation through an earthen cap has been scarce.

Laboratory column tests conducted by Stormont and Morris (2000) and Bathurst et al. (2007) showed that the presence of a single layer of geotextile in the system impedes the downward movement of wetting front. This demonstrates the presence of capillary break. Stormont and Morris (2000) carried out constant infiltration tests on a

column consisting of a silty sand over coarse sand and compared it to the response of identical column where a nonwoven geotextile was placed between the two layers. Additional column test was conducted wherein a nonwoven geotextile was placed between two layers of silty sand. All tests compare the suction response of the soil immediately above and below the soil interface when breakthrough occurs. Results show that the suction head developed above the interface during breakthrough for columns with geotextile layer is significantly lower than those without the geotextile. Lower suction indicates greater water content which is caused by the presence of the geotextile. Similarly, Bathurst et al. (2007) evaluated the effect of a woven geotextile layer sandwiched between two sand layers under constant head infiltration. Pore water pressure time response developed in the sand located above the geotextile interface showed a detectable positive increase as the wetting front reach the geotextile layer. This was not observed in the identical column without the geotextile. The jump in positive pore water pressure corresponds to instantaneous water ponding above the geotextile layer which indicates the presence of capillary barrier effect.

Numerical simulations have been conducted to evaluate the effect of a geotextile layer on the water balance of earthen covers under actual meteorological conditions (Benson et al. 2005; Scanlon et al. 2005; Ogorzalek et al. 2008; Bohnhoff et al. 2009). In contrast with a typical unit gradient boundary, a seepage face boundary is used to approximate the capillary break formed at the base of the lysimeter due to the geotextile layer. Alternatively, a seepage face boundary can also be represented by including a thin layer of coarse-grained soil (e.g. gravel) at the base of the profile (Scanlon et al. 2002). Ogorzalek et al. (2008) and Bohnhoff et al. (2009) have shown that regardless of which

lower boundary conditions were used, the resulting soil water storage, runoff, and evapotranspiration are unaffected. With regard to the resulting percolation, Benson et al. (2005) and Ogorzalek et al. (2008) showed little difference on simulated percolation. Bohnhoff et al. (2009) observed minimal difference while Scanlon et al. (2005) noticed significant difference on percolation values. Scanlon et al. (2005) also found an overestimation of soil water storage which has caused the underestimation of free drainage indicating capillary barrier effect.

The presence or absence of capillary barrier effect due to the geocomposite drainage layer that lines the base of earthen cover lysimeters is not straightforward. Hence, the need to quantify the magnitude of capillary barrier effect introduced by the geotextile is important in order to assess lysimeter measured percolation. Parameters such as soil hydraulic properties, infiltration rate, and meteorological conditions are hypothesized to be key factors that determine occurrence of capillary break.

OBJECTIVES

The key objectives of the study presented in this paper are to: (1) determine the magnitude of capillary barrier effect due to the geocomposite drainage layer used in lysimeters to evaluate the water balance of earthen caps; (2) identify the factors that facilitate formation of capillary break; and (3) compare the capillary barrier effect due to the presence of a geotextile in lysimeters to that due to the waste layer that is present in actual caps.

In this numerical study, the effect of GDL consisting of a nonwoven geotextile on the water balance of the cap was evaluated by numerically simulating three monolithic

earthen covers. 1-D soil columns with a height of 90 cm were simulated as lysimeters or actual caps (with underlying waste) using UNSAT-H. Constant infiltration simulations were conducted to easily identify and quantify when capillary break occurs. In addition, long-term simulations were carried out to quantify the magnitude of capillary barrier effect under actual meteorological conditions in semi-arid and humid climates.

NUMERICAL MODELING

The finite-difference model UNSAT-H (Fayer 2000) was used in this study. UNSAT-H numerically solves a modified form of Richards' equation to compute the flow of water through both saturated and unsaturated soil. This model has been routinely used for water balance modeling of earthen caps (Khire et al. 1997; Khire et al. 2000; Benson et al. 2005; Scanlon et al. 2005; Ogorzalek et al. 2008; Bohnhoff et al. 2009). For this study, one-dimensional simulations were carried out using UNSAT-H Version 3.0.

A schematic of the conceptual model used in the numerical simulations is shown in Figure 4-1. For the lysimeter, the lower boundary either included or did not include a nonwoven geotextile. In order to simulate an actual cap, the soil cap was assumed to have underlain by a 30-cm thick waste layer. Additional simulations with thicker waste layer were also carried out. However, thicker waste layer did not significantly influence the percolation and soil water storage of the simulated caps.

Material Properties

Table 4-1 summarizes the saturated and unsaturated hydraulic properties of the soils and the waste used to simulate the lysimeter presented in Figure 4-1. Unsaturated hydraulic

conductivity functions were estimated using the closed-form van Genuchten-Mualem expression where the pore interaction term was set to 0.5 (van Genuchten 1980). Hydraulic properties of the municipal solid waste (MSW) reported by Kazimoglu et al. (2005, 2006) were assumed to represent the waste layer in the actual cap. Kazimoglu et al. (2005, 2006) determined the waste retention properties for a laboratory prepared waste specimen which has composition similar to the waste found in Lyndhurst landfill in Australia that is located at shallow depth with a dry density of 0.57 g/cm^3 . Stoltz and Gourc (2007) published similar waste retention curves for loosely compacted MSW

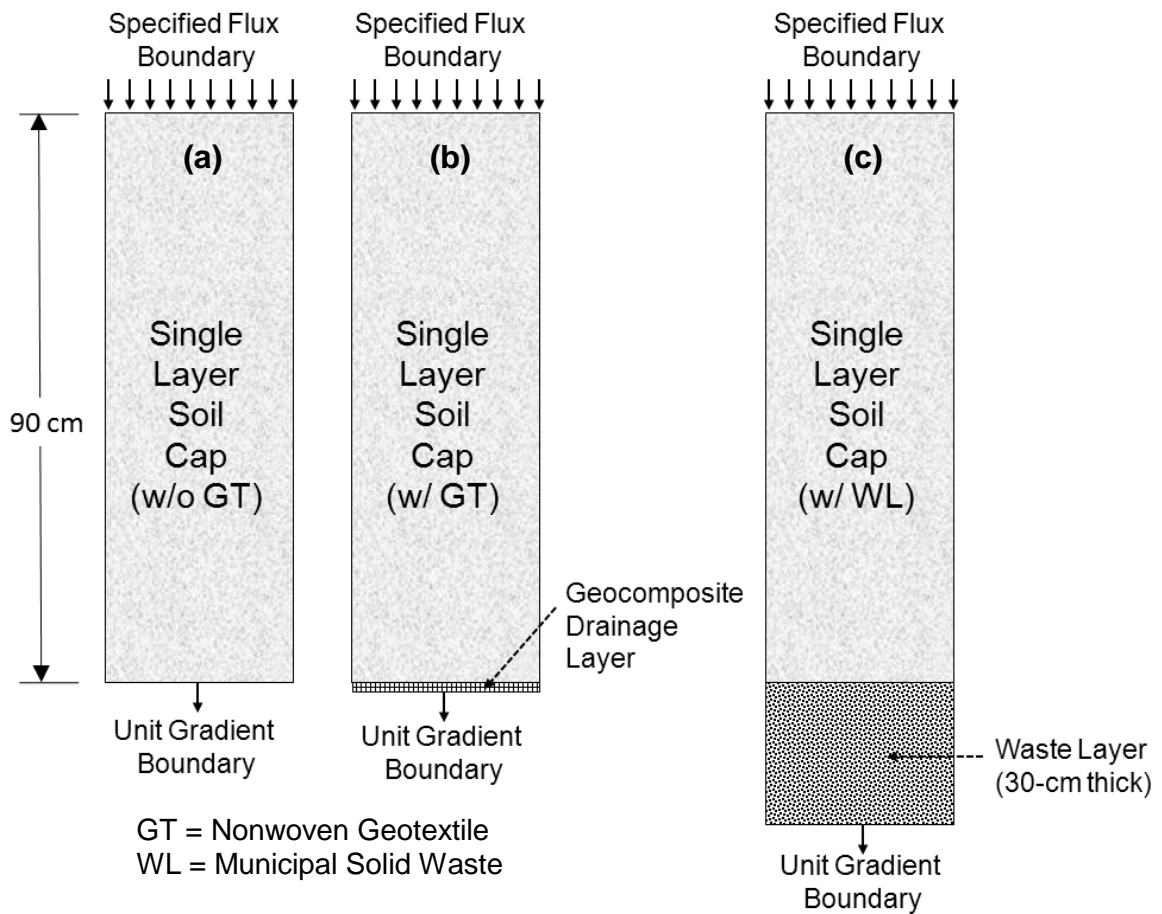


Figure 4-1: Conceptual model used to simulate a lysimeter without (a) and with (b) a nonwoven GT and an actual cap with waste layer (c).

having a dry unit weight equal to 0.54 g/cm^3 . For loosely compacted MSW such as those found within landfills at shallow depth (i.e. beneath the final cover), a saturated hydraulic conductivity of 10^{-3} cm/s has been reported (Mukherjee 2008).

Hydraulic properties of nonwoven geotextile were obtained from Park and Fleming (2006). The nonwoven, polypropylene, needle-punched, continuous fiber geotextile has a mass per unit area of 550 g/m^2 with a thickness of 4.0 mm and an opening size of 0.05 to 0.15 mm. It has similar properties to that of the geotextile used in the study of Stormont and Morris (2000). van Genuchten fitting parameters were obtained based from the data points measured by Park and Fleming (2006) for the geotextile's water retention curve (Figure 4-2).

Figure 4-2 shows the soil water characteristic curves and the hydraulic conductivity functions for the geotextile and the waste presented in Table 4-1.

Table 4-1: Saturated and unsaturated hydraulic properties.

Soil/Material	θ_s [cm ³ /cm ³]	θ_r [cm ³ /cm ³]	α [1/cm-H ₂ O] (kPa ⁻¹)	n	K_s [cm/s]	Reference
Geotextile	0.82	0	0.066 (0.66)	3.99	1.5×10^{-1}	Park and Fleming (2006)
OK 110 Fine Sand	0.35	0.03	0.016 (0.16)	2.5	6.4×10^{-3}	Mukherjee (2008)
SM Soil	0.42	0.02	0.005 (0.05)	1.48	2.7×10^{-4}	Khire et al. (2000)
SM-ML Soil	0.35	0.02	0.012 (0.12)	1.123	9.0×10^{-6}	Khire et al. (2000)
Waste	0.58	0.14	0.15 (1.5)	1.6	1.0×10^{-3}	Kazimoglu et al. (2006)

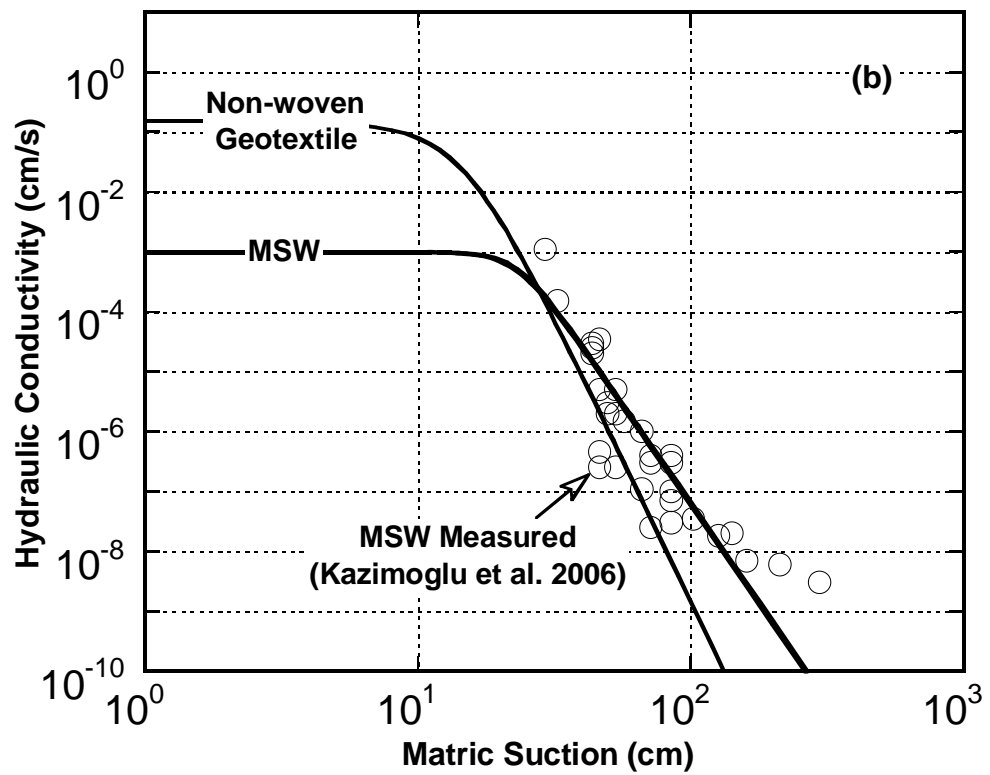
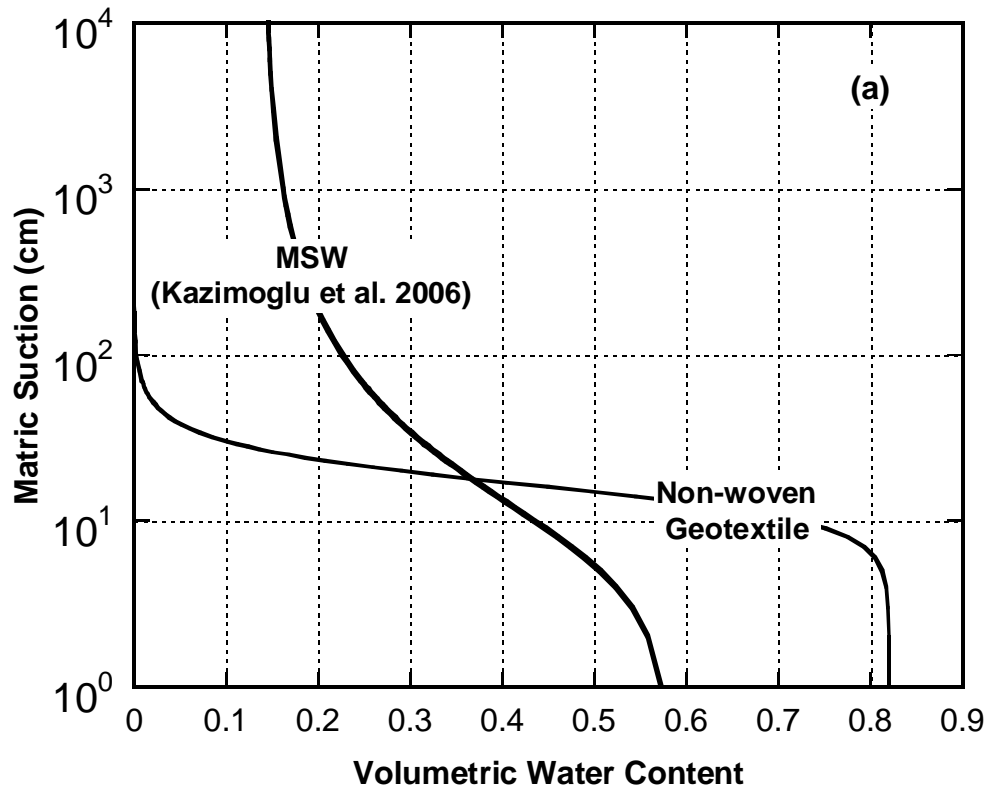


Figure 4-2: Measured soil water characteristic curves (a); and predicted hydraulic conductivity function (b) for nonwoven geotextile and MSW.

Figure 4-2(b) shows that the unsaturated hydraulic conductivities of the nonwoven geotextile and low unit weight MSW are about the same at matric suctions greater than 20 cm.

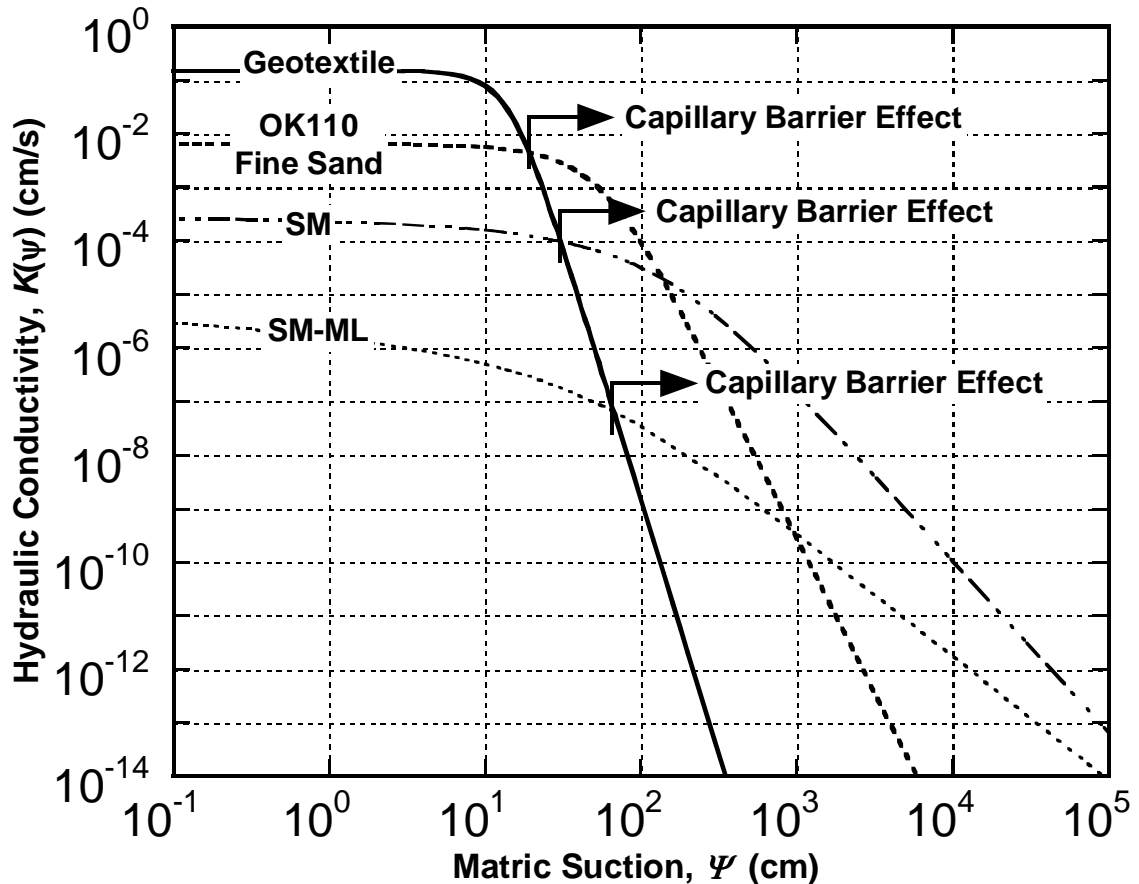


Figure 4-3: Unsaturated hydraulic conductivity functions of the cap soils and the underlying nonwoven GT to illustrate the contrast in $K(\psi)$ relationships which is conducive to the occurrence of capillary barrier effect.

Figure 4-3 shows the unsaturated hydraulic conductivity functions for the three soils used to simulate the monolithic earthen cap and the underlying geotextile (GT) layer for lysimeter. In order for capillary barrier effect to occur, the minimum condition is that the unsaturated hydraulic conductivity of the underlying coarser-grained porous material

needs to be less than the overlying finer-grained soil layer (Khire et al. 2000). Figure 4-3 shows that the unsaturated hydraulic conductivity of the geotextile (GT) is less than the overlying OK110 sand at matric suctions greater than about 20 cm. At 20 cm suction, the hydraulic conductivity of OK110 sand is relatively high ($\sim 6.0 \times 10^{-3}$ cm/s). Figure 4-3 also shows that for the SM-ML soil, at about matric suction equal to 70 cm, the hydraulic conductivity of the GT drops below that of the SM-ML soil. The hydraulic conductivity of the SM-ML soil at 70 cm suction is about 10^{-7} cm/s, which is relatively low. Hence, while capillary barrier effect may occur for all three soils, its effect on percolation is expected to be relatively small when SM-ML soil ($K_s = 9.0 \times 10^{-6}$ cm/s) is used.

Initial and Boundary Conditions and Numerical Control Parameters

For constant infiltration simulations, a specified flux was applied at the ground surface (Figure 4-1) for the lysimeter as well as for the actual cap. While the upper boundary of the cap is typically modeled as an atmospheric boundary, a specified flux boundary provides a condition to readily identify and quantify when capillary break occurs. The specified flux was 1.5×10^{-4} cm/s, 6.1×10^{-6} cm/s, and 2.1×10^{-7} cm/s for the OK110 fine sand, the SM soil, and the SM-ML soil, respectively. The flux values were selected such that no runoff would be generated for the simulated cap and the value was low enough to simulate unsaturated conditions in the cap. A unit gradient boundary condition was imposed on the lower boundary of the model domains. The unit gradient boundary used for the actual cap was applied to the bottom of the waste layer. Fayer et al. (1992) and Khire et al. (1997) have used this boundary condition for lysimeters. Khire and

Mijares (2008) and Mijares et al. (2010) have used the same lower boundary condition for simulations with waste layer.

Initial conditions were specified using matric suctions corresponding to an average degree of saturation of about 40%. This value was used for all simulations for consistency. A relatively drier (or wetter) initial condition for soil caps impacted the onset of percolation but did not impact steady-state soil water storage and rate of percolation. Spatial discretization of the model domain was optimized by conducting sensitivity analysis. This was done by repeatedly refining the nodal spacing until insignificant changes in simulated water balance parameters were achieved. The nodal spacing between the nodes located near the upper and lower boundaries was relatively small (1 mm). A maximum time step of 0.1 hr and a minimum time step of 10^{-7} hr were used for all the simulations. At any given time step, the maximum allowable mass balance error for the whole profile was set at 10^{-5} cm. For all numerical analyses, total mass balance errors were less than 1%.

For field-scale simulations, monolithic earthen covers that were instrumented in the field and numerically modeled by Khire et al. (1997) were reanalyzed in this study. Instrumented field lysimeter test sections in East Wenatchee, Washington and Atlanta, Georgia provided water balance assessment of earthen covers under semi-arid and humid climates, respectively. In this paper, numerical simulations conducted by Khire et al. (1997) were extended to incorporate a geocomposite drainage layer at the base of the actual soil profiles to determine whether a capillary break occurs due to the GT for the two test sections. Soil properties, meteorological data, boundary and initial conditions, spatial discretization, and numerical controls were patterned from the original

simulations of Khire et al. (1997). Aside from including a geotextile layer at the base of the models, additional simulations using SM and SM-ML soils were carried out to determine the effect of soil properties on occurrence of capillary break under field meteorological conditions. In all scenarios, the first year meteorological data was repeated three times to model the long-term soil water storages and percolation. Extending the simulation results to additional 10 years did not change the long-term predictions.

RESULTS

Constant Infiltration Simulations

Figure 4-4 presents the cumulative percolation and soil water storage for OK 110 sand subjected to a specified flux equal to 1.5×10^{-4} cm/s at the upper boundary. The predicted cumulative percolation and soil water storage for OK110 sand with geotextile or with waste are almost identical. However, without GT, the soil water storage is relatively low and percolation onset is early. The cumulative percolation without GT is about 250% of the cumulative percolation with GT or waste. The difference in the percolation is about 5 cm. Due to the relatively low unsaturated hydraulic conductivities of GT or waste when they are relatively dry, the soil water storage of OK110 sand builds up high enough to increase the degree of saturation of the GT or the waste high enough to increase their hydraulic conductivities to carry the imposed flux at the top boundary. Figure 4-4 shows the evidence of capillary break created by nonwoven GT or waste layer when the overlying soil is a relatively permeable soil such as OK110 sand.

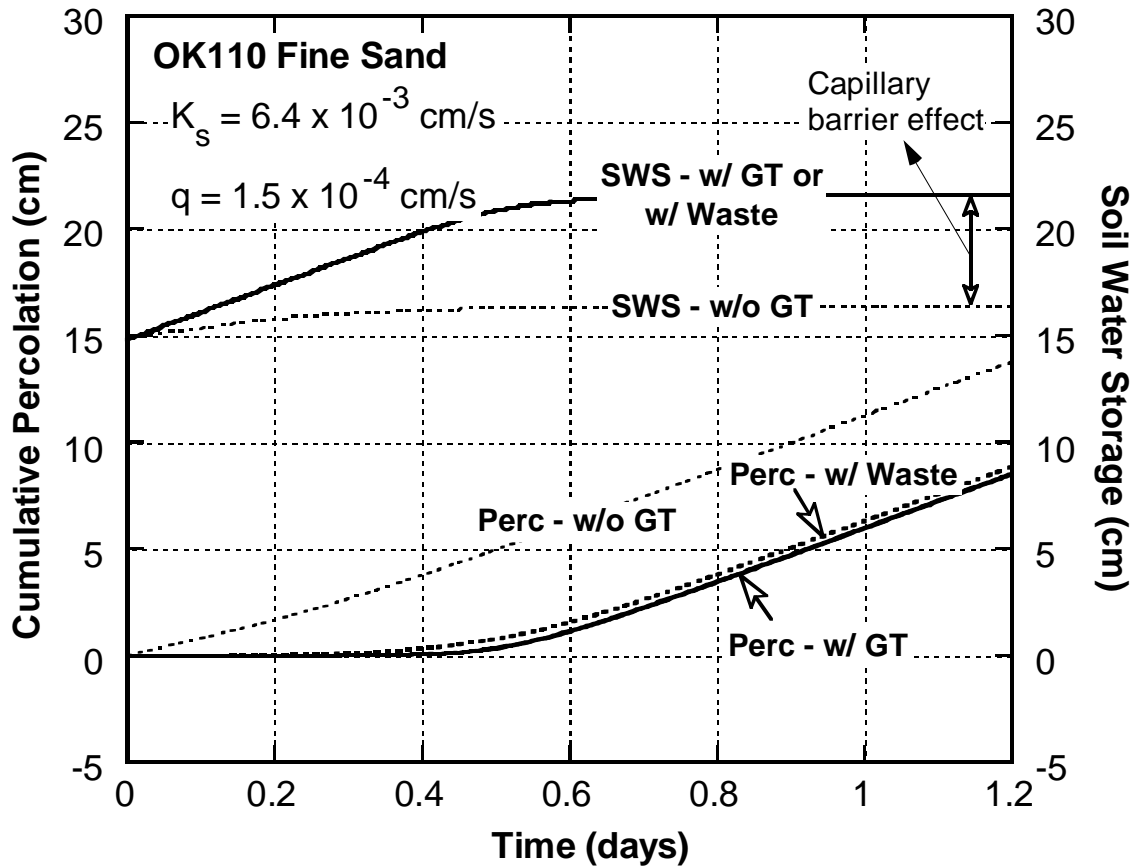


Figure 4-4: Simulated cumulative percolation and soil water storage for OK110 fine sand under specified flux boundary condition.

Figure 4-5 presents the cumulative percolation and soil water storage for SM soil subjected to a specified flux equal to $6.1 \times 10^{-6} \text{ cm/s}$ at the upper boundary. The predicted cumulative percolation and soil water storage for SM soil with a geotextile and with waste are slightly different. The cumulative percolation without GT is about 210% of the cumulative percolation with GT or waste. The difference in the percolation is about 5 cm. The percolation onset for the lysimeter with GT is slightly early compared to the waste. However, without GT, the soil water storage is relatively low and percolation

onset occurs much earlier. Figure 4-5 shows the evidence of capillary break created by nonwoven GT or waste layer when the overlying soil is an SM soil.

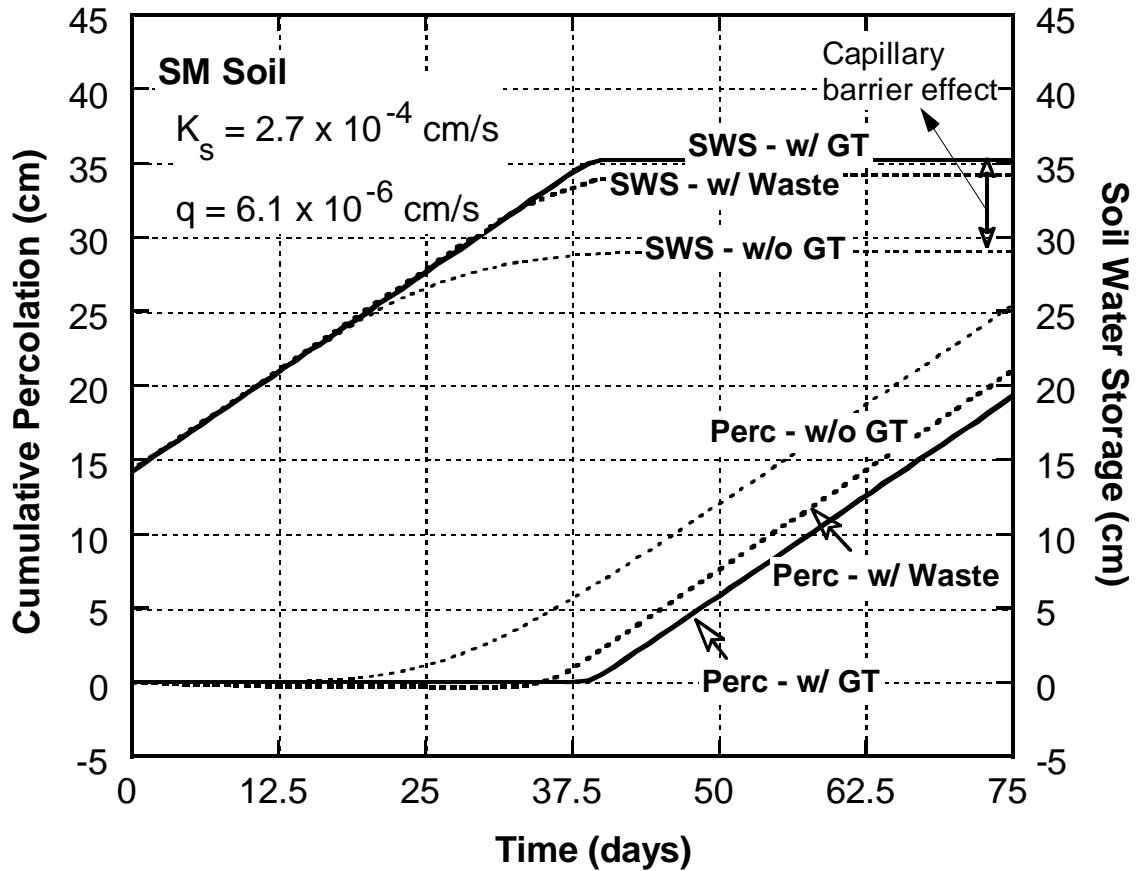


Figure 4-5: Simulated cumulative percolation and soil water storage for SM soil under specified flux boundary condition.

Figure 4-6 presents the cumulative percolation and soil water storage for SM-ML soil subjected to a specified flux equal to $2.1 \times 10^{-7} \text{ cm/s}$ at the upper boundary. The predicted cumulative percolation and soil water storage for SM-ML soil with a geotextile, without geotextile, and with waste are about the same. The cumulative percolation without GT is about 50% of the cumulative percolation with GT or waste. The difference

in the percolation is about 0.7 cm. Thus, while Figure 4-3 shows that the capillary barrier effect is possible based on the differences in hydraulic conductivities of the SM-ML soil and the GT or the waste interface, due to relatively low hydraulic conductivity of the SM-ML soil, the capillary barrier effect does not yield lower percolation or significantly greater soil water storage when a GT or waste layer exists below the cap. Thus, capillary barrier effect is less pronounced when the soils used for the cap have relatively low hydraulic conductivity.

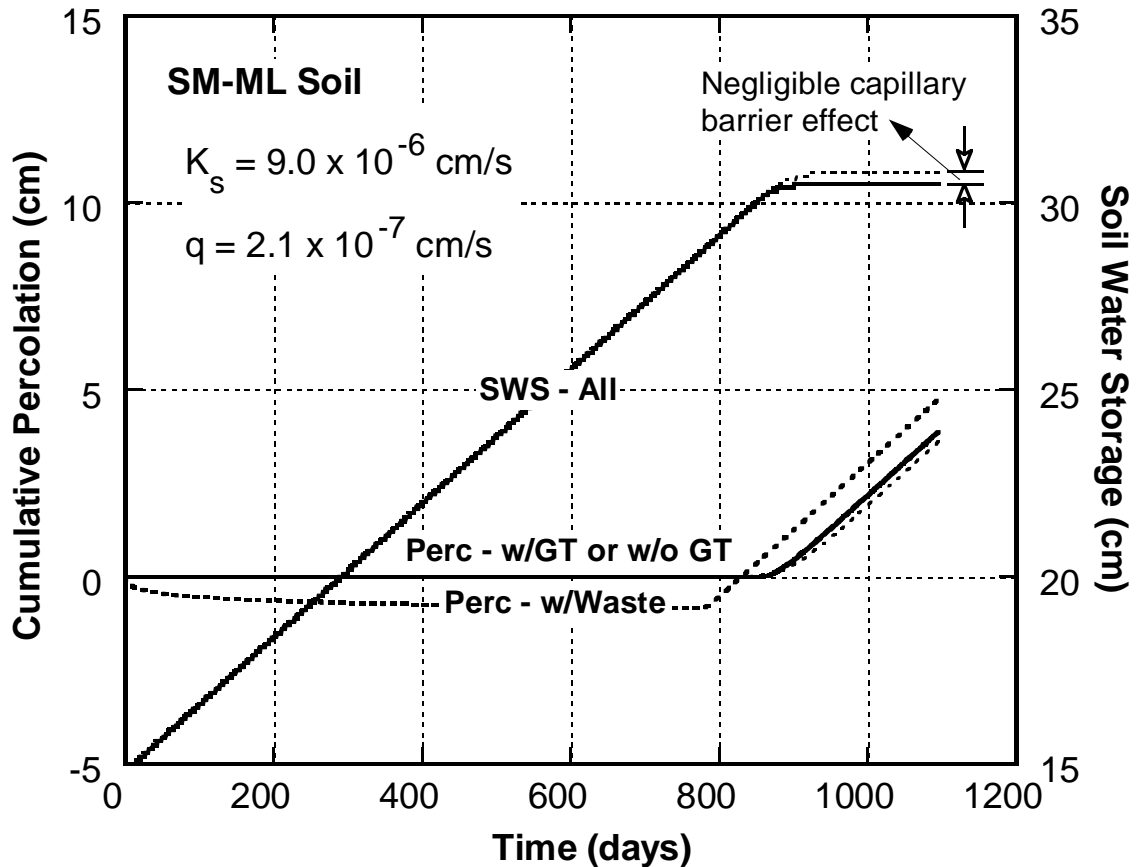


Figure 4-6: Simulated cumulative percolation and soil water storage for SM-ML soil under specified flux boundary condition.

Practical Implications

Based on the numerical results (Figures 4-4 to 4-6), evidence of capillary barrier effect is characterized either by a significant relative delay in the onset of percolation or difference in the peak soil water storage of the soil cover. For a monolithic soil cover, if the underlying geotextile that is typically used at the lower boundary in a lysimeter is not used, in order to satisfy the unit gradient lower boundary condition for the specified flux at the top boundary, the matric suction at the lower boundary of the soil shall equate the suction value corresponding to $K(\psi_f) = q$ (the applied or specified flux) as shown in Figure 4-7. This suction shall correspond to ψ_f in the unsaturated hydraulic function of the soil where its unsaturated hydraulic conductivity is equal to the applied infiltration rate q . Hence, the soil profile would acquire a uniform water content equal to θ_f as determined from its soil water characteristic curve (Figure 4-7a).

For a soil cap with underlying coarser layer, such as in a lysimeter with a geotextile or an actual cap overlying a waste layer, the imposed unit gradient lower boundary condition would require the matric suction in the coarser layer to drop to ψ_c , which corresponds to the unsaturated hydraulic conductivity of the layer at the applied infiltration rate q (Figure 4-7b). Consequently, at the interface, the suction is ψ_c in the GT (or waste) and the overlying soil layer to satisfy continuity. Hence, the suction distribution across the soil profile would be ψ_c at the bottom, increasing nonlinearly

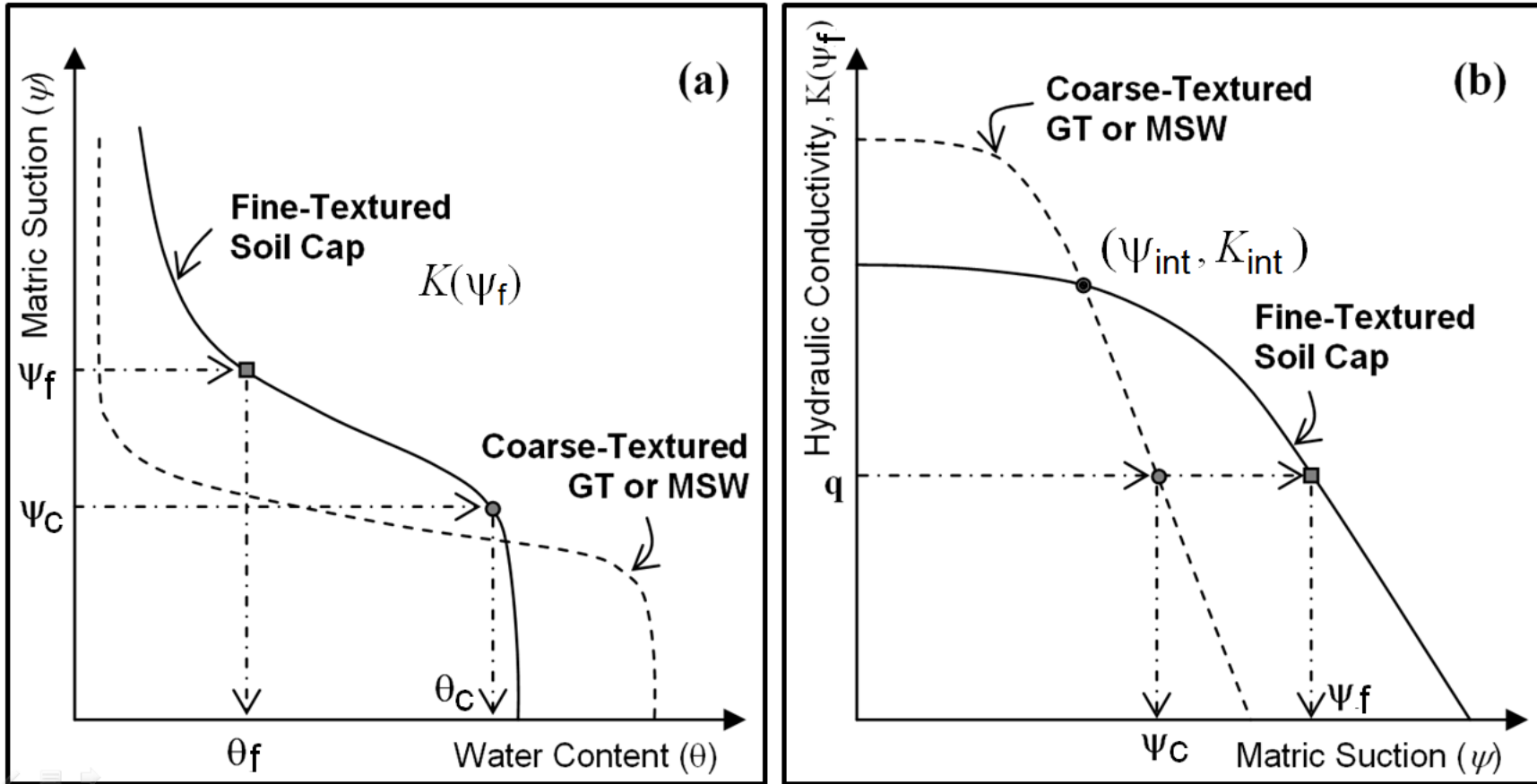


Figure 4-7: Water retention curves (a); and unsaturated hydraulic conductivity functions (b) for fine-textured soil cap and coarse-textured GT or MSW.

upwards satisfying Richards' equation but would not exceed a value of ψ_f . Because ψ_c is less than ψ_f , θ_c would be greater than θ_f . This phenomenon, also referred to as the capillary barrier effect, results in an increase in the soil water storage of the soil cap when a geotextile layer (or waste layer) is present. The increase in soil water storage results in a significant delay in the onset of percolation as shown in Figures 4-4 and 4-5.

Figures 4-4 to 4-7 show that while capillary break is always present when a nonwoven geotextile layer is placed below a soil cap, the magnitude of the capillary barrier effect varies depending upon the hydraulic properties of the soil cap and the infiltration rate. Generally, as q decreases, the difference between ψ_c and ψ_f increases relatively rapidly and results in significant increase in the soil water storage. Thus, the degree or magnitude of capillary barrier effect is higher when the infiltration rate is smaller. As shown in Figure 4-7b, capillary break only occurs whenever $q < K_{int}$. For a typical atmospheric boundary condition that exists for caps, the infiltration rate varies. While the scenarios modeled in Figures 4-4 to 4-6 assume constant infiltration rate to illustrate the magnitude of capillary barrier effect for soils having varying saturated hydraulic conductivity, for earthen caps, the net infiltration rate fluctuates by orders of magnitude on a weekly to seasonal time scales.

Hence, in order to evaluate the magnitude of the capillary barrier effect, the specified rate of infiltration was varied by several orders of magnitude for both SM soil and SM-ML soil and the resulting effect on the SWS of the cap, with and without GT, is presented in Figure 4-8. SWS ratio was calculated by dividing the SWS of the cap with the GT layer by the SWS of the cap without GT. SWS ratio closer to one indicates

minimal capillary barrier effect while higher SWS ratio signifies greater capillary barrier effect. Figure 4-8 shows that the SWS ratio is close to 1.0 for specified fluxes close to the saturated hydraulic conductivity of the SM soil and SM-ML soil (no capillary barrier effect), respectively. As the specified flux was decreased, the difference in the soil water storage became consistently higher. For SM soil, a sharp increase in the SWS ratio occurred indicating the presence of capillary break over a wide range of specified fluxes.

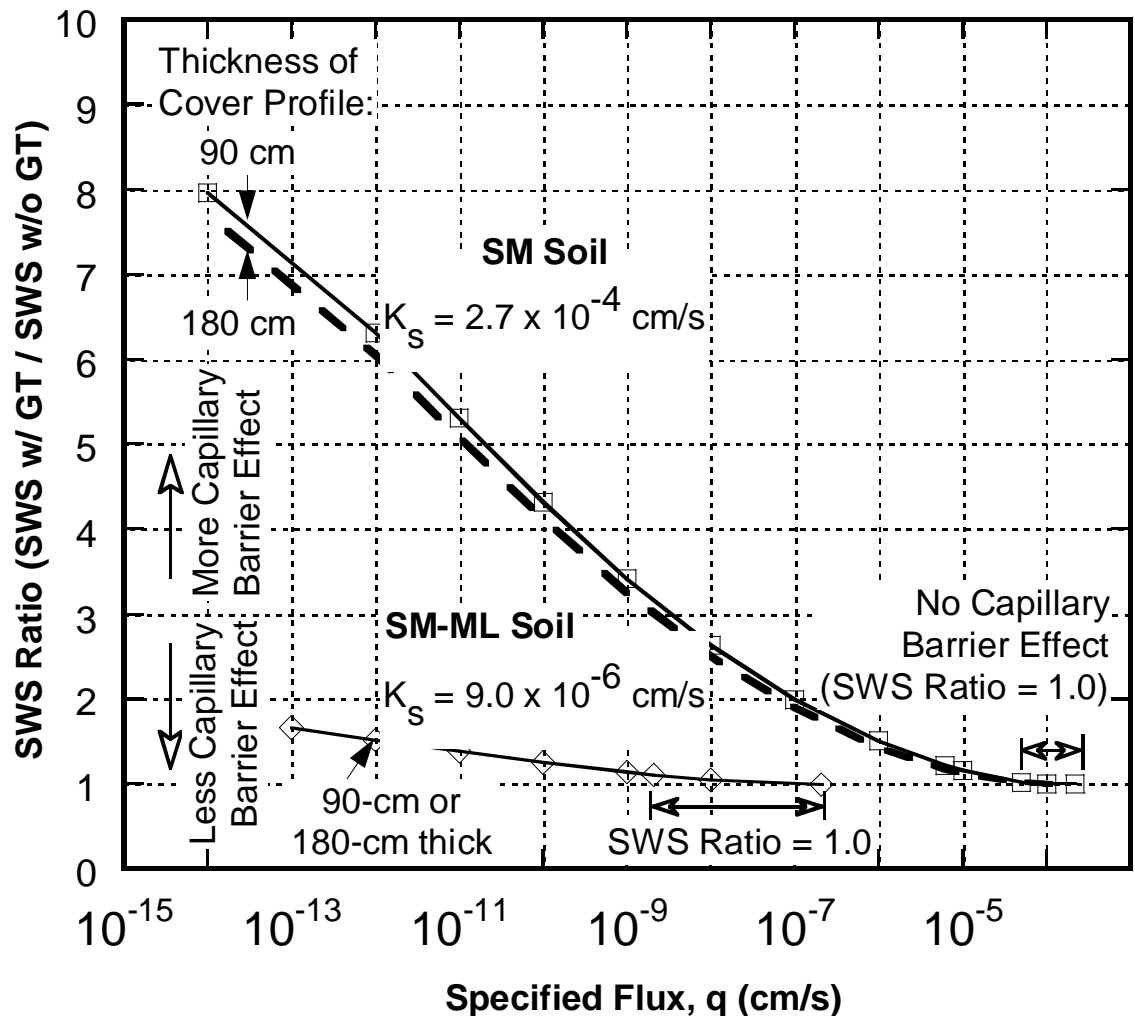


Figure 4-8: Relative magnitude of capillary barrier effect as a function of applied specified flux for SM and SM-ML soils.

For SM-ML soil, decrease in specified flux resulted only to slight increased in SWS ratio indicating a lower degree of capillary barrier effect.

A set of simulations was repeated by considering a thicker soil cap (180-cm thick) for both SM and SM-ML soils to determine whether cap thickness would have an impact on SWS ratio. As shown in Figure 4-8, the thickness of the cap had insignificant effect on the SWS ratio.

Thus, for earthen cover lysimeters which are typically built in arid and semi-arid climates where the net infiltration rate through the cap is generally smaller than in humid climates, the magnitude of capillary barrier effect would be higher and therefore needs to be considered in modeling the cap or assessing the field results of lysimeter. However, the results also show that regardless of the infiltration rate, earthen covers made up of soils having relatively low hydraulic conductivities (less than 10^{-5} cm/s) would result in insignificant capillary barrier effect.

Field-scale Simulations

To confirm the key findings of the previously presented constant infiltration simulations, selective field-scale simulations were conducted for instrumented field-scale lysimeters located in semi-arid and humid climates.

Semi-arid Climate

Figure 4-9 shows the simulated percolation and SWS for a soil profile instrumented in East Wenatchee, Washington by Khire et al. 1997. This simulation represents an earthen cap in a semi-arid climate built with 60-cm thick compacted Wenatchee silty clay as

cover soil having a saturated hydraulic conductivity of 2.2×10^{-7} cm/s. A 15-cm thick topsoil layer is included with a saturated hydraulic conductivity of 4.5×10^{-5} cm/s for surface vegetation.

For the first year, the measured percolation is 0.79 cm, whereas simulated by UNSAT-H without including the GT is 1.08 cm and 0.05 cm when the GT was included. For the second year, the simulated percolation by UNSAT-H without including the GT is 1.53 cm and 0.86 cm when the GT was included. For the third year, the simulated percolation is 1.57 cm (without GT) versus 0.87 cm (with GT). Due to the effect of the

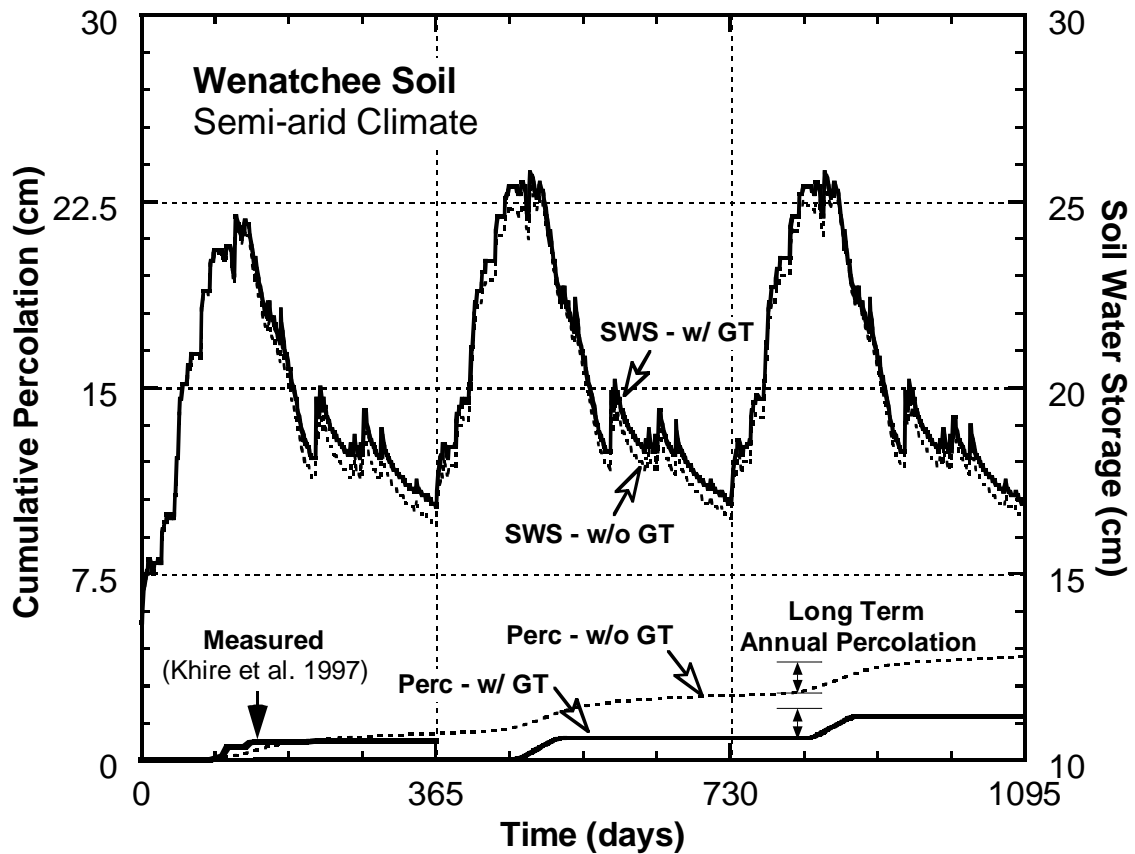


Figure 4-9: Simulated cumulative percolation and soil water storage for Wenatchee soil under semi-arid climate boundary condition.

initial condition, while there is difference in the simulated percolation with and without GT, the difference in percolation is relatively small whether GT is considered or not when long-term values of percolation are compared (3rd year in this case). Figure 4-9 shows that the simulated SWS when GT was considered versus when GT was not considered are almost identical. Hence, it can be inferred that, at this semi-arid site, the effect of capillary break introduced by the GT on long-term percolation is insignificant.

Figures 4-10 and 4-11 show the simulated percolation and SWS for SM soil and SM-ML soil, respectively, with and without GT under a semi-arid climate similar to the

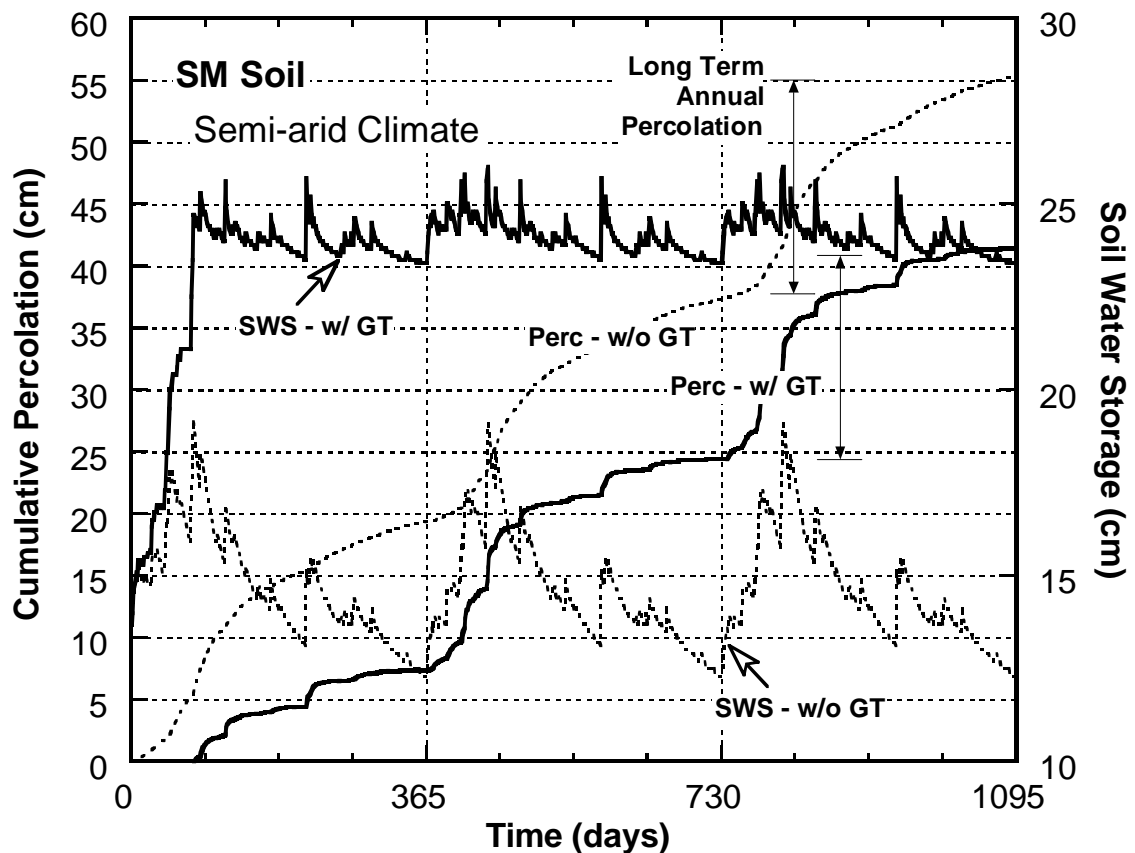


Figure 4-10: Simulated cumulative percolation and soil water storage for SM soil under semi-arid climate boundary condition.

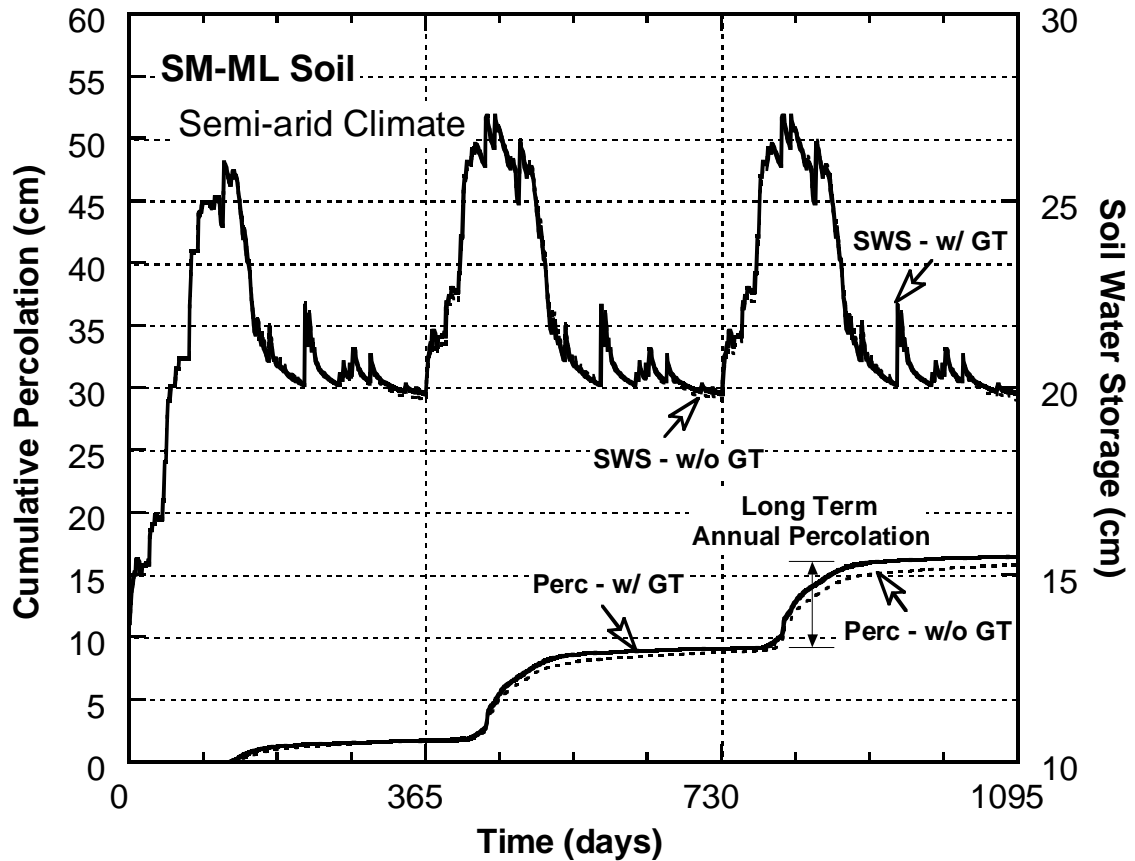


Figure 4-11: Simulated cumulative percolation and soil water storage for SM-ML soil under semi-arid climate boundary condition.

Wenatchee soil cap. The thickness of the soil profile and all other variables were kept the same except for the topsoil layer wherein relatively permeable uniformly graded medium sand (SP) was used to reduce or eliminate runoff to allow a consistent platform to compare the results. The saturated hydraulic conductivity assigned to the SP topsoil was 2.9×10^{-3} cm/s.

As shown in Figure 4-10, for the SM soil, the resulting SWS with GT is generally higher than SWS without GT. Consequently, the percolation for a lysimeter with GT is less than the percolation for a lysimeter without GT which indicates significant capillary

barrier effect. In contrast, for the SM-ML soil, minimal difference between simulated soil water storage and percolation occurred for lysimeter without GT versus lysimeter with GT (Figure 4-11). Hence, the difference in the simulated percolation for the SM-ML soil with and without GT is relatively small.

Peak SWS for SM soil with GT is 26.0 cm while for SM soil without GT is 19.1 cm or a 36% increase in storage capacity due to significant capillary barrier effect. Whereas the peak SWS for SM-ML soil with and without GT are both 27.3 cm. For the original Wenatchee soil, peak SWS with GT is 25.8 cm while peak SWS without GT is 25.5 cm. Thus, the peak soil water storage can be used as an indicator for assessing the magnitude of the capillary barrier effect as shown in SWS plots presented in Figures 4-8 to 4-11.

In order to compare the simulated SWS for all soil types with and without GT, simulated SWS for lysimeters with GT was plotted against simulated SWS for lysimeters without GT (Figure 4-12). The 1:1 line shows the region where SWS values are the same for a lysimeter with and without GT. Points above the 1:1 line correspond to higher SWS for earthen cap lysimeters underlined with GT and indicates the presence of capillary barrier effect. As shown in Figure 4-12, SWS values for the original Wenatchee soil are scattered near the 1:1 line indicating that there is insignificant difference between the soil cap with GT and without GT for field conditions that covered dry periods as well as wet periods. Similar trend is observed for SM-ML soil. Data points for SM soil are scattered far from the 1:1 line, in the upper left corner. Few data points for SM soil that are near the 1:1 line represent the initial condition wherein the same starting values of soil suction was applied for both simulations with and without GT. As the initial wetting front moves

through the SM soil, the soil cap with GT retains more water compared to the soil cap without GT resulting in the data points to shift above the 1:1 line. This indicates that capillary barrier effect is indeed significant for SM soil.

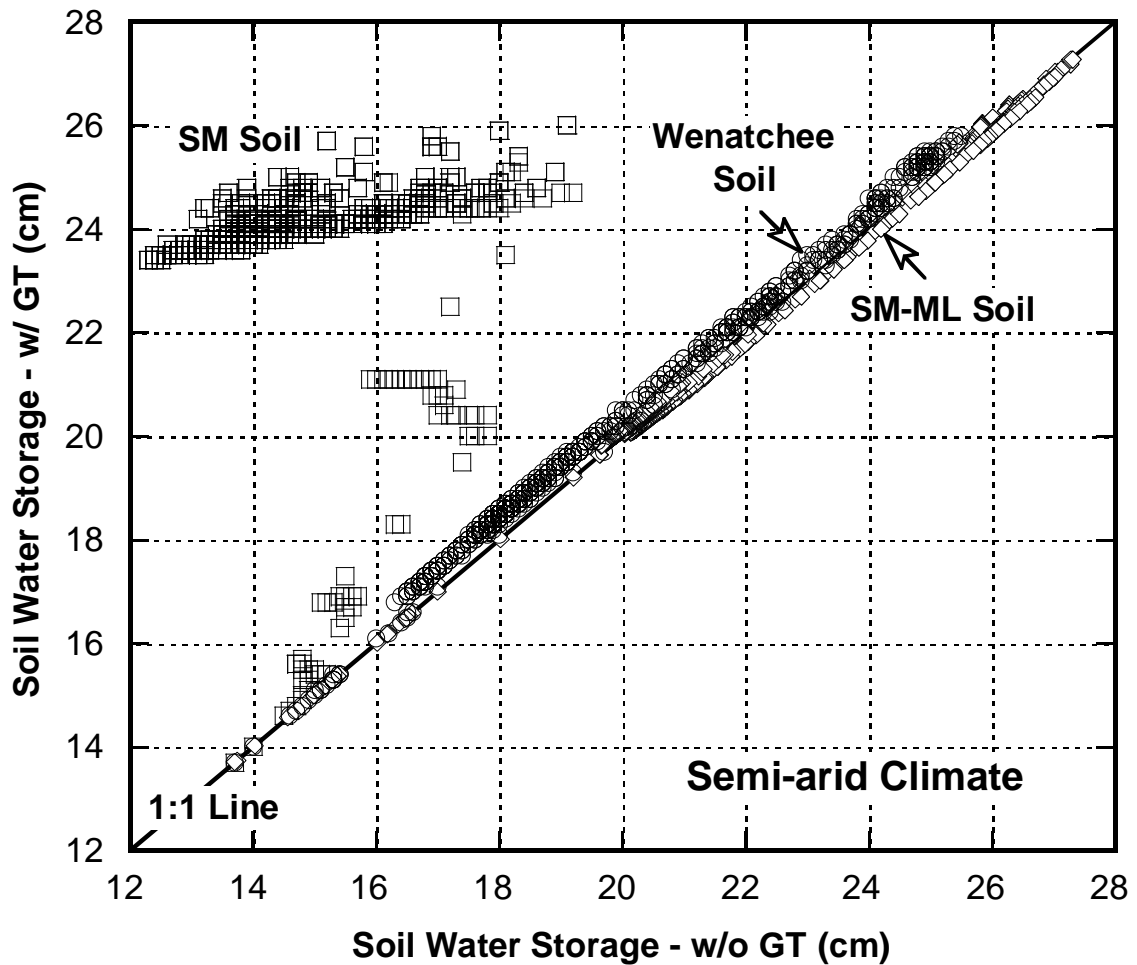


Figure 4-12: Simulated soil water storage for lysimeter with GT versus without GT under semi-arid climate boundary condition.

Humid Climate

Figure 4-13 shows the simulated percolation and SWS for an instrumented lysimeter located in Atlanta with and without GT. The field measured percolation and SWS for this

lysimeter are presented in Khire et al. (1997). The earthen cap in this humid climate consisted of 90-cm thick compacted Georgia red clay as cover soil having a saturated hydraulic conductivity of 3.2×10^{-6} cm/s. The cap also consisted of a 15-cm thick topsoil layer having a saturated hydraulic conductivity of 1.0×10^{-4} cm/s.

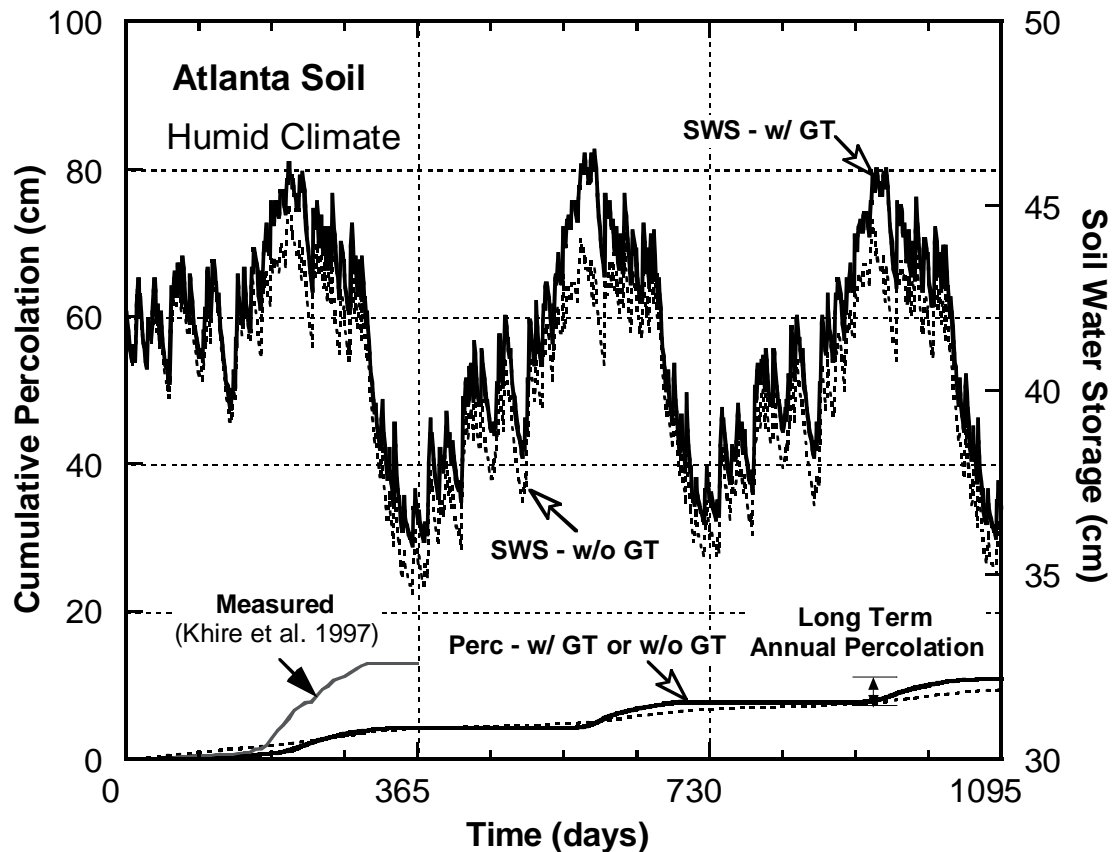


Figure 4-13: Simulated cumulative percolation and soil water storage for Atlanta soil under humid climate boundary condition.

The first year percolation simulated by UNSAT-H without GT is similar to the result published by Khire et al. (1997). The resulting percolation is 4.15 cm for a lysimeter without GT and 4.18 cm for a lysimeter with GT. UNSAT-H underpredicted

percolation because it overestimated the surface runoff (Khire et al. 1997). For the third year which would represent a long-term scenario, the resulting percolation is 2.69 cm (without GT) versus 3.10 cm (with GT). It can also be observed that percolation for simulation with GT is slightly greater than that for simulation without GT. The relatively small difference is attributed to the mass balance error reported by the model which is about the same as the observed difference. Nevertheless, negligible difference between simulated percolations occurs for earthen cap without GT versus with GT. Figure 4-13 also shows that simulated SWS for earthen cap without GT is very close to the simulated

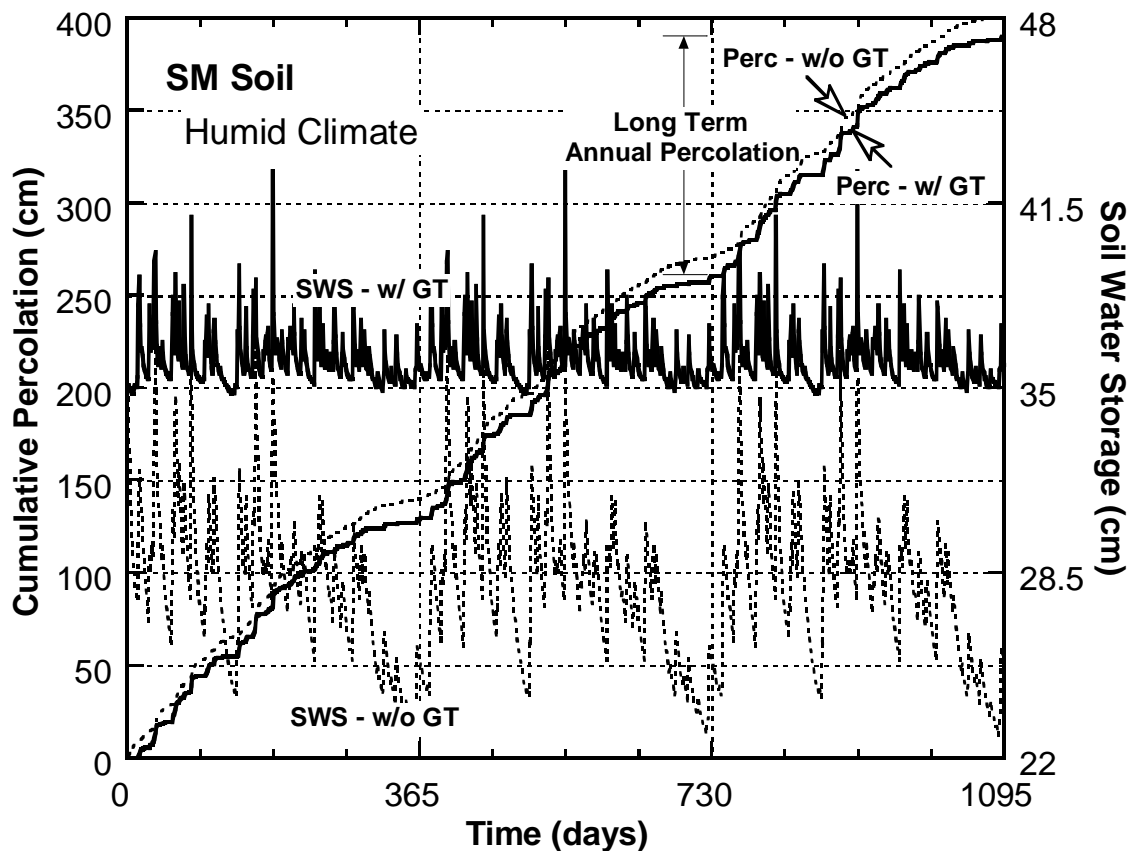


Figure 4-14: Simulated cumulative percolation and soil water storage for SM soil under humid climate boundary condition.

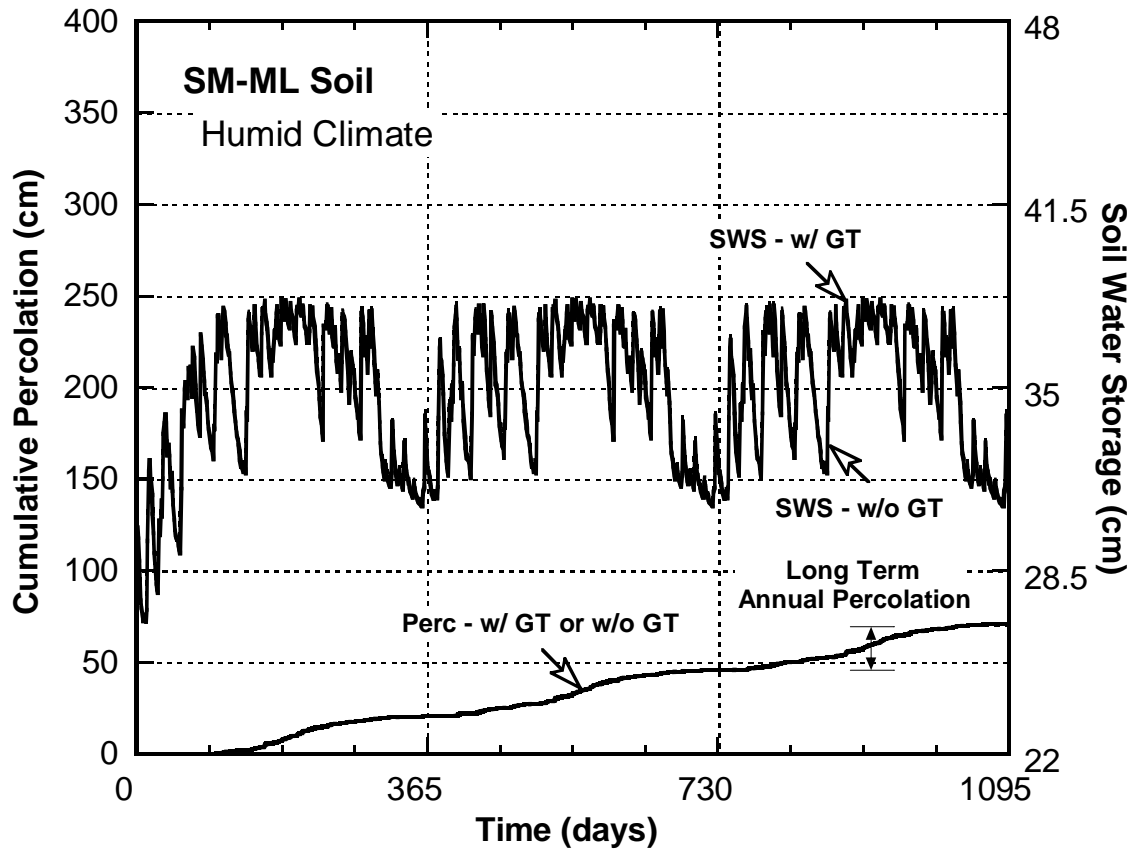


Figure 4-15: Simulated cumulative percolation and soil water storage for SM-ML soil under humid climate boundary condition.

SWS with GT. Thus, the peak SWS ratio is close to one. Hence, it can be inferred that the magnitude of capillary barrier effect for this field study was insignificant.

Figures 4-14 and 4-15 show the simulated percolation and SWS for SM soil and SM-ML soil, respectively, with and without GT for the humid site. The thickness of the soil profile and all other variables were kept the same except for the topsoil layer where SP soil was used instead. For SM soil, the resulting SWS with GT are greater than the SWS without GT. In fact, the maximum SWS for the soil cap without GT is only approximately equal to the minimum SWS for soil cap with GT. Peak SWS for SM soil

without GT is 36.7 cm while peak SWS for SM soil with GT is 42.6 cm or a 16% increase in storage capacity. Although this signifies significant capillary break, the increase in SWS due to capillary barrier effect in a humid climate is not as high as the increase in SWS for a semi-arid climate. The inherent frequently high precipitation rate at the humid location compared to the semi-arid location results in higher net infiltration rate for the soil cap. The resulting infiltration rate is often closer to the saturated hydraulic conductivity of the soil cap. As Figure 4-8 illustrates, the magnitude of capillary barrier effect under such conditions is less significant.

For SM-ML soil, peak SWS with and without GT is about the same (38.1 cm). Hence, capillary barrier effect is insignificant because both soil caps, with and without GT, achieved similar water content at the onset of percolation breakthrough. This is also evident from the cumulative percolation plot shown in Figure 4-15 wherein both curves (with and without GT) overlap.

Figure 4-16 shows the comparison of simulated SWS for lysimeters with GT versus lysimeters without GT for all soil types for the humid site. Data points for both SM-ML soil and the original Atlanta soil spread near the 1:1 line indicating negligible capillary barrier effect. In contrast, data points for SM soil are scattered far from the 1:1 line signifying greater magnitude of capillary barrier effect.

Results of the field-scale simulations agree with the observations obtained from constant infiltration simulations. The hydraulic properties of cover soils and the applied infiltration rate(s) determine whether significant capillary barrier effect can be expected or not when a nonwoven GT is considered or not in the numerical simulation. The magnitude of capillary barrier effect, as defined by the effect on long-term percolation,

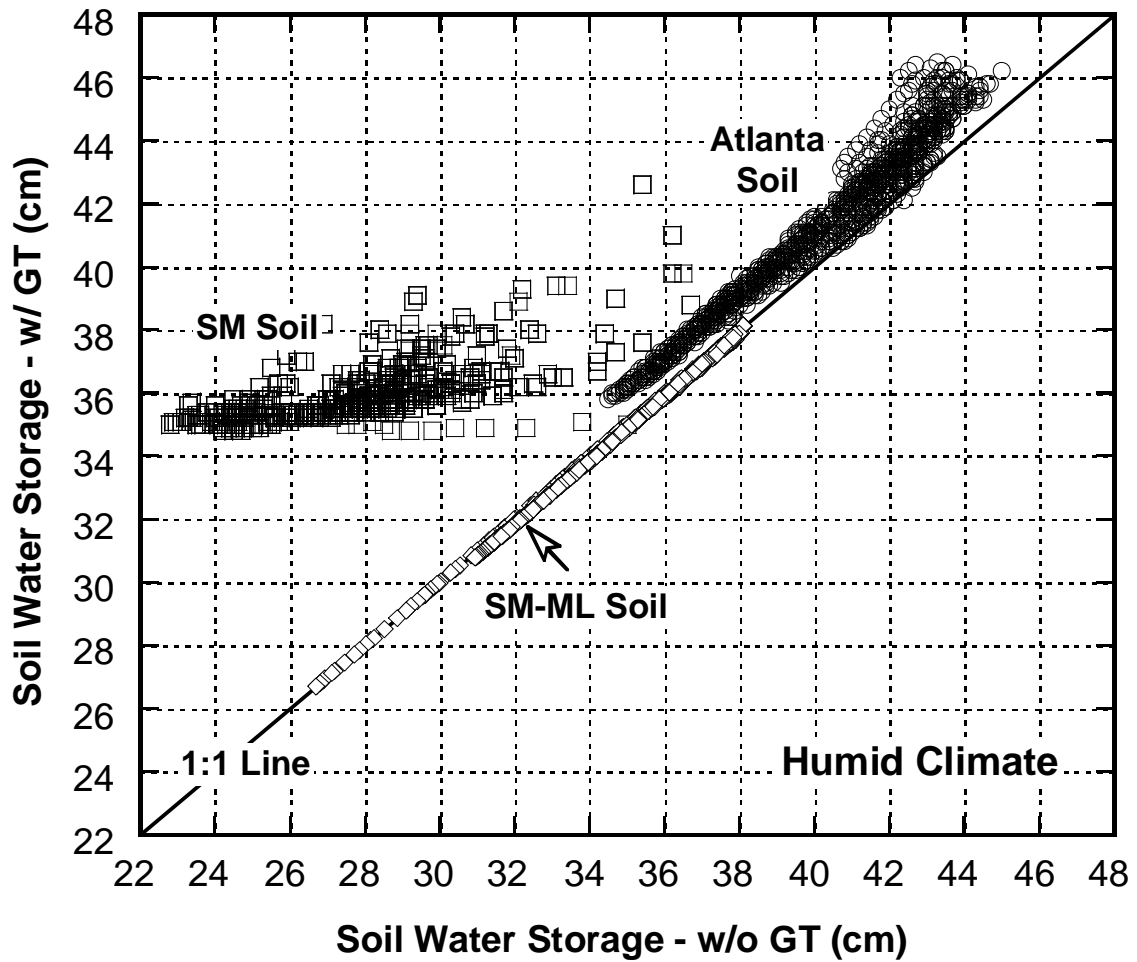


Figure 4-16: Simulated soil water storage for lysimeter with GT versus without GT under humid climate boundary condition.

introduced by the non-woven geotextile in the geosynthetic drainage layer of a lysimeter is negligible when the saturated hydraulic conductivity of the cap is less than 10^{-5} cm/s.

Figure 4-17 summarizes the annual percolation difference between the lysimeter without GT and the lysimeter with GT for the first year and long-term scenarios. Because landfill earthen caps more often consist of soils having hydraulic conductivity that is less than or equal to 10^{-5} cm/s, the effect of GT on the long-term percolation is expected to be

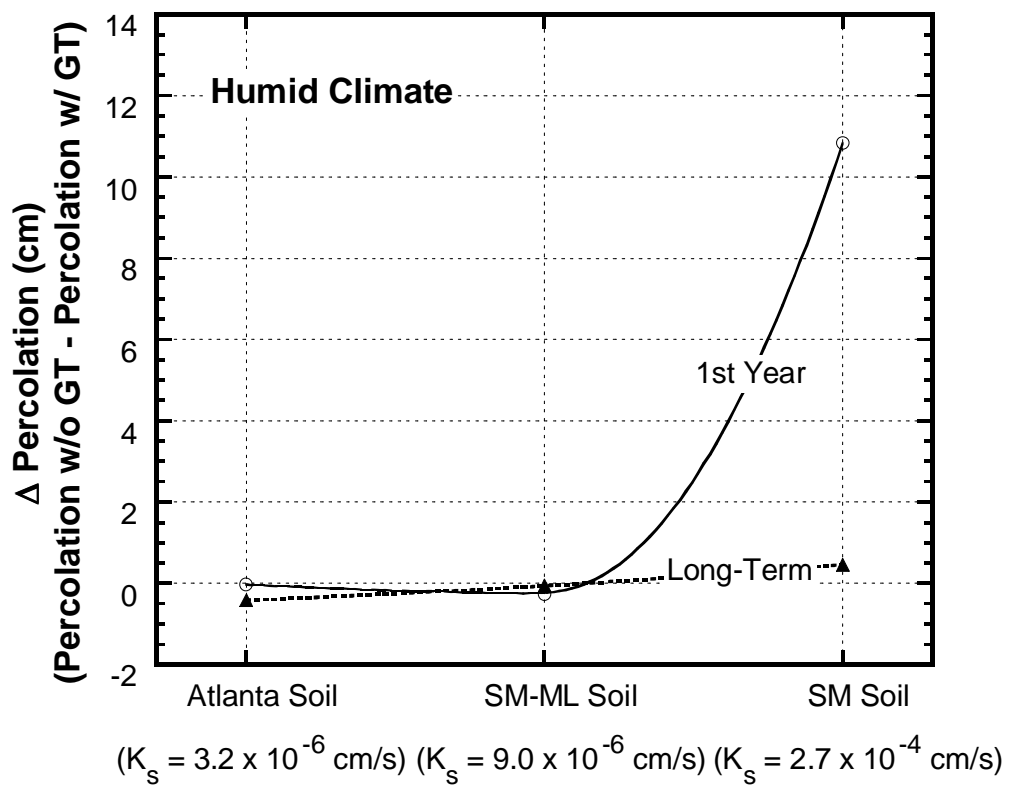
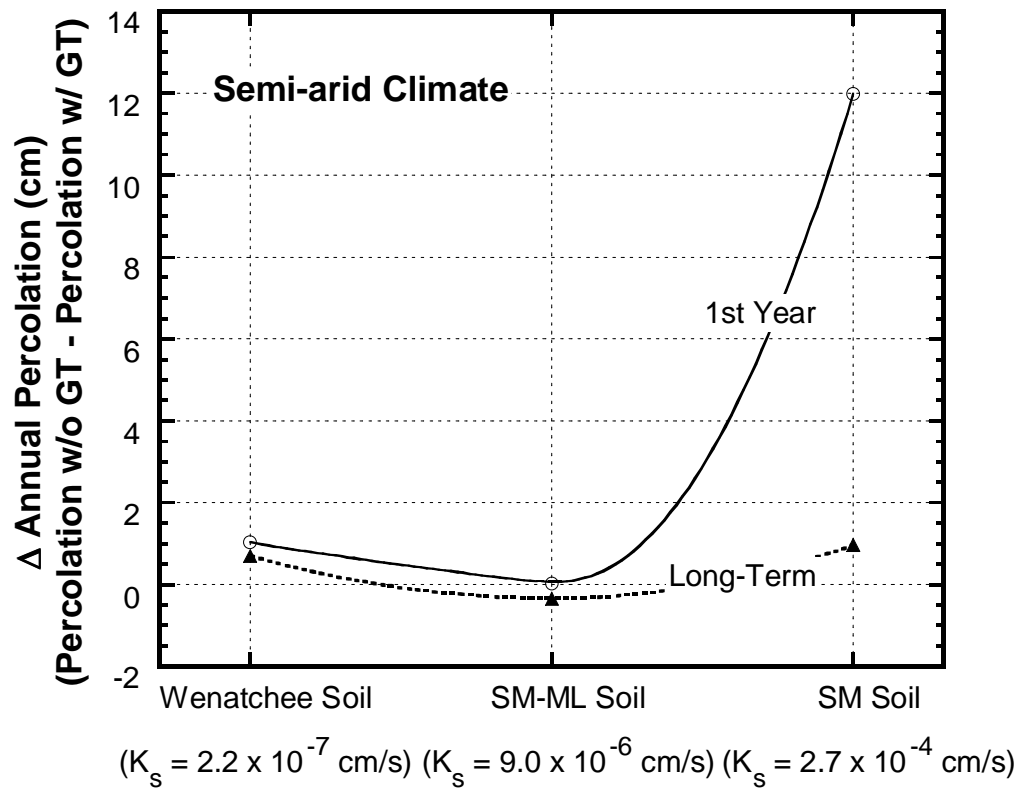


Figure 4-17: Annual percolation difference between lysimeter without GT and lysimeter with GT for semi-arid (a); and humid climates (b).

insignificant. Previous study of Scanlon et al. (2005) where significant capillary barrier effect have been observed under a long-term (25-yr) numerical simulation of an earthen cover for their Texas site. The saturated hydraulic conductivity of the soil cover that was simulated is 2.3×10^{-4} cm/s. Hence, the results of Scanlon et al. (2005) are consistent with the findings of this study. The capillary barrier effect may be significant if the hydraulic conductivity is greater than 10^{-5} cm/s.

SUMMARY AND CONCLUSIONS

This numerical study demonstrates that capillary break is introduced when an earthen cap is underlain by a nonwoven geotextile or low unit weight municipal solid waste. While a geotextile or a waste layer both create a capillary break, the magnitude of the capillary barrier effect on the simulated percolation is negligible when the saturated hydraulic conductivity of the cover soils is 10^{-5} cm/s or less.

Results from the field-scale simulations further show that whenever capillary break exists, the capillary barrier effect maybe significant during the first year, irrespective of the soil type or meteorological conditions. As the soil water storage of the cap increases due to precipitation and when percolation occurs, capillary break is breached and will only be restored if the cap dries up and returns to the original state prior to percolation breakthrough. For humid climates, the capillary barrier effect is not as significant as for the drier climates regardless of the hydraulic conductivity of the soils. Hence, for long-term percolation prediction, nonwoven geotextile may not be considered when modeling earthen cap lysimeters.

REFERENCES

REFERENCES

- Albright, W., Benson, C., Gee, G., Roesler, A., Abichou, T., Apiwantragoon, P., Lyles, B., and Rock, S. (2004). "Field Water Balance of Landfill Final Covers," *Journal of Environmental Quality*, 33 (6): 2317-2332.
- Baker, R., and Hillel, D. (1990). "Laboratory Tests of a Theory of Fingering During Infiltration into Layered Soils," *Soil Science Society of America Journal*, 54: 20–30.
- Bathurst, R., Ho, A., and Siemens, G. (2007). "A Column Apparatus for Investigation of 1-D Unsaturated-Saturated Response of Sand-Geotextile Systems," *Geotechnical Testing Journal*, 30 (6): 1-9.
- Benson, C., and Khire, M. (1995). "Earthen Covers for Semi-arid and Arid Climates, *Landfill Closures*, GSP No. 53, ASCE, Reston, VA: 201-217.
- Benson, C., Albright, W., Roesler, A., and Abichou, T. (2002). "Evaluation of Final Cover Performance: Field Data from the Alternative Cover Assessment Program (ACAP)," *Proceedings, Waste Management 2002*, Tucson, AZ.
- Benson, C., Bohnhoff, G., Ogorzalek, A., Shackelford, C., Apiwantragoon, P., and Albright, W. (2005). "Field Data and Model Predictions for an Alternative Cover," *Waste Containment and Remediation*, GSP No. 142, ASCE, Reston, VA: 1-12.
- Bohnhoff, G., Ogorzalek, A., Benson, C., Shackelford, C., and Apiwantragoon, P. (2009). "Field Data and Water-Balance Predictions for a Monolithic Cover in a Semiarid Climate," *Journal of Geotechnical and Geoenvironmental Engineering*, 135 (3): 333–348.
- Fayer, M., Rockhold, M., and Campbell, M. (1992). "Hydrologic Modeling of Protective Barriers: Comparison of Field Data and Simulation Results," *Soil Science Society of America Journal*, 56: 690-700.
- Fayer, M. (2000). "UNSAT-H Version 3.0: Unsaturated Soil Water and Heat Flow Model – Theory, User Manual, and Examples." PNNL-13249, Pacific Northwest Laboratories, Richland, Washington.
- Iryo, T., and Rowe, R. (2003). "On the Hydraulic Behavior of Unsaturated Nonwoven Geotextiles," *Geotextiles and Geomembranes*, 21: 381-404.
- Kazimoglu, Y., McDougall, J., and Pyrah, I. (2005). "Moisture Retention and Movement in Landfilled Waste," *Proceedings, GeoProb 2005: International Conference on Problematic Soils*, Famagusta, Northern Cyprus, May 2005.
- Kazimoglu, Y., McDougall, J., and Pyrah, I. (2006). "Unsaturated Hydraulic Conductivity of Landfilled Waste," *Proceedings, Unsaturated Soils 2006*, GSP No. 147, ASCE, Reston, VA: 1525-1534.

- Khire, M., and Mijares, R. (2008). "Influence of the Waste Layer on Percolation Estimates for Earthen Caps Located in a Sub-humid Climate," *Proceedings, GeoCongress 2008*, GSP No. 177, Geotechnics of Waste Management and Remediation, ASCE, Reston, VA: 88-95.
- Khire, M., Benson, C., and Bosscher, P. (1997). "Water Balance Modeling of Earthen Final Covers," *Journal of Geotechnical and Geoenvironmental Engineering*, 123 (8): 744-754.
- Khire, M., Benson, C., and Bosscher, P. (1999). "Field Data From a Capillary Barrier and Model Predictions with UNSAT-H," *Journal of Geotechnical and Geoenvironmental Engineering*, 125: 518-528.
- Khire, M., Benson, C., and Bosscher, P. (2000). "Capillary Barriers: Design Variables and Water Balance," *Journal of Geotechnical and Geoenvironmental Engineering*, 126 (8): 695-708.
- Mijares, R., Khire, M., and Johnson T. (2010). "Lysimeters Versus Actual Earthen Caps: Numerical Assessment of Soil Water Storage," *Proceedings, GeoFlorida 2010*, GSP No. 199, Advances in Analysis, Modeling and Design, ASCE, Reston, VA: 2849-2858.
- Mukherjee, M. (2008). "Instrumented Permeable Blankets for Estimating Subsurface Hydraulic Conductivity and Confirming Numerical Models Used for Subsurface Liquid Injection," *Ph.D. Dissertation*, Michigan State University, East Lansing, Michigan, 278 p.
- Nyhan, J., Hakonson, T., and Drennon, B. (1990). "A Water Balance Study of Two Landfill Cover Designs for Semiarid Regions," *Journal of Environmental Quality*, 19: 281-288.
- Ogorzalek, A., Bohnhoff, G., Shackelford, C., Benson, C., and Apiwantragoon, P. (2008). "Comparison of Field Data and Water-Balance Predictions for a Capillary Barrier Cover," *Journal of Geotechnical and Geoenvironmental Engineering*, 134 (4): 470-486.
- Park, K., and Fleming, I. (2006). "Evaluation of a Geosynthetic Capillary Barrier," *Geotextiles and Geomembranes*, 24: 64-71.
- Scanlon, B., Christman, M., Feedy, R., Porro, I., Simunek, J., and Flerchinger, G. (2002). "Intercode Comparisons for Simulating Water Balance of Surficial Sediments in Semiarid Regions," *Water Resources Research*, 38: 1323-1339.
- Scanlon, B., Reedy, R., Keese, K., and Dwyer, S. (2005). "Evaluation of Evapotranspirative Covers for Waste Containment in Arid and Semiarid Regions in the Southwestern USA," *Vadose Zone Journal*, 4: 55-71.

- Stoltz, G., and Gourc, J. (2007). "Influence of Compressibility of Domestic Waste on Fluid Conductivity," *Proceedings*, 18th Congres Francais de Mecanique, Grenoble, France.
- Stormont, J., Henry K., and Evans, T. (1997). "Water Retention Functions of Four Nonwoven Polypropylene Geotextiles," *Geosynthetics International*, 2 (6): 661-672.
- Stormont, J., and Anderson, C. (1999). "Capillary Barrier Effect from Underlying Coarser Soil Layer," *Journal of Geotechnical and Geoenvironmental Engineering*, 125: 641–648.
- Stormont, J., and Morris, C. (2000). "Characterization of Unsaturated Nonwoven Geotextiles," *Proceedings*, Geo-Denver 2000, GSP No. 99, Advances in Unsaturated Geotechnics, ASCE, Reston, VA: 153–164.
- Tami, D., Rahardjo, H., Leong E., and Fredlund, D. (2004). "A Physical Model for Sloping Capillary Barriers," *Geotechnical Testing Journal*, 27: 1–16.
- van Genuchten, M. (1980). "A Closed-Form Equation for Predicting the Hydraulic Conductivity of Unsaturated Soils," *Soil Science Society of America Journal*, 44: 892-898.
- Ward, A., and Gee, G. (1997). "Performance Evaluation of a Field-Scale Surface Barrier," *Journal of Environmental Quality*, 26: 694–705.

PAPER NO. 5: NUMERICAL ASSESSMENT OF PAN LYSIMETERS USED FOR ESTIMATION OF GROUNDWATER RECHARGE FOR NATURAL SYSTEMS

ABSTRACT

A laboratory soil column consisting of fine sand with a saturated hydraulic conductivity of 4.5×10^{-3} cm/s was built and instrumented to measure its hydraulic response to constant infiltration of 1.5×10^{-4} cm/s. The numerical model UNSAT-H with a water table lower boundary condition was able to accurately predict the percolation and soil water storage of the column. The calibrated numerical model was used for field-scale simulations that were conducted to determine whether percolation estimates obtained from pan lysimeters are representative of the groundwater recharge rate for the corresponding natural system. Natural systems consisting of monolithic soil profile were simulated for semi-arid and sub-humid climates. This study demonstrates that when pan lysimeters are used for estimating groundwater recharge, the lysimeter should be thick enough to overcome the capillary barrier effect introduced by the lower drainage boundary. Thinner soil profiles used for constructing lysimeter underestimate the recharge due to the capillary barrier effect. The higher the hydraulic conductivity of the soil profile, the thicker the soil profile needs to become in order for the lysimeter to estimate the recharge accurately. Furthermore, in wetter climates, the thickness of the soil profile for the lysimeter could be less than the required profile thickness for a drier climate. Generally, a lysimeter thickness of 1.2 m would be enough to capture the groundwater recharge for the natural system.

INTRODUCTION

The primary source of groundwater recharge for natural systems is precipitation. The groundwater recharge rate, which is also known as the rate of replenishment of the water in aquifers, is dependent on the rate of infiltration across the vadose zone. Estimating groundwater recharge may be undertaken under different spatial and temporal scales depending on the required application and accuracy. Scanlon et al. (2002) categorized the techniques used in quantifying groundwater recharge based on the three hydrologic zones: surface water, unsaturated zone, and saturated zone. Within each of these zones, the estimation techniques are further classified as physical, tracer, or numerical modeling.

Among all the techniques used for recharge estimation, the only method that is considered direct for estimating natural groundwater recharge from the ground surface is via the construction of a pan lysimeter. A pan lysimeter also can provide accurate measurement of the various components of field water balance which include percolation, surface runoff, soil water storage, basal percolation, and evapotranspiration. Lysimeter studies have been performed since the end of the 17th century (Seiler and Gat 2007). In the past, lysimeters are generally constructed using deep cylindrical pots with an open surface area of about 1 m^2 . These cylindrical lysimeters were typically used for estimating groundwater recharge and were mechanically balanced to accurately measure fluctuations in soil water storage and measure the deep percolation. For landfill earthen cover application, pan lysimeters are more common. These lysimeters have much larger surface area to capture the field-scale heterogeneities such as soil macropores and fractures (Benson et al. 1994; Khire et al. 1997). Changes in the soil water storage are determined by installing water content sensors to monitor the water content across the

soil profile. A diversion berm is constructed along the perimeter in order to divert surface runoff from upslope of the lysimeter while directing the surface runoff within the monitoring area to the collection system. The deep percolation is collected by installing a pea gravel drainage layer or a geocomposite drainage layer at the lower boundary of the pan lysimeter.

Recharge rates obtained from a lysimeter can be estimated at time scales from minutes to years with a good precision of at least 1 mm/year (Gee and Hillel 1988; Scanlon et al. 2002). Because lysimeters yield good data to study recharge mechanisms, Gee and Hillel (1988) pointed out that quantification of drainage across a soil profile using lysimeters for a long period under field meteorological conditions could provide the basis for calibrating numerical models used for estimating regional or local groundwater recharge. Flow of infiltrated water through the unsaturated zone to the water table is controlled by the saturated and unsaturated hydraulic properties of the soil (Krishnamurthi et al. 1977). In addition to the hydraulic properties, boundary conditions also influence the estimation of recharge when pan lysimeters are used because the lysimeters introduce a drainage boundary that does not exist in the natural system it attempts to emulate.

OBJECTIVE

The key objective of the study presented in this paper is to numerically evaluate the accuracy of the use of pan lysimeter to estimate natural recharge. Natural groundwater recharge rate is defined in this paper as the resulting rate of deep drainage that reaches the groundwater table as a consequence of redistribution of water across the soil profile in

response to the gradients in the energy state of the water (Fayer 2000). Lysimeter basal percolation rate is compared to the deep drainage rate to evaluate the accuracy of using pan lysimeter in estimating natural groundwater recharge. The key parameters evaluated include hydraulic conductivity, thickness of the soil profile, and climate. In order to validate the unsaturated flow model, a laboratory soil column underlain by a geocomposite drainage layer was built and instrumented to monitor its soil water storage and deep percolation under constant infiltration. The calibrated numerical model was used to conduct numerical simulations to predict groundwater recharge rates in semi-arid and sub-humid climates using pan lysimeters.

LABORATORY SOIL COLUMN

A soil column consisting of OK110 fine sand underlain with a geocomposite drainage layer was built and instrumented to monitor its response under a one-dimensional constant infiltration event. OK110 is a uniformly graded sand having D_{50} equal to 0.11 mm and USCS classification of SP (poorly graded sand). Figure 5-1 shows the photo and the schematic of the 30 cm diameter soil column which was 90 cm tall. The column was made up of a PVC pipe that was capped at its bottom. The PVC cap was modified by inserting a circular plane to create a sloping impermeable bottom boundary where a geocomposite drainage layer was placed. The geocomposite drainage layer consisted of a geonet sandwiched between two nonwoven geotextiles. Table 5-1 shows the properties of the soil and the geotextile used to fabricate the soil column. A perforated plastic tubing was placed around the circumference of the geocomposite drainage layer to facilitate drainage of infiltrated water. A 2-cm diameter outlet tubing was placed at the bottommost

point to collect the percolation and measure the resulting outflow rate. The entire set-up was placed on top of a weighing scale to accurately measure and record the changes in the soil water storage.

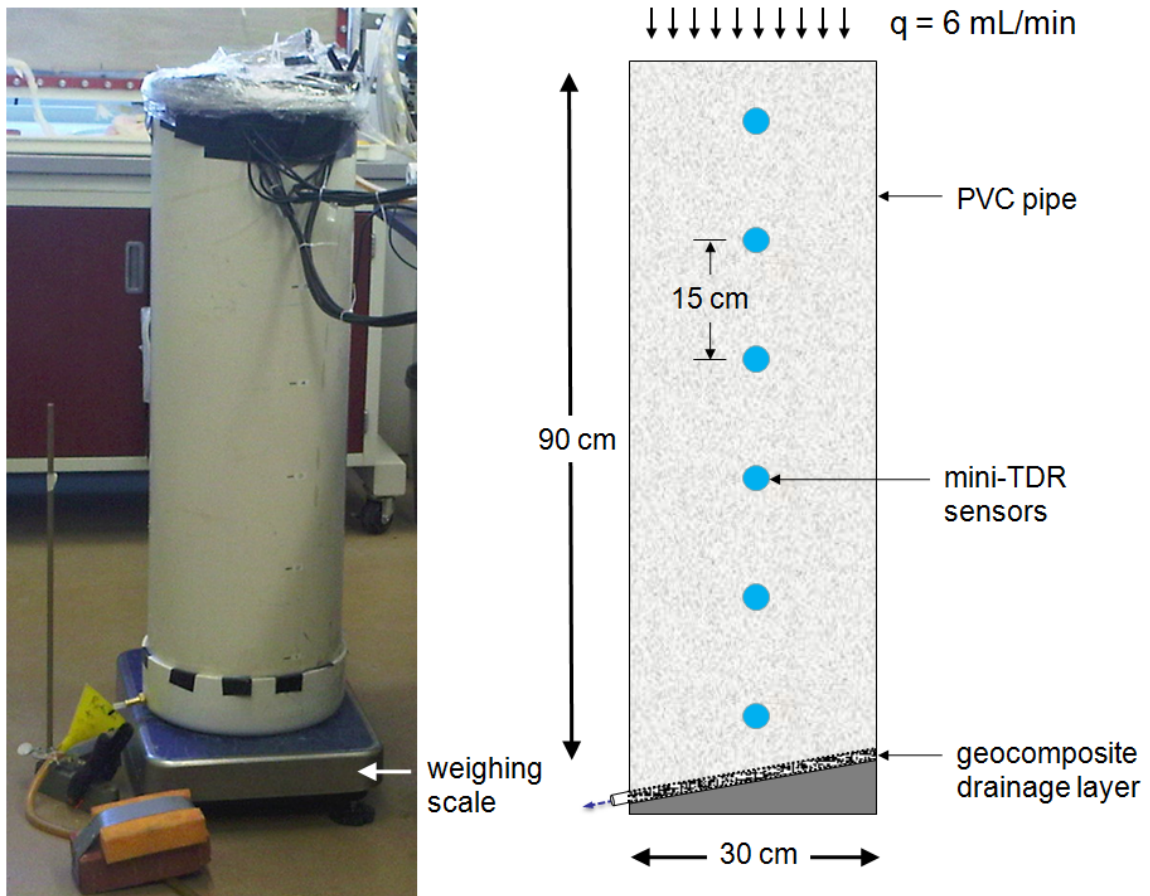


Figure 5-1: Photo and schematic of instrumented laboratory soil column.

The laboratory soil column was instrumented with water content sensors to monitor the soil water storage. Six time domain reflectometry (TDR)-based water content sensors were placed across the soil column with a vertical spacing of 15 cm. The mini-TDR water content sensor has three pointed stainless steel rods mounted into a polymer head. The probe rods are 6 cm long, have a diameter of 0.15 cm, and are spaced by

0.6 cm. The mini-TDR water content sensor was placed horizontally in the initially dry column of fine sand and was connected to a multiplexer and a datalogger to continuously monitor and record the apparent dielectric constant. The empirically derived calibration equation by Topp et al. (1980) was used to convert the measured dielectric constants to the instantaneous volumetric water contents.

To facilitate the application of a constant flux at the surface of the sand column, an elevated Mariotte bottle was connected to a coil of perforated tubing placed on the sand surface that irrigated the column. A 15-cm thick pea gravel layer wrapped with a polymer insect mesh was also placed on top of the soil column to achieve a uniform wetting front.

Table 5-1: Saturated and unsaturated hydraulic properties of the materials used to build the laboratory soil column.

Soil/Material	θ_s (cm ³ /cm ³)	θ_r (cm ³ /cm ³)	α (1/cm)	n	K_s (cm/s)	Reference
OK110 Fine Sand	0.36	0.03	0.016	6.5	4.5×10^{-3}	Mukherjee (2008)
Geotextile	0.82	0	0.066	3.99	0.15	Park and Fleming (2006)
GP Soil	0.30	0.01	0.574	2.44	1.0	Khire et al. (2000)

NUMERICAL MODELING

The finite-difference water balance model UNSAT-H (Fayer 2000) was used in this study to mathematically simulate the response of the instrumented laboratory soil column

subjected to constant flux. Once UNSAT-H was validated for the lab sand column, it was extended to conduct field-scale simulations to evaluate how lysimeter can simulate groundwater recharge rates.

UNSAT-H numerically solves a modified form of Richards' equation to compute the flow of water through both saturated and unsaturated soil and is capable of simulating steady-state and transient conditions. Equation 5-1 shows the governing equation that UNSAT-H solves to mathematically simulate the flow of water in soil:

$$\frac{\partial \theta}{\partial \psi} \frac{\partial \psi}{\partial t} = - \frac{\partial}{\partial z} \left[K_T(\psi) \frac{\partial \psi}{\partial z} + K_L(\psi) + q_{VT} \right] - S(z, t) \quad (5-1)$$

where θ is the volumetric water content; ψ is the matric suction head; z is the vertical coordinate, t is time; $K_L(\psi)$ is the unsaturated hydraulic conductivity for a given ψ , $K_T(\psi) = K_L(\psi) + K_V(\psi)$ where $K_T(\psi)$ is the isothermal water vapor conductivity for a given ψ ; q_{VT} is the thermal vapor flux density; and S is the sink term that represents the water uptake by vegetation as a function of both depth and time. The thermal vapor flux density is calculated by applying Fick's law of vapor diffusion. Equation 5-1 assumes that fluid is incompressible, liquid water flow is isothermal, and air phase is continuous and at constant atmospheric pressure. Khire et al. (1997) summarizes key features of UNSAT-H as they apply to simulating field-scale pan lysimeters.

UNSAT-H assesses the water balance of the soil profile using Equation 5-2:

$$P_r = P - RO - E - T - \Delta S \quad (5-2)$$

where P_r is the basal percolation, P is the precipitation, RO is the surface runoff, E is the surface evaporation, T is the plant transpiration, and ΔS is the change in soil water storage during a specified period of time. At the ground surface, UNSAT-H separates the applied precipitation input into infiltration and surface runoff. The model does not include as input the surface run-on or overland flow that runs onto the area being modeled. It does not have algorithms for snowmelt and ground freezing during winter. UNSAT-H also does not consider interception of water by the plant canopy nor delayed infiltration of collected water in depressions on the soil surface. Whenever precipitation exceeds the infiltration capacity of the soil profile, surface runoff is generated to prevent ponding on the surface. Once water has infiltrated, it moves upward or downward across the soil profile, depending on the prevailing evapotranspirative and hydraulic gradients.

Potential evapotranspiration is calculated from daily maximum and minimum air temperatures, daily average dewpoint, net solar radiation, wind speed, and cloud cover using a modified form of the Penman equation as reported by Doorenbos and Pruitt (1977). Surface evaporation is calculated using an integrated form of Fick's law of diffusion that addresses the interrelationships between these three processes: (1) the flow of heat to and from the soil surface; (2) the flow of water to the soil surface from below; and (3) transfer of water vapor from the soil surface to the atmosphere (Hillel 1980; Fayer 2000). Transpiration is calculated by applying the potential transpiration demand, which is a function of the leaf area index and the growing season for the vegetation, across the root zone in proportion to the relative root density at a particular depth. Soil

water storage is calculated by integrating the volumetric water content across the soil profile. The resulting flux along the lower boundary is the basal percolation or deep drainage for the soil profile. UNSAT-H was specifically developed to estimate deep drainage rates. This model has also been routinely used for water balance modeling of earthen caps (Khire et al. 1997; Khire et al. 2000; Benson et al. 2005; Scanlon et al. 2005; Ogorzalek et al. 2008; Bohnhoff et al. 2009). For this study, one-dimensional simulations were carried out using UNSAT-H Version 3.0.

Material Properties

Laboratory Soil Column

Saturated and unsaturated hydraulic properties of the materials used to build and simulate the laboratory soil column are presented in Table 5-1. Unsaturated hydraulic conductivity functions were estimated using the closed-form van Genuchten-Mualem expression where the pore interaction term was set to 0.5 (van Genuchten 1980).

Hydraulic properties of nonwoven geotextile were obtained from Park and Fleming (2006). The nonwoven, polypropylene, needle-punched, continuous fiber geotextile has a mass per unit area of 550 g/m^2 with a thickness of 4.0 mm and an opening size of 0.05 to 0.15 mm. It has similar properties to that of the geotextile used in the study of Stormont and Morris (2000). van Genuchten fitting parameters were obtained based from the data points measured by Park and Fleming (2006) for the geotextile's water retention curve (Figure 5-2).

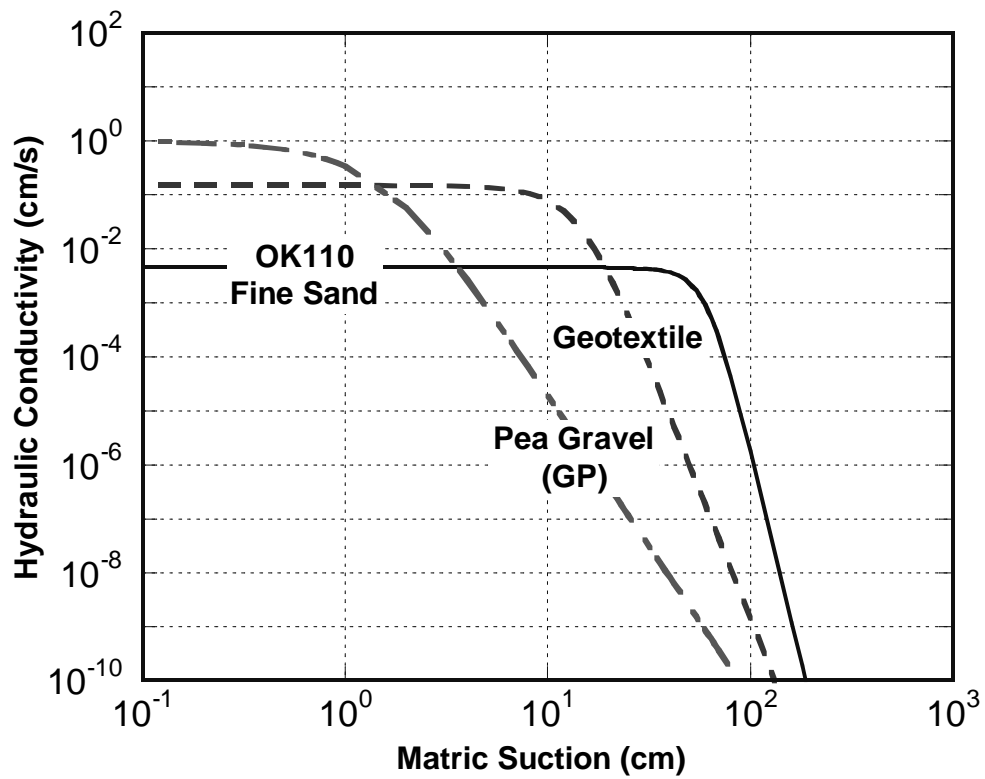
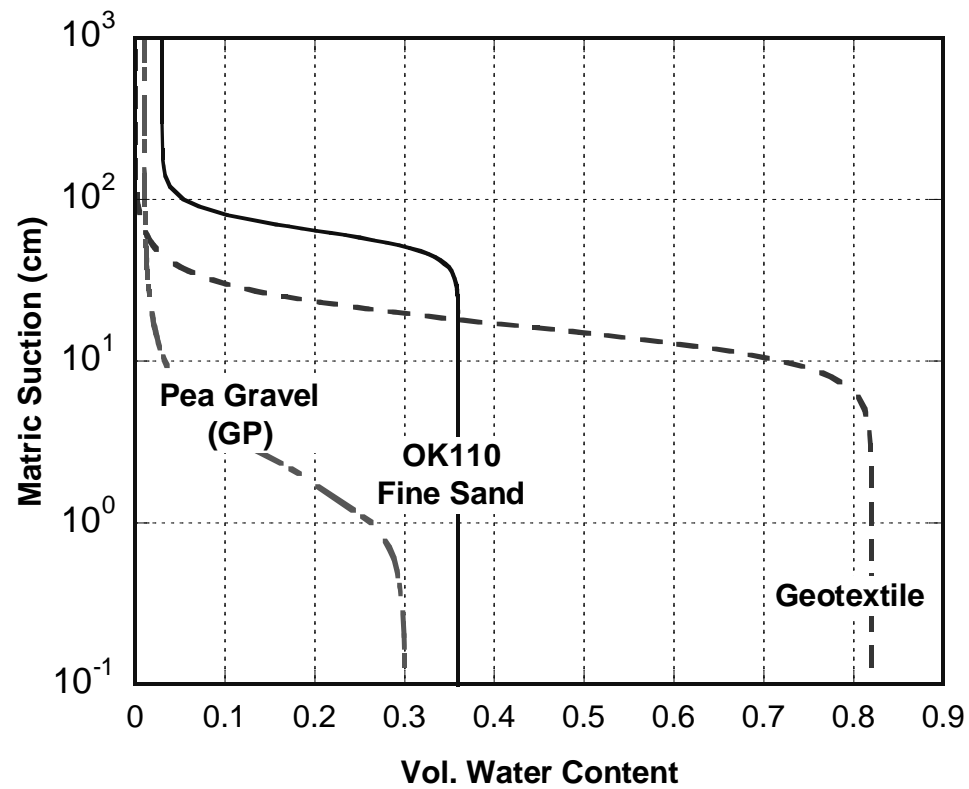


Figure 5-2: Water retention curves (a); and predicted hydraulic conductivity functions (b) for the materials used in the laboratory soil column.

Field-scale Simulations

Table 5-2 shows the saturated and unsaturated hydraulic properties of the soils used to simulate the groundwater recharge for natural systems. The natural system considered in this study consisted of monolithic soil profile under semi-arid and sub-humid climates. Figure 5-3 shows the soil water characteristic curves and the unsaturated hydraulic conductivity functions for the soils presented in Table 5-2.

Table 5-2: Saturated and unsaturated hydraulic properties of the soils used to simulate groundwater recharge rates.

Soils	θ_s (cm³/cm³)	θ_r (cm³/cm³)	α (1/cm)	n	K_s (cm/s)	Reference
GP Soil	0.30	0.01	0.574	2.44	1.0	Khire et al. (2000)
SP Soil	0.40	0.01	0.038	2.69	2.9×10^{-3}	Khire et al. (2000)
SM Soil	0.42	0.02	0.005	1.48	2.7×10^{-4}	Khire et al. (2000)
SM-ML Soil	0.35	0.02	0.012	1.123	9.0×10^{-6}	Khire et al. (2000)
ML Soil	0.52	0.08	0.035	1.25	3.2×10^{-6}	Khire et al. (2000)

Initial and Boundary Conditions

Laboratory Soil Column

The initial condition was specified using a matric suction corresponding to the initially dry OK110 fine sand. A specified flux was applied at the surface of the OK110 soil column (Figure 5-1) which was equal to the actual rate of sprinkled water during the laboratory experiment. These lower boundary conditions were simulated to determine

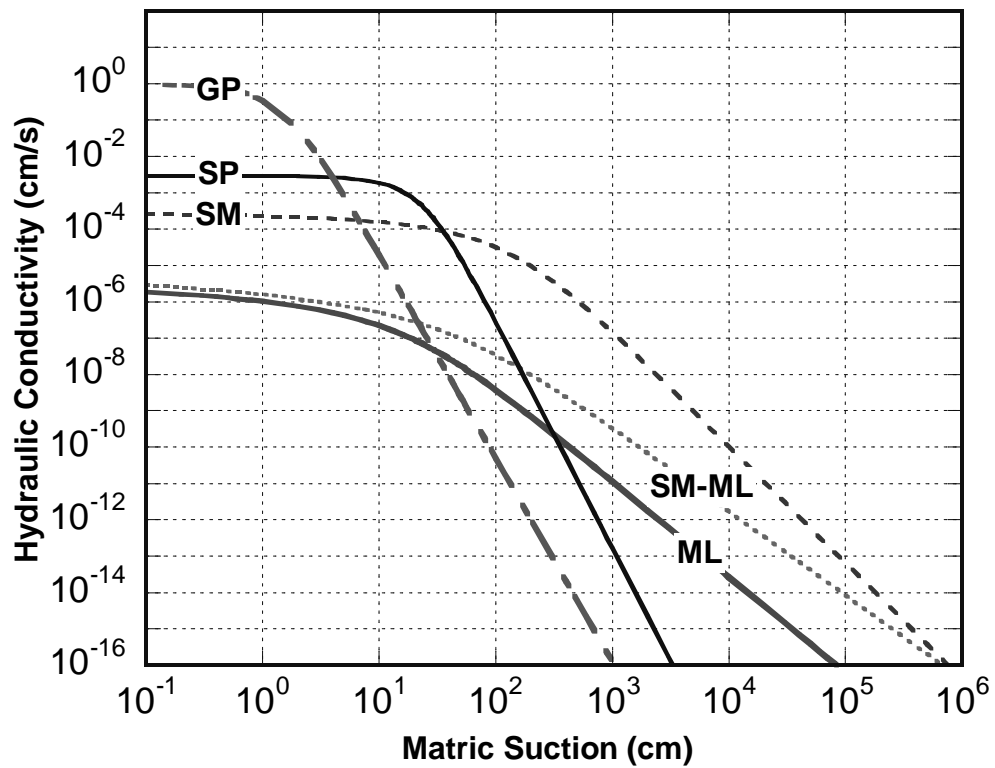
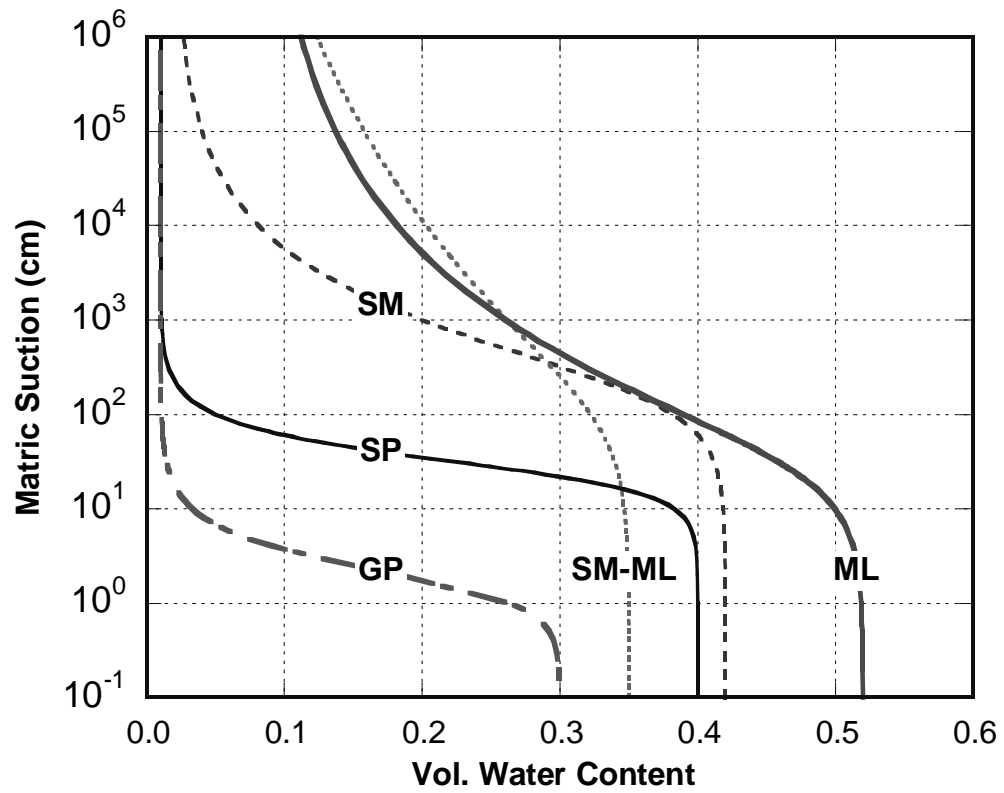


Figure 5-3: Soil water characteristic curves (a); and predicted hydraulic conductivity functions (b) for the soils used to simulate groundwater recharge rates.

which would better predict the measured response of laboratory soil column under the constant infiltration event: (1) a unit gradient boundary at the base of the OK110 sand column; (2) a unit gradient boundary at the base of the nonwoven geotextile that lines the OK110 soil column; and (3) a constant water table at the base of a 90-cm thick coarse gravel (GP) that was hypothetically placed underneath the OK110 soil column. The coarse gravel was necessary to be able to apply a constant water table boundary condition and the thickness was selected such that no upward flux of water will be generated on the OK110 soil column due to capillarity of the gravel layer. Similar lower boundary has been used for the field-scale pan lysimeters built in Detroit as presented in Paper No. 1.

Field-scale Simulations

For field-scale simulations, an atmospheric boundary condition was applied at the surface of the monolithic natural system. The meteorological data obtained by Khire et al. (1997) for East Wenatchee, Washington and Mijares et al. (2010) for Wayne, Michigan were used to simulate the semi-arid and sub-humid climate conditions, respectively. The precipitation was applied at an hourly frequency specifically during the time intervals it occurred during a particular day. To simulate long-term scenario, the meteorological data was successively repeated at least 10 times to generate a cyclic multi-year data. The total number of years of simulations or the number of times the meteorological data was repeated varied depending on the soil profile. To determine the long-term steady-state condition, the criterion that was met was that the annual initial and final soil water storage of the system should be equal. This was done to minimize the effect of the initial conditions on the simulated water balance quantities.

Numerical Control Parameters

Spatial discretization of the model domain was optimized by conducting sensitivity analysis. This was done by repeatedly refining the nodal spacing until insignificant changes in simulated water balance parameters were achieved. The nodal spacing between the nodes located near the upper and lower boundaries was relatively small (1 mm). A maximum time step of 0.1 hr and a minimum time step of 10^{-7} hr were used for all the simulations. At any given time step, the maximum allowable mass balance error for the whole profile was set at 10^{-5} cm. For all numerical analyses, total mass balance errors were less than 1%.

RESULTS

Laboratory Soil Column

Figure 5-4 shows the measured cumulative percolation and soil water storage response of the OK110 sand column subjected to a constant infiltration rate of 1.5×10^{-4} cm/s (6 mL/min) at its surface. The flux that was selected was low enough to maintain unsaturated conditions in the soil column and that no surface water ponding would be generated. A much smaller flux value would not have been possible due to the limitation of the Mariotte bottle and the perforated tubing used to irrigate water on the top surface of the sand column.

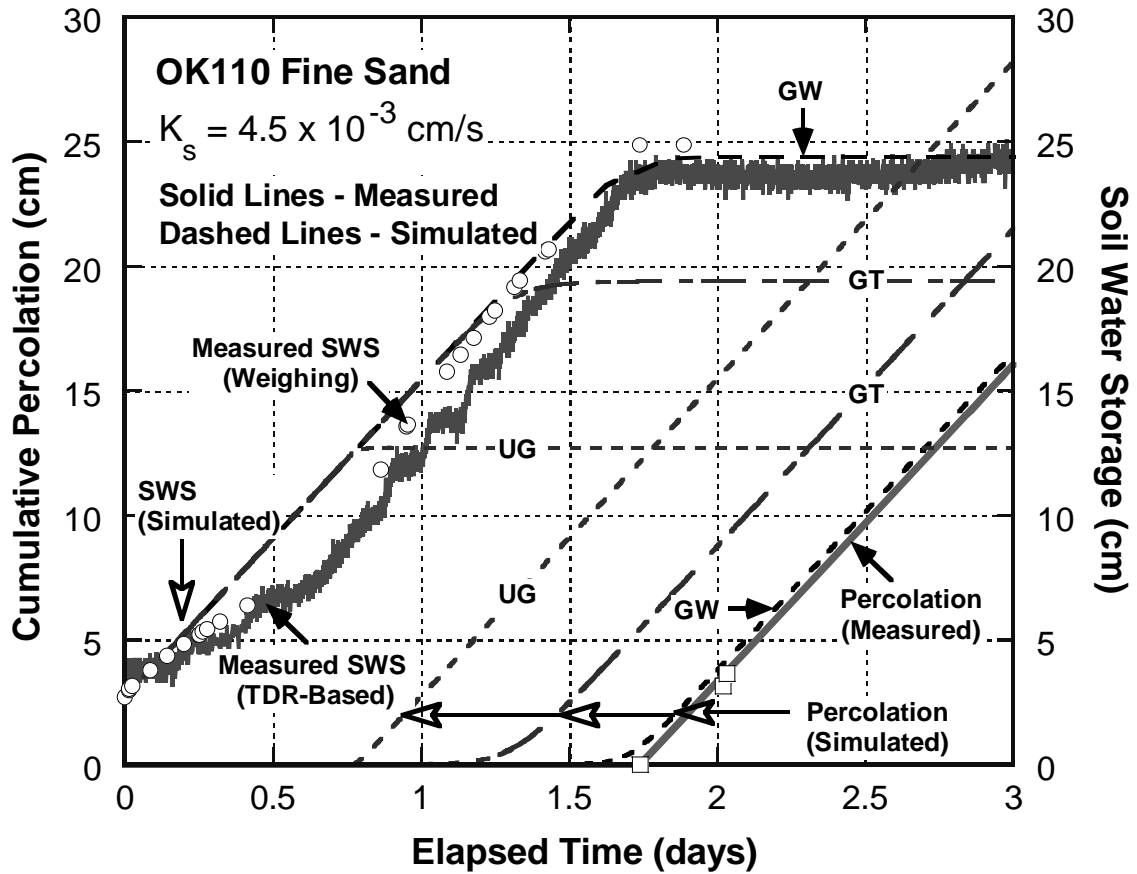


Figure 5-4: Measured and simulated UNSAT-H cumulative percolation and soil water storage for OK110 sand column.

As shown in Figure 5-4, the initially dry soil column reached a steady-state condition after 1.75 days of constant infiltration. Beyond this period, percolation breakthrough occurred and the resulting rate of outflow became equal to the applied inflow rate. The measured soil water storage was determined by integrating the measured water contents from the six mini-TDR sensors that were placed within the soil column. The measured soil water storage agrees well with the measured increase in the mass of the soil column obtained from the weighing scale where the soil column was placed as a weighing lysimeter. Figure 5-4 shows that the soil water storage initially increased at a

rate approximately equal to the applied infiltration rate. Afterwards, it reached its maximum value of about 24 cm after 1.75 days which corresponds to the time when percolation breakthrough occurred.

The measured cumulative percolation and soil water storage obtained from the laboratory soil column experiment provides a dataset to validate the UNSAT-H model for various lower boundary conditions that are typically used. In addition the validated model is used to make predictions for field scenarios. Several boundary conditions were considered to determine which condition would better simulate the measured flow in the OK110 sand column. Figure 5-4 shows the simulated cumulative percolation and soil water storage obtained from three types of lower boundary conditions used in the model: (1) UG which is a unit gradient boundary at the base of the monolithic OK110 soil column; (2) GT which is a unit gradient boundary at the base of the nonwoven geotextile that lines the OK110 soil column; and (3) GW which is a constant water table at the base of a 90-cm thick coarse gravel (GP) that was hypothetically placed underneath the OK110 soil column.

As presented in Figure 5-4, the simulated cumulative percolation and soil water storage obtained when the lower boundary is simulated as a fixed GW within a gravel layer best predicts the measured cumulative percolation and soil water storage, respectively. The UG and GT lower boundary conditions underestimated the time when percolation breakthrough occurs. Both UG and GT lower boundary conditions also underestimated the maximum soil water storage reached by the soil column under steady-state condition.

For the fixed GW within a gravel layer lower boundary, the measured and simulated water content profiles are about the same. It can also be observed from Figure 5-5 that due to the presence of the geocomposite drainage layer in the OK110 soil column, water builds up near the base of the soil column when percolation breakthrough occurs. This phenomenon indicates the occurrence of capillary barrier effect. Khire and Mijares (2010) pointed out that a geosynthetic capillary break occurs when the saturated hydraulic conductivity of the finer grained soil layer in the capillary barrier is greater than 10^{-5} cm/s. This finding is consistent with the data collected from the sand column.

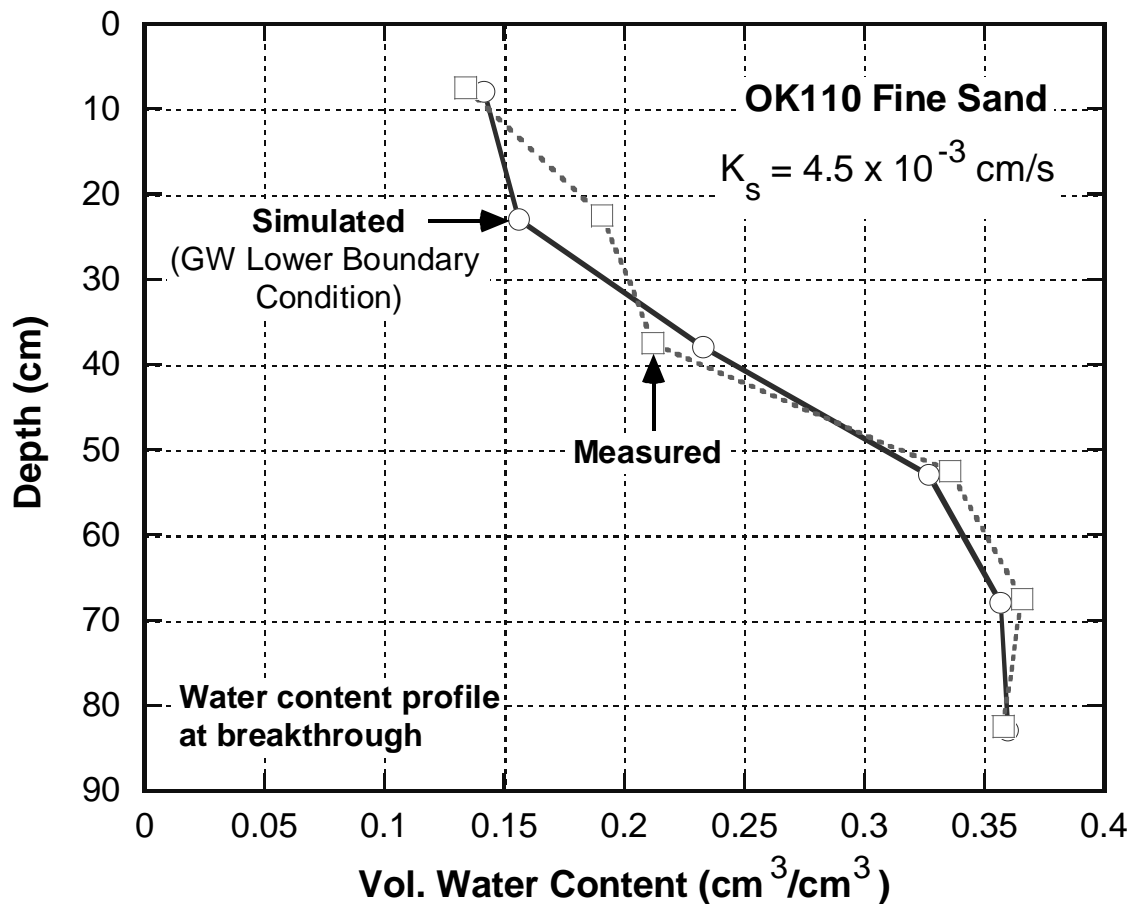


Figure 5-5: Measured and simulated water content profile for OK110 fine sand column at breakthrough.

Field-scale Simulations

Field-scale simulations were conducted to predict natural groundwater recharge rates in semi-arid and sub-humid climates. Annual precipitation for East Wenatchee, Washington is 26.5 cm with an annual potential evapotranspiration of 109.12 cm (PET/P ~ 4.12) was selected to represent the semi-arid condition. Annual precipitation for Wayne, Michigan is 86.2 cm with an annual potential evapotranspiration of 87.30 cm (PET/P ~ 1.01) was selected to represent the sub-humid condition.

Monolithic natural systems consisting of 7.5 m thick soil profile were simulated to determine the resulting groundwater recharge rates from the applied meteorological data. A deeper soil profile up to 60 m thick was also considered to determine whether the thickness affected the estimates for groundwater recharge. Actual fluxes were determined at different depths of the soil profile and compared to lysimeter simulations. Lysimeter simulations consisted of the same soil profile with thickness equal to the depths where the actual fluxes for the natural system were determined. Figure 5-6 shows the conceptual model of the monolithic natural system and lysimeter used for the simulations. Based on the accuracy of GW boundary observed from the sand column experiment, a fixed GW within a gravel layer lower boundary condition was used to determine the percolation through a lysimeter and the recharge for the natural system.

Semi-arid Climate

Figure 5-7 shows the simulated groundwater recharge rates for a natural system consisting of SP soil (poorly graded sand; $K_{\text{sat}} = 2.9 \times 10^{-3}$ cm/s) under a semi-arid

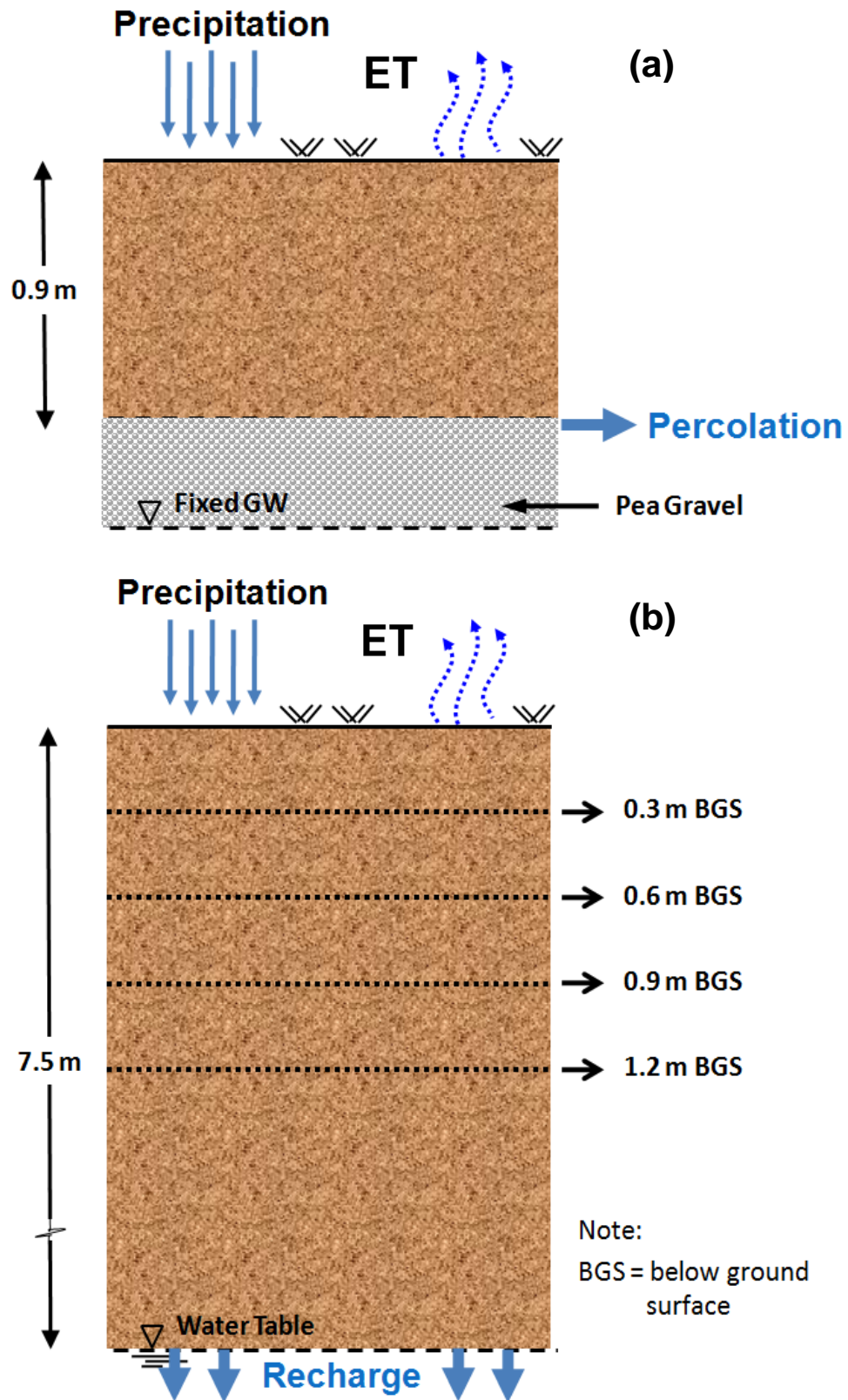


Figure 5-6: Schematic of a lysimeter (a); and a monolithic natural system (b) used to estimate natural groundwater recharge rates.

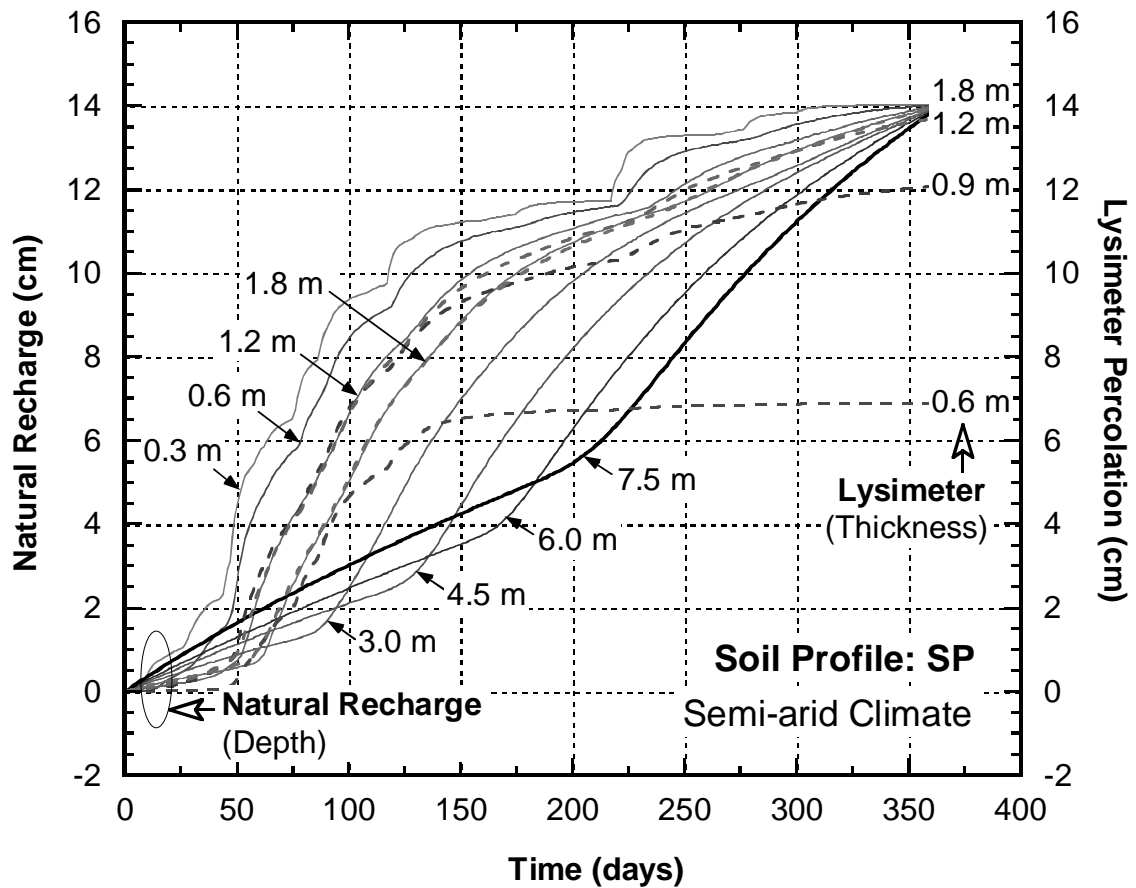


Figure 5-7: Simulated natural groundwater recharge rates and lysimeter percolations for SP soil in a semi-arid climate.

climate. The annual long-term recharge rate is about 14.0 cm which is approximately 53% of the precipitation received at the ground surface. Figure 5-7 also shows the actual fluxes at different depths across the soil profile. Because the simulation represents long-term scenario under steady-state condition, the cumulative fluxes at various depths across the soil profile are the same. This finding is consistent with the continuity and conservation of mass that must be satisfied. However, as shown in Figure 5-7, the plot of cumulative flux at shallower depths shows greater fluctuations. At deeper depths, the fluctuations dampen because the effect of evapotranspirative gradient is less significant.

Figure 5-7 also presents the cumulative percolation obtained by simulating corresponding lysimeters having soil profile thickness ranging from 0.6 m to 1.8 m. Figure 5-7 shows that lysimeter having soil profile thickness less than 1.2 m underestimates the groundwater recharge. As the lysimeter thickness increases, the percolation captured by the lysimeter more closely approximates the groundwater recharge. Thus, for SP soil, which has a K_{sat} of 2.9×10^{-3} cm/s, under a semi-arid climate, would require at least 1.2 m thick soil profile for the lysimeter to be representative of the natural system.

Figure 5-8 shows the simulated groundwater recharge rates for a natural system consisting of SM soil (silty sand; $K_{sat} = 2.7 \times 10^{-4}$ cm/s) under a semi-arid climate. The annual long-term recharge rate is 0 cm. This shows that the hydraulic conductivity of the soil impacts the natural recharge. Lower hydraulic conductivity yield a lower recharge rate. Similar to SP soil, the plot of cumulative flux at shallower depths shows greater fluctuations and the fluctuations dampen at deeper depths. However, in this particular case, due to the hydraulic conductivity of the SM soil being an order of magnitude lower than SP soil, the resulting groundwater recharge becomes zero. Lysimeter simulations consisting of 0.6 to 1.2 m thick profiles also predicted zero percolation for the SM soil in the semi-arid climate. Field measured percolation for the Hanford site (Fayer et al. 1999) in Richmond, Washington similarly resulted to zero percolation rates for 1.0 and 1.5 m thick silt loam lysimeters.

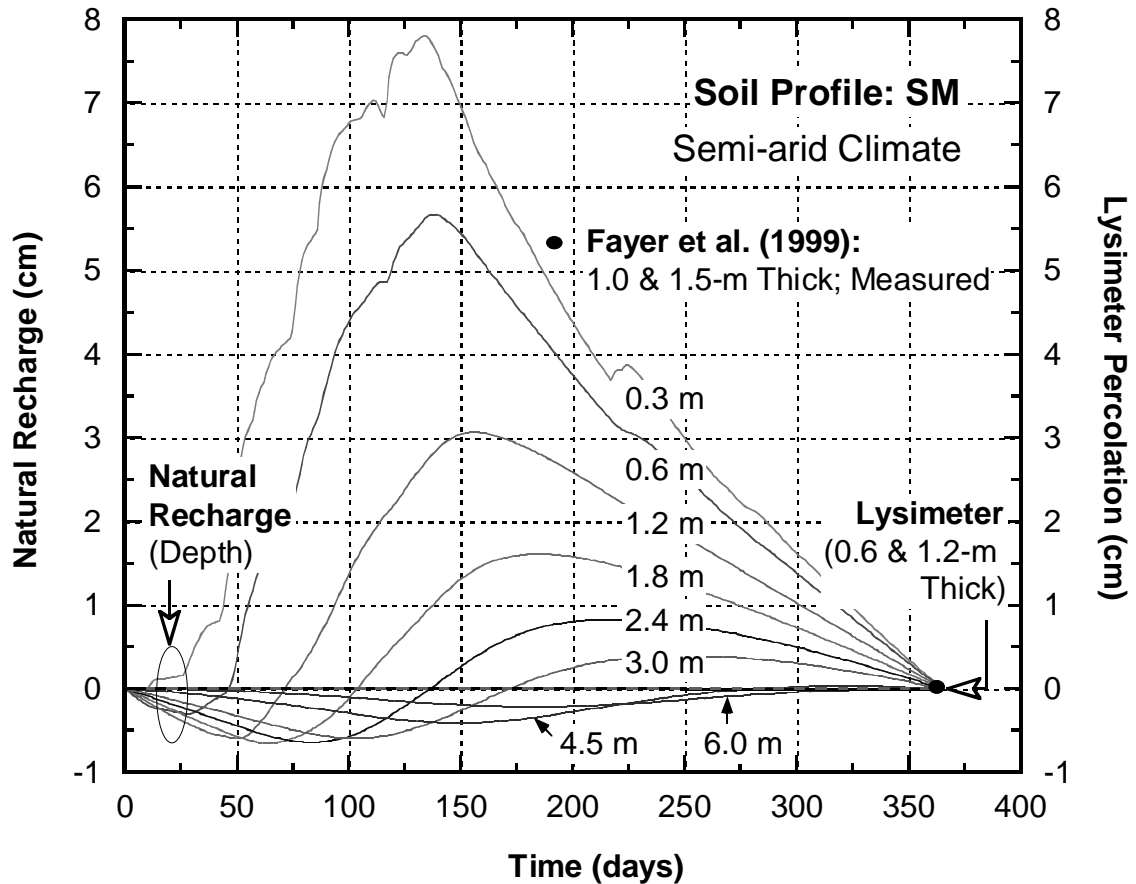


Figure 5-8: Simulated natural groundwater recharge rates and lysimeter percolations for SM soil in a semi-arid climate.

Since the SM soil profile yielded zero recharge rate and lysimeter percolation for the semi-arid climate, an SP-SM soil having hydraulic conductivity in between SP and SM was simulated. SP-SM soil (poorly graded sand with silt) has a K_{sat} of 5.8×10^{-4} cm/s and has unsaturated hydraulic properties that are similar to the SP soil. Figure 5-9 shows the simulated groundwater recharge rates for a natural system consisting of SP-SM soil. The annual long-term recharge rate is about 13.3 cm and is slightly lower than the annual long-term recharge rate for the SP soil due to a lower hydraulic conductivity. Figure 5-9 also shows that a lysimeter having a soil profile thickness of at least 0.9 m would be

needed to capture the natural groundwater recharge rate. This thickness is less compared to that required for SP soil due to a lower hydraulic conductivity. Thus, a lower hydraulic conductivity of a soil profile requires less thick lysimeter to be equivalent to the natural system.

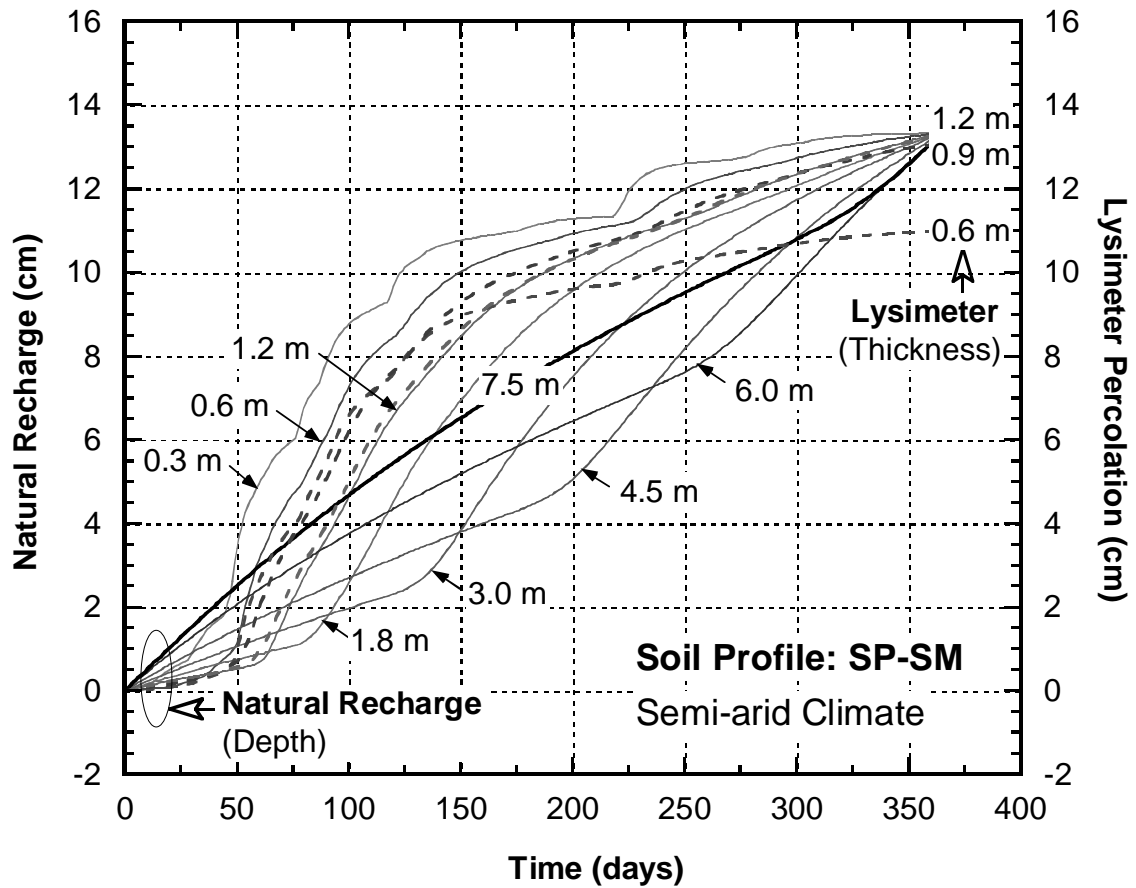


Figure 5-9: Simulated natural groundwater recharge rates and lysimeter percolations for SP-SM soil in a semi-arid climate.

Sub-humid Climate

Figure 5-10 shows the simulated groundwater recharge rates for a natural system consisting of SM soil in a sub-humid climate. The annual long-term recharge rate is about

15.5 cm which is approximately 18% of the precipitation. Figure 5-10 also shows the cumulative percolation obtained from lysimeter simulations with different thicknesses (1.8 to 6.0 m thick). It can be seen that the lysimeter underestimates the groundwater recharge rate. A lysimeter with a thickness greater than 6.0 m is necessary to capture the annual groundwater recharge rate.

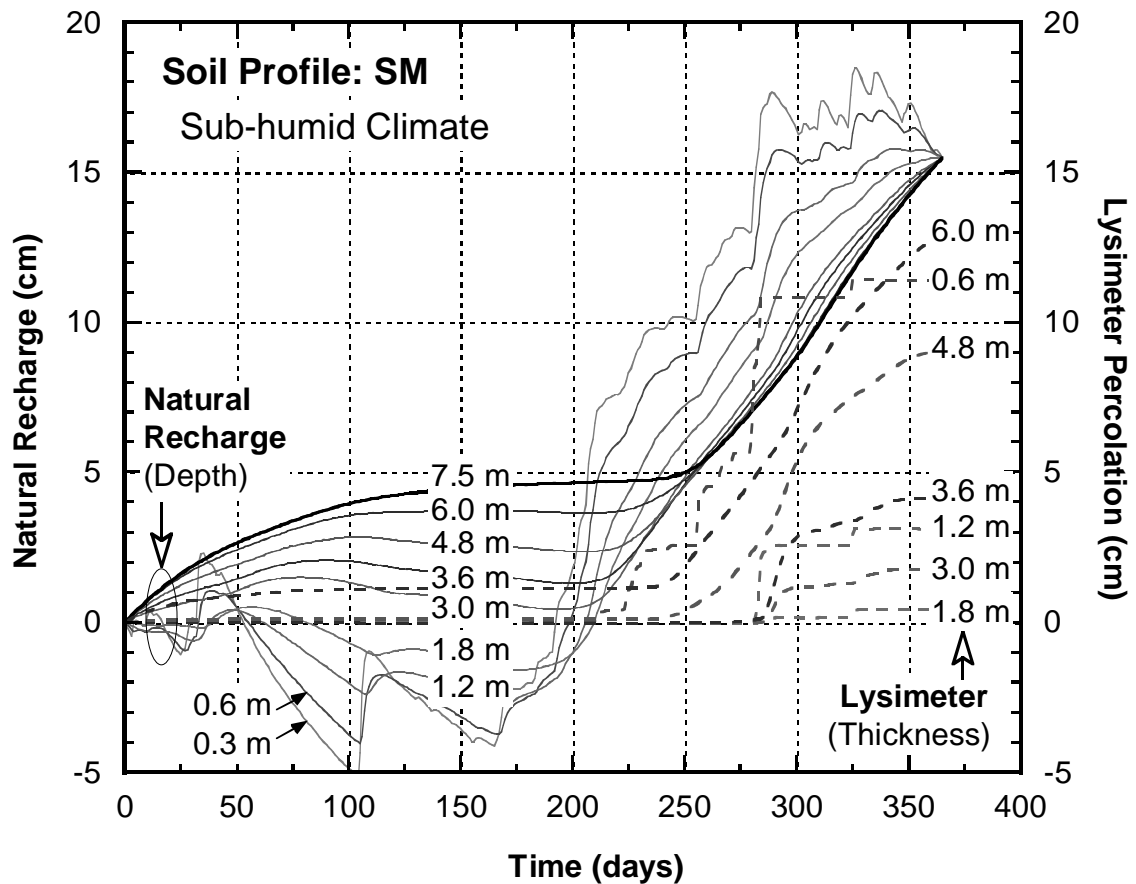


Figure 5-10: Simulated natural groundwater recharge rates and lysimeter percolations for SM soil in a sub-humid climate.

Figures 5-11 and 5-12 present the simulated groundwater recharge rates for a natural system consisting of SM-ML and ML soils, respectively, under a sub-humid

climate. SM-ML is sandy silt with $K_{\text{sat}} = 9.0 \times 10^{-6}$ cm/s and ML soil is silt with $K_{\text{sat}} = 3.2 \times 10^{-6}$ cm/s. In order to eliminate surface runoff, a 0.6 m thick topsoil layer consisting of SM soil was considered. The annual long-term recharge rate for SM-ML soil is approximately 6.65 cm and 5.66 cm for ML soil due to lower hydraulic conductivities. For both soils in sub-humid climate, Figures 5-11 and 5-12 show that at least 0.6 cm thick lysimeter (with a 0.6 cm topsoil layer) is necessary to capture the annual groundwater recharge rate for the natural system.

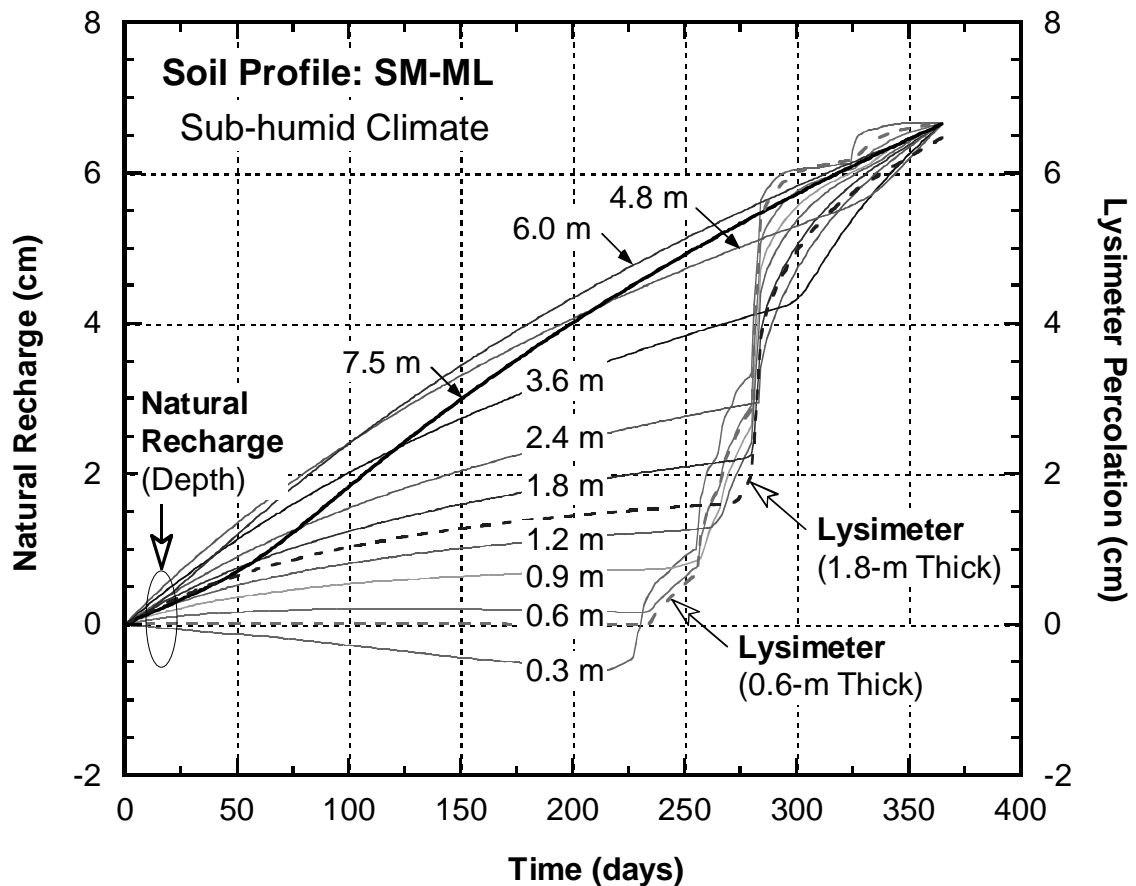


Figure 5-11: Simulated natural groundwater recharge rates and lysimeter percolations for SM-ML soil in a sub-humid climate.

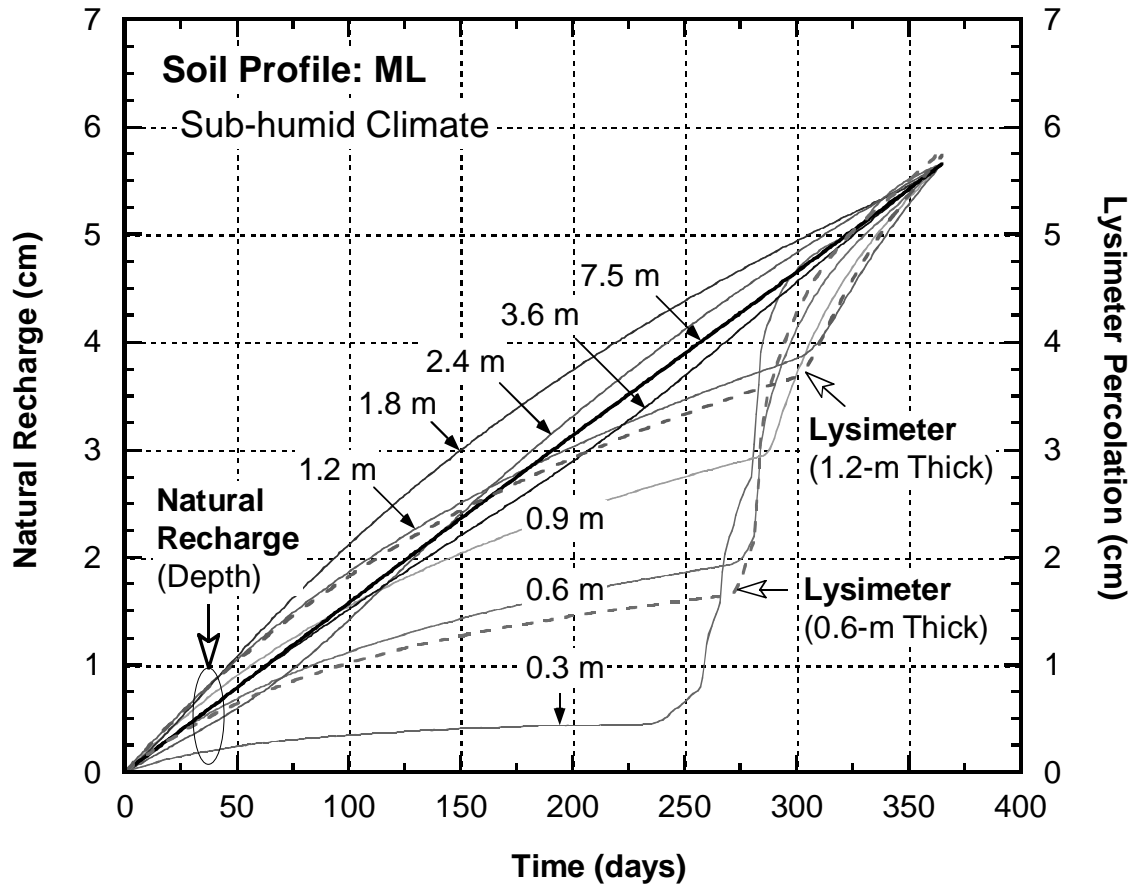


Figure 5-12: Simulated natural groundwater recharge rates and lysimeter percolations for ML soil in a sub-humid climate.

Practical Implications

Figure 5-13 shows the ratio of groundwater recharge rate for a natural system and percolation estimates obtained from a lysimeter using various thicknesses of the soil profile. Figure 5-13(a) shows that for semi-arid climates, for soils with saturated hydraulic conductivity greater than 10^{-3} cm/s, the lysimeter needs to be relatively thick to obtain representative recharge estimates. Whereas for sub-humid climates as shown in Figure 5-13(b), for soils with saturated hydraulic conductivity greater than 10^{-5} cm/s, the

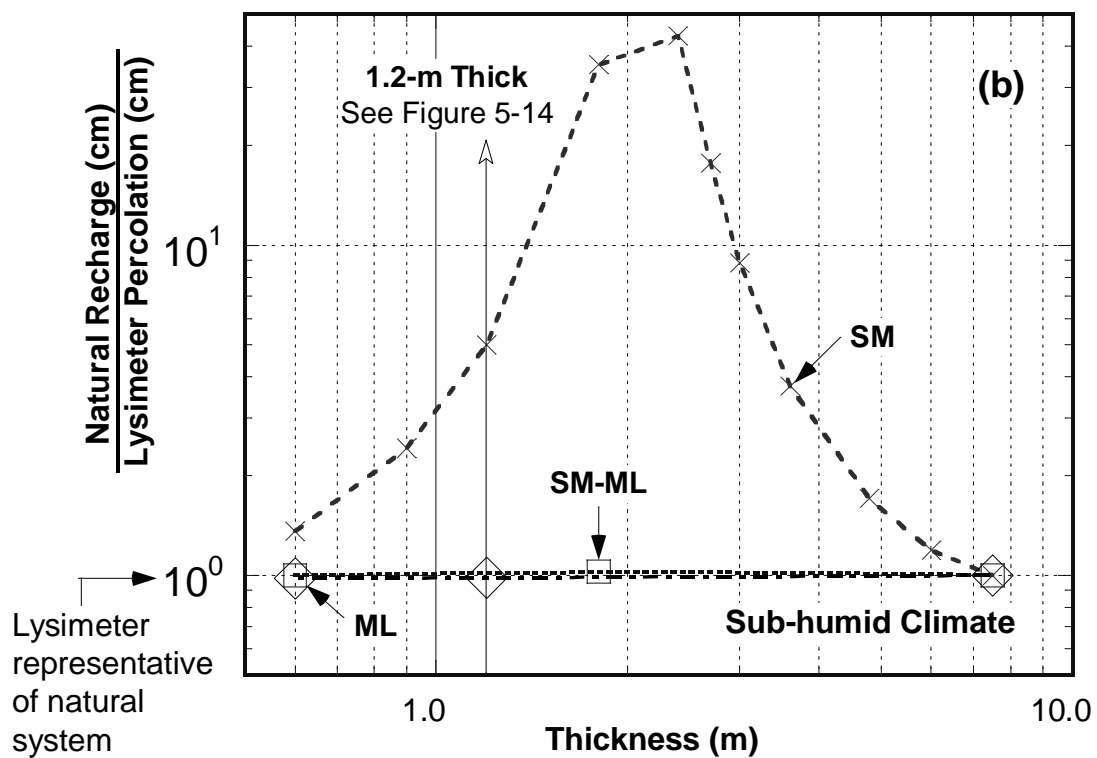
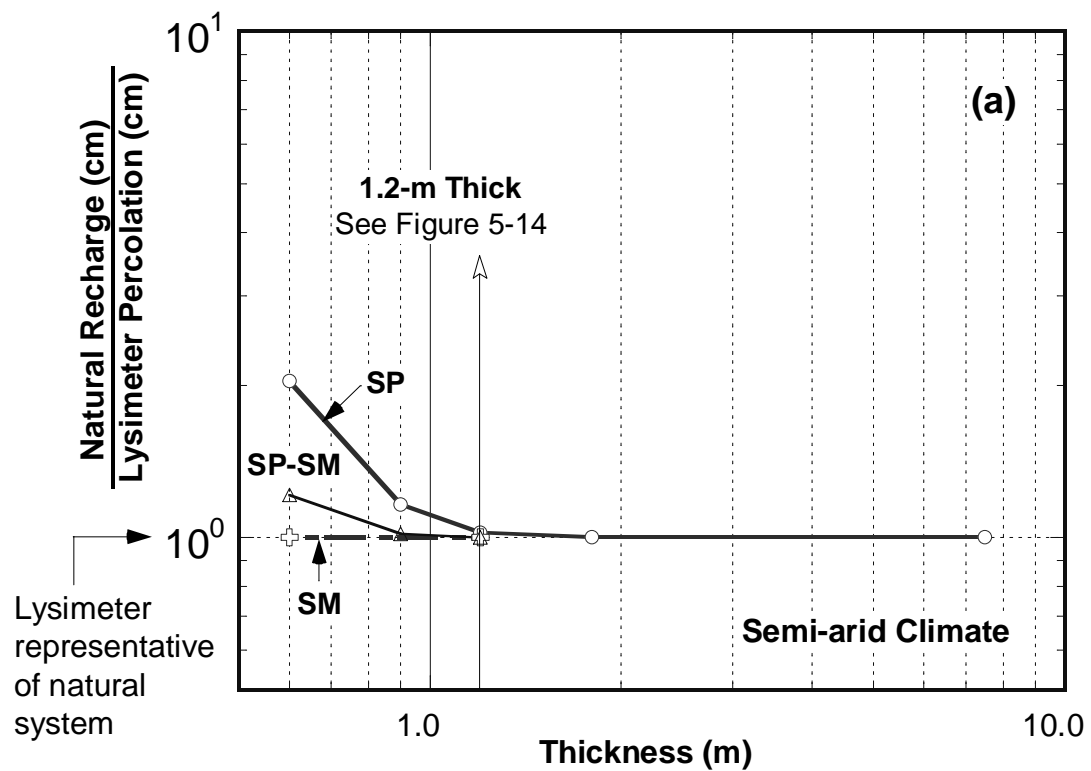


Figure 5-13: Ratio of natural groundwater recharge and percolation estimates for various lysimeter profile thicknesses in semi arid (a); and sub-humid (b) climates.

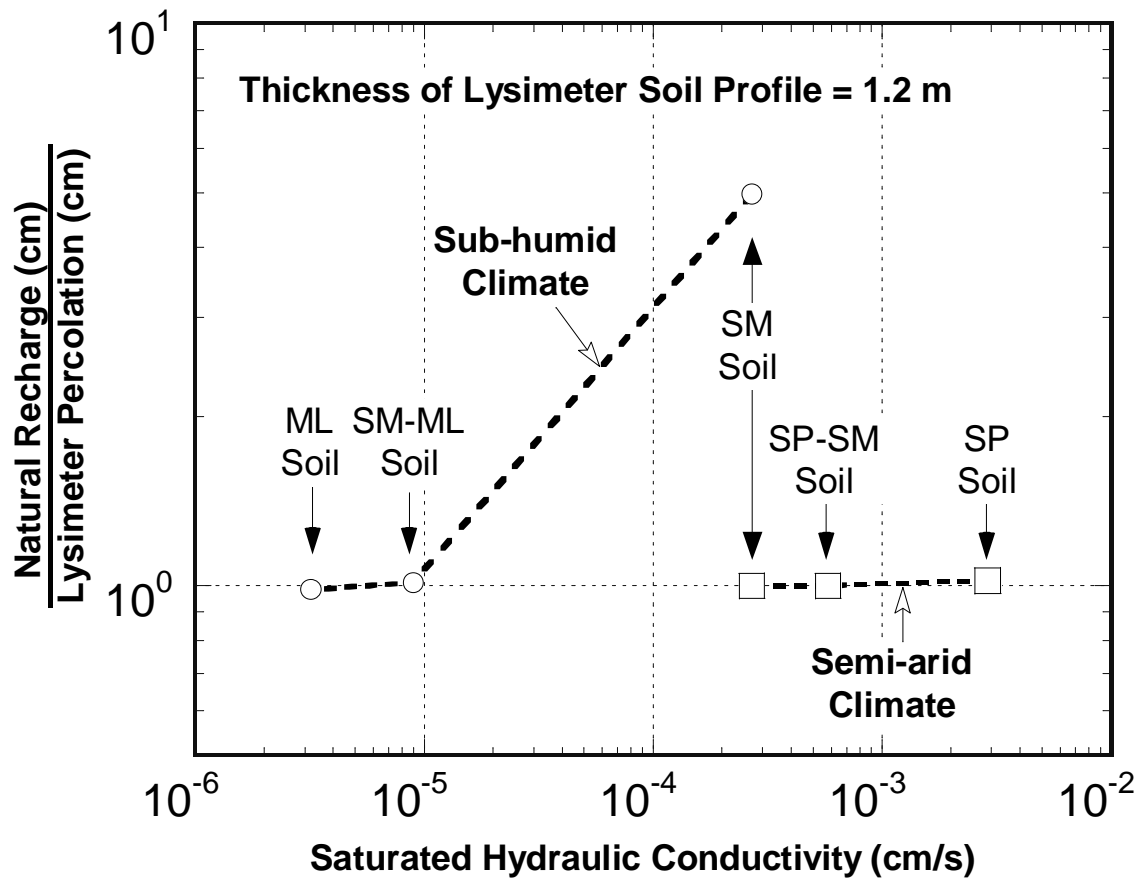


Figure 5-14: Ratio of natural groundwater recharge and percolation estimates for various saturated hydraulic conductivity of the soil.

lysimeter needs to be very thick (6 m or more) to obtain representative recharge estimates. This is because the capillary barrier effect is significant for these permeable soils that would cause the lysimeter to measure lower percolation, thereby underestimating the recharge rate. Figure 5-14 shows the ratio of groundwater recharge rate for a natural system and percolation estimates obtained from a 1.2 m thick lysimeter for various saturated hydraulic conductivity of the soil. It can be seen that for a given lysimeter thickness, as the soil becomes permeable, the lysimeter percolation further underestimates the recharge rate.

SUMMARY AND CONCLUSION

This study presents a numerical assessment of recharge rate estimated by lysimeters as a function of thickness of soil profile, hydraulic properties of soils, and the climate. A laboratory soil column consisting of fine sand underlain by a geocomposite drainage layer was built and instrumented to monitor its response under constant infiltration of water from the surface. Among the UNSAT-H simulations that were carried out, the numerical model with a fixed GW table within a gravel layer lower boundary condition was able to capture the measured cumulative percolation and soil water storage for the instrumented soil column relatively accurately. The calibrated model was used for field-scale simulations to determine natural groundwater recharge rates for natural systems consisting of monolithic soil in semi-arid and sub-humid climates. Lysimeter simulations were also conducted to determine whether percolation estimates obtained from a lysimeter are representative of the groundwater recharge rate for the corresponding natural system.

The numerical results suggest that the lysimeter soil profile needs to be thick enough to minimize the capillary barrier effect that is inevitably introduced at the lower boundary. The capillary barrier effect results in the underestimation of natural groundwater recharge rate. In general, in wetter climates, the thickness of the soil profile for the lysimeter could be less than that required for a drier climate. In addition, a lower hydraulic conductivity soil profile would require a thinner soil profile to capture the recharge as opposed to a higher hydraulic conductivity soil profile. Therefore, site specific water balance simulations need to be carried out to size the lysimeter in order to account for the effect of these key parameters.

REFERENCES

REFERENCES

- Benson, C., Bosscher, P., Lane, D., and Pliska, R. (1994). "Monitoring System for Hydrologic Evaluation of Landfill Final Covers," *Geotechnical Testing Journal*, 17 (2): 138-149.
- Benson, C., Bohnhoff, G., Ogorzalek, A., Shackelford, C., Apiwantragoon, P., and Albright, W. (2005). "Field Data and Model Predictions for an Alternative Cover," *Waste Containment and Remediation*, GSP No. 142, ASCE, Reston, VA: 1-12.
- Bohnhoff, G., Ogorzalek, A., Benson, C., Shackelford, C., and Apiwantragoon, P. (2009). "Field Data and Water-Balance Predictions for a Monolithic Cover in a Semiarid Climate," *Journal of Geotechnical and Geoenvironmental Engineering*, 135 (3): 333-348.
- Doorenbos, J., and Pruitt, W. (1977). "Guidelines for Predicting Crop Water Requirements," *FAO Irrigation Paper No. 24*, 2nd ed., Food and Agriculture Organization of the United Nations, Rome, Italy: 1-107.
- Fayer, M., Murphy, E., Downs, J., Khan, F., Lindenmeier, C., and Bjornstad, B. (1999). "Recharge Data Package for the Immobilized Low-Activity Waste 2001 Performance Assessment," PNNL-13033, Pacific Northwest National Laboratory, Richland, Washington.
- Fayer, M. (2000). "UNSAT-H Version 3.0: Unsaturated Soil Water and Heat Flow Model – Theory, User Manual, and Examples," PNNL-13249, Pacific Northwest Laboratories, Richland, Washington.
- Gee, G., and Hillel, D. (1988). "Groundwater Recharge in Arid Regions: Review and Critique of Estimation Methods," *Hydrological Processes*, 2: 255-266.
- Hillel, D. (1980). *Applications of Soil Physics*, Academic Press, Inc., New York.
- Khire, M., and R. Mijares. (2010). "Effect of Geocomposite Drainage Layer on Water Balance of Earthen Cap Lysimeters," *Proceedings*, 2010 Global Waste Management Symposium, San Antonio, TX.
- Khire, M., Benson, C., and Bosscher, P. (1997). "Water Balance Modeling of Earthen Final Covers," *Journal of Geotechnical and Geoenvironmental Engineering*, 123 (8): 744-754.
- Khire, M., Benson, C., and Bosscher, P. (2000). "Capillary Barriers: Design Variables and Water Balance," *Journal of Geotechnical and Geoenvironmental Engineering*, 126 (8): 695-708.
- Krishnamurthi, N., Sunada, D., and Longenbaugh, R. (1977). "Mathematical Modeling of Natural Groundwater Recharge," *Water Resources Research*, 13 (4): 720-724.

- Mijares, R., Khire, M., and Johnson T. (2010). "Lysimeters Versus Actual Earthen Caps: Numerical Assessment of Soil Water Storage," *Proceedings, GeoFlorida 2010, GSP No. 199, Advances in Analysis, Modeling and Design*, ASCE, Reston, VA: 2849-2858.
- Mukherjee, M. (2008). "Instrumented Permeable Blankets for Estimating Subsurface Hydraulic Conductivity and Confirming Numerical Models Used for Subsurface Liquid Injection," *Ph.D. Dissertation*, Michigan State University, East Lansing, Michigan, 278 p.
- Ogorzalek, A., Bohnhoff, G., Shackelford, C., Benson, C., and Apiwantragoon, P. (2008). "Comparison of Field Data and Water-Balance Predictions for a Capillary Barrier Cover," *Journal of Geotechnical and Geoenvironmental Engineering*, 134 (4): 470-486.
- Park, K., and Fleming, I. (2006). "Evaluation of a Geosynthetic Capillary Barrier," *Geotextiles and Geomembranes*, 24: 64-71.
- Scanlon, B., Healy, R., and Cook, P. (2002). "Choosing Appropriate Techniques for Quantifying Groundwater Recharge," *Hydrogeology Journal*, 10: 18-39.
- Scanlon, B., Reedy, R., Keese, K., and Dwyer, S. (2005). "Evaluation of Evapotranspiration Covers for Waste Containment in Arid and Semiarid Regions in the Southwestern USA," *Vadose Zone Journal*, 4: 55-71.
- Seiler, K., and Gat, J. (2007). *Groundwater Recharge from Run-off, Infiltration and Percolation*, Water Science and Technology Library, Vol. 55, Springer, The Netherlands, 244 p.
- Stormont, J., and Morris, C. (2000). "Characterization of Unsaturated Nonwoven Geotextiles," *Proceedings, Geo-Denver 2000, GSP No. 99, Advances in Unsaturated Geotechnics*, ASCE, Reston, VA: 153-164.
- Topp, G., Davis, J., and Chinnick, J. (1980). "Electromagnetic Determination of Soil Water Content: Measurements in Co-axial Transmission Lines," *Water Resources Research*, 16 (3): 574-582.
- van Genuchten, M. (1980). "A Closed-Form Equation for Predicting the Hydraulic Conductivity of Unsaturated Soils," *Soil Science Society of America Journal*, 44: 892-898.

SUMMARY AND CONCLUSIONS

This dissertation aimed to evaluate the difference in the hydraulic performance of a lysimeter versus an actual earthen cap with underlying landfilled waste.

Field-scale test sections were built and instrumented at a landfill near Detroit, Michigan consisting of compacted and uncompacted native glacial till (clay) soils. These caps were 1.8 m thick. Lysimeter pans were installed in the middle of each test sections to collect and quantify the percolation through the soil covers. The instrumented area of the test section was expanded upslope and downslope of the lysimeter to monitor the soil water storages within and beyond the lysimeter footprint in order to evaluate the effect of a lysimeter lower boundary.

Water balance models UNSAT-H and Vadose/W were used to simulate the field measured percolation and soil water storage and to estimate the percolation across the interface between the overlying soil cap and the underlying landfilled waste. Field-scale simulations under semi-arid and humid climates were also conducted to determine the effect of the hydraulic properties of the cover soils and the underlying waste, as well as the presence of a nonwoven geotextile, on percolation values measured by the lysimeter.

The key findings of this study are as follows:

- (1) Percolation for the compacted clay test section was about few millimeters per year versus it was in tens of centimeters for the uncompacted test section due to about two orders greater field hydraulic conductivity.
- (2) The soil water storages for the portions of the uncompacted test section that were underlain by the waste were typically greater than those for the corresponding

lysimeters. However, for the compacted test section, there was no significant difference between the soil water storage for the actual cap and the lysimeter.

- (3) UNSAT-H and Vadose/W were able to simulate the measured percolation through the compacted test section. However, both numerical models were not able to capture the macropore flow through the uncompacted test section primarily due to incapability of these models to simulate non-Darcian flow. Variations in the field measured soil water storages were generally captured by the numerical models.
- (4) Estimated percolation across the interface between the overlying soil cap and the underlying landfilled waste showed upward fluxes of water which indicates that the overlying soil cap has the capability to pull moisture from the underlying material under evapotranspirative gradients. Thus, net percolation for actual caps predicted by the validated models was negative.
- (5) The numerical results indicate that lower soil water storage corresponds to greater percolation, and vice versa. The lysimeter generally has lower soil water storage than the corresponding actual cap. The lysimeter, in general, results in greater percolation compared to the corresponding actual cap. The lysimeter versus actual cap hydrologic performance difference becomes relatively small if the hydraulic conductivity of the soil is less than 10^{-6} cm/s.
- (6) The capillary barrier effect that is introduced by a nonwoven geotextile used as a drainage layer in a lysimeter influences the long-term percolation significantly only when the saturated hydraulic conductivity of the soil is greater than

10^{-5} cm/s. In addition, for humid climates, the capillary barrier effect is not as significant as for the drier climates regardless of the hydraulic conductivity of the soil.